



FACULTEIT LANDBOUWKUNDIGE EN
TOEGEPASTE BIOLOGISCHE
WETENSCHAPPEN



Academiejaar 2003-2004

ACTIVATED SLUDGE FLOCCULATION DYNAMICS: ON-LINE MEASUREMENT METHODOLOGY AND MODELLING

DYNAMICA VAN ACTIEF-SLIB FLOCCULATIE: ON-LINE MEETMETHODOLOGIE EN MODELBOUW

door

ir. Ruxandra Govoreanu

*Thesis submitted in fulfillment of the requirements for the degree of
Doctor (Ph.D.) in Applied Biological Sciences: Environmental Technology*

*Proefschrift voorgedragen tot het bekomen van de graad
van Doctor in de Toegepaste Biologische Wetenschappen: Milieutechnologie*

op gezag van

Rector: **Prof. Dr. A. De Leenheer**

Decaan:

Prof. Dr. ir. H. VAN LANGENHOVE

Promotor:

Prof. Dr. ir. P. VANROLLEGHEM

ISBN 90-5989-031-0

The author and the promoter give the authorization to consult and to copy parts of this work for personal use only. Any other use is limited by the Laws of Copyright. Permission to reproduce any material contained in this work should be obtained from the author.

De auteur en de promotor geven de toelating dit doctoraatswerk voor consultatie beschikbaar te stellen, en delen ervan te kopiëren voor persoonlijk gebruik. Elk ander gebruik valt onder de beperkingen van het auteursrecht, in het bijzonder met betrekking tot de verplichting uitdrukkelijk de bron te vermelden bij het aanhalen van de resultaten van dit werk.

Gent, June 2004

De promotor:

De auteur:

Prof. Dr. ir. Peter Vanrolleghem

ir. Ruxandra Govoreanu

To Bogdan

Acknowledgement

Gratitude is the heart's memory.

--- *French Proverb*

It is hard to believe that I'm now about to write the final words of my Ph.D. book. Everything happened so fast and in the mean time so extraordinary! This journey wouldn't have been possible without the company of so many great people I am surrounded by. I would like to thank you all for your professional attitude, for your enthusiasm and team spirit and, needless to say, for your friendship.

First of all, I am very grateful to my supervisor, Prof. Peter A. Vanrolleghem. He is simply amazing! Professionalism and scientific guidance, energy and spontaneity, joyfulness and friendly attitude, just to mention a few attributes that make him the supervisor any Ph.D. student could wish for. I am very grateful to Peter for giving me the opportunity to pursue Ph.D. research under his supervision, for the warm welcome in his group; for his kind encouragements, flexibility and understanding; for his help with administrative procedures and for making my research financially possible.

To work with Peter means being a member of a big family – the PVR@BIOMATH research group. I would like to thank all my colleagues, for contributing with their “multidimensional” personality to this unique workplace. They managed to find the perfect balance between scientific and social activities, being a permanent source of brilliant ideas, challenging questions and good mood, which can hardly be forgotten. Thank you Bob, Ingmar, Gurkan, Guclu, Dirk, Eveline, Klaas, Frederik, Jeriffa, Stijn, Tolessa, Usama, Tao, Dae Sung, ChangKyoo, Kris, Gaspard, Karel, Thilo, Tinne, Jing and Griet (well, there has to be a last, but not a least!).

I greatly appreciated the close collaboration I had within the Sedifloc project with my Biomath colleagues, Ingmar and Bob (also, many thanks to Bob for taking the time to read and correct my Ph.D. and for the valuable suggestions). I am very grateful to Prof. Paul Van der Meeren and to Hans, for substantially contributing to the progress of the project and for the countless interesting discussions we had. I also owe them a special thank for kindly providing me access to the lab equipment, for a long period of time, for their flexibility and understanding. Without that, an important part of this thesis would not have been possible. I also want to acknowledge the technical assistance of other "PAINT" people, from which I benefited a lot. I would particularly like to mention Denis, Eric and Annie.

I also had the great opportunity to work with "the molecular group" of LabMET. I am very grateful to Prof. Willy Verstraete for making this collaboration possible and for his valuable suggestions. To Dave and Nico, my warm thanks for their help in performing and analysing the DGGE results. Also to Siska, many thanks for the experimental work and technical assistance.

I am grateful to the members of the reading committee, for accepting to evaluate my thesis, and for their valuable comments and suggestions, which substantially contributed to improving the manuscript: Prof. Paul Van der Meeren, Dr. Catherine Biggs (I also acknowledge the fruitful collaboration we had, and her competent advice and stimulating discussions), Dr. Marie-Noëlle Pons (also for her professional remarks and help in developing the image analysis system) and Prof. Eberhard Morgenroth (also for the challenging discussions with various occasions).

To Olivier and Lieve, many thanks for the help in performing the statistical analysis.

I acknowledge the wonderful assistance provided by Viv, Annie, Roos and Rony.

To Griet, a very special thank for the help in performing the experimental work, and for always being a supportive friend. I am especially grateful for her generous effort during the last summer campaign (thanks Marie, as well, for enduring that!:)). I'll not forget the *ad hoc* Dutch classes (I promise to try harder, next time I have the chance!) and the daily chats, flavoured with fun.

To my colleague, Gurkan, with whom I shared good and difficult moments during all these years, my thanks for his friendship, help and encouragements, and for his patience with my countless questions.

I would like to thank the management and my new colleagues of Ankersmid N.V. for their flexibility and understanding in the last couple of months, when I went through the final phases of this Ph.D.

I also want to thank Prof. Ionel Constantinescu, Prof. Cristina Costache and all the colleagues from the Technical University of Bucharest, for the good collaboration we had.

Thanks to all my friends for spending together many enjoyable moments, here, in Belgium. I am also thankful to my friends at home, in Romania, for remaining the best friends, no matter the time or distance.

I would like to thank with all my heart to my family for their continuous encouragements and support. I owe deep gratitude to my parents for educating me and for their endless love and understanding. Ionuț, my dear brother, thank you very much for your love and support. You all missed me so much during all these years. Thank you! (*Aș vrea să mulțumesc din inima familiei mele pentru încurajările și suportul lor continuu. Părinților mei le datorez o profunda grațitudine pentru educația primită și nemăsurata lor dragoste și înțelegere. Ionuț, dragul meu frate, mulțumesc mult pentru dragostea și sprijinul tău. Buni, voi aprecia întotdeauna grija ta pentru mine. Mi-ați lipsit tot așa de mult, în toți acești ani. Mulțumesc!*).

Finally, the words are not enough to express my gratitude to my husband, Bogdan. Without him, this work wouldn't have been possible. His love, support, patience, encouragements and ambition fuelled my determination to start my Ph.D. and reach this point.

Ruxandra Govoreanu

Ghent, June 2004

Contents

1.Introduction	1
1.1. Aim.....	3
1.2. Research approach.....	5
1.3. Outline of the thesis.....	7
2.Literature review.....	9
2.1. Wastewater treatment.....	9
2.1.1. <i>The activated sludge process</i>	10
2.2. Solid-liquid separation in secondary clarifiers.....	11
2.2.1. <i>Measurement of the activated sludge settleability in secondary clarifier</i>	11
2.2.2. <i>Separation problems in secondary clarifiers</i>	14
2.3. Activated sludge flocculation process.....	17
2.3.1. <i>The composition of the activated sludge flocs</i>	17
2.3.2. <i>Flocculation mechanisms</i>	21
2.4. A set of relevant factors for the flocculation process.....	28
2.4.1. <i>Mixing intensity</i>	28
2.4.2. <i>Cations</i>	28
2.4.3. <i>Temperature</i>	29
2.4.4. <i>Dissolved Oxygen</i>	30
2.4.5. <i>Activated sludge concentration</i>	31
2.5. Conclusions.....	30
3. On-line quantification of floc morphological properties.....	33
3.1. Introduction.....	33
3.2. Activated sludge floc morphological properties: state of the art.....	34
3.2.1. <i>Size and size distribution</i>	34
3.2.2. <i>Fractal dimension</i>	38
3.3. Activated sludge floc morphological properties: measurement techniques.....	39
3.3.1. <i>Sizing techniques</i>	39

3.3.2. <i>Techniques used in this study for on-line measurement of floc size distribution and fractal dimension</i>	46
3.4. Influence of experimental conditions for on-line determination of floc size and size distribution.....	59
3.4.1. <i>Experimental methods and setups</i>	59
3.4.2. <i>Influence of mixing</i>	61
3.4.3. <i>Influence of sonication</i>	62
3.4.4. <i>Influence of dilution</i>	64
3.4.5. <i>Influence of the setup components</i>	65
3.4.6. <i>Conclusions</i>	67
3.5. From spherical particles to activated sludge distribution - simultaneous investigation by different techniques.....	67
3.5.1. <i>Materials and methods</i>	68
3.5.2. <i>Evaluation of devices dilution requirement concentration influence</i>	71
3.5.3. <i>Effect of particle shape on the particle size distribution</i>	73
3.5.4. <i>Influence of devices measurement principle on activated sludge floc size distribution</i>	77
3.6. Fractal dimension measurement by using on-line techniques.....	83
3.6.1. <i>Fractal dimension obtained by using MastersizerS device</i>	83
3.6.2. <i>Fractal dimension obtained by using TOT</i>	86
3.6.3. <i>Fractal dimension by using SHAPE</i>	86
3.6.4. <i>Fractal dimension obtained from IMAN</i>	87
3.6.5. <i>The dynamics in fractal dimension as recorded with MastersizerS</i>	88
3.7. Conclusions.....	89
4. Monitoring of the activated sludge properties in a Sequencing Batch Reactor.....	91
4.1. Introduction.....	91
4.2. Sludge stability evaluation.....	91
4.2.1. <i>Operation principle of the SBR technology</i>	92
4.2.2. <i>Monitoring the SBR activated sludge properties</i>	94
4.3. Construction and monitoring of a lab-scale SBR.....	96
4.3.1. <i>Description of the set-up</i>	96
4.3.2. <i>Influent characteristics</i>	99
4.3.3. <i>Description of the SBR cycle</i>	100
4.3.4. <i>SBR monitoring</i>	101

4.4. Evaluation of the SBR activated sludge stability.....	104
4.4.1. Long-term SBR monitoring	104
4.4.2. Short-term SBR monitoring.....	111
4.4.3. Conclusions.....	114
5. Methodology for experimental design and analysis.....	115
5.1. Introduction.....	115
5.2. Experimental layout.....	115
5.2.1. Experimental set-up.....	115
5.2.2. On-line control and data logging.....	117
5.2.3. Off-line measurements.....	115
5.3. Experimental design.....	121
5.3.1. Background.....	121
5.3.2. Time development of a measurement cycle.....	122
5.3.3. DOE considerations: working methodology and experimental matrix.....	124
5.4. Fundamentals of the response surface methodology (RSM).....	128
5.5. Conclusions.....	134
6. The influence of different physical and chemical parameters on the (de)flocculation dynamics.....	135
6.1. Introduction.....	135
6.2. Evaluation of the SBR's activated sludge properties during the experimental period...135	
6.2.1. Microbial community.....	136
6.2.2. Activated sludge structural properties.....	137
6.2.3. Conclusions.....	139
6.3. Quantification of the influence of different factors on the (de)flocculation dynamics...139	
6.3.1. The effect of average velocity gradient (G).....	139
6.3.2. Activated sludge concentration.....	146
6.3.3. Calcium concentration.....	147
6.3.4. Temperature.....	154
6.3.5. Dissolved oxygen concentration.....	157
6.3.6. Conclusions.....	158
7. Study of the influence of physical and chemical factors on the (de)flocculation process by using the DOE and RSM.....	161

7.1. Introduction.....	161
7.2. Floc size.....	162
7.2.1. $\Delta D[4,3]$	162
7.2.2. <i>Final D[4,3]_f</i>	168
7.2.3. <i>Conclusions</i>	170
7.3. Sludge volume index (SVI).....	170
7.3.1. ΔSVI	171
7.3.2. <i>Final SVI</i>	175
7.3.3. <i>Conclusions</i>	178
7.4. Zeta potential.....	178
7.4.1. $\Delta Zeta$	179
7.4.2. <i>Final zeta potential</i>	181
7.4.3. <i>Conclusions</i>	183
7.5. Turbidity.....	184
7.5.1. $\Delta Turb$	184
7.5.2. <i>Final turbidity</i>	186
7.5.3. <i>Conclusions</i>	188
7.6. Supernatant suspended solids concentration.....	189
7.6.1. ΔTSS	189
7.6.2. <i>Final TSS</i>	187
7.6.3. <i>Conclusions</i>	193
7.7. Conductivity.....	193
7.7.1. $\Delta Conductivity$	193
7.7.2. <i>Final conductivity</i>	196
7.7.3. <i>Conclusions</i>	197
7.8. pH.....	197
7.8.1. ΔpH	198
7.8.2. <i>Final pH</i>	201
7.8.3. <i>Conclusions</i>	202
7.9. Process optimisation by using RSM.....	202
7.9.1. <i>Seven response optimisation</i>	203
7.9.2. <i>Five response optimisation</i>	204
7.9.3. <i>Conclusions</i>	206
7.10. Conclusions.....	206

8. Conclusions and perspectives.....	209
8.1. Evaluating and obtaining stable sludge samples.....	210
8.1.1. <i>Further developments and recommendations</i>	210
8.2. A systematic approach for the on-line quantification of the flocculation dynamics.....	211
8.2.1. <i>Methodology for on-line measurement of the floc size distribution (FSD)</i>	211
8.2.2. <i>Factors selection and development of the DOE methodology</i>	212
8.2.3. <i>The experimental technique</i>	213
8.2.4. <i>Further developments and recommendations</i>	213
8.3. Response surface modelling and analysis of the influence of different physico-chemical factors on the (de)flocculation process.....	214
8.3.1. <i>The effect of individual factors on (de)flocculation dynamics</i>	214
8.3.2. <i>Modelling the interactive effect of the studied factors on (de)flocculation by using DOE and RSM</i>	216
8.4. General conclusions.....	219
Appendices.....	223
Appendix to Chapter 3	223
Appendix to Chapter 4	224
Appendix to Chapter 5.....	225
Appendix to Chapter 6.....	229
Appendix to Chapter 7.....	230
References.....	245
List of Abbreviations and symbols.....	261
Summary.....	265
Samenvatting.....	269
Curriculum Vitae.....	273

Chapter 1

Introduction

The increasing shortage of water in the world caused by the steady growth of the population and by the industrial and economical development raises serious concerns about the need for appropriate water management practices. Nowadays, large quantities of wastewater are produced from different human activities, leading to a growing awareness of the impact of sewage contamination on rivers and lakes.

The water bodies contamination could raise severe problems associated not only to the environmental pollution and aesthetic aspects but can also affect the population's health. Accordingly, a careful assessment of health, environmental effects and community concerns should govern the principles and the guidelines for a proper wastewater management and fix the targets for comprehensive research related to wastewater.

For a successful implementation of the sustainable development concept, the environment pollution is one of the major concerns. Consequently, an Integrated Waste Management program was recently launched (UNEP, 2000) and proposed that practices such as wastewater, stormwater and solid waste management should be linked for a proper management.

In nature, waste materials are produced by living organisms (plants, animals and people). Yet streams and rivers flowing through a pristine environment usually have an excellent water quality due to the natural processes that purify the naturally produced wastes. Discharge of wastewater and stormwater into an environment exceeding the natural purification capacity of that environment will result in the accumulation of organic materials, nitrogen, phosphorus or other pollutants that cannot be absorbed by the ecosystem. If nutrients, such as nitrogen and phosphorus are discharged to a river they are accumulated by the water body and finally lead to eutrophication (Figure 1.1). Hence, severe negative consequences for the ecosystem occur, making the quality of the aquatic life to decrease significantly and the water becoming impracticable for any human activity (fishing, swimming, etc...) and unsafe for the population's health.

Accordingly, sustainable wastewater management system is required. Its main principle consists in less discharge and more reuse of the pollutants. As a result, the problem of resource depletion and pollution of the river can be overcome by closing the material cycles. Figure 1.2 emphasises the need to treat industrial wastewaters containing toxic substances separately, and not to mix industrial wastewaters with domestic wastewater. In addition stormwater should be separately collected and treated and infiltrated locally.

Although sustainable development principles show the targets for a clean environment and clean production, still large quantities of wastewater are discharged in rivers and create serious pollution problems. Consequently, good technological practices and strict regulations are definitely required to overcome this problem.

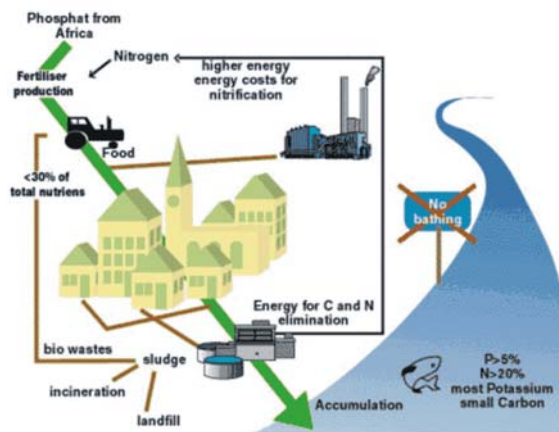


Figure 1.1 Unsustainable wastewater management exceeding the natural capacity of the receiving environment (UNEP, 2000)

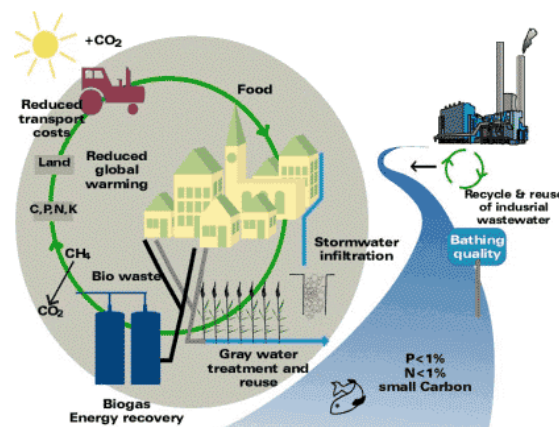


Figure 1.2 Sustainable wastewater management practice (UNEP, 2000)

In this context, the EU Water Framework Directive (WFD – directive 2000/60/EC) sets the common principles and the overall framework for actions regarding water protection measures in the European Union. One of the main objectives of the WFD related to wastewater treatment is to protect the environment against adverse effects of wastewater discharges. This goal should be achieved through application of several measures including:

- Ensuring that appropriate wastewater treatment plants exist for a proper treatment of the wastewater prior to discharge to the receiving waters.
- Establishing emission limit standards for concentration of specific substances in urban and industrial discharges.

The standards however have to adhere to *"the general rule that secondary (biological) treatment is required for all areas"*.

Among the biological treatment processes, the most widespread one is the activated sludge process. The main objectives of this process consist in the pollutant degradation by microorganisms, which grow as suspended flocs. Next, the flocs are separated from the effluent in a secondary clarifier. The process effectiveness is not only related to the pollutant degradation but also to the separation process. If the separation process is not efficient, a large

amount of the suspended solids is discharged in the receiving waters, which leads to an increase of the Chemical Oxygen Demand (COD) and nutrients (phosphorous and nitrogen).

It is estimated that at least 70% of the activated sludge treatment plants encounter settling problems at least once a year (Pujol and Canler, 1992). Even if the design, operating and monitoring procedures have been subjected to continuous development for process improvement, combating the occurrence of sludge settling problems is still a challenging task for researchers and plant operators. However, most of the separation problems are related to the formation, nature and the characteristics of the biological flocs. Accordingly, sludge bulking and a poor flocculation process are often mentioned as major causes affecting the efficiency of the solids-liquid separation and therefore the overall activated sludge process.

Although not completely solved yet, considerable research work has already been devoted to the sludge bulking phenomena. By contrast, less importance is given to the flocculation process, especially when new process developments are introduced. Because of this, it may happen that even the most sophisticated treatment plants may encounter problems due to poor flocculation properties.

In order to obtain a successful solid-liquid separation and to meet the latest regulations regarding effluent quality, an efficient flocculation process must prevail. Hence, improving knowledge on the flocculation step is an essential requirement for optimal biological wastewater treatment.

The activated sludge flocculation is a very complex process in which many factors interact and may have an influence. Since many of these influences are poorly understood, the characteristics related to the floc-formation are still difficult to be predicted and controlled. Any change of the environmental conditions is considered to affect the structural properties of the flocs. Nevertheless, the major difficulty consists in a lack of techniques capable to directly measure and quantify the parameters required to describe the flocculation mechanisms. As a consequence, modelling of the activated sludge processes often ignores the effect of changing conditions on floc structure and their implication on important phenomena such as sludge settling, dewatering and compaction.

In this thesis, the attention is focused on the development of a systematic approach which allows for a direct quantification of the activated sludge flocculation dynamics as it occurs under the variation of some physico-chemical factors. Furthermore, the obtained data are used to evaluate the joint effect of these factors by means of empirical models and to develop a more comprehensive flocculation model.

In the next section the objectives and the research approach of the thesis are presented. At the end of this chapter an outline of the thesis is presented as well .

1.1. Aim

The work described in this thesis was conducted within the framework of the "Sedimentation and Flocculation" (*SediFloc*) project. It is a joint project of BIOMATH (Department of Applied Mathematics, Biometrics and Process Control) and PAINT (Particle and Interfacial Technology Group), at the Faculty of Agricultural and Applied Biological Sciences (Ghent University). The objectives of this comprehensive project are to quantify and model the flocculation process as it occurs in secondary clarifiers by accounting for the influence of different physico-chemical parameters. Putting together insights concerning the flocculation dynamics with the subsequent modelling efforts may represent one step forward in the

understanding of the process and a more accurate prediction of the effluent quality of the treatment plant.

Starting from the on-line monitoring technique and Population Balance Modelling (PBM) approach introduced by Biggs (2000), this project aimed at improving the previous findings by accounting for the joint effects of more process parameters on the flocculation dynamics and therefore to gather knowledge which will allow to develop an advanced flocculation model based on the PBM approach. Ultimately, the PBM needs to be incorporated in a Computational Fluid Dynamics (CFD) framework, which represents a numerical model predicting the flow and the solids concentration field in the settling tank. Hence, the PBM in this CFD model is believed to improve the prediction of effluent quality.

In the framework of this project a conceptual CFD model focusing on the model structure and its phenomenological submodels such as rheology, solid settling and solid removal mechanism was already finalised and full-scale validated. The main achievements were presented in a dissertation thesis entitled:

Computational fluid dynamics of settling tanks: development of experiments and rheological, settling and scraper submodels (De Clercq, 2003)

The present work aims at developing a methodology for the on-line evaluation of the flocculation dynamics and at investigating the process response to the variation of different physico-chemical parameters.

In order to study the influence of these parameters independent of biological variations, the sludge properties need to be standardised. To this end, a pilot-scale Sequencing Batch Reactor (SBR) was selected and operated under as stable as possible environmental conditions. The sludge stability should be evaluated and an intensive monitoring of the stability in terms of settling properties, floc size and size distribution and microbial community has to be performed.

Then, this standardized sludge is to be applied to a five litres flocculator in which the (de)flocculation can be studied under imposed conditions. The process dynamics can be evaluated on-line by using specific sensors, while after each experiment a few of the relevant parameters on settling and clarification process should be measured.

To evaluate the process parameters in a systematic way a statistical experimental design is adopted. Finally, the joint effect of these parameters is to be investigated. To this end, Design of Experiment (DOE) and Response Surface Methodology (RSM) approaches can be used. The knowledge obtained from this systematic study is then to be used to explain the behaviour of a set of process characteristics.

The collected data and insights will be further used and applied for developing an advanced population balance model. This will be presented in a dissertation thesis, currently in preparation:

Modelling Physico-Chemical Influences on the Activated Sludge Flocculation Process: Population Balance Approach (Nopens, 2004).

To summarise, an overview of the SediFloc project in which the focus of this thesis is highlighted is schematically shown in Figure 1.3.

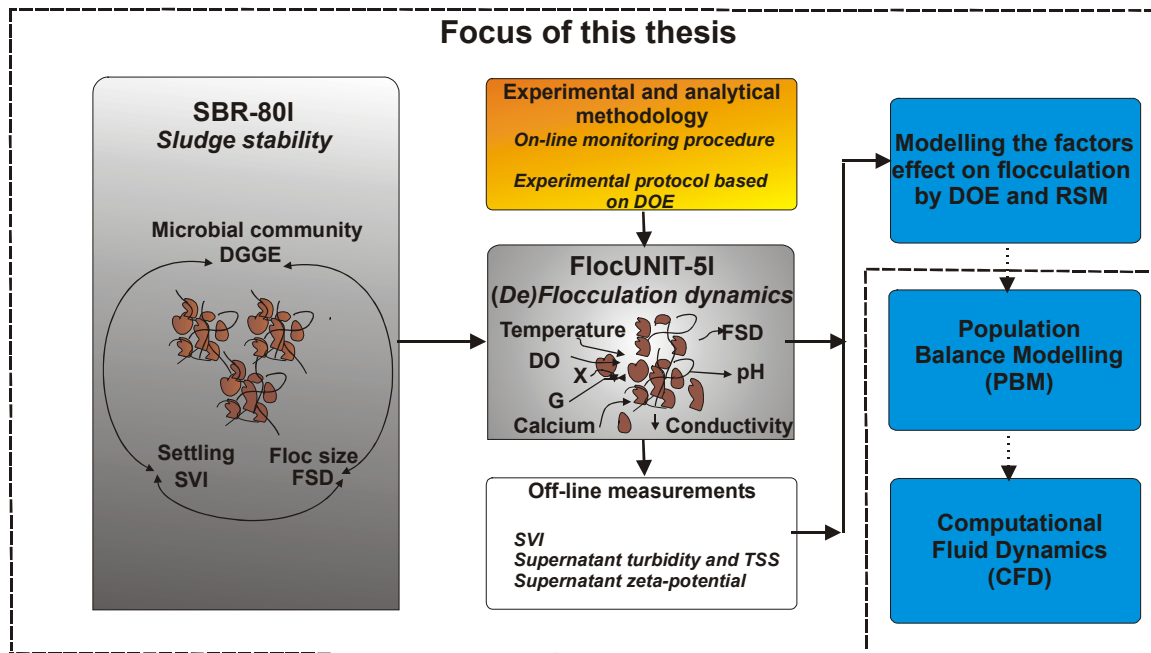


Figure 1.3 The focus of this thesis as part of the SediFloc project

(Abbreviations: **SBR** – Sequencing Batch Reactor, **DGGE** – Denaturing Gradient Gel Electrophoresis; **SVI** – Sludge Volume Index; **FSD** – Floc Size Distribution; **DO** – Dissolved Oxygen concentration; **X**– Sludge concentration; **G** – Shear rate; **TSS** – Total Suspended Solids Concentration; **DOE** – Design Of Experiment; **RSM** – Response Surface Methodology)

1.2. Research approach

In general, the activated sludge flocculation is described as a two stage process (Biggs, 2000). In the first stage, microcolonies are formed as a results of cationic bridges created by the polyvalent cations between the microorganisms and the extracellular polymers. The second stage facilitates the formation of larger flocs, which can be well separated from the treated water in the secondary clarifier.

In spite of its importance, little is known about how the process parameters affect the flocculation occurrence and its mechanisms. Accordingly, a direct evaluation of the flocs aggregation and breakage by means of measurement of their size and size distribution helps to improve the flocculation understanding and to develop a good modelling framework, as shown previously by Biggs, 2000.

To achieve the overall aim – *development and evaluation of a methodology for direct quantification and modelling of the activated sludge flocculation* – the thesis objectives are divided in three main parts as follows:

I. Stability of the analysed sludge sample

In order to be able to evaluate the flocculation and deflocculation dynamics, the initial characteristics of the activated sludge sample should be well defined and standardised. In this context the sludge needs to be obtained from an activated sludge process working under stable environmental conditions. To this end, a lab-scale Sequencing Batch Reactor (SBR) is operated and monitored such as to achieve stable sludge properties.

Consequently, the flocculation study is limited to a particular lab-scale sludge sample with specific and stable characteristics and biological composition. Moreover, since the emphasis of the SBR operation is put on obtaining stable sludge characteristics and properties, less attention is paid to optimal nutrient removal. The microbial populations existing in the floc matrix at the time of performing the experiments are monitored qualitatively by means of a molecular technique (Denaturing Gradient Gel Electrophoresis). However, their identification is beyond the scope of this study.

II. Development of an experimental protocol and analysis methodology for on-line quantification of the flocculation dynamics

The first step towards evaluating the flocculation dynamics is to set up a methodology that allows for the direct quantification of the relationship between the flocculation process and different operational parameters. Due to the fragile and complex structure of the activated sludge flocs, the development of the experimental procedure requires a special attention as it is necessary to avoid as much as possible the influences of the measurement procedure on the obtained results. Moreover, in view of the final scope, quantification of the flocculation dynamics using the on-line sensors represents a requirement that should be fulfilled as much as possible.

With this remark in mind, the main steps followed to develop the experimental methodology are:

- *Screening out the most important floc properties to be investigated and choosing the most suitable techniques and procedures to be used for their measurement.*
- *Developing an experimental set-up in which the flocculation experiments can be performed under controlled operating conditions.*
- *Elaborating on the experimental protocol based on the DOE theory, which allows the quantification of the joint effect of different considered factors on the activated sludge flocculation dynamics.*

The effect of five factors (average gradient velocity, calcium, temperature, dissolved oxygen, sludge concentration) on activated sludge dynamics is investigated in this thesis. Even if some other factors (wastewater composition, pH, ...) could interact and also have an influence on the flocculation process, the number of factors that can be studied is restricted due to the limitations imposed by experimental procedure. This mainly depends on the time in which relatively stable sludge samples characteristics are present.

To evaluate the flocculation dynamics the effect of the considered factors on a set of variables such as floc size, pH, conductivity as well as of variables related to the separation step (SVI, supernatant turbidity) is analysed.

III. Investigating the effect of several physico-chemical factors on the (de)flocculation process

The effect of each of the five factors on the floc size dynamics is investigated on-line. It is intended to estimate to which extent each of the considered factors affects the floc aggregation and breakage phenomena and to determine the most significant factors for the (de)flocculation process.

Empirical models built using the DOE/RSM approach are used to evaluate the effect of the considered five factors on a set of process responses such as mass mean diameter of the flocs, supernatant characteristics (suspended solids concentration, zeta potential, turbidity), pH, conductivity, sludge settling characteristics (Sludge Volume Index).

The evaluation is restricted to a relatively short time scale evaluation (up to 6 hours) of the effects produced by the imposed factors on the floc size and size distributions. Also, the empirical models constructed are tied to the particular type of sludge used. However, the methodology is rather general.

1.3. Outline of the thesis

The PhD thesis is organised as follows.

- **Chapter 2** starts with a literature study of the wastewater treatment and activated sludge process. The solid–liquid separation step and the importance and characteristics of the flocculation process are highlighted.
- **Chapter 3** focuses on the evaluation of the morphological properties of the activated sludge flocs. Following a comprehensive review of the available sizing devices, the most suitable techniques for on-line measurement of the flocs' morphological properties are selected and their performances are critically assessed.
- **Chapter 4** describes the monitoring procedure that was used for evaluating the sludge stability in a pilot-plant SBR activated sludge treatment system. To this end, the sludge settling properties, floc size and size distributions and microbial community dynamics are investigated.
- **Chapter 5** deals with the elaboration of the experimental technique and protocol for on-line quantification of the flocculation dynamics. The influence of five relevant factors (temperature, shear stress, dissolved oxygen concentration, sludge concentration and calcium concentration) on a set of selected process responses (floc size, SVI, supernatant turbidity and suspended solids concentration, zeta potential, pH, conductivity) is evaluated by using a DOE approach. The RSM methodology is subsequently used for data analysis and an optimisation study is carried out as well.
- **Chapter 6** presents the results of the evaluation of the sludge sample stability during the experimental period by using the developed monitoring procedure described in Chapter 4. Next, the effect of each considered factor on the floc size and size distribution dynamics is presented and discussed.
- **Chapter 7** discusses the joint effect of all five factors on the considered responses. The responses were evaluated by using quadratic polynomial models in normalised factor space. A statistical model analysis and model identification is used for the analysis of each response. Finally, a process optimisation is performed and the results are subsequently discussed.
- **Chapter 8** summarises the general conclusions of the thesis. In the last part, a general discussion and the perspectives for the continuation of the present work are outlined.

Literature review

2.1. Wastewater treatment

Wastewater treatment is a process of crucial importance for several reasons related to the social and economic aspect, of human life, such as public health, environmental protection, aesthetics. Irrespective of the source (domestic, industrial or storm water) the wastewater must be collected and treated before returning it into natural water cycle.

Depending on the source, a complex mixture of compounds (dissolved or particulate) may be found in the wastewater composition. Thus, large quantities of organic matter, inorganic particulates as well as numerous pathogenic and disease causing microorganisms are often contained in the wastewaters. The discharge of these pollutants into the receiving waters can have severe negative consequences for the ecosystem, starting from eutrophication of the waters due to the excessive growth of vegetation and malodorous gases emissions due to the decomposition of the organic matter. These cause a decrease of the aquatic life, make the waters unsuitable for other activities and become a very dangerous source of diseases.

The role of the wastewater treatment is to reduce these contaminants to acceptably low concentrations, in order to not create any harmful effect to the receiver waters. The contaminants present in water may be removed by following a series of steps, which practically involved physical, chemical and biological unit processes (Tchobanoglous et al, 2003), which may be accordingly classified as shown in Table 2.1

Table 2.1 Levels of wastewater treatment (Tchobanoglous et al, 2003)

Treatment level	Description
<i>Preliminary</i>	Removal of the gross solids from wastewater such as rags, sticks, floatables, grit and grease which may cause maintenance or operational problems with the treatment operations, processes and ancillary systems.
<i>Primary</i>	Removal of a portion of the suspended solids and organic matter from the wastewater.
<i>Advanced Primary</i>	Enhanced removal of suspended solids and organic matter from wastewater. Typically realised by chemical addition or filtration.
<i>Secondary</i>	Removal of biodegradable organic matter (in solution or suspension) and suspended solids. Disinfection is included usually at this level.
<i>Secondary with nutrient removal</i>	Removal of biodegradable organics, suspended solids and nutrients (nitrogen and/or phosphorous)
<i>Tertiary</i>	Removal of residual suspended solids, usually by granular medium filtration or microscreens. Disinfection is also part of tertiary treatment and nutrient removal is often included as well.
<i>Advanced</i>	Removal of dissolved and suspended materials remaining after biological treatment when various water reuse applications are required.

The treatment and disposal of the sludge produced during the wastewater treatment levels is achieved in during sludge processing step. Methods such as thickening, conditioning and dewatering are used to remove the moisture from the sludge while digestion, composting and incineration are used to treat or stabilize the organic material in the sludge. Among the processes involved in the wastewater treatment, sludge processing represents the most complex and difficult part.

Different plant operating scenarios and technical solutions are available for each treatment unit involved in the wastewater treatment processes. However, the necessity of an optimal treatment process represents a continuous challenge for the researchers due to the increasingly stringent standards regarding effluent quality and sludge processing. Moreover, minimisation or restriction of using some chemicals, as well as the necessity to reduce the energy consumption, direct the attention to the biological treatment processes. With a proper analysis and control, almost all wastewaters can be treated biologically (Tchobanoglous and Burton, 1991). Therefore, it is essential that efforts are concentrated on understanding the characteristics of the very complex biological processes, which occur in the wastewater treatment, in order to ensure optimal process operation.

2.1.1. The activated sludge process

The activated sludge process represents the most widespread biological wastewater treatment method. In its conventional form (Figure 2.1), this process is based on the aeration of wastewaters with mixed bacterial cultures, which carry out the biological conversion of the contaminants and form a flocculated biomass known as flocs. In the next step, the treated water is separated from the biomass to produce a clear effluent. Usually, the separation of the biomass from the treated wastewater is performed by settling (Ganczarzyk, 1983). Part of the settled biomass is then wasted, and the remainder is returned to the system. The reason for returning the sludge is to maintain a concentration of activated sludge in the aeration tank sufficient for the desired degree of treatment. The excess activated sludge should be wasted to maintain the desired solids concentration in the aeration tank.

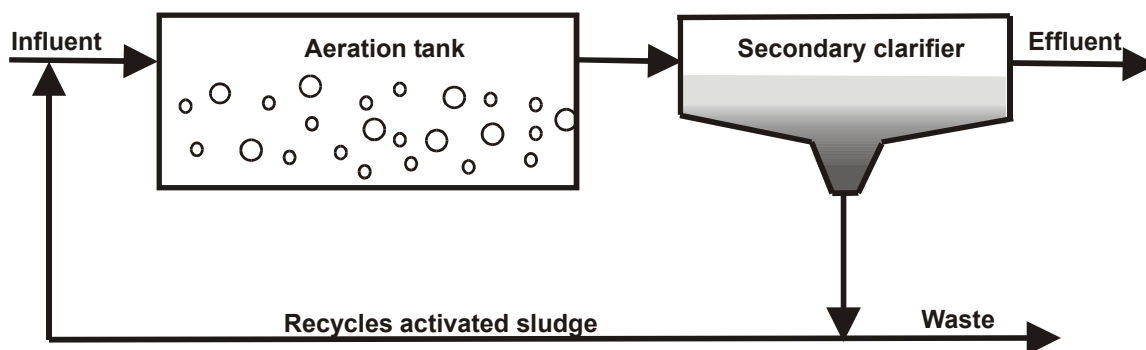


Figure 2.1 Basic concept of the activated sludge process

It is often difficult to predict the response of this system to the environment since the microbial population may change its composition in a dynamic way depending on the different process conditions (Eikelboom, 2000). The wastewater composition, the oxygen concentration, pH and temperature are among the most important process parameters to which the microorganisms were found to be very sensitive.

Initially the aim of the activated sludge process was to reduce the biodegradable organic load in the wastewaters. With the recent developments, biological nitrogen and phosphorous

removal can be achieved as well, by expanding the conventional process with anoxic and anaerobic zones. As a result, the activated sludge process has been subjected to many modifications and different process configurations are available nowadays, which often lead to significant improvements of the removal capacities.

However, due to the process complexity a series of knowledge gaps have been identified and a large variety of tools and expertise is required to improve the process. Respirometry, new chemical analyses, microsensors, gene-based identification, microbial physiology techniques and integrated modelling and simulations were the novel tools identified by Keller et al. (2002) which may help in the continuing process development. Moreover, the effectiveness of the activated sludge process is related to the ability of the sludge flocs to settle and compact. A major source of the problems, which lead to a poor activated sludge effluent quality, result from the inability of the secondary clarifier to efficiently remove the activated sludge biomass from the treated wastewater (Jenkins et al., 1993).

2.2. Solid-liquid separation in secondary clarifiers

The secondary clarifier is often considered as the most critical step of the wastewater treatment plant operation (Grijpspeerdt, 1996) and therefore considerable research work is directed to this step.

Three important functions have to be satisfied by the secondary clarifier:

- Produce a clear effluent achieved by the separation of activated sludge floc from the treated water through settling.
- Allow sludge thickening, which is requested for the sludge to be returned to the aeration basin for maintaining its efficient operation. According to Verstraete and VanVaerenbergh (1986) recycle sludge should be at least three times more concentrated in comparison with the mixed liquor.
- The clarifier should have a storage capacity in order to be able to cope with hydraulic disturbances.

Failing to achieve one of these functions leads to severe malfunctions of the process, characterised especially by a poor effluent quality and an excessive loss of solids. The functions of the secondary clarifier are however dependent of those of the aeration tank, inducing a very dynamic activated sludge process. Hence, various physical, chemical and biological factors interact and affect the settling properties and solids removal efficiency of the secondary clarifier (De Clercq, 2003).

2.2.1. Measurement of the activated sludge settleability in secondary clarifier

To monitor the solid-liquid separation of activated sludge routine methods aiming to quantify the settling rate of the sludge are used. Accordingly, the Sludge Volume Index (SVI) and settling velocity measurements are among the most used tests for sludge settleability characteristics, while the non-settleable solids are usually evaluated by measuring their concentrations.

2.2.1.1. SVI

The SVI is a rough measure of the settling properties in everyday operation of the wastewater treatment plant. It may be defined as the volume occupied by 1 g of sludge after 30 minutes of settling in a cylinder (APHA, 1992). It gives an indication of how far the thickening process

has reached after a standard time of 30 minutes. As a result, it is possible that two kinds of sludge with the same SVI have different settling properties (Dick and Vesilind, 1969). This suggests that it is meaningless to compare the SVI's from different WWTP plants.

Due to its simplicity and easy measurement, the SVI was widely adopted (Wahlberg and Keinath, 1988) and it is still used as a quantitative measure of the settling properties of the sludge (Bye and Dold, 1998).

However, many criticisms are addressed to the SVI-test. Dick and Vesilind (1969) enumerated a number of reasons for which using the SVI may be inappropriate. The most important ones were the difficulties related to a correct prediction of the dependence on sludge concentration and the influence of the wall effects on the measurements.

Therefore, modifications of the standard SVI are often suggested in order to minimize the mentioned drawbacks of the SVI –test. The most recommended is the diluted SVI (DSVI) (Lee et al., 1983). Other reported SVI modifications consist in stirred specific volume index (SSVI) and sludge quality index (SQI) (Hultman et al., 1991; Thompson and Forster, 2003).

The SVI-type measurements are often used as alternative methods for the determination of the zone settling velocity (ZSV) (Giokas et al., 2003) which is more laborious but also more representative for describing the settling process in the secondary clarifier (Ozinsky and Ekama, 1995).

2.2.1.2. Settling velocity

The settling velocity is a useful parameter for evaluating the sludge settling properties, as its measurement leads to an evaluation of the secondary clarifier loading capacity.

During the sedimentation process, four types of settling phenomena may occur (discrete, flocculant, hindered and compression), which are mostly depending of the solids concentration and the interaction between the particles (Tchobanoglous and Burton, 1991).

Discrete settling refers to the sedimentation that happens at low solid concentrations. It occurs especially in the upper part of the secondary clarifier. Particles settle as individual entities and no significant interactions between the particles take place. Therefore, the discrete settling velocity depends mostly of the individual particle characteristics such as particle size, porosity and density (Li and Ganczarczyk, 1987).

Flocculant settling occurs as well for rather diluted suspension of particles. By contrast with the discrete settling, the particles flocculate during the sedimentation, increase in mass and settle faster. Patry and Takács (1992) showed that the average settling velocity of particles in the flocculant settling zone of the secondary clarifier is correlated with the suspended solids concentrations. In order to evaluate the settling characteristics of flocculant particles, standard batch column settling tests have to be performed (Zanoni and Blomquist, 1975).

Hindered settling refers to a suspension of intermediate concentration in which interparticle forces are sufficient to allow the particles to hinder each other in their movements. Therefore, the particles in contact tend to settle as a zone and form a relatively clear layer of water above the particles in the settling region. The hindered settling velocity is independent of the particle size and the settling velocity decreases as the solids concentration increases (De Clercq, 2003).

As settling continues, a compressed layer of particles forms at the bottom of the clarifiers. The particles form a structure in this region and further settling can occur only by the compression of this structure. For a better sludge compaction, stirring is often used to break-up the flocs and therefore to diminish the water channels present in the formed structure. Accordingly,

Dick and Ewing (1967) showed that mixing produced a better settling in the hindered settling region as well.

For high sludge concentrations all four settling phenomena may occur at the same time, as shown in Figure 2.2 for a concentrated suspension of activated sludge, which settles in a cylinder.

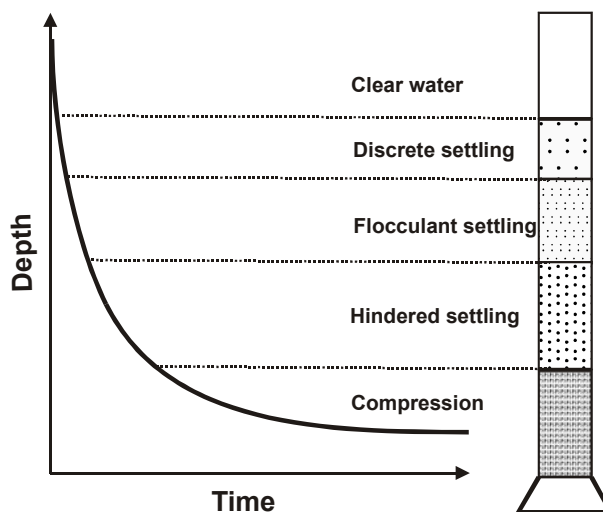


Figure 2.2 Settling regions for activated sludge (from Tchobanoglous and Burton, 1991)

By measuring the settling velocity of different sludge concentrations, the settling properties of the sludge may be evaluated, usually described by the solid-flux theory (Dick and Ewing, 1967). Nowadays, the modelling of the secondary clarifiers is in general based on the solid-flux theory (Takács et al., 1991), although more complex models have been introduced for this purpose (Lakehal et al., 1999; De Clercq, 2003).

2.2.1.3. Non-settleable solids evaluation

To evaluate the effectiveness of the settling process, the effluent quality is highly important. After settling, a part of the solids, which consists mainly in small flocs and free bacteria, may not settle and therefore remains in the supernatant.

The amount of suspended solids in the effluent should be carefully controlled and evaluated. Failure to achieve the required suspended solids (SS) removal as a result of poor clarification, may result in a nonfulfilment of the effluent quality standards, even though the secondary clarifier might be functioning perfectly as a thickener and the aerobic tank might be producing the required biological treatment efficiency. Therefore, Fuchs and Staudinger (1999) showed that activated sludge with similar sedimentation curves can produce extremely different effluent quality.

The most used method for measurement of the suspended solids concentration is the turbidity (Baudu et al., 1995; Mikkelsen et al. 1996), often called residual turbidity after settling. Wahlberg et al. (1994) monitored the clarification process by using turbidity measurements and found that a calibration of the suspended solids in the supernatant with turbidity can be performed.

When the sludge flocs settle, small flocs that can not settle by themselves are trapped in the floc matrix. Therefore, it may be considered that the residual turbidity can be affected by the activated sludge floc morphology (Wilén, 1999).

2.2.1.4. Automatic methods for activated sludge settling evaluation

The methods used for evaluating the sludge settling consist mainly in batch tests, which may be performed with a relatively low frequency. It is therefore difficult to evaluate the settling process in a dynamic way. Consequently, automated and on-line sensors were recently developed, which allow a fast detection of the short-term changes in activated sludge settleability. The most popular one refers to the localization of the sludge blanket. Vanrolleghem and Lee (2003) refer to three measurements techniques, which have been used for this purpose, namely ultrasonic absorption, ultrasonic scanning and turbidity sensors. Among these methods, the turbidity sensors on a rotating drum are the most used. The method consists in lowering a turbidity sensor until the sludge blanket is reached. As a result, the sludge blanket depth is determined from the distance until the sludge blanket. Another possibility consists in locating three turbidity sensors at fixed but different depths in the clarifiers and evaluating the presence or absence of the sludge blanket at these positions.

The measurement of the sludge blanket, coupled with an automatic estimation of the sludge concentration, is used to determine sludge sedimentation curves, settling velocity and the sludge volume index expressed as SVI, SSVI or DSVI (Vanrolleghem et al., 1996; Vanderhasselt and Vanrolleghem, 2000). Alternatively, Rasmusen and Larsen (1997) detected the short-term changes of the sludge stability by measuring the dynamic variation of the settling velocity in a continuous settling column.

It may therefore be concluded that the development of automatic sensors and systems for monitoring the processes that take place in the secondary clarifier are useful tools, which provide an early indication of the settling problems and allow to take appropriate actions in time. However, these systems required costly investments and therefore are not easily accessible to any treatment plant (Daigger et al., 1992).

2.2.2. Separation problems in secondary clarifiers

Among all possible separation causes in the secondary clarifiers six are identified (Table 2.2) and largely accepted in literature (EPA, 1987; Jenkins et al., 1993; Wanner, 1994) as major sedimentation problems.

Table 2.2. Solids separation problems. Classification of the descriptions and effects

Type of problem	Description of the problem	Effect of the problem
Dispersed growth	No floc formation	Turbid effluent, no zone settling
Pinpoint flocs	Small and weak floc formation	Low SVI and highly turbid effluent
Filamentous bulking	Abundance of filamentous bacteria	High SVI and very clear effluent. Low return and waste activated sludge solids concentration
Rising Sludge	Release of nitrogen gas due to denitrification	Activated sludge scum is formed on the surface of the secondary clarifier
Viscous (non-filamentous) bulking	Overproduction of exocellular slime	Reduce settling and compaction rate. Sometimes viscous foam is formed.
Foaming and scumming	Abundance of <i>Nocardia</i> spp. or nondegradable surfactants	Large amount of solids float to the surface of the clarifier due to the foam production

Many operational process characteristics may be responsible for the occurrence of the above mentioned solids separations problems. De Clercq (2003) classified these parameters as function of their nature (biological, physico-chemical and hydraulic) and also suggested that a clear distinction between their influences is difficult to formulate.

In this context, many studies have been performed to identify and isolate the major causes of solid-liquid separation problems in secondary clarifiers, although these remain relatively poorly understood.

In connection with the complexity of the settling problems, Parker et al. (2000) proposed a Structured Diagnostic Approach (SDA). Accordingly, a DSS/TSS test was used to explain the problems, which may occur due to the flocculation and/or hydraulic effects. Consisting in a series of three measurements (Effluent Suspended Solids –ESS; Dispersed Suspended Solids – DSS and Flocculated Suspended Solids – FSS) the test proved to be able to locate and to investigate the clarification step failures. When high ESS concentrations were determined four possible causes may be identified as summarised in Table 2.3.

Table 2.3 Causes of clarifications problems as predicted by DSS/TSS test (Parker et al., 2000)

DSS	TSS	Problem
high	high	Flocculation not adequate due to a biology problem
high	low	Flocculation not adequate, but it can be corrected (physical flocculation)
medium	low	Combined hydraulic and flocculation problem
low	high	Impossible
low	low	Hydraulic problem

However, most of these problems are related to the formation and structural characteristics of the activated sludge flocs. Accordingly, in relation with the settling properties Sezgin et al. (1978) define an "ideal" floc as being formed by floc-forming bacteria and a moderate number of filamentous bacteria. It was shown that for this case the filaments form a backbone onto which the floc-forming bacteria attach. Such "ideal" floc is schematically shown in Figure 2.3 as compared with the other two extreme cases. One possibility is that the activated sludge contains only floc-forming bacteria. In this case pinpoint or dispersed flocs are often formed, which settle slowly. Consequently, a poor clarification process occurs, characterised by a turbid effluent (Jenkins et al., 1993) and a decrease of sludge dewaterability (Mikkelsen et al., 1996; Kjellerup et al., 2001). When an abundant growth of filamentous bacteria occurs, again the sludge ability to settle and compact are significantly affected and less efficient.

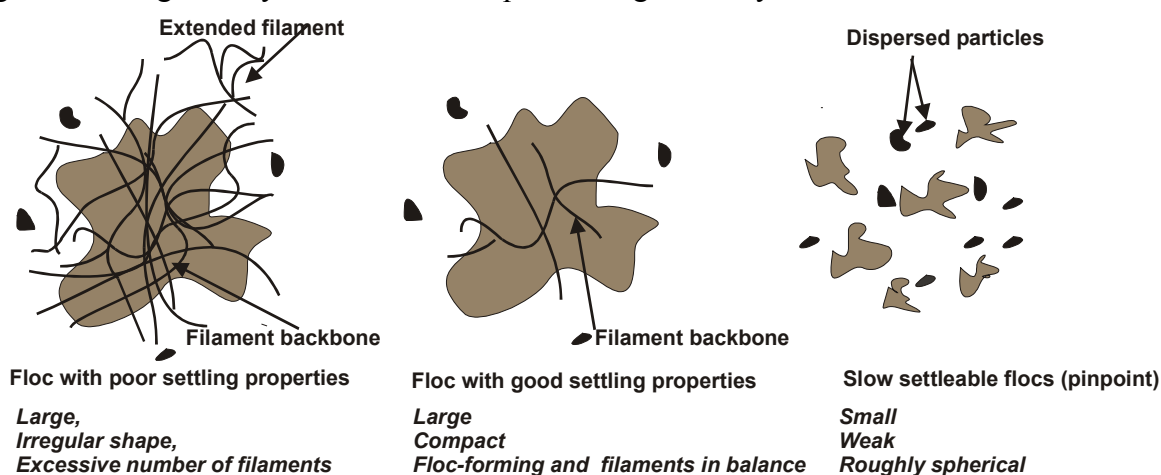


Figure 2.3 Activated sludge floc types which have an influence in solid-liquid separation on secondary clarifiers

Bulking sludge

Among the settling problems occurring in secondary clarifiers, sludge bulking is the most complex. In general, bulking sludge is due to an excessive growth of filamentous bacteria.

The term bulking sludge is sometimes also used for non-filamentous sludge with poor settling properties. This phenomenon is commonly known as Zoogloea bulking sludge and is caused especially by the strong binding of water by the flocs and the presence of the zoogloal microorganisms. Zoogloal microorganisms form finger-like colonies that excrete EPS and create large and slimy flocs (Novák, 1993). An excessive amount of such microorganisms leads to very poor settling properties and may cause foaming and scumming as well (Novák, 1993, Peng et al., 2003).

However, the problems arising from filamentous sludge grabbed the attention of numerous studies especially due to their complexity and frequently reported occurrence. According to Eikelboom (2000), filamentous sludge bulking phenomena were reported at more than 50% of all WWTP characterised by very high SVI values (400-600 mg/l). Nowadays, due to the activated sludge process stability improvements, bulking sludge occurs rarely, especially in the winter, but the SVI remains usually lower (250-300 mg/l).

To characterise the bulking sludge phenomena it is important to correctly identify the filamentous bacteria involved. However, this is usually not an easy task since many types of filaments are still not identified. The most often used technique is microscopical evaluation, which allows to examine the types, abundance and sometimes to identify the filamentous species present in the activated sludge structure. The obtained information is combined with the process parameters and performance in order to identify and isolate the possible causes of sludge bulking. Accordingly, fast and easy microscopical methods used for quantification of the filaments were proposed by Jenkins (1993) and Eikelboom (2000). These methods are known as 'subjective scoring of the filament abundance' and 'filament index' respectively.

The recent developments of image analysis techniques made it possible to faster evaluate the sludge bulking occurrence (Grijspeerdt, 1997). An automatic image analysis technique was developed by Cenens et al. (2002) for measurement of the floc and filamentous concentrations in the activated sludge while Dagot et al. (2001) combined an automated image analysis technique with measurements of sludge rheological properties for evaluating the filamentous bacteria settleability.

The advanced molecular techniques are becoming also more and more used in analysing the bulking process. In a review, Martins et al. (2004) suggested that the recently developed molecular methods such as DGGE and FISH, as well as the automatic molecular techniques like microarray/DNA chips and flow cytometry in combination with automated image analysis systems represent promising methods for more accurate quantification of the sludge bulking phenomena.

The most severe bulking problems are reported to be caused by *Microthrix parvicella* (Eikelboom et al., 1998). A classification of the filamentous bacteria as function of the settling problems encountered is presented by Warner (1994) while Martins et al. (2004) classified the filamentous bacteria in four groups, depending on their relationships with operational parameters. However, causes favouring the growth and proliferation of filamentous bacteria in the activated sludge process are numerous and often contradictory when a classification is performed (Séka, 2002). Jenkins (1992) divided the factors responsible for bulking formation into general and specific ones. The general factors are sludge age, aeration basin configuration and secondary clarifier design. The most important and frequently mentioned specific factors are low dissolved oxygen concentration, nutrients concentration, pH, low temperature, nature and biodegradability of the organic substances in the wastewater.

The remediation of sludge bulking often proceeds by addition of the biocides; ballasting agents or coagulating and flocculating agents directly to the sludge (Jenkins et al., 1993). Séka

(2002) proposed a multi-component additive consisting in a combination of three agents listed before. The superiority of this multi-component additive to the traditional methods was proven by a fast improvement of the sludge settling properties and a destructive effect of the filamentous bacteria.

However, sludge bulking is still far from being a solved problem for the activated sludge processes and the causes of the proliferation of filamentous microorganisms are still not very well identified and controlled.

2.3. Activated sludge flocculation process

The activated sludge flocculation is a very complex process, which involves physical, chemical and biological phenomena. Large flocs formation, which settle rapidly and incorporate the discrete particles that typically would not settle alone represent the ideal case for an effective clarification process.

The flocs can be regarded as individual microsystems with particular and interactive physical, chemical and biological functions or behaviours operating within the floc matrix. A continuous interaction between the flocs and their surroundings provides the energy, nutrients and chemicals required for biological growth, chemical reactions and morphological developments and regulate the water quality (Droppo et al., 1997).

2.3.1. Composition of activated sludge flocs

Activated sludge flocs contain a mixture (Figure 2.4) of different microorganisms, dead cells, organic and inorganic matters. Large amounts of extracellular polymeric substances (EPS) are present as well within the activated sludge floc structure. The EPS surrounds the microbial cells (Li and Ganczarzyk, 1990) and play a role in binding the floc components together (Snidaro et al., 1997).

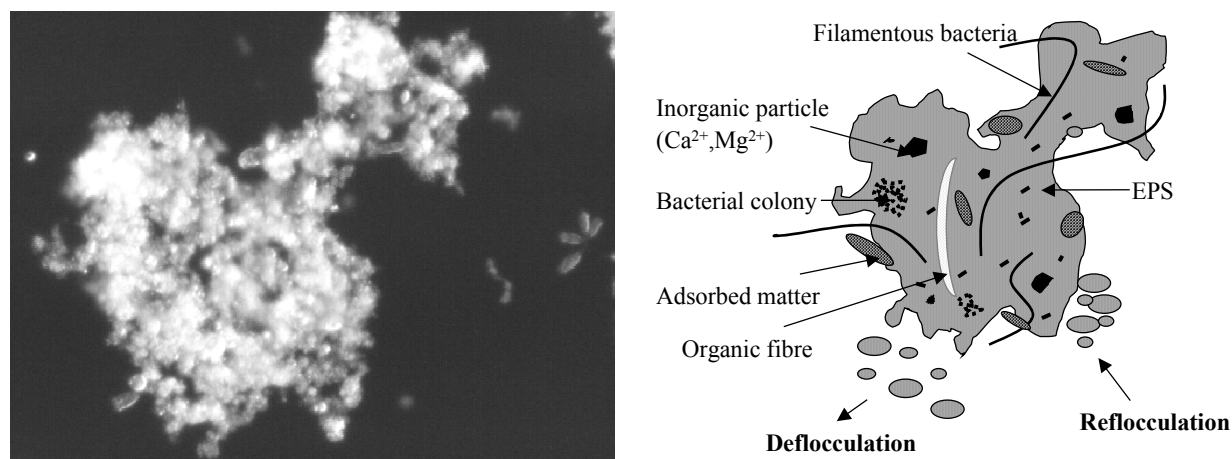


Figure 2.4. Image of an activated sludge floc (left) and its composition (right)

2.3.1.1. Microorganisms

The microorganisms present in the flocs are in a wide variety of bacteria, fungi, protozoa and metazoa (Jenkins et al., 1993). The most predominant and active are the heterotrophic bacteria, which use the organic material as a source of carbon and energy. From a flocculation point of view the microorganisms can also be classified as floc-forming and filamentous microorganisms.

Traditionally, *Zoogloea ramigera* was considered as a single floc-forming bacteria due to its flocculent growth habit (Ganczarczyk, 1983). Nowadays, many other bacteria are identified to behave as floc-forming microorganisms. Novel molecular techniques allowed to better isolate the floc-forming organisms, in order to proceed with their identification. Thomsen et al. (2004) showed that the microorganisms belonging to the *Betaproteobacteria* group exhibited very strong floc-forming properties. Schmid et al. (2003) related the occurrence of poor settling properties in different wastewater treatment plants to the presence of floc-forming bacteria. It was observed that the enrichment of settling problems corresponded to a decrease of *Betaproteobacteria* from about 62% to 40% and *Alphaproteobacteria* from about 15% to 7% in one plant, while in another the abundance of *Alphaproteobacteria* dropped from 35% to 10%. However, the knowledge related to the most dominant floc-forming bacteria is still limited and many bacteria still need to be identified.

Eikelboom (2000) classified the most commonly found filamentous microorganisms in the activated sludge as function of their impact on the sludge settling properties (SVI), as shown in Table 2.4.

Table 2.4. Effect of filamentous microorganisms on sludge settling properties (SVI) (adapted from Eikelboom, 2000).

Filamentous microorganisms	Effect on SVI	Characteristics
<i>S. natans</i>	High	Protrude from the flocs or are mainly present in the water phase between the flocs. Prevent the floc formation
<i>Thiothrix</i>	High	
Type 021N	High	
Type 0803/0914	Medium	
<i>Actinomyces</i>	Medium	May form open structured flocs, which settle slowly and compact poorly.
<i>M.parvicella</i>	High	
Type 0092/1701	Medium	
Type 1863	Low	Practically these organisms never cause bulking sludge. They form flexible tiny filaments or grow as flocs.
<i>N.limicola</i>	Low	

To explain the selection between the floc-forming and filamentous microorganisms the kinetic selection theory introduced by Chudoba et al. (1973 a,b,c) is used most. It states that the growth of filaments and floc formers follows a Monod kinetics under assumption of different kinetic constants K_s (half – saturation constant, g/l) and μ_{max} (maximum growth rate, 1/h). According to this theory, filaments have a lower K_s and higher μ_{max} at lower substrate concentration. By contrast, the floc-forming microorganisms have high K_s and μ_{max} for soluble substances at higher substrate concentrations. Moreover, the affinity of filaments for nutrients and oxygen is higher than that of the floc-forming. Despite the theory popularity, it was recently shown that other factors contribute to the selection process as well. Accordingly, Cenens et al. (2000) combined the filamentous backbone theory with the kinetic selection theory to account for the fraction of filaments incorporated in the floc as backbone.

However the theory based on growth kinetics proposed by Chudoba et al. (1973, a,b,c) is not the only one used to explain the competition between floc-forming and filamentous bacteria. A review of the theories which may explain this competition, is given by Martins et al. (2004).

Thus, storage and regeneration phenomena are considered as significant for the description of metabolic processes that occur in bulking and non-bulking systems (Martins et al., 2003). According to these phenomena the filamentous bacteria are assumed to have less capacity to accumulate carbon reserves as compared with the floc-forming microorganisms which store the substrate under high substrate concentration. However, it was shown that filamentous

microorganisms can have similar or even higher storage capacity as compared with the floc-forming microorganisms and therefore the advantage of the floc-forming bacteria to store the substrate can not be considered to be a general rule.

2.3.1.2. Organic and inorganic particulate matter

In the floc structure, a heterogeneous mixture of non-biodegraded organic matter or colloidal particles are present. These consist mainly in cell walls, different minerals, animal tissues and plant residues (Zartarian et al., 1994). An activated sludge floc may contain approximately 30-40% inorganic matter and 60-70% organic matter (Wilén, 1999). These particles are mostly transported with the influent and encapsulated in the floc structure. The inorganic particles in general possess a larger refractive index than the other floc materials (Eikelboom, 2000) and therefore their amount may influence the floc properties measurements performed by using techniques based on light diffraction.

Sometimes sludge ballasting by addition of mineral materials is used to improve the sludge settleability and filterability (Vanderhasselt et al., 1999). Piirtola et al. (1999) showed that the addition of mineral materials, which contain a large amount of divalent cations (Ca/Mg), such as clinoptilolite, talc and montmorillonite, creates denser flocs, which settle better. An important role in sludge ballasting is played by the cations, which form flocs due to the cation bridging phenomena occurring between the negatively charged minerals and activated sludge particles. Due to their largely recognised importance, the cations effect is discussed next separately, below.

2.3.1.3. Cations

There is no consensus on the role of monovalent cations, especially Na and K, on flocculation. Novak et al. (1998) and Murthy and Novak (2001) showed that an excess of monovalent cations or a replacement of divalent cations with monovalent cations promote a release of the biopolymers causing deflocculation. Therefore, a deterioration of the settling properties and sludge characteristics occurred (Higgins and Novak, 1997b). By contrast, Zita and Hermansson (1994) found that the monovalent cations enhanced flocculation. In agreement with this, Cousin and Ganczarzyk (1998) showed that an increase of the Na⁺ ions concentration leads to an improvement of the floc structural properties characterised by larger floc size and an improved floc porosity.

It was however, generally accepted that divalent cations facilitate flocculation due to the formation of cation bridging phenomena (Cousin and Ganczarzyk, 1999; Sobek and Higgins, 2002). By increasing the divalent cations concentration, particularly Ca²⁺ and Mg²⁺, an improvement of the settling properties and an increasing floc strength was observed. Among the divalent cations, calcium is accepted as the most common and significant factor responsible for floc formation (Eriksson and Alm, 1991; Keiding and Nielsen, 1997; Higgins and Novak, 1997c). Bruus et al. (1992) showed that removal of Ca²⁺ and Mg²⁺ ions from the floc structure leads to a deterioration of the floc properties.

When both monovalent and divalent cations are present in the system their ratio is highly important in determining their effect on flocculation. Therefore, Higgins and Novak (1997b) showed that when the sum of the monovalent cation concentration (Na⁺; NH₄⁺ and K⁺) divided by the sum of the divalent cation concentrations (Ca²⁺ and Mg²⁺) was higher than 2 the floc properties deteriorated.

Some other cations were identified to play a role in flocculation as well. Bruus et al. (1992) observed that a replacement of Ca²⁺ with Cu²⁺ leads to a more stable floc structure. Stasinakis

et al. (2003) showed that the addition of Cr^{6+} caused an effluent quality deterioration which was mainly explained by the appearance of pin-point flocs and free dispersed bacteria.

Nielsen and Keiding (1998) showed that iron ions and especially Fe^{3+} create very strong bonds within the flocs and therefore, their replacement caused a higher deflocculation effect as compared with Ca^{2+} . However, Wilén (1999) showed that the chemical oxidation of Fe^{2+} which was formed during the anaerobic conditions to Fe^{3+} has less important effects on sludge reflocculation as compared with the aerobic microbial activity itself.

2.3.1.4. Extracellular polymeric substances

Besides microorganisms and water the EPS are the third major component of the flocs (Li and Ganczarczyk, 1990) and represent the most important parameter with respect to the sludge structure (Mikkelsen and Keiding, 2002). It was found that the EPS have the property to keep the floc together in a three-dimensional matrix (Rudd et al., 1983), which is mainly produced by binding with bivalent cations (Higgins and Novak, 1997c) and hydrophobic interactions (Urbain et al., 1993).

According to Urbain et al. (1993) the EPS may originate from the metabolism or lysis of microorganisms (protein, DNA, polysaccharides and lipids) and from the wastewater itself (cellulose, humic acids). Liu and Fang (2003) showed that the extraction procedure influences the analysis of the EPS constituents significantly. The composition of the EPS as reported by different studies is presented in Table 2.5 and show that the proteins and carbohydrates represent the main components of the EPS. In this context, Nielsen et al. (1996) found that the EPS contain approximately 2-4 times more proteins than the rest of the sludge. Humic substances, uronic acids and DNA constitute just a small fraction of the EPS and only a few methods were able to identify and quantify them.

Table 2.5. The EPS composition in activated sludge (adapted from Liu and Fang, 2003)

Extraction procedure	EPS constituents and quantities (mg/g VS*)					Reference
	Carbohydrates	Proteins	Humus	Uronic acid	DNA	
Centrifugation	17-25	15	-	-	-	Murthy and Novak, 1999
Centrifugation	7.7	7.9	6.4	0.5	0.06	Liu and Fang, 2002
Heating	8	121	-	-	-	Frølund et al., 1996
Heating	13	44.9	-	-	-	Liu et al., 2001
Sonication	86	310	-	-	71	Jorand et al., 1995
Sonication	3.5-15.6	6.1-97.8	-	-	5-17.7	Urbain et al., 1993
Homogenisation	3	1	-	-	-	Örmeci and Vesilind, 2000
Homogenisation	7-21	21-93	-	-	-	Eriksson and Alm, 1993
Cation exchange resin	37-37.7	90-127	-	-	-	Jorand et al., 1998
Cation exchange resin	6.8-8.8	64-75	-	3.2-3.3	-	Frølund and Keiding, 1994
EDTA	4.3	30.0	-	-	-	Wuertz et al., 2001
NaOH	22	96	-	-	-	Frølund et al., 1996
Sonication+ Exchange resin	11.4	242	-	-	-	Dignac et al., 1998

*VS – volatile solids

The influence of different EPS on the flocculation is not completely known. Various studies are presented in literature, which try to explain the role of the EPS on floc formation. However, contradictory results are sometimes presented.

Liao et al. (2001) suggested that the flocculation is influenced by surface properties, hydrophobicity, surface charge and composition of the EPS rather than their quantity. Li and Ganczarczyk (1990) showed that the EPS play an important role in substrate and product transfer to and from the microbial cells in the floc. A reduced presence of EPS was observed when the flocs were exposed to high organic loads.

Higgings and Novak (1997c) showed that the divalent cations may serve as bridges between the negatively charged EPS and the microbial cells and stabilise the flocs network structure. Therefore, it was found that by increasing the concentration of Ca^{2+} and Mg^{2+} in the influent resulted in an increase of the amount of extracellular protein and a decrease of the effluent suspended solids concentration. By contrast, when the concentrations of Na^+ ions was increased, a decrease of the bounded proteins and an increase of effluent suspended solids occurred. Urbain et al. (1993) and Dignac et al. (1998) showed that cations bind preferentially with the proteins and also the amount of the proteins in EPS is increasing with the concentration of divalent cations (Ca^{2+} and Mg^{2+}).

In relation with the sludge settling properties Urbain et al. (1993), Eriksson and Alm (1991) and Liao et al. (2001) showed that an increase of the amount of EPS results in a linear increase of the SVI. By contrast, Yun et al. (2000) showed that the SVI decreases with the amount of EPS, while Jorand et al. (1998) reported that no correlation may be found.

Wilén (1999) concluded that physical and chemical properties of the activated sludge flocs are decided by the amount and structure of EPS. Moreover, dense EPS are found inside the flocs while the outer parts of the flocs are bound by weaker forces and are very sensitive to the changes in the environmental conditions.

2.3.2. Flocculation mechanisms

Due to its heterogeneous composition and therefore complex structure, many factors may interact and influence the floc formation in the activated sludge process. This makes it almost impossible to evaluate the flocculation process by only a single mechanism.

Several studies are presented in literature to identify and characterise the mechanisms involved in the flocculation process. Conceptual floc-formation models are often described by considering the influence of different parameters (Wilén, 1999). Among them the most known approaches deal with the effect of cations and polymers in bridging the floc structure and the physico-chemical influence.

From a biological influence point of view, the filamentous backbone theory introduced by Parker (1971) is considered to be responsible for the large floc formation. A good balance between filamentous and floc forming bacteria is essential for a well settling and compacting floc (Sezgin et al. 1978). Accordingly, Sanin and Vesilind (1999) showed that a lack of filamentous microorganisms in a synthetic sludge formed weaker flocs and led to more turbid effluent. In contrast, Chudoba (1989) stated that the filamentous bacteria do not play a role in stronger floc formation. It is supposed that the EPS forms a firm binding of the flocs. Jenkins (1992) suggested that the two theories related to the role of filamentous bacteria and EPS on floc formation are not mutually exclusive.

However, a clear distinction and separation between different mechanisms which may be responsible for floc formation is difficult and consequently one has to consider them separately. Furthermore, there are not only the physico-chemical aspects that must be taken

into account, since the composition of the flocs is constantly changing due to microbial degradation and the formation of new products. Some properties of the sludge flocs change on a long-term scale (structure, bacterial population), while other properties change fast (surface chemistry, floc size) (Ganczarzyk, 1983).

Since this research emphasises on the short-term physico-chemical influence on the floc formation by assuming no significant biological changes, the flocculation mechanism will be further discussed in this context.

The need for a general approach led to the conventional way to describe flocculation based on two discrete steps dealing with the transport and attachment of the particulate material into flocs respectively (Thomas et al., 1999). In turn, the flocculation can be characterised by three distinct mechanisms:

- Perikinetic flocculation
- Orthokinetic flocculation
- Differential settling

Based on the size of the involved particles, Tchobanoglous et al. (2003) define the perikinetic flocculation as microfloculation which is significant for particles that are in the size range from 0.001 to about 1 μm . Orthokinetic flocculation and differential settling are defined as macrofloculation and refer to the aggregation of particles larger than 1 or 2 μm (Figure 2.5,a).

Perikinetic flocculation occurs due to the random thermal motion of fluid molecules (Brownian motion). Orthokinetic flocculation is imposed by velocity gradients created by mixing. As shown in Figure 2.5,b particles which are moving faster overtake slower-moving particles in a velocity field. Due to the collision which occurs between the particles larger particles are formed that will be easier to remove by gravity separation.

The differential settling is determined by differences in settling velocity between different particles size. Larger particles overtake smaller particles, collide and stick together, forming larger particles that settle faster (Figure 2.5, c).

Even related mostly to the transport phenomena of the particles, these mechanisms include the attachment phenomena as well. In this respect, the effectiveness of the attachment will depend on the collision efficiency between the particles, significantly affected by electrostatic forces, floc structural properties and hydrodynamic interactions (Kuster, 1991; Serra et al, 1997; Chin et al., 1998).

The fundamentals of the flocculation mechanisms were presented by Smoluchowski (1917), who described them based on collision frequency functions and changes in particle size. From this concept, different approaches are taken in order to establish a good conceptual flocculation mechanism.

2.3.2.1. The hydrodynamic interaction model

The model proposed by Smoluchowski (1917) offers a rectilinear view of the collisions in which the changes in fluid motion as particles approach each other are neglected. In reality, when particles collide the space between them is diminished, forcing the liquid to flow out. By this fluid motion, the particles deviate from their linear path and rotate relative to one another. The alternative of the rectilinear approach is the so called curvilinear approach in which the liquid motion forces are considered. A comparison of those two models based on flocculation mechanisms was provided by Han et Lawer (1992). It was shown that for the

rectilinear approach, the particles' size plays a dominant role in determining the flocculation mechanisms. Hence, the perikinetic flocculation occurs only when particles are very small (less than 1 μm), while the orthokinetic flocculation is the dominant process occurring in general for particles larger than 10 μm . Differential settling dominates the process only when one of the particles is significantly larger than the others.

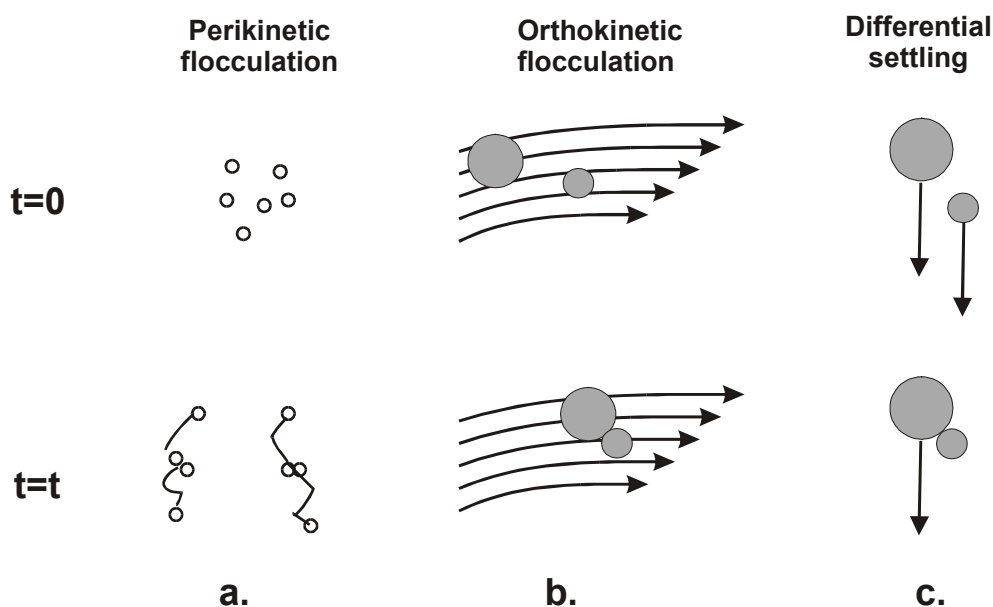


Figure 2.5 Schematic illustration of the flocculation mechanisms: a. Perikinetic flocculation; b. Orthokinetic flocculation; c. Differential settling (adapted from Tchobanoglous et al., 2003)

The development of the curvilinear model, as compared with the rectilinear model, showed the importance of including other properties, such as particle density and sludge viscosity. Moreover, it was shown that the orthokinetic flocculation is a less dominant process as predicted by the rectilinear approach and therefore the role of the root-mean-square velocity gradient G , is only to keep the particles in suspension, in order to allow particles collision by differential settling and perikinetic flocculation. However, as shown by Thomas et al. (1999) practice demonstrated that the rectilinear or the curvilinear models may not be entirely applicable to the flocculation process and the real situation is eventually somewhere in between these two models.

Recent developments in evaluating the hydrodynamic effects on flocculation considered the drag forces exerted on the floc as a prerequisite for an accurate prediction of its motion. To estimate the drag forces, knowledge regarding the drag coefficient, primary particles density and a correction factor for advection flow are required (Wu et al., 1998). Also important is the determination of the floc porosity. Accordingly, Veerpaneni and Wieser (1996) and Li and Logan (1997) calculated the flow by considering nonuniform porosity. Wu and Lee (1998) showed that Stokes' regime for drag forces upon a porous aggregate can be extended as compared with a solid sphere. Therefore, it was suggested that the lack of knowledge related to the flocs' interior permeability results in difficulties to accurately estimate the floc density. In this sense, the evaluation of the fractal dimension of the flocs and its inclusion in the new models may represent a step forward to understand the process mechanisms.

2.2.2.2. The colloidal interaction model

The Smoluchowski model considers that all collisions between particles lead to attachment and forces such as electrostatic repulsion and van der Waals attractions are ignored. The DLVO theory (Derjaguin and Landau, 1941; Verwey and Overbeek, 1948) considers the combined effect of these forces by assuming that the particles are in general electrically charged surfaces. Accordingly, the DLVO theory is used for determining the Gibbs energy between two surfaces as function of the separation distance by assuming that the van der Waals attractive interactions and the electrostatic double layer repulsion are additive.

The van der Waals attractive forces can be calculated by considering the separation distance between the particles, the system geometry and the Hamaker constant. The electrical repulsion depends on the width of the double layer and varies inversely proportional with the root of the ionic strength (Wilén, 1999).

The calculation of the van der Waals and electrostatic repulsions at various separation distances resulted in a dependency of the interaction energy on separation distance that reveals the presence of two minima separated by a maximum (Figure 2.6). This maximum is usually expressed as the energy barrier and occurs when the repulsion forces are higher than the attractions. In order to allow the particles to come in contact, the energy barrier must be surmounted. The lowest interaction energy is found at the minimum occurring at the smallest separation distance. This represents the most favourable case in which attraction between the particles takes place. However, in a suspension of dispersed particles, the flocculation frequently occurs in the secondary minimum at a larger separation distance.

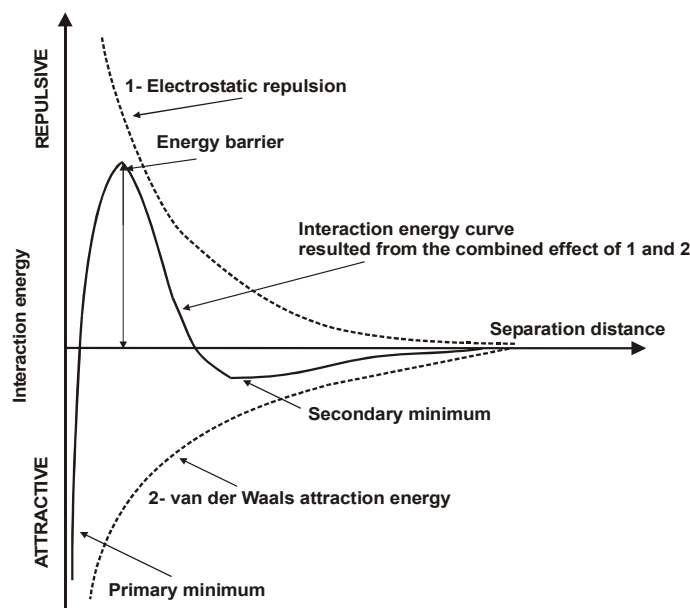


Figure 2.6 Representation of DLVO theory. The solid curve gives the interaction energy between two particles as function of the separation distance.

Originally, the DLVO theory was developed to describe the processes that occur between colloidal particles. However, taking into account that the activated sludge flocs carry a net negative charge (Gregory, 1989), many research studies extended this theory in order to explain the activated sludge flocculation mechanisms.

The role of cations in flocculation is often described by using the DLVO theory. The addition of positively charged cations was shown to result in a decrease of the energy barrier and to

promote aggregations. Therefore, Cousin and Ganczarczyk (1998) and Zita and Hermansson (1994) showed that addition of cations indifferent of their valence produced similar effects on the particles' stability and improved the structural properties of the flocs by increasing their size and porosity. Other influences of process parameters such as addition of sulphide and detergent, changing the pH may be described by DLVO theory as well (Mikkelsen, 2001)

Mikkelsen (1999) showed that the turbulence or thermal fluctuations as given by orthokinetic and perikinetic flocculation, respectively may increase the particles kinetic energy. Hence, the particles flocculated in the secondary minimum may escape leading to deflocculation. These observations suggest that in the secondary minimum flocculation and deflocculation occur simultaneously. When the kinetic energy is high enough, the particles flocculate in the first minimum in an irreversible manner.

Zita and Hermansson (1994) suggested that the floc stability is highly affected by the ionic strength of the medium and the interactions between the floc components as described by the DLVO theory.

Opinions relating to the role of DLVO theory in explaining the flocculation mechanisms are contradictory. Sobek and Higgins (2002) showed that the addition of monovalent cations (especially sodium) resulted in a deterioration of the floc strength and settling properties, while Keiding and Nielsen (1997) found that the deflocculation process observed by removal of the Ca ions from the floc structure occurred due to an increase in the negative surface charge, as given by the zeta potential.

2.3.2.3. Breakage and aggregation model

The model developed by Smoluchowski considers that the collisions between the particles follow the above described rectilinear model and therefore that particle transport and attachment take place in a laminar flow. Later on, Camp and Stein (1943) introduced the root-mean-square velocity gradient, G , and extended the model to the turbulent flow regime. Only aggregation was considered in these models. The floc breakup process has been included in a turbulent diffusion model by Argaman and Kaufman (1970). Parker et al. (1971) showed that the aggregation and breakage occur simultaneously and developed a model that described the net rate of change in the number of primary particles concentration:

$$\frac{dn}{dt} = k_B X G^m - k_A X n G \quad (2.1)$$

where n is the primary particles number concentration (number/l); t is the time (s); X is the mixed liquor suspended solids concentration (g/l); G is the root-mean-square velocity gradient (s^{-1}); k_A is the floc aggregation rate coefficient (l/g); k_B is the floc break-up rate coefficient (numbers. s^{m-1} /g) and m is the floc breakup rate exponent.

The root-mean-square velocity gradient is calculated by using the Camp and Stein (1943) formula:

$$G = \sqrt{\frac{\varepsilon}{\nu}} \quad (2.2)$$

where ε (m^2/s^3) the local rate of energy dissipation and ν (m^2/s) is the kinematic fluid viscosity.

By assuming that k_A , k_B and G are independent of time and using a value of 2 for m , the integration of equation (2.1) resulted in:

$$n_t = \frac{k_B G}{k_A} + \left(n_0 - \frac{k_B G}{k_A} \right) e^{-k_A X G t} \quad (2.3)$$

where n_t is the number of primary particles at time t (number/l); n_0 is the number of primary particles at time $t=0$ (number/l).

With the previous assumptions of time independent k_A , k_B and G , equation (2.3) can be written in the following generic form:

$$n_t = \alpha + \beta e^{-\lambda t} \quad (2.4)$$

where: α is the equilibrium primary particle number concentration (number/l), β is the difference between the initial and equilibrium primary particle number concentrations (number/l) and λ is the overall primary particle removal rate constant (s^{-1}).

Using the parameters given by equations (2.3) and (2.4) the activated sludge flocculation characteristics from different plants were compared and evaluated. To this end, Parker et al. (1972) showed that the aggregation coefficient k_A and breakup coefficient k_B depend on physical-chemical factors, which may affect the particles destabilisation and the floc strength. It was also shown that the breakage and aggregation phenomena are significantly affected by the G values. Therefore, at low G values the number of primary particles decreases, indicating a flocculation process, while at high G values the number of primary particles increases.

Wahlberg et al. (1994) investigated the model proposed by Parker et al. (1971) for 30 activated sludge samples obtained from 21 wastewater treatment plants. For model validation, each of the individual parameters (k_A ; k_B , n_0 , α , β , λ) were evaluated separately. It was found that k_A and k_B may vary with of the flocculation devices and especially the mixing device. The α parameter indicates that there is a limit below which the flocculation cannot be used to further reduce the turbidity, while the β parameter quantifies the improvement in the removal capacity of suspended solids through flocculation. Poor flocculation is indicated by large estimates of β and gives an indication that sludge conditioning is required.

Mikkelsen and Keiding (1999) analysed the model developed by Parker et al (1971) by including the desorption of the primary particles in response to high turbulent values of G ($500-1700s^{-1}$) and different suspended solids concentrations. The results showed disagreement with Parker's model since it was found that the equilibrium turbidity level is also dependent of the solids content and not only of G as found by Parker et al (1971) and Wahlberg et al. (1994). In order to describe the effects of solids content and G on sludge deflocculation Mikkelsen and Keiding (1999) proposed an adhesion-erosion model. This was built using the similarity with gas-liquid phase transition in which the adsorption-desorption equilibrium of primary particles incorporation into flocs was described by using a diffusion process very similar with the Langmuir adsorption isotherm. The model gives the possibility to predict the equilibrium colloidal concentration as function of sludge solids content and G , obtained when the sludge is mixed for an infinitely long time.

Population balance modelling

Recently, Biggs (2000) developed a new concept based on population balance modelling (PBM) for the activated sludge flocculation. The major advantage as compared with the model introduced by Parker et al. (1971) is that by using PBM, an investigation of the whole distribution of floc size during flocculation becomes possible rather than just the primary particles' size.

According to the PBM approach, the time evolution of different properties may be derived for individual flocs. In Biggs' approach the aggregation and breakage were considered as the only

processes involved in flocculation. Therefore, the dynamics of the number concentration of the flocs (N_i) in different size classes (i) can be written as:

$$\frac{dN_i}{dt} = \text{aggregation} + \text{breakage} \quad (2.5)$$

According to Hounslow et al. (1988) "birth" and "death" terms should be included into the population balance. This is necessary as it allows to explain the formation or depletion of the number concentration. Hence, both aggregation and breakage lead to "birth" and "death" of flocs of a certain size and the equation (2.5) becomes:

$$\frac{dN_i}{dt} = \text{Birth}_{\text{aggregation}} - \text{Death}_{\text{aggregation}} + \text{Birth}_{\text{breakage}} - \text{Death}_{\text{breakage}} \quad (2.6)$$

The aggregation and breakage dynamics given in equation (2.6) were illustrated by Biggs (2000) as shown in Figure 2.7.

By using an on-line technique to monitor the floc size dynamics, Biggs (2000) concluded that PBM is a suitable method to describe the flocculation process. It was found that the model prediction accurately described the experimentally determined dynamics of the mass mean floc size diameter, which was used as a size parameter. The effects of two parameters, shear rate, G , and calcium addition were evaluated by using the PBM approach. It was observed that the breakage rate coefficient increased with increasing G according to a power-law relationship. The collision efficiency decreased when G was increased and increased when calcium ions were added. However, being the first attempt of applying the PBM for the activated sludge flocculation, Biggs's model needs further improvement.

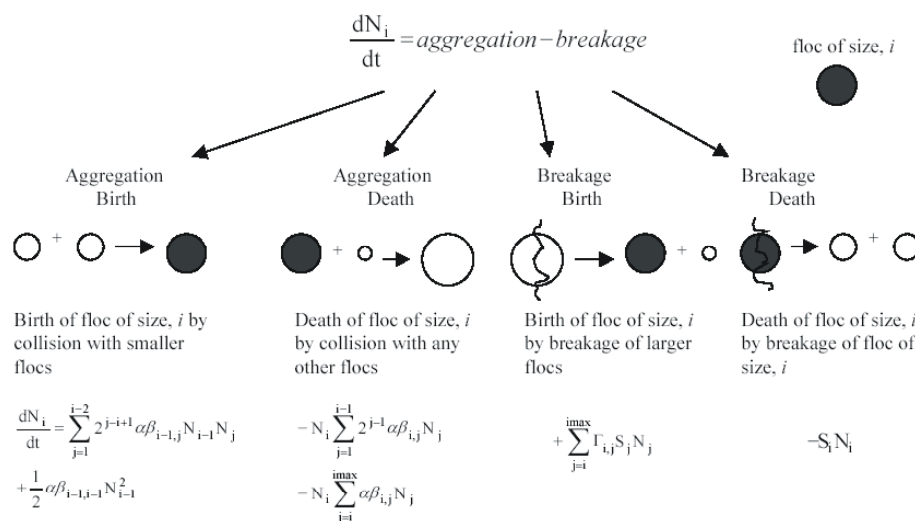


Figure 2.7 Aggregation and breakage dynamics of the discretised population balance (Biggs, 2000)

Nopens et al. (2002), evaluated the model developed by Biggs and isolated the most sensitive points that should be considered for improving the model. A lack of flexibility was found and it was suggested that the model structure should be extended by including more process parameters and by changing the current process description. To achieve these goals however, it is necessary to find better relationships between the key model parameters and the process characteristics and floc properties. It is believed that this will lead to an improved understanding of the activated sludge flocculation mechanisms.

2.4. A set of relevant factors for the flocculation process.

The knowledge related to the flocculation process can be improved only by a careful analysis of the factors that produce and affect the process. Moreover, any change of the environmental conditions can affect the floc properties. As shown before, the composition of the activated sludge plays a significant role in floc formation and therefore in removal characteristics. Simultaneously, the flocculation occurrence and its properties are influenced by a series of physico-chemical factors. In this research, the role of a set of five relevant factors for the flocculation process are considered. A short motivation of the selection of these factors based on the literature study is given below in this section.

2.4.1. *Mixing intensity*

The influence of mixing on the efficiency of flocculation has been subject of many studies that recognise it as one of the major factors affecting the process. From the aeration basin to the clarification process and sludge recycling, different degrees of turbulence affect the fragile structure of the biological flocs causing its breakup or aggregation. To quantify the turbulent shear rate the root-mean-square velocity gradient (G) introduced by Camp and Stein (1943) is often used.

However, the application of the G concept to the flocculation process has been criticised by many researchers. In this context, Han and Lawler (1992) found that orthokinetic flocculation is no longer seen as being directly proportional with G as predicted by Camp and Stein (1943) and only a minimum G is required to keep particles in suspension. Contrary, Wahlberg et al. (1994) demonstrated that the shear played an important role on floc breakage and aggregation mechanisms, which were considered to be the key phenomena for floc formation. Even with the existing criticisms G is the most used parameter for quantifying the effect of shear on flocculation. For typical processes the activated sludge flocs experience a G range from 20 s^{-1} to 150 s^{-1} (Tchobanoglous and Burton, 1991). Some full-scale treatment plants have a G value designed to be larger than 200 s^{-1} to avoid settling of biomass in the aerated reactor (Galil et al., 1991). Parker et al. (1972) and Galil et al. (1991) found a power-law relationship between G and floc size showing that the floc size decreases with increasing shear. This was later on confirmed by Biggs and Lant (2000) by on-line quantification of the floc size dynamics under different shear stress values. The role of mixing in the flocculation process is essential to induce particle-particle interactions. Its importance should not be neglected and must be taken into consideration when the flocculation process is investigated. In this study the effect of mixing on flocculation is quantified and its interaction effects with other physico-chemical parameters are examined as well.

2.4.2. *Cations*

The role of cations in flocculation can be explained by three different theories: Derjaguin, Landau, Verwey and Overbeek (DLVO) theory, divalent cation bridging (DCB) theory and the alginate theory.

According to the DLVO theory, the addition of cations would decrease the size of the double layer of counterions that surround the particles. In this way, the repulsive forces between the particles decrease, allowing short-range forces to promote aggregation. Zita and Hermansson (1994) sustained the DLVO theory by showing that the ionic strength affects the particles stability and the addition of K^+ and Ca^{2+} produced similar effects.

The alginate theory was introduced by Bruus et al. (1994) and showed that the bacterially produce alginate polysaccharide form alginate gels in the presence of calcium ions.

Comparative experiments performed with different cation additions (Ca^{2+} , Mg^{2+} and Na^+) showed that the biopolymer had a higher affinity for Ca^{2+} than Mg^{2+} and Na^+ addition deteriorated the floc properties.

The DCB theory is the most widely accepted theory up to now and shows that the cations are involved in flocculation through ionic bridging. Intensive research work of Novak and coworkers (Higgins and Novak, 1997a; Novak et al. 1998; Sudhir and Novak, 2001) sustains this theory. In this respect, it is suggested that the ratio of monovalent to bivalent cations is an important parameter for improving the process performance in terms of settling, dewatering and effluent quality. By studying the effect of cations addition on the floc size dynamics, Biggs (2000) demonstrated that the affinity of cations to improve flocculation was $\text{Ca}^{2+} > \text{Mg}^{2+} > \text{Na}^+$, which supports the role of cations in flocculation as cation bridging. Moreover, Sobeck and Higgings (2002) compared the three theories available for describing the mechanism of cation-induced flocculation and showed that the addition of bivalent cations (Ca^{2+} and Mg^{2+}) into the feed of a lab-scale activated sludge system resulted in improvement in floc properties. An identical test showed that the addition of Na^+ deteriorated the floc properties. Based on these results, the authors concluded that the DCB theory best described the role of cations in flocculation. Independent of the theory, it seems to be largely accepted that calcium addition improves flocculation, although many of the studies concluded that its effect becomes more effective after long-time exposure (Higgins and Novak, 1997b). In this research, the short-term influence of calcium addition was investigated.

2.4.3. Temperature

For the activated sludge treatment, the temperature has a complex influence. The temperature effect is mostly related to changes in the wastewater viscosity and its surface tension. When temperature increases, the wastewater viscosity decreases, improving the mixing and the molecular diffusion of substrate and products of biochemical reactions. Sürücü and Çetin (1989) further found that the separation properties of the activated sludge decreased with temperature increase due to a change in the function and charge of the EPS. Krishna and van Loosdrecht (1999) investigated the long term effects of temperature on the activated sludge structural and settling properties. They found that the SVI increased with an increase in temperature, which in the same time created a decrease in the production of storage polymers in the sludge (PHB) and an increase in the amount of extracellular polysaccharides. The microorganisms show specific optimum temperatures for growth and substrate utilisation. This leads to their classification into psychrophiles, mesophiles and thermophiles (Ganczarzyk, 1983). However, the specific temperature range for each organism group is not well defined. The temperature influence on microbial growth may be explained by temperature dependent enzymatic transformations, specific to particular species. The short-term temperature effect may also have a significant effect on the treatment efficiency acting sometime as a shock effect on the microbial community and the structural properties of the activated sludge flocs. The short-term effect evaluations performed by Wilén (1999) showed that different degrees of deflocculation occurred by changing the temperature of the system. A relationship between the floc strength and temperature was also found in the sense that cooling of the sludge weakened the floc strength while a moderate heating increased the floc strength. Moreover, at higher applied shear levels the effect of cooling on deflocculation was more pronounced. However, very little is known about the direct impact of the short-term temperature effect on floc size dynamics and how strong its effect is in comparison with other significant factors that may affect the flocculation process.

2.4.4. Dissolved oxygen

Oxygen deficiency is one of the main factors involved in the biological dysfunction. Many studies available in literature focused on the relationship between the DO concentration and microbial community evolution and especially with the growth of filamentous bacteria (Jenkins, 1992; Gaval and Pernelle, 2003). Pochana and Keller (1999) hypothesized that simultaneous sludge nitrification/denitrification is caused by an oxygen diffusion limitation into the flocs thereby generating anoxic conditions around the center of the flocs. Abbassi et al. (1999) suggested that an increase of the dissolved oxygen concentration in the mixed liquor can cause the reduction of excess sludge production. Li and Ganczarzyk (1993) found that the organic loading and the availability of dissolved oxygen are the most significant factors which influence the size distribution of activated sludge flocs. However, an intensive research study regarding the effect of DO concentration on flocculation has been performed by Wilén (1999). It was concluded that the effect of DO concentration can be divided into short-term effects (from minutes up to a few hours) and long-term effects (from days up to weeks). When the long-term effects were examined, it was found that the low DO concentrations (0.5-2 mg/l) produced flocs with poorer settling properties than the high DO concentrations (2-5 mg/l). The inferior settling was mainly due to the excessive growth of filamentous bacteria and the higher flocs porosity. From a short-term perspective, oxygen limitation had a pronounced effect on the amount of small flocs in the supernatant after settling and an increase in effluent turbidity, although the size and structure of the larger flocs was not significantly affected.

2.4.5. Activated sludge concentration

For the clarification step, the sludge concentration is a very important parameter being directly interrelated with the settling properties of the sludge. De Clercq (2003) showed by in situ measurements of particles sizes in secondary settling tanks that the solids concentration plays an important role in flocculation. In this context, it was found that the aggregation rate increased with increasing solids concentration. Similar results have been obtained by Chaignon et al. (2002) for the case of low sludge concentration (3.5 – 140 mg/l) reporting a linear correlation between the flocs size and suspended solids content. This is in agreement with Mikkelsen and Keiding (1999) who observed a linear dependence between the supernatant turbidity and low solids concentration (approx. < 3g/l), while for higher solids contents the effect of solids increases dramatically. However, for the clarification process at high solids concentration it is believed that the hindered settling rates are independent of the individual particle characteristics. The structural properties of the particles become more important at lower concentrations where flocculent and discrete settling occur (De Clercq, 2003).

2.5. Conclusions

The secondary clarifier represents the most important and critical step of the activated sludge process. Its main objectives are to provide an effluent of good quality and a thickened activated sludge.

Combating and especially preventing the sludge settling problems is one of the major challenges for the further optimisation of the activated sludge process. Different design, operating and monitoring procedures are continuously developed and implemented for process improvement.

Most of the separation problems are related to the nature and the characteristics of the flocculent growth. Sludge bulking and a poor flocculation process have been characterised as major causes that affect the overall activated sludge process and especially the efficiency of the solids-liquid separation. Considerable research work has been made in order to control and solve sludge bulking. However, due to the high diversity of filamentous species and their different optimal growth conditions, the bulking phenomena still represent a major and frequently occurring problem for the activated sludge process.

Often, less importance is given to the floc properties when new process developments are introduced. It may happen that the most sophisticated treatment plants encounter problems due to the poor flocculation properties they induce.

It is therefore essential to pay special attention to the flocculation mechanisms, as it is still considered a bottleneck in understanding the activated sludge process and consequently, in controlling its performances.

A complex mixture of diverse constituents makes up flocs of which behaviour is difficult to be predicted and controlled under different environmental conditions. Among them, it is generally accepted that the EPS and the cations are the principal constituents involved in the floc formation. The EPS represent the major organic fraction of the flocs, acting as glue between the other components. Hence, the amount and properties of the EPS have a significant influence on the floc properties. However, little is known about what EPS constituents are mostly responsible for floc formation. A lack of consensus regarding the EPS composition and properties exists and this is partly due to the different extraction procedures used.

Overall recognised is the importance of calcium in flocculation. The effect of other cations is still doubtful and this is especially due to different mechanistical approaches presented in literature.

As a result of its complex nature the flocculation process can not be described by a single mechanism. However, a general approach exists that describes the flocculation as function of three distinct transport mechanisms: perikinetic flocculation, orthokinetic flocculation and differential settling. Different models accounting for hydrodynamic influences or colloidal interactions are presented to explain these mechanisms. However, these theoretical models are often contradicted by experiments and no attempts were found in literature in which the interactions between these models are considered. Considering them isolated, a comprehensive model able to describe the whole flocculation mechanism is difficult to be found.

It was shown that during the flocculation, the aggregation and breakage phenomena occur simultaneously. A few research studies stress the importance of considering these phenomena as key mechanisms able to explain floc formation. The model introduced by Parker et al. (1971) allowed to investigate the change in the primary particles concentration and to relate these changes to several process parameters.

In extension to this model, the most promising approach to gather insights in the flocculation process is the approach based on population balance modelling. Introduced by Biggs (2000) for the activated sludge process, the PBM enabled to follow the aggregation and breakage rates for the entire size distribution. It is considered that improving this model so as to account for the influence of as many as possible process parameters on floc properties will lead to a solid and comprehensive flocculation model.

This latest requirement is nevertheless the most important issue, which should be considered in evaluation of the flocculation. Insufficient insight in the impact of these parameters makes

the models to fail in their predictions and to ignore the effect of changing conditions on important phenomena such as sludge settling, dewatering or compaction.

Only a deeper, thorough investigation on the interactive effects, which the environmental conditions and process parameters have on floc properties will eventually allow to understand the complex processes related to the floc formation and to ultimately improve the activated sludge performance.

In this context, the present research will deal with an evaluation of the effect of five important factors on the flocculation process. Accordingly, average velocity gradient, dissolved oxygen, calcium concentration, temperature and sludge concentrations will be investigated and their role on flocculation dynamics as well as their interactive effects will be discussed.

On-line quantification of floc morphological properties

3.1. Introduction

For the activated sludge process, the bioflocculated microbial aggregates are essential components of the system. Removal and transformation of the organic matter from the wastewater and incorporation of the colloidal particles into settleable solids are examples of processes for which the biological flocs are responsible. On the other hand, many major problems such as filamentous bulking or formation of small and light flocs, which occur in solid-liquid separation may be as well attributed to the floc's properties. It is therefore straightforward to state that the floc characteristics are of utmost importance for the activated sludge process performance.

For a comprehensive insight into the floc characteristics and their impact on the sludge settleability and compressibility, a series of parameters and properties must be investigated as shown in Figure 3.1. Jin et al. (2003) proposed and analysed an integrated approach for investigating the floc characteristics and sludge properties and found that the morphological properties of the flocs (size, fractal dimension and filament index) were the major parameters associated with settling and compressibility of the sludge. Moreover, using a similar approach Wilén et al. (2003) observed that the same parameters were the most important factors governing the floc stability.

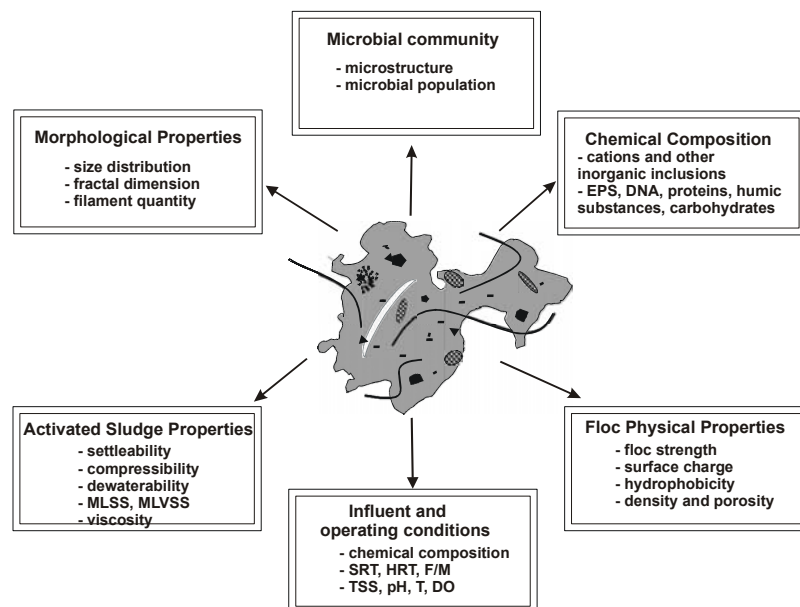


Figure 3.1 Integrated investigation of floc characteristics and sludge properties in the activated sludge process (adapted from Jin et al., 2003).

This chapter focuses on the evaluation of the morphological properties (size and fractal dimension) of the activated sludge flocs. Due to the fragile biological nature, irregular structure and heterogeneous composition of the flocs, the measurement procedures and the used techniques may affect the results and often lead to a misinterpretation of the data. It is therefore necessary to screen out the available techniques and to evaluate their strengths and weaknesses before performing an experiment in order to develop a good experimental protocol in which the disturbance produced by sample preparation and manipulation are reduced as much as possible.

The structure of this chapter is as follows:

- Review of the state of the art of activated sludge morphological properties, with emphasis on floc size and fractal dimension evaluation.
- Evaluation of the capabilities of the available sizing techniques for measurement of floc morphological properties.
- Investigation of optimal experimental conditions for on-line measurement of the floc properties.
- Evaluation of the shape effect on the size distribution results.
- Simultaneous determination of the floc size distribution and the fractal dimension by using different techniques.

3.2. Activated sludge floc morphological properties: State of the art

3.2.1. Size and size distribution

The floc size and size distribution are the result of a dynamic equilibrium state between formation, transformation and breakage of the microbial aggregates. Depending on the variations in the process parameters that may occur, the size of the floc may vary in a broad range of values.

Large and dense flocs, which settle faster and give low effluent turbidity are an indication of an efficient flocculation and good settling and dewatering performance (Li and Ganczarczyk, 1988, Dammel and Schroeder, 1991). Based on this observation, Han et al. (2002) demonstrated that the measurement of the floc size dynamics during different stages of the activated sludge process allowed to detect trivial mistakes in the design and operation of a WWTP such as particles break-up at the opening between flocculation basins and flocculation and sedimentation in the distribution channel. Moreover, the floc size and size distributions evaluation proved to be a very useful tool to understand the influence of some process parameters such as: substrate loading (Barbusinski and Koscielniak, 1995); shear forces (Parker et al, 1971; Galil et al. 1991; Biggs and Lant, 2000), sludge age (Andreadakis, 1993) and dissolved oxygen concentration (Pochana and Keller, 1999, Wilén, 1999).

In spite of the practical importance of flocculation, its mathematical modelling has not been well established. This is mostly due to the inability to correctly measure and evaluate the size of the flocs. Detailed information regarding the rate of flocs aggregation and breakage, which are required for understanding the flocculation mechanisms and developing a suitable modelling framework are directly linked with the floc size dynamics. Recently, activated sludge flocculation has been successfully described using population balances (Biggs and Lant, 2003; Nopens et al., 2002). The authors stressed the importance of a good determination

of the floc size and size distribution, which is a necessary condition for the correct evaluation and interpretation of the mathematical models.

Moreover, modelling of the final clarification step needs a deep understanding of the settling properties, which are directly linked to the floc's characteristics. Patry and Takács (1992) pointed out that knowledge related to the particle size is of high importance in modelling the settling velocity of the floc in the upper layers of the secondary clarifier, while De Clercq (2003) used in-situ floc size distribution measurements to model the clarifiers by using Computational Fluid Dynamics (CFD).

3.2.1.1. Floc size

In a typical activated sludge there is a wide range of particle sizes, starting from single bacteria with dimensions in the order of 0.5 to 5 μm up to large aggregates (flocs) that can reach sizes of more than 1000 μm .

Derived diameters are determined by measuring a size dependent property of the particle and relating it to a single linear dimension (Table 3.1).

Table 3.1 Definitions of particles diameters (adapted from Allen, 1997).

Symbol	Diameter	Definition	Formula
d_v	Volume	Diameter of a sphere having the same volume as the particle	$V = \frac{\pi}{6} d_v^3$
d_s	Surface	Diameter of a sphere having the same surface area as the particle	$S = \pi d_s^2$
d_{sv}	Surface-volume	Diameter of a sphere having the same external surface to volume ratio as the particle	$d_{sv} = (d_v^3 / d_s^2)$
d_d	Drag	Diameter of a sphere having the same resistance to motion as the particle in a fluid of the same viscosity (μ) and the same velocity (v)	$F_d = 3\pi d_d \mu v$
d_{St}	Stokes	Diameter of a sphere having the same free-falling speed (V) as a particle of the same density (ρ) in the laminar flow region ($Re < 2$)	$d_{St} = \sqrt{\frac{18 * \mu * V}{g * \Delta \rho}}$
d_c	Perimeter	Diameter of a circle having the same perimeter as the projected outline of the particle	$P = \pi d_c$

The most often used application of such equivalent diameters is the individual floc settling velocity measurement, which led to an evaluation of the free settling ability of the flocs (Tambo and Watanabe, 1979; Li and Ganczarczyk, 1987). In this case, if an activated sludge floc is allowed to settle in a settling column, its terminal velocity may be compared with the terminal velocity of a sphere of the same density settling under similar conditions and the Stokes diameter may then be calculated. However, in the laminar flow region the flocs settle in a random orientation and a single floc may generate a range of equivalent diameters depending on its orientation. Li and Ganczarczyk (1987) found a linear function between the settling velocity and the cross-sectional diameter or the longest dimension of the floc. Their results were consistent with the one calculated from Stoke's equation by assuming a constant density of the flocs. However, due to the heterogeneity of the floc structure the aggregates cannot be considered as dense particles and Stoke's law cannot be used to describe the settling velocity (Jorand et al., 1995).

An average diameter represents a convenient way to analyse and describe the population of flocs by a single number. All average diameters are calculated starting from the size distributions and represent a measure of central tendency, which is unaffected by the

relatively few extreme values in the tails of the distributions. The average diameters may be calculated by using the mode, median and mean diameter.

The mode indicates the most frequent size in the sample. More than one mode may be present in a distribution, case in which the distribution is called multi-modal. In practice, the mode is rarely used since it has no practical significance as a measure of central tendency.

The median divides the distribution into two equal parts and may be deduced easily as the 50% size corresponding to 50% cumulative particles distribution.

The mean is the most used average diameter and represents the centre of gravity of the distribution. Different means can be defined for a given size distribution as pointed out by Allen (1997) (Table 3.2).

Table 3.2 Definitions of mean diameters.

Mean diameter	Formula
Number, length	$x_{NL} = D[1,0] = \frac{\sum x \Delta N}{\sum \Delta N}$
Number, surface	$x_{NS} = D[2,0] = \sqrt{\frac{\sum x^2 \Delta N}{\sum \Delta N}}$
Number, volume	$x_{NV} = D[3,0] = \sqrt[3]{\frac{\sum x^3 \Delta N}{\sum \Delta N}}$
Length, surface	$x_{LS} = D[2,1] = \frac{\sum x^2 \Delta N}{\sum x \Delta N}$
Length, volume	$x_{LV} = D[3,1] = \sqrt{\frac{\sum x^3 \Delta N}{\sum x \Delta N}}$
Surface, volume	$x_{SV} = D[3,2] = \frac{\sum x^3 \Delta N}{\sum x^2 \Delta N}$
Volume moment	$x_{VM} = D[4,3] = \frac{\sum x^4 \Delta N}{\sum x^3 \Delta N}$
Mass moment	$x_{WM} = D[4,3] = \frac{\rho \sum x^4 \Delta N}{\rho \sum x^3 \Delta N}$

3.2.1.2 Floc size distribution

The measurement of floc size distribution gives more information than a single diameter. Evaluating the frequency of the particles occurrence in different specific size classes represent a fast way to detect the floc size variability under varying conditions during the wastewater treatment. Therefore, it may lead to a more profound understanding and improve control of the activated sludge process.

Distributions expressed as number, surface area, volume or mass are often used for characterising the frequency of floc occurrence in each size class. Traditionally, a relationship between these distributions is reported based on the assumption of sphericity of the flocs. Allen (1997) converted the number distributions defined as $\Delta P_i = \Delta N_i / N$ (where ΔN_i is the number of flocs within the size interval i , and N is the total number of flocs) to distributions by volume, surface area and mass by using the following formulas

$$\Delta A_i \propto \bar{x}_i^2 \Delta P_i \quad (3.1)$$

$$\Delta V_i \propto \bar{x}_i^3 \Delta P_i \quad (3.2)$$

$$\Delta M_i \propto \bar{x}_i^3 \rho \varepsilon(\bar{x}) \Delta P_i \quad (3.3)$$

where \bar{x}_i is the characteristic size of the i^{th} class interval; ρ is the density of the solid content of the flocs (constant for a given sample) and $\varepsilon(\bar{x})$ is the solid fraction of the flocs.

A series of frequency distribution functions have been investigated and used to fit and transform the measured size distribution. Accordingly, Li and Ganczarczyk (1991) and Barbusinski and Koscielniak (1995) found that the measured data fitted well with a log-normal distribution:

$$f(x) = \frac{1}{x\sqrt{2\pi\ln\sigma_g}} \exp\left[-\frac{(\ln(x/x_g))^2}{2\ln^2\sigma_g}\right] \quad (3.4)$$

where: x is the particle size, $f(x)$ is the probability density function, x_g is the geometric mean of the distribution and σ_g is the geometric standard deviation.

Good log-normal fit was reported also for the volume distributions of the flocs by Jorand et al. (1995); Wilén and Balmér (1999) and Biggs (2000).

Another frequency distribution function used to fit the measured floc size distributions is the power-law. Hillgardt and Hoffmann (1997) fitted a floc size range interval of 3-300 μm to power-functions, while Li and Ganczarczyk (1991) found that the number distribution of the activated sludge flocs across a large size spectrum (from 0.5 to $> 500 \mu\text{m}$) correlated well with a power-law (equation (3.5)) and Rosin-Rammler (equation (3.6)) statistical models. The power-law model is described by:

$$\Delta N_i / \Delta x_i = C x_i^{-\beta} \quad (3.5)$$

where: ΔN_i is the number of flocs within the size interval i , x_i is the floc size, Δx_i is the length of the size interval i , and C and β are constants.

The Rosin-Rammler model is given by:

$$f(x) = 100nbx^{n-1} \exp(-bx^n) \quad (3.6)$$

where: x is the particle size, $f(x)$ is the probability density function and n and b are the shape and scale parameters.

Different activated sludge floc size distributions have been measured and reported in literature. Many times the results were contradictory. This is most probably due to the different measurement techniques used or to the differences in sampling and pre-treatment procedures. For instance, Parker et al. (1971) studied the number distribution of the activated sludge flocs and found a bimodal distribution, with very few flocs situated in the interval 5-25 μm . These results were contradicted later by Li and Ganczarczyk (1991) who showed that flocs size covered the whole investigated size spectrum and stated that flocs larger than 50 μm are the major source of surface area, volume and mass provided by activated sludge flocs while the flocs smaller than 2 μm have a significant number contribution (up to 18%).

The size spectrum of the activated sludge is often divided due to the size range limitations of the measurement techniques. Accordingly, different techniques are used (Wilén and Balmér, 1999) and/or combined in order to perform a complete evaluation over the whole size range (Li and Ganczarczyk, 1991). This practice, however, needs to be avoided as much as possible

since it may represent a source of errors due to the incompatibility between different measurement principles.

3.2.2. Fractal dimension

Li and Ganczarczyk (1989) showed that an activated sludge floc may be characterized as a highly porous fractal-like aggregate of many primary particles and the cross-sectional morphology of the floc section appeared to be self-similar. A simple illustration of the self-similarity concept is given by Gregory (1997) as a triplet of equal spheres (Figure 3.2). In reality, the essence of self-similarity aggregates is much complicated and involve different aggregation levels from large-scale structures down to individual primary particles (Gregory, 1997).

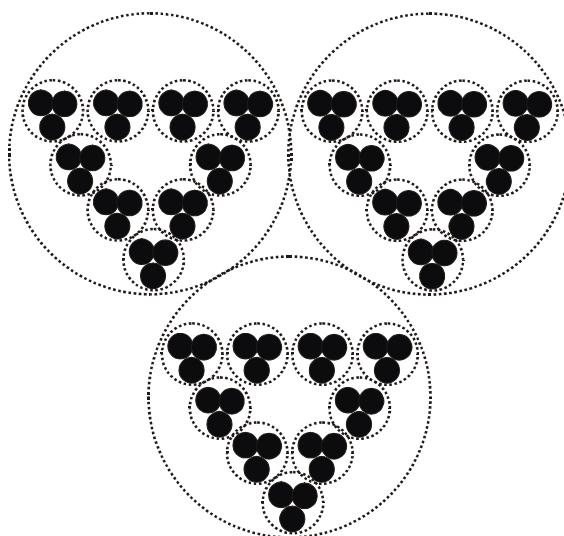


Figure 3.2 Two-dimensional model of a self-similar aggregate structure (Gregory, 1997).

The fractal dimension is often defined in linear, planar or volumetric terms, resulting in so-called one, two- or three dimensional fractals. Jiang and Logan (1991) derived the equations for the fractal aggregates as function of their properties such as mass, volume, density, porosity and settling velocity. Equations (3.7)-(3.9) are among the most used for fractal dimension evaluation, especially when microscopy and image analysis techniques are applied (Jiang and Logan 1996). Microscopy relies on the examination of the aggregates with two dimensional fractal dimension taking values less than 2 (Bushell and Amal, 2000; Chakraborti et al., 2003).

$$P \propto l^{D_1} \quad (3.7)$$

$$A \propto l^{D_2} \quad (3.8)$$

$$V \propto l^{D_3} \text{ or } N \propto l^{D_3} \quad (3.9)$$

where:

l – the maximum aggregate length

A – the projected aggregate area

V – the solid volume

N_a – number of particles in the aggregate

D_1, D_2, D_3 – fractal dimensions

Another tool for characterizing the fractal dimension is based on small angle laser light scattering (LALLS) (Guan et al., 1998a; Waite, 1999; Wu et al., 2002). Changes in the

biological floc structure due to modifications of the process parameters such as cations or polymers addition (Guan et al, 1998a; Cousin and Ganczarczyk, 1999) or different turbulent regimes (Li and Logan, 1997; Spicer et al. 1998; Serra and Logan, 1999; Wilén et al, 2003) were found to correlate well with those observed in fractal dimension.

The rate of aggregation has been observed to have a considerable influence on the fractal dimension. Larger fractal dimensions may be obtained for aggregates formed under reaction limited aggregation (RLA) conditions as compared with those obtained under diffusion limited aggregation (DLA) conditions. DLA implies that there is no repulsion between colliding particles and then each collision leads to an attachment. RLA emerges when there is inter-particle repulsion and the collision efficiency between particles is reduced (Gregory, 1997). Waite (1999) reported fractal dimensions in the range of 1.7 –1.8 for flocs formed under DLA conditions while for RLA the typical fractal dimension values range is 2.2-2.3. Of high importance is the aggregation mechanism involved in floc formation, which as shown by Gregory (1997) can be particle–cluster aggregation or cluster–cluster aggregation. For the case of particle-cluster aggregation, it is assumed that the particle may easily penetrate into the cluster before encountering another particle. This leads to a dense structure, which in general is characterised by high fractal dimension values in the range of 2.5 up to 2.6. However, a more realistic aggregation model is that describing the cluster–cluster aggregation. This usually leads to a more open structure with a fractal dimension of around 1.8 for the case of DLA and of around 2.1 for RLA.

3.3. Activated sludge floc morphological properties: Measurement techniques

Due to the very broad floc size distributions and to the very fragile and heterogeneous structure of the floc, size measurements turned out to be a very difficult task. Often contradictory results are reported in literature, which is mostly due to the different measurement principles of the devices used to perform the analysis. Moreover, during sampling and the measurement procedure itself, it is difficult to avoid possible alterations of the activated sludge flocs. Extremely important as well is the treatment to which the flocs are exposed before being analysed, since sample dilution are often required to make possible the size measurements.

An excellent review of the most used sizing techniques has been presented by De Clercq (2003). In this section, a general overview of the methods reported in literature is presented and the measurement principles are shortly described and evaluated. Emphasis is put on detecting the main advantages as well as the drawbacks of each technique with regard to its suitability to perform activated sludge floc size and size distribution measurements. Finally, the sizing devices used in this study are presented and a motivation for their selection is given.

3.3.1. Sizing techniques

A very diversified range of commercial sizing techniques is available. The differences between them usually consist in the measurement principle and/or in the size detection range. An important step in the selection of a device is to point out the most important conditions that should be fulfilled for achieving the measurement goal. For performing the size measurements of the activated sludge floc, the following criteria were considered for selecting the sizing device:

1. The technique should allow the measurement of a broad size range as it is often found to be the case for the activated sludge flocs.
2. The sample preparation should not require special treatments, as it may create severe alterations of the flocs' properties.
3. The measurement procedure itself must not exert significant shear forces or other obstructions that may create structural change of the flocs.
4. The sizing techniques allowing on-line or on-situ measurements are preferred for the quantifications of the floc size dynamics.

Techniques such as sieving or sedimentation were excluded from beginning since they are not appropriate for a flocculation process evaluation (Kusters, 1991).

For convenience, the sizing techniques are classified and described based on their measurement principle. In this way, a separate technique is the microscopy connected to an image analysis system. The other techniques can be divided as suggested by Allen (1997) in two categories: stream scanning and field scanning. A short overview of each of the considered methods is presented below.

3.3.1.1. Microscopy and image analysis

Optical microscopy is reported as a good tool for the determination of the floc size and size distribution (Parker et al., 1971, Sezgin et al. 1978, Galil et al. 1991, Barbusinski and Koscelniak, 1995). It represents an excellent technique for directly examining the individual flocs size, shape and structural properties.

However, manual microscopy requires elaborate sample preparation and only a few particles can be examined at once. Due to this, the technique is known as time consuming, since for a statistical relevant determination of the number based size distribution it requires the analysis of at least five slides containing minimum 500 particles in total (Vigneau et al., 2000). For a mass distribution evaluation at least 25 particles in the largest size category (Allen, 1997) are necessary. When using the microscopy a size analysis by number is recommended to be performed instead of an analysis by mass. One of the most important limitations is its small depth of focus resulting in only a few particles in focus in any field of view for samples having a wide range of sizes, as is the case for activated sludge. It may be concluded that manual microscopy represents a slow and tedious technique, which can give rise to considerable error when size distributions are of interest.

More recently, by connecting the microscope to automated image analysis software, a faster evaluation of the activated sludge floc properties became possible. As a general definition, the image analysis consists in the digitisation of an image to a grid of image elements or pixels, the measurement of the intensity of the light in each point, either in grey scale or in full colour and the interpretation of these data (Russ, 1990).

The introduction of automated image analysis systems has virtually eliminated manual methods. Initially, the image analysis consisted basically in the connection of the microscope to a video camera that was further linked to image analysis software. Sample preparation remained however similar to the one used for manual microscopy.

The automatic image analysis requires dispersed particles, which are clearly separated from each other so that the analyser is not confused by touching particles. Agar and resin embedded samples (Cousin and Ganczarczyk, 1999) or slide disposal (Dagot et al., 2001; Motta et al., 2002) are the most used methods for activated sludge sample preparation.

On-line techniques were developed recently based on on-line image analysis. Grijspeerdt and Verstraete (1997) built up an on-line image analysis system for activated sludge flocs properties evaluation by pumping the sample through a flow cell connected to the microscope. Another on-line technique for rapid determination of the FSD was introduced by Sievers et al. (2003). It consists in scanning the acquired images line by line by using a CCD-line scan camera. The grey-scale line scanned was transformed into a binary image and the FSD have been generated in terms of cumulative length distribution. The method showed to be fast enough for on-line monitoring and no sample preparation was needed.

On-line image analysis may be considered a suitable and very promising technique for evaluation of the activated sludge floc size and size distribution, as it allows, together with the size determination, to visualise the sample and to evaluate the shape of the floc. These are considered as being important advantages, which are often not available with other sizing techniques. One of the main drawbacks of on-line image analysis is the size detection range which is limited to the magnification of the lens used. In general, optical microscopy restricts the small size range limit to about 3 μm . The theoretical lower limit is approximately 0.2 μm but the diffraction halo around the particle gives a gross overestimation of the particle size (Allen,1997). Grijspeerdt and Verstraete (1997) restricted the measurements to flocs larger than 10 μm in order to have a statistically correct evaluation of the FSD.

3.3.1.2. Stream scanning methods for particle size measurements

Stream scanning methods allow to examine the particles one at a time and their interaction is taken as a measure of their size. Stream scanning is generally limited to low concentration suspensions and suits better for the determination of the size distribution by number. According to Allen (1997), the conversion of a number distribution to mass or volume distributions can result in large errors unless the width of the distribution is narrow. Consequently, in order to obtain accurate volume distribution data, it may therefore be necessary to size millions of small particles in order to get a statistically acceptable count at the coarse end of the distribution. The streaming systems are based on different principles and accordingly various commercial devices can be found in this category.

A few of the most used devices based on stream scanning methods are presented below with an emphasis on activated sludge floc size measurements.

Electrical particle counters

The electrical sensing zone method (the Coulter principle)

The Coulter principle is based on the determination of the number and size distribution of particles suspended in an electrolyte solution, which is drawn through a small aperture. The voltage applied across the apertures creates a sensing zone. Each particle, passing through the aperture dislocates its own volume of conducting liquid creating an increase of the aperture impedance. The change in the electrical impedance generates pulses that are directly proportional to the volume of the particle that produced it. The generated pulses are amplified, sized and counted from the derived data and the particle size distribution is determined.

A relatively large size range may be used for performing the particle size analysis, which generally ranges between 0.4 and 1200 μm . In order to cover the whole range, a number of different apertures is required. The operating range of each aperture is from around 2% to 60% of the orifice diameter (e.g. from 2 to 60 μm for a 100 μm aperture). Moreover, if particles are larger than about half of the aperture diameter they give an increasingly non-linear response and tend to block the aperture.

It seems therefore that for particles with a size range as wide as that of activated sludge flocs is necessary to use multiple apertures. Using only one aperture (200 μm) Andreadakis (1993) analysed the floc ranges from 2 μm to 75 μm , which represents a rather limited size range for biological flocs.

Although it is considered an easy and reliable technique for many applications the Coulter technique is hardly suitable for biological floc size measurement. The main disadvantages are:

- *Sample suspension in electrolyte.* Usually the electrolyte consists of a highly concentrated solution of NaCl. Zita and Hermansson, 1994 showed that the changes in salinity alter the ionic composition of the medium and affect the electrostatic interactions, while Cousin and Ganczarzyk (1998) found that by increasing the NaCl concentration formation of the larger flocs was detected. Moreover, when the divalent cations are present within the floc structure, an increase in the concentration of Na^+ ions has been found to decrease the floc stability and the bacterial adhesion via an ion exchange mechanisms (Higgins and Novak, 1997a). It is therefore suggested that the electrolyte creates changes in the floc size, which may affect the reproducibility of the results.
- *Changing and clogging of the aperture.* It is not possible to perform a wide size range measurement with only one aperture. When passing through the aperture, the flocs are exposed to considerable squeezing forces. Also aperture clogging can occur due to the presence of large flocs. It is likely that measurement errors will occur due to breakage and compression of the flocs. Because of these limitations, the Coulter technique is preferred only for small particles and in stable environments (Li and Ganczarzyk, 1991).
- *On-line measurements.* The available devices are suitable only for small sample volume measurement and on-line or in-situ measurements are not possible.

Optical particle counters

Considerable design approaches are available for optical particle counters. In general, the instruments' response depends on particle size, particle shape, particle orientation, the wavelength of the light, liquid flow rate or the relative refractive index between the particle and its surroundings. Due to the very diverse instruments market and measurement principles only two devices will be discussed further in detail namely, FBRM (Lasentec, USA) and CIS-100 (Ankersmid, Belgium). According to literature, these two devices are the most suitable for particles analysis in wastewater treatment.

The focused beam reflectance measurement – FBRM (Lasentec, USA)

The main advantage of this method as compared to the other is that it allows in-situ measurements of the particle size at high solids concentration, i.e up to 50 g/l (De Clercq, 2002a). The device consists in a FBRM probe, which projects a laser beam through a sapphire window. The beam is highly focused and illuminates individual particles in its path. As particles pass by the window surface, the focused beam will intersect the edge of a particle and the laser light will be backscattered by the particle. The backscattered light pulses are picked up by a non-scanning stereoscopic detection system. The size of each particle is determined by measuring the time that the particle is in the beam. Hence the size is recorded as a chord length. Typically, thousands of chords are measured per second and the generated results are in a number-by-chord length distribution. The available devices can cover a size range between 0.5 μm and 2.5 mm.

Due to its in-situ measurement capabilities the FBRM method has a wide range of application in different particle characterization fields. Recently, the method also gained interest in the field of flocculation processes (Blanco et al., 2002) for the characterisation of the particle size distribution in activated sludge clarifiers (De Clercq et al. 2002a,b); biofilm detachment (Choi and Morgenroth, 2003) or microbial hydrolysis of particulate organic matter (Michaud and Morgenroth, 2003).

A FBRM M500 device was successfully used by De Clercq et al. (2002a) to measure the activated sludge floc size distribution in-situ in a secondary clarifier. The authors demonstrated the devices' applicability for a wide range of solids concentrations. It was also shown that for reliable results the device needs a careful manipulation and a few issues should be treated with special attention:

- The most important aspect is the focal point of the laser beam. It was found that by changing its position different size distributions were obtained. It was further demonstrated that in order to achieve reproducible results, the focal point should be put near the optical window.
- The particles' velocity in the suspension medium should be high enough to avoid particles to reside on the sensor window. A small mixing device placed in front of the optical window could avoid the occurrence of this phenomenon. Note that attention should be paid to its influence on the flocculation process.
- The horizontal positioning of the probe is preferred for the case in which particle sedimentation is followed.

Due to its in-situ measurement capabilities of highly concentrated samples, the FBRM device seems to be an excellent and appropriate technique for following the activated sludge (de)flocculation processes. Moreover, the short time interval required for generating a size distribution (10 sec.- Choi and Morgenroth, 2003) demonstrates the capability of this technique to monitor the floc size dynamics. It may therefore be concluded that this technique satisfies all requirements initially imposed for the purpose of this study, if precautions are taken in order to avoid the main drawbacks listed before, which may lead to a misinterpretations of the results.

Time-of-Transition – TOT (CIS devices)

For the CIS devices manufactured by Ankersmid N.V. (Belgium) a few models are available. Two measurement techniques are combined in the same instrument. One technique is known as Time-of-Transition, while the other one consists in a CCD video camera, which allows for an on-line image analysis.

Since the advantages and high applicability of on-line image analysis were discussed separately in this chapter, only the TOT principle is shortly discussed here and its suitability for activated sludge floc size measurements is investigated.

Basically, the measurement principle is based on a rotating laser beam that scans the single particles within its focus. The diameter of the particle is directly correlated to the time spent by the scanning beam on a particle, which is called time-of-transition. In contrast to the zone-counters, the size is determined by the pulse width and not by the pulse height.

Compared with the first generation of devices (CIS-1) which were considered as relatively slow, in the last years significant improvements have been made to this techniques. These increased the device accuracy and the measurement speed (Weiner et al., 1998).

Even with the above mentioned drawback the CIS-1 device found wide applicability especially for characterising the size of biological flocs and organic materials. This is mainly due to several advantages as compared to other techniques:

- Measurements are performed on individual particles.
- Particles refractive indexes are not required for the measurements.
- Problems of orifice clogging are avoided by using interaction pulse analysis to provide an optically defined measurement zone, rather than a mechanically defined orifice.
- Interchangeable sample cells allow the analysis of a wide variety of samples. In between them, a liquid flow-through cell accessory allows on-line measurements.

Tsai and Rau (1992) found that CIS-1 device represented the only laser-based device that satisfied the requirements for performing the size measurement of suspended particles in oceans. It was demonstrated that the device did not cause significant breakage or aggregation of the analysed particles and the results had a high reproducibility. The only limitation found was the relatively limited size range (0.5 –150 μm). However, this does not represent a problem with the new devices (CIS-50 and CIS-100) since they cover a size range from 0.5 to 3600 μm , which may be acquired by just changing a single lens.

In wastewater treatment the size measurements performed with CIS devices were used successfully for different purposes.

Hiligardt and Hoffmann (1997) used a CIS-1 to characterise activated sludge floc settling properties. Neis and Tiehm (1997) and Tiehm et al. (1999) analysed the particle size distribution of primary and secondary clarifiers effluents by using a CIS-100. The results showed to be reliable and specific distributions were found for different wastewater treatment plants.

However, as for most counting techniques, the accuracy of the measurements increase when the particle size spectrum is narrower (Tsai, 1996). This disadvantage can be avoided by counting a high enough number of particles, which allows to obtain a statistically correct size distribution. For highly concentrated samples, which is the case for activated sludge samples, this technique requires dilution for a correct measurement. The recommended sample concentration as given by the manufacturer, is up to 10^9 particles/cc (for 1 μm particles).

This technique is suitable for the objectives of this study, since it satisfies almost all requirements. Attention should be paid to the sample dilution when necessary. However, this is a drawback of almost all available counting devices except for the in-situ devices.

3.3.1.3 Field scanning methods for particle size measurement

Field scanning methods measure the size distribution of an ensemble of particles and are widely recognized as best suited for performing on-line analysis.

Low angle laser light scattering (LALLS)

Low angle laser light scattering devices are the most popular techniques reported in literature. Thanks to the principle's on-line measurement capabilities and rapid measurement performance this technique is often used to control and evaluate processes such as crystallisation, flocculation or precipitation.

The LALLS devices operate by predicting the light scattering behaviour of particles that scatter light in all directions with an intensity that is dependent on their size. The scattering

pattern is described by taking into account that the particles are optically homogenous and spherical. For deconvoluting the scattering pattern two optical theories, namely the Mie and the Fraunhofer may be used to yield the unknown size distribution. The Mie theory requires knowledge of the optical properties (refractive indexes) of the particles and suspension medium. The Fraunhofer theory is limited to particles that are in general opaque or large as compared to the wavelength of light and hence the diffraction is considered.

Spherical monosized particles give an enhanced diffraction pattern. Non-spherical particles are measured over all orientations and this causes a broadening in the measured size distribution. Moreover, textured particles tend to give enhanced weighting to the fine end of the distribution (Allen, 1997).

The obtained distributions are volume based. A very broad size distribution can be measured by using LALLS devices, which can go from a lower size of about 0.04 μm to up to 3 500 μm .

In recent years many studies reported the use of LALLS devices for the characterization of the activated sludge floc size distribution. Such techniques were applied for on-line determination of the changes in floc structure such as fractal dimension (Waite et al., 1998; Wilén et al., 2003) or direct size distribution (Biggs, 2000; Chaignon et al., 2002). It was demonstrated that this method represents a fast and reliable technique for determining the size of flocs, covering a relatively wide floc size range. Moreover, it allows to follow the flocculation dynamics and the data were already used to model the activated sludge flocculation/deflocculation process by using a population balance approach (Biggs, 2000; Nopens et al., 2002).

The main drawbacks consist in the requirements for sample dilution, since a too concentrated sample may lead to multiple scatterings and also in the difficulty to determine the optical properties of the biological flocs.

Several devices are commercially available and sometimes considerable differences exist between the instruments, both from a hardware and software point of view, thus making it difficult to compare and interpret data generated by different instruments (Allen, 1997). Among the most used devices for monitoring and evaluating the dynamics of the processes are the Mastersizer devices (Malvern, UK) (Guan et al. 1998; Spicer et al., 1998; Houghton et al., 2002). These are preferred due their highest reproducibility of the data as found by Allen (1997) when a set of more than 25 devices was investigated by using standard quartz powders.

3.3.1.4. Conclusions

Several techniques using different measurement principles were considered and their suitability for following the activated sludge flocculation dynamics was assessed based on their characteristics.

It is concluded that each device has both advantages and drawbacks, inherent to the measurement principle and a perfect technique is difficult to be found. Therefore, some compromises are necessary while selecting a device.

Accordingly, the following conclusions have been drawn, which provided the basis for the selection of a few instruments fulfilling the purposes of the present research.

- An on-line image analysis system gives an indication of the shape of the flocs, which may be necessary for understanding the results and allows a direct visualization of the samples. However, this technique may not be fast enough to allow a statistically correct evaluation of the rapid floc size dynamics which may

take place. This problem may occur especially when very large size particles are formed. This leads to a considerable decrease of the number of particles that may be counted on each image and then a large number of acquired images is necessary.

- A relatively wide particle size range characterises the devices. However, for most of them and especially for the counting techniques this can only be obtained by interchanging the lens, which is not convenient for on-line analysis when floc size dynamics is followed. Due to this, the devices allowing wider size range measurements by using only one lens are preferred. This feature is characteristic usually to the LALLS devices, but special attention should be paid when considering these devices for analysis of smaller size particles, since the Mie theory is difficult to be applied to biological flocs.
- Only the FBRM method has the capability to measure the floc size distribution in-situ at high enough concentration. This technique however requires special care in manipulation especially with regard to the correct positioning of the focal point. For on-line measurements, the LALLS techniques proved to have high reproducibility and to be reliable for fast measurement of the floc size dynamics.
- It may be however of high interest to also consider a counting device which would allow for a direct evaluation of the number distribution as the process takes place. Therefore, combining two sizing devices with different measurement principles allowing a direct evaluation of the number and volume distributions may represent an interesting opportunity for evaluating the activated sludge flocculation dynamics and validating the results. Allen (1997) carried out a comprehensive study, investigating the accuracy and precision of many particle size measurement instruments. It was shown that the laser diffraction technique is more precise than other particle sizing techniques. In contrast, the counting and sedimentation techniques are more accurate than the light scattering techniques (especially at the tails of the distributions). Knowledge of the particles number and concentration are however required for model implementation, including the new PBM approach (Biggs, 2000). This will avoid the artefacts occurring when a volume-based distribution is transformed to number distribution.

Taking into account all the above considerations and also their easy availability a MastersizerS (Malvern, UK), a CIS-100 (Ankermid, Belgium) and an image analysis system developed in house by using LabView (National Instruments, USA) were chosen in this study. All considered devices allow on-line sample analysis due to their flow-through-cell capabilities and similar requirements for sample dilution. It is therefore considered that connecting all these devices in series, the samples will be treated in the same way and then information regarding particles volume, number and shape will be obtained for the same sample.

3.3.2. Techniques used in this study for on-line measurement of floc size distribution and fractal dimension

A detailed evaluation of the devices used in this study will be given in this section. The intention is also to point out some features and characteristics of these devices, which should be taken into consideration for the activated sludge flocs investigation.

3.3.2.1. MastersizerS

The MastersizerS uses a low power He-Ne laser of wavelength of 632.8 nm to form a collimated and monochromatic beam of light of maximum 18 mm in diameter. It is referred to as the analyser beam since it interacts with the particles causing the light to scatter. A lens forms the far field diffraction pattern based on the principle that particles in a laser beam scatter the laser light at angles that are inversely proportional to the size of the particles. In this way, large particles scatter at small forward angles while small particles scatter light at wider angles.

The device utilises two forms of optics based on a "conventional Fourier" or "reverse Fourier" approach. The second is used to allow the measurement size range to be extended down to 0.05 μm . By using Fourier optics, this scattering is imaged to an array of detectors at the focal plane of the optics. There is a direct relationship between the distribution of the scattered light energy on these detectors and the particle size distribution.

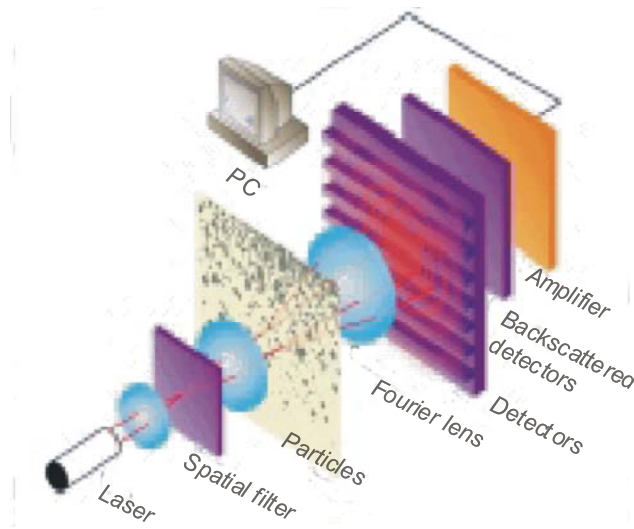


Figure 3.3 The measurement principle of Mastersizer S (Malvern, 2004).

To calculate the size distribution the MastersizerS uses Mie theory. For particles smaller than the wavelength of the incident light, the Mie theory is reduced to the Rayleigh-Gans theory. When particles are larger than the wavelength of the incident light, the Mie theory reduces to the Fraunhofer theory. Therefore, for particles larger than 10 μm Fraunhofer diffraction theory may be used. The angular distribution of a light flux $I(\theta)$ for a single opaque spherical particle, as given by the Fraunhofer equation is shown in equation (3.10) in terms of the Bessel function $J_1(\theta)$ (Allen, 1997):

$$I(\theta) = I(0) \left[\frac{2J_1(\alpha\theta)}{\alpha\theta} \right]^2 \quad (3.10)$$

Where $I(0)$ is the intensity of the incident beam, $\alpha = \pi D/\lambda$, D is the particle diameter and λ is the wavelength of light in the surrounding medium. For a distribution of particle sizes, equation (3.10) becomes:

$$I(\theta) = I(0) \int_0^{\infty} \left(\frac{2J_1(\alpha\theta)}{\alpha\theta} \right)^2 f(D) dD \quad (3.11)$$

In two situations the Fraunhofer assumption can not be applied. The simplest situation occurs when very small particle sizes have to be analysed. As the particle diameter approaches the

wavelength of the incident light, the interaction between light and particle becomes more complex. The second situation occurs when the differential refractive index is low. This rarely occurs in normal measurements due to the commonly occurring ranges of dispersing fluids and solid particles (Malvern, 2004).

In the small particle range (lower than 10 μm), the refractive index dependence becomes significant due to the fact that at such small sizes the light coupled into the particle is not completely absorbed and can emerge as a refracted ray. The Mie theory specifies an increase in forward light scatter intensity with particle size, refractive index of particles and dispersion medium (van de Hulst, 1981). In this case the Mie theory may be simplified to the Rayleigh-Gans approximation.

For the particular case of analysing the activated sludge floc size the optical properties are difficult to be considered and only the Fraunhofer theory can be used (Biggs, 2000). Due to this, errors in the small range particle measurements may be expected. To illustrate the differences, which may occur different FSD's were generated for one single measurement by using different real refractive index values (Figure 3.4) or different imaginary refractive index values (absorbance) (Figure 3.5). For generating the results, reported literature data were taking into consideration.

The dispersed medium of the particles was filtered effluent (0.45 μm). Biggs (2000) found that the refractive index of the effluent was the same as that of water (1.33). Guan et al. (1998) mentioned that the refractive index of the biological systems may be considered as being 1.05. Moreover, a refractive index of 1.04 was found for bacteria (Robertson et al., 1998) and for bacterial film (Busalmen et al., 1998). Twardowski et al. (2001) reported an imaginary index (absorption) taking values between 0.001 and 0.1 for bulk particles found in ocean waters. The same numbers are reported by Malvern (2004) for the organic materials.

Figure 3.4 and Figure 3.5 clearly show that significant differences occur in the small size ranges between the results generated by Fraunhofer and Mie theories even under small variations of the refractive index values. It is however difficult to correctly approximate the characteristic values for biological flocs. Therefore, the Fraunhofer theory is preferred but attention should be paid to the interpretation of the small size class results.

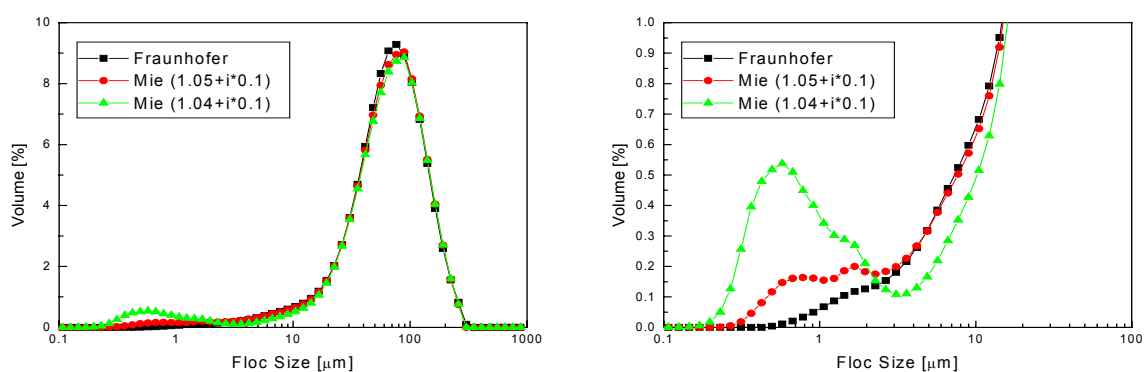


Figure 3.4 FSD generated for one single data set by using Fraunhofer and Mie theories with different real refractive indices. ($m+im'$ – where m is the real refractive index and m' the imaginary refractive index). Whole distribution (left) and detail in the small size classes (right).

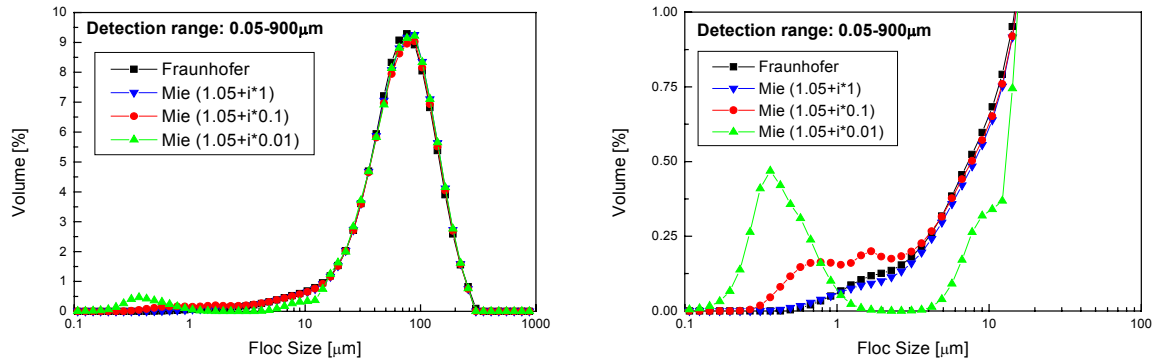


Figure 3.5 FSD generated for one single data set by using Fraunhofer and Mie theories with different imaginary refractive indices . Whole distribution (left) and detail in the small size classes (right).

As shown in Table 3.3 two different lenses may be used to perform the measurements with the MastersizerS .

Table 3.3 The size detection range of MastersizerS

Lens	300RF (Reverse Fourier)	1000 (Fourier)
Size Range [μm]	0.05-900	4-3500

Another point to be considered while interpreting the results from laser diffraction is that the size distribution derived by this technique is volume based expressed as volume proportion in each considered size class in the total volume of the particles. The most reported diameter used to describe the size distribution is the volume (mass) moment mean diameter ($D[4,3]$) (see Table 3.2).

One of the major drawbacks of this device, as well as all laser diffraction devices, is the necessity to dilute the sample prior to analysis since a too concentrated sample leads to multiple scattering. To control the dilution the obscuration level is used.

If the amount of sample added is too low, the obscuration is low, leading to noisy data. If the sample concentration is too high then light scattered from a particle may be scattered again by a second particle. Obscuration (equation (3.12)) is expressed in percents and an optimal range for the MastersizerS is between 10-30%.

$$Ob = 1 - \frac{L_s}{L_b} \quad (3.12)$$

Here L_s is the light intensity measured in the central detector when a sample is present in the cell and L_b the light intensity measured with clean dispersant.

If attention is paid to the small size range measurements and to the sample dilution the MastersizerS may be considered as being a suitable technique for fast monitoring of the floc size dynamics, as already proved by Biggs, 2000.

3.3.2.2. CIS-100

The CIS-100 device combines a laser channel, which provides size measurements based on the time-of-transition (TOT) principle, with an image analysis channel which allows a dynamic size and shape characterization (SHAPE) (Figure 3.6).

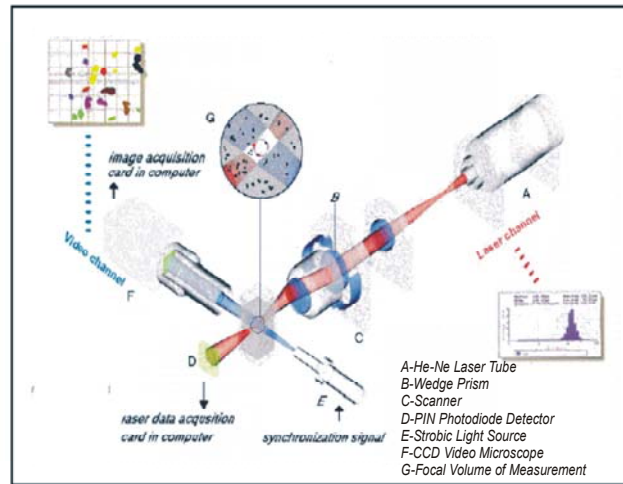


Figure 3.6 Measurement principle of CIS-100 (Ankersmid, 2004).

The laser channel (TOT)

The measurement set-up (Figure 3.7) consists in a collimated He-Ne laser beam (wavelength $\lambda = 632.8 \text{ nm}$) (A), which performs circular scanning by a rotating wedge prism (C) (angular frequency $\omega = 2\pi\nu$) of the sample measurement volume (G).

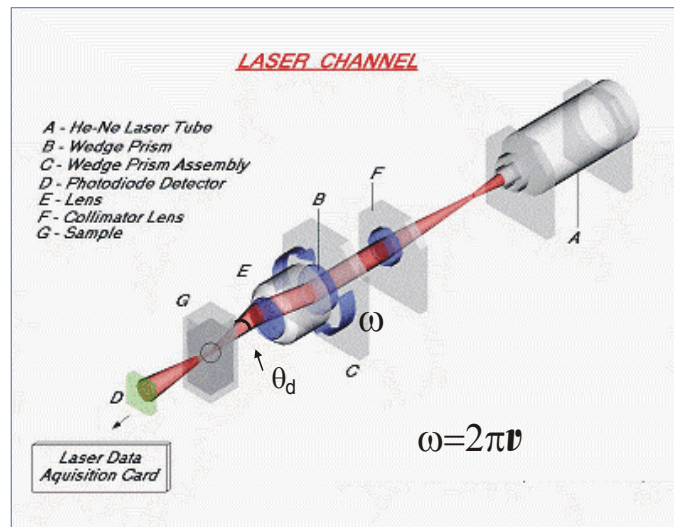


Figure 3.7 Basic optics for TOT method (Ankersmid, 2004).

When the laser beam passes through the wedge prism, it deviate from the optical axis by the deflection angle θ_d . A lens (F) focuses the beam down to a spot size of $1.2 \text{ }\mu\text{m}$ using a collimated lens (F) of a focal length (f). As the particles within the sample volume are individually bisected by the laser spot, interaction signals are generated. These signals are then detected by a PIN photodiode (D). The signal on the photodiode is lower during the time when the beam is crossing the particle. By measuring the pulse width (Δt) (Figure 3.8) and multiplying by the tangential velocity, $v_T = \omega f \tan \theta_d$ the distance the beam travelled across the particle may be determined. Since the beam rotates at a constant speed, the size of each particle can be calculated from the duration and form of the beam obscuration signal. The time of obscuration (TOT) is directly related to the particle diameter by equation (3.13).

$$D = v_T \times \Delta t \quad (3.13)$$

where:

D – particle diameter

v_T – tangential velocity of the laser beam

Δt – Time of Transition

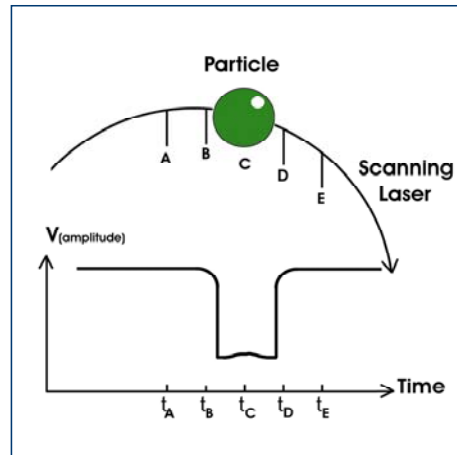


Figure 3.8 Particle size measurement based on TOT (laser beam – particle interaction).

Compared to the high speed of the rotating laser, the particles are nearly stationary. This eliminates possible errors due to particle movement. Moreover, the device has a relatively high resolution since the measurements are made on individual particles.

The interaction signals are collected by a data acquisition card and analysed in 600 discrete size intervals. Pulse analysis algorithms are employed to reject out-of-focus and off-center interactions.

The TOT measurement covers a size range of 0.1 - 3600 μm . Two lenses are available, each of them covering two different size intervals as shown in Table 3.4

Table 3.4 The size range available for laser channel of CIS-100 device

Lens	Size range (μm)	
A	0.1 – 300	2 – 600
B	2 – 600	10 – 3600

The technique allows an easy adaptation to different size ranges by changing the focal length, the deflection angle and the rotational frequency.

For on-line analysis a liquid flow cell GCM-104A (Ankersmid, Belgium) with a cross section of 1 cm x 1 cm may be used. The available software allows to perform repetitive measurements in which the frequency in time of the performed measurements as well as the number of the experiments to be performed may be set by the user.

It is important to correct charge the device settings according to the sample properties. In this sense, the transparency of the particles is an important issue to which the device is very sensitive. Therefore, in order to make the size determination independent of the particle opacity it is necessary to correctly select the so called "*samples modes*". The following options are available:

The "Regular" mode is specific for materials that are neither completely opaque, or not completely transparent.

The "Special" mode is recommended for transparent materials or a mixture of transparent and opaque materials.

The "Super regular" mode is a working mode for particles that are absolutely opaque.

For activated sludge floc analysis the "Special" mode was used. For this case, attention is paid to the interpretation of the volume-based results, where in certain conditions the "Special" mode may interpret two very close opaque particles as one transparent particle producing a second peak in the displayed data. When using the "Super Regular" mode, the detection algorithm does not perform the transparency check, which can be an important issue in view of the activated sludge structure. When working in "Regular" mode, the small and transparent particles can be rejected.

An indication about the concentration range of the sample is given by using the Signal Normalisation Factor (S.N.F) and Solution Density Uncalibrated (S.D.U.).

The S.N.F. represents the light intensity reaching the cell's particle detector. The particles obscure light from the laser beam. When the S.N.F. is relatively low it indicates that the dispersion is over-concentrated or the particles are transparent. A high number indicates an under-concentrated solution or compact particles. Usually, the S.N.F. takes values between 0.5 and 1.0 when "Regular" mode or "Super Regular" mode are used and between 0.39 and 1.0 for "Special" mode.

The S.D.U. represents a relative measurement of the concentration of particles in the mixture, as an expression of the total number of particles per unit volume (depending of a size of particles). It is based on the number of interactions between the laser beam and particles and it is proportional to the sample concentration.

It may be concluded that the TOT method can be applied for analysis of the activated sludge flocs. Counting the particles one-by-one with no need for knowledge of the particles refractive indexes represents the major advantage of this method. If the sample has a broad distribution ranges the measurement time may increase in order to obtain statistical relevant information. However, sometimes the samples must be diluted.

The image analysis channel (SHAPE)

The video channel of the CIS-100 (SHAPE) is an alternative analysis channel that allows for size and shape characterisation that can be performed by acquiring images of moving particles and analysing them with the provided image analysis software.

Two-dimensional shape information is essential for the true characterisation of non-spherical particles and aggregates. In order to perform this, the CIS-100 device uses an automatic image analysis system. A CCD video camera microscope provides images for processing. Acquired images are passed to a frame-grabber card for analysis and are then displayed on a monitor for viewing.

Features such as rejection of out-of-focus particles, separation of touching particles and automatic light correction enable optimisation of the sample measurement. Software algorithms allow for the calculation of a variety of characteristics including different size diameters, area, perimeter, shape factor and aspect ratio. The device also allows selection of different lenses with varying objective magnifications as summarised in (Table 3.5)

Table 3.5 The size range available for the image analysis channel of the CIS-100 device.

Lens	Field of view (μm)	Size range (μm)
CW	430	2-150
DW	1400	10-600
EW	5400	20-3600

3.3.2.3 Image analysis (IMAN)

Setup description

An image analysis system (IMAN) was developed for automated investigation of the floc size and shape parameters. Basically, the IMAN setup components and the measurement principle can be described as follows:

Images of activated sludge samples are taken using a CX40 optical microscope (Olympus, Japan) connected to a ICD-46E CCD camera (Ikegami Electronics Inc., USA) and digitised with a frame grabber PCI-1411 (NI, USA). The digitised images are processed on a PC, by means of specific software developed in LabView 6i (NI, USA). A 4x-magnification lens is used in measurements and in order to enlarge the image view on the PC a 0.35x C-mount adapter (Olympus, Japan) was placed between the CCD camera and the microscope resulting in an image window of size 4.5 mm x 3.5 mm. In this way, a relatively large number of particles can be observed in a single picture. The major drawback of this choice is related to the detection of small size particles, due to the limited resolution (1 pixel = 5.81 μm). A quantification of the particles shape is difficult to be carried out at this low magnification. According to Pons et al. (1999), to allow a correct shape evaluation at least 400 pixels per object are necessary. Hence, a 10X- magnification lens (1 pixel = 2.37 μm) or 40 – magnification lens (1 pixel = 0.50 μm) may be used for characterising the shape of enough large particles. However, attention should be paid to the case of activated sludge in which a broad range of the floc size may create difficulties in a precise estimation of the shape characteristics. For calibration, a calibration grid MIC110 (VWR, Belgium) was used.

To carry out the automatic measurements, the sample flow is directed through a rectangular cell (40 mm X 10 mm X 1 mm) fixed to the microscope. Two Sirai – Z110A valves (Bussero, Italy) controlled by LabView allow a automatic flow control by stopping the flow through the cell when an image is acquired. To allow simultaneous measurements by the other devices, the flow is directed via a bifurcation to a tube that is not directly connected to the microscope (Figure 3.9). When an image is acquired the flow stops and a snapshot is taken.

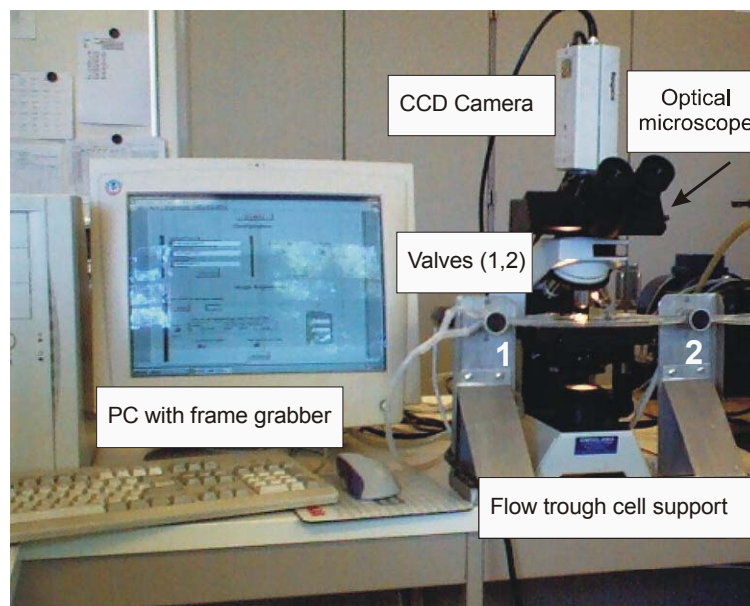


Figure 3.9 The IMAN setup.

IMAN software description

In this section a brief description of the IMAN software is given. Detailed information about the developed software as well as the used procedure may be found in Govoreanu et al. (2003).

For prototyping and testing, the image processing algorithms included in the IMAQ Vision Builder (NI, USA) were used. After prototyping, LabVIEW software was used to implement the algorithm and to perform real-time acquisition, analysis and storage of the images.

The image analysis software consists of 3 main steps as shown in Figure 3.10:

- 1: Configuration – file logging, take the background and the threshold.
- 2: Image acquisition – acquire the images (manual or automated).
- 3: Image analysis – perform the image analysis and save the results.

First the background is automatically acquired and saved by using the dispersed medium of the particles (e.g. filtered effluent 0.45 μ m).

Next, the particles are added to the dispersant medium and a manual threshold operation is performed which enables to select the desired range of greyscale pixel values (Figure 3.11). For a real-time acquisition, an image is taken and the background is first automatically extracted for the acquired image. Once the threshold value is set, it will be used for the coming acquired images. An example of the manual thresholding is illustrated in Figure 3.12. At this step, the valves may be operated manually allowing to choose the most representative image for setting the threshold.

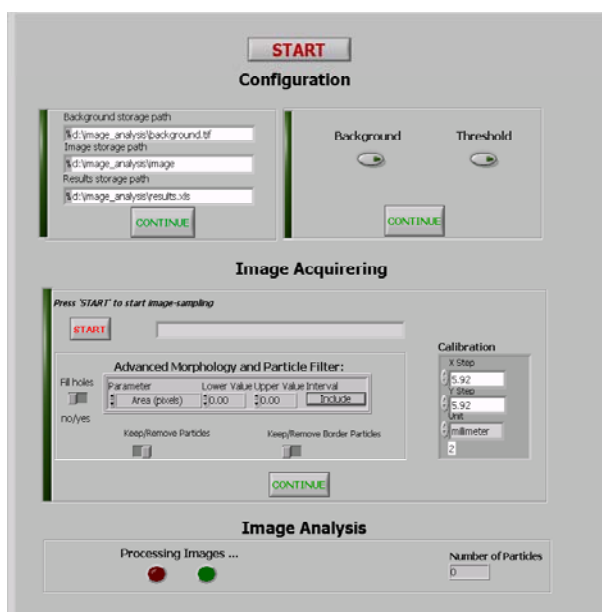


Figure 3.10 The image analysis front panel (LabView, NI)

The threshold consists of segmenting an image into two regions: a particles region and a background region. This process works by setting to 1 all pixels that belong to a grey-level interval, called threshold interval, and setting all other pixels in the image to 0. The manual threshold values, which are set in this way in the configuration menu, are further used for all acquired images. This is based on the assumption that no other changes in the microscope configuration occur after the threshold is set. During the image processing the thresholded images are displayed on the screen.

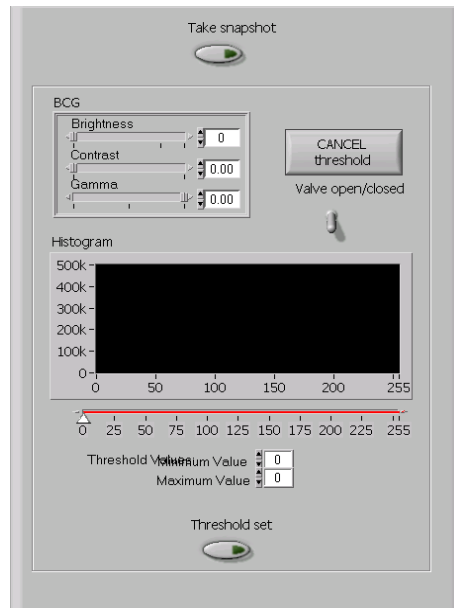


Figure 3.11 The threshold front panel (LabView,NI)

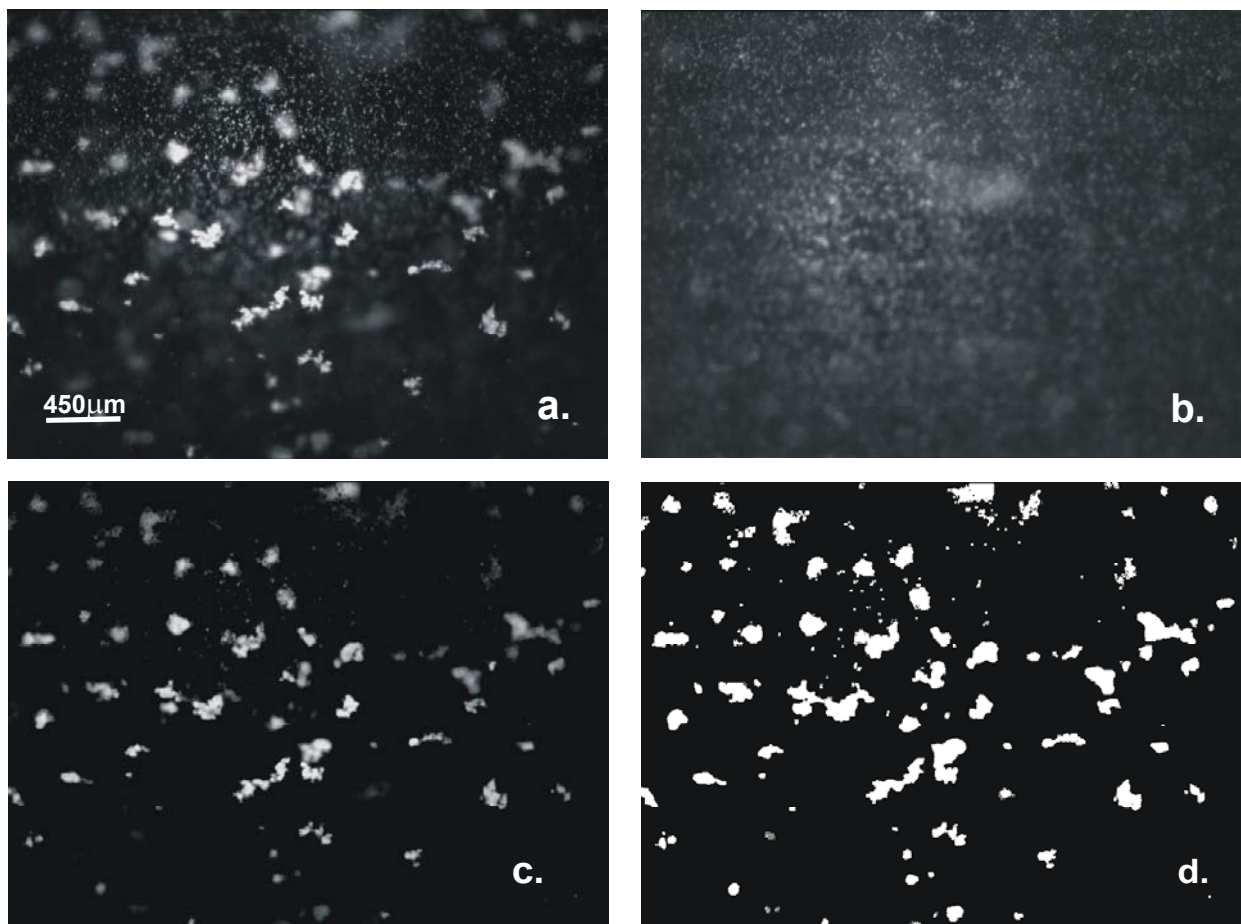


Figure 3.12 Manual thresholding: a. Original image; b. Background; c. Image after background subtraction, c. Thresholded image.

When starting the image acquisition sequence, a dialog box pops up, which gives the possibility to choose either an automated or a manual image acquiring procedure.

The automated image acquisition gives the possibility to set the number of pictures to be acquired and also the images acquisition frequency. When a manual acquisition is selected, it gives the possibility to select the images and save them manually. In case of an automatic image acquisition, the valves are synchronized depending on the time set between two consecutive pictures. For the case of manual acquisition the valves can be closed manually before taking an image.

The following sequence is further applied to each acquired image for performing the image analysis:

1. **Background subtraction** - The acquired background is subtracted from the pictures.
2. The **lookup table** (LUT) transformations highlight details in areas containing significant information and are used to improve the contrast and brightness of an image by modifying the dynamic intensity of regions with poor contrast. A LUT transformation converts input grey-level values into other grey-level values.
 - The *equalize* function alters the grey-level values of pixels so that they become evenly distributed in a defined greyscale range (0 to 255 for an 8 bit image). This transformation is very useful in increasing the contrast in images that do not use all grey levels. The produced image reveals details in the regions that have intensity in the equalization range, while other areas are cleared (Figure 3.13-a).
 - The *exponential* function expands high grey level ranges while compressing low grey-level ranges. Applying an exponential transformation on the image pixels will decrease the overall brightness of the image and will increase the contrast in bright areas (Figure 3.13 -b).

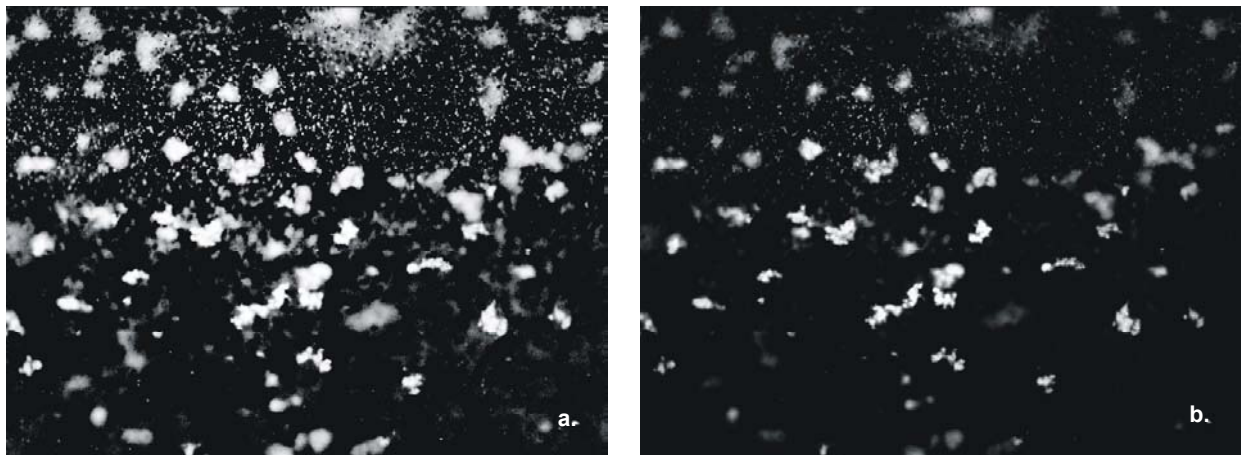


Figure 3.13 LUT transformations: a. Equalize; b. Exponential.

3. The **threshold** values determined before are applied to every acquired image.
4. A simple **calibration** is used to transform the pixels into microns. Calibration is the process of transforming pixels in real-world units. The calibration was performed separately for each available magnification lens by using a calibration grid. The obtained values were recorded in the software, which allows to choose the calibration in function of the used magnification lens.
5. The **advanced morphological operations** give the possibility, if necessary, to remove the particles that touch the border of the image and/or to fill holes inside the particles. These transformations are very useful for preparing images for quantitative analysis.
6. The **particles filter** allows to set the particles size range which are to be analysed.

7. Finally, the *particle analysis* gives information about the size and the shape of the particles, which have been analysed during the image processing. These results are automatically generated and saved.

Typical Results

For generating the results, the features defined in IMAQ Vision Builder were used. There are two basic types of measurements that could be performed on images. The first is a global determination of the image parameters and the second involves measured values for each individual feature that is present. Because the present study aims at evaluating the flocs characteristics, only the second measurement type is taken into account. For convenience, the selected particle analysis parameters are separated in two groups. The first covers measures of size and the second deals with various aspects of particle shape. Within each of these categories, there is a variety of individual parameters that can be measured or calculated from others that are measured directly. From the IMAQ Vision Builder particles analysis application, 21 parameters (Appendix 3-1) are selected and their values are automatically saved in the results file.

- ***Size measurements***

The size measurement results are firstly evaluated starting from the equivalent spherical diameter with the assumption of the particle's spherical shape and secondly from the real size parameters of the flocs (area, perimeter, length, width, i.e.)

- *Size measurements based on spherical assumption*

A linear measure of the size is often more useful than the area and it is common to convert the measured area to the *equivalent sphere diameter*. In the IMAQ Vision Builder software this is named the *Waddel disk diameter* and is calculated by using the equation (3.14).

$$D_s = 2\sqrt{\frac{\text{Particle area}}{\pi}} \quad (3.14)$$

Starting from this diameter the mean floc size diameters may be calculated.

Particle size distributions are further generated as function of number, perimeter, area (with and without holes) and volume function of the equivalent circle diameter.

Distribution parameters and derived diameters are calculated from the fundamental distribution using the summation of the contributions from each size band. In performing this calculation the representative diameter for each band is considered to be the geometric mean of the size band limits.

Particle size distributions are further obtained as function of number, length, area and volume. The distributions are generated as histograms on a semi-logarithmic scale.

The data analysis is performed by using a program implemented in Matlab. Assuming spherical particles the generated image processing results are taken directly from the results file (ASCII type). For an easy comparison with other techniques and also for more flexibility in generating and interpreting the results, the minimum and maximum particles range and also the number of histogram bands can be set. After introducing these data the results are calculated, displayed and also saved in an output file.

- *Size measurements without spherical assumption*

For this evaluation histograms based on frequency number distributions are generated for different size parameters. The most important parameters considered in this case are: the particles area, particles number, particles perimeter, particles length, width, height, longest segment length, mean chord length.

- **Shape factors**

A major category of measurement parameters describes the particles shape. The shape factors are generally dimensionless numbers and usually are obtained by combining size parameters in various ways. For example, Russ (1990) used the *form factor* as being an important shape parameter. It is calculated as:

$$FF = \frac{4\pi Area}{Perimeter^2} \quad (3.15)$$

The form factor is 1 for a perfect circle. Any other shape will have a higher perimeter for the same area and the form factor will describe this increase. For a square the form factor is 0.785, and for more irregular particles it becomes smaller.

The image analysis software (IMAQ Builder Vision) uses the so-called *Heywood circularity factor (HCF)*, which represents the ratio of a particle parameter to the perimeter of the circle with the same area. It is defined as:

$$HCF = \frac{Perimeter}{2\sqrt{\pi Area}} \quad (3.16)$$

As can be easily observed there is a direct relationship between these parameters and in fact they both describe the same property of the particles. For convenience, the HCF was used as a shape parameter for describing the circularity of the particles.

The main use of these shape factors is to compare different forms of the particles. In addition to this purpose, some interpretation of the flocs morphology is sometime immediate from the shape factors. For example, Russ (1990) described that a plot of *form factor* versus some measure of size, such as length, for the entire particles analysed will show a definite trend. If the *form factor* increases with size, it indicates that the particles becomes rounder as they increase in size, and more irregular as they become smaller. This could be an indication that the smaller objects have been produced by fragmentation of the larger ones. Conversely, a trend of decreasing form factor with increasing size often indicates that the larger objects have been formed by agglomeration of the smaller ones.

The *elongation factor* represents the ratio of the longest segment within a particle to the mean length of the perpendicular segment. The more elongated the shape of the flocs, the higher is its elongation factor. It is defined as:

$$EF = \frac{\text{Maximum intercept}}{\text{Mean perpendicular intercept}} \quad (3.17)$$

The ratio of a particle area to the area of the smallest rectangle containing the particle represents the *compactness factor*. It is defined as:

$$CF = \frac{\text{Particle area}}{\text{breadth} \times \text{width}} \quad (3.18)$$

The compactness factor belongs to the interval [0,1]. It shows how close the particle shape is to a rectangle. The compactness factor is 1 in the case of a perfect rectangular shape.

There are a wide variety of shape descriptors available. Grijspeerdt and Verstraete (1997) used the *aspect ratio (AR)* and *roundness (RD)* for shape quantification. These parameters can be easily calculated from the results generated by image analysis.

For an entire population of particles with random orientation the so-called three-dimensional aspect ratio can be estimated based on equation (3.19) It is sensitive (like the elongation

factor) to the extension of an object. The more elongated it is, the larger the value of this parameter. A circle has an AR of one.

$$AR = 1.0 + \frac{4}{\pi} \left(\frac{Length}{Width} - 1.0 \right) \quad (3.19)$$

The roundness (RD) is mainly influenced by the elongation of an object. It looks very much like the form factor but instead of the perimeter, the roundness uses the length of the particle. This makes it more sensitive to how elongated the feature is rather than indicating how irregular its outline may be. The RD varies between 0 and 1. A circle has an RD of one. The RD is calculated as:

$$RD = \frac{4 \cdot Area}{\pi \cdot (Length)^2} \quad (3.20)$$

To conclude, the developed image analysis system represents a useful automated tool, which may be used for evaluation of activated sludge flocs' size and structural properties. Moreover, together with other on-line techniques it provides additional useful information for characterisation of the flocculation process.

3.4. Influence of experimental conditions for on-line determination of floc size and size distribution

In order to develop an experimental technique for on-line monitoring of the activated sludge (de)flocculation dynamics, it is necessary to optimise first the experimental conditions. In this section, the influence of some setup components and of the operating parameters are investigated.

3.4.1. Experimental methods and setups

Sampling: The activated sludge samples were collected from the Ossemeersen domestic wastewater treatment plant (WWTP) located in Ghent, Belgium. The suspended solids concentration was determined to be $X = 4.1 \div 4.5$ g/l. After collection, the samples were stored at 4°C and preserved for a maximum of 3 days.

Size measurements: Floc size measurements were performed by using the MastersizerS. A 300RF lens was used for the experiments, corresponding to a size range 0.05-900 µm. The samples dilution was performed by using filtered effluent (0.45µm) and deionised water. For effluent filtration an Optisep (Schleider&Schuell, Germany) filtration module connected in parallel was used.

Sonication and Mixing: The possibility to break-up the flocs was investigated by using a VC-130 Ultrasonic Processor Vibracell (Analis, Belgium). The impact of sonication on the FSD was investigated on-line for different sonication time periods (1-8 min.) and sonication powers (10-50 W). For mixing an RW-20.n IKA stirrer motor (IKA, Germany) was used at a mixing intensity varied between 60-320 rpm. These values corresponded to the minimum (60 rpm) and maximum (320 rpm) mixing speeds possible with the used mixing device.

Experimental Setups:

The flocculation reactor used for performing the tests is presented in Figure 3.14. The reactor had a capacity of 2 l.

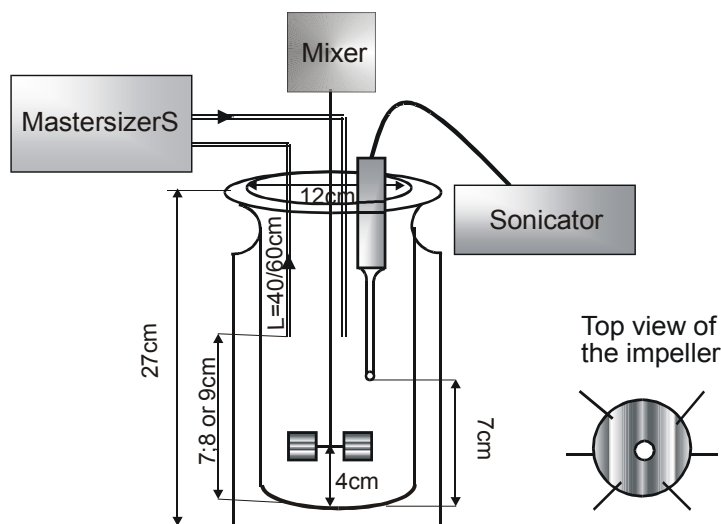


Figure 3.14 Flocculation reactor and experimental settings of the principal components inside the reactor.

For all the tests performed the following settings were used:

- The mixing system was placed in the middle of the vessel at 4 cm from the bottom of the reactor.
- The sonication tip was placed in the right part of the vessel at 7 cm from the bottom of the reactor.

The length of tube performing the sampling and connected to the MastersizerS was varied between 40 and 60 cm in order to permit an evaluation of the tube effect. PVC tubes with a the diameter of 9/11 mm (internal/external) were used. For the case in which the sludge was returned in the flocculation reactor the corresponding returning tube was placed in the opposite part of the sampling tube.

The following experimental setups were evaluated:

Setup 1

The main purpose of this setup (Figure 3.15-left) was to investigate the possibility of evaluating the flocculation dynamics for different sludge concentrations in the vessel (higher than the sizing device can measure). In order to perform this, the sludge needs to be diluted in-line. For dilution, filtered effluent was used. The dilution was performed by pumping the effluent with a peristaltic pump 505U (Watson Marlow- P_2) via a tubes bifurcation (T-part) directly into the tube transporting the sludge to the sizing device. The flow rate of the pump (P_2) was set to a range that allowed to keep an obscuration level of 15% in the MastersizerS and varied as a function of the sludge concentration in the vessel. Several dilution ratios ($X/2$; $X/4$; $X/8$) of the initial activated sludge concentration (X) were used. A second peristaltic pump Masterflex L/S (P_1) controlled the total flow rate (3 ml/s) through the MastersizerS. The flow rate was selected according to Biggs (2000) who found that the pumps should be set for a dilution of approximately 5 % vol. of activated sludge in order to minimise the shear, corresponding to a flow rate of 3 ml/s. The pump P_1 was placed after the sizing device to prevent any disturbances of the sludge before measurement. The sludge pumped to the Malvern instrument was drained to avoid changing the sludge concentration in the flocculation reactor. To allow performing enough measurements, a large sample volume is therefore required.

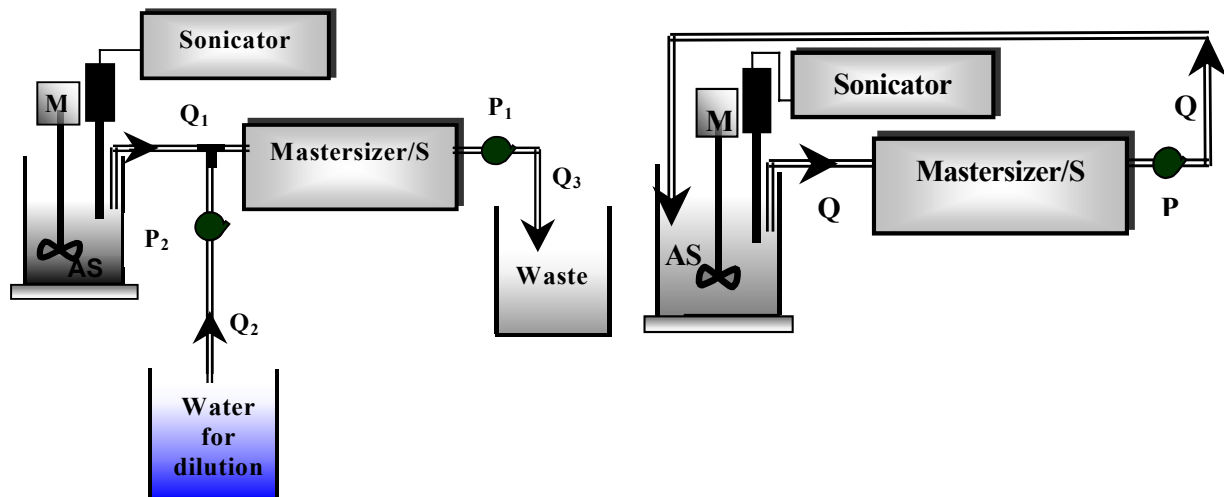


Figure 3.15 Experimental Setups: Setup1 (in-tubes dilution - left) and Setup2 (in-vessel dilution - right) (P_1, P_2, P - pumps; $Q, Q_3 = Q_1 + Q_2 = 3 \text{ ml/s}$ - flow rate; M - mixer; AS - activated sludge).

Setup 2

Setup 2 (Figure 3.15-right) is similar with the one developed by Biggs (2000). In this case the disturbing effect created by using an in-situ sonication in a large volume of sample was evaluated. Moreover, the effect of some components of the setup was checked as well. The sludge concentration in the vessel was determined by the necessary obscuration level required by the sizing device to obtain a good diffraction pattern (15 %). A dilution ratio of $X/20$ was found to be optimal for these experiments. The in-line dilution was removed and sludge was continuously recirculated to the vessel. This option led to the possibility of performing a larger number of on-line analyses of the size distribution and thus to monitor the (de)floculation for a longer time.

3.4.2. Influence of mixing

Investigating the influence of mixing has two main purposes:

- To evaluate the floc breakage and aggregation at different sludge concentrations in the vessel for a relatively large volume of sample.
- To find the minimum mixing intensity that creates a homogenous mixing in the vessel and maintains the flocs in suspension.

For these experiments sonication was not used.

Figure 3.16 shows the influence of mixing on the particle size distribution for two sludge concentrations ($X/2$ and $X/20$). Similar effects have been observed when the mixing was applied to two other dilution ratios ($X/4$ and $X/8$). By increasing the mixing intensity the floc break-up effect was recorded for all investigated cases and the magnitude of the disturbance increased when the mixing intensities were increased. The very fast effect of the mixing should also be remarked since for recording the FSD shown in Figure 3.16 the mixing speed was increased in the vessel every 2 min.

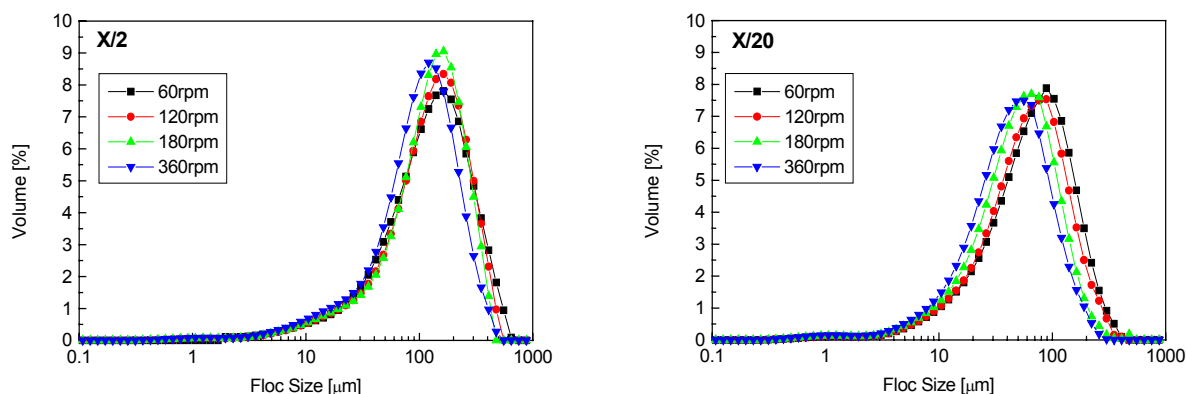


Figure 3.16 Influence of mixing on the FSD for a sludge concentration of X/2 (left) and X/20 (right) The measurements were performed by using Setup 1 for the sludge concentration of X/2 and Setup 2 for the sludge concentration of X/20. Sonication was not used.

The smallest changes in the time evolution of PSD were observed for mixing at 60 rpm. Also, by sampling the sludge at different points in the vessel a very similar FSD was observed. This gives an indication of reaching the conditions of homogenous mixing in the vessel. This mixing speed was therefore considered to be the best for maintaining the sample in suspension without creating other effects that can lead to difficulties in evaluating sonication effects on floc size.

As a preliminary conclusion, it was observed that mixing is an effective method for monitoring the (de)floculation dynamics in a relatively large volume of sample and at different sludge concentrations.

3.4.3. Influence of sonication

Sonication is an alternative method to the mixing for floc break-up. According to Jorand et al. (1995), sonication is a physical method that does not contaminate the sample with chemical reagents and represents a good way of dispersing bacterial aggregates. It is often used to enumerate bacteria or for the extraction of EPS. The technique was successfully applied by Biggs (2000) for disturbing a sludge sample (100 ml) for the purpose of studying the reflocculation phenomena in a controlled environment. It was found that sonication of the activated sludge flocs for 3 minutes at 50 W reduced the floc size to a consistently small size without causing significant cell lysis.

In this study, based on the method developed by Biggs (2000), the possibility of using a sonication tip for flocs break-up in a large sample volume (2 l) and for different sludge concentrations was investigated. Initially, only the effect of sonication power and time on FSD was investigated. At this stage, the impact of sonication on the microbial activity was not considered since the main purpose was to verify the applicability of this method under the imposed operating conditions.

By studying the influence of the sonication power it was remarked that in general a high sonication power must be applied to create floc disruption (Figure 3.17). It was also observed that the high sonication power had a higher floc break-up effect at low sludge concentrations (Figure 3.17-right).

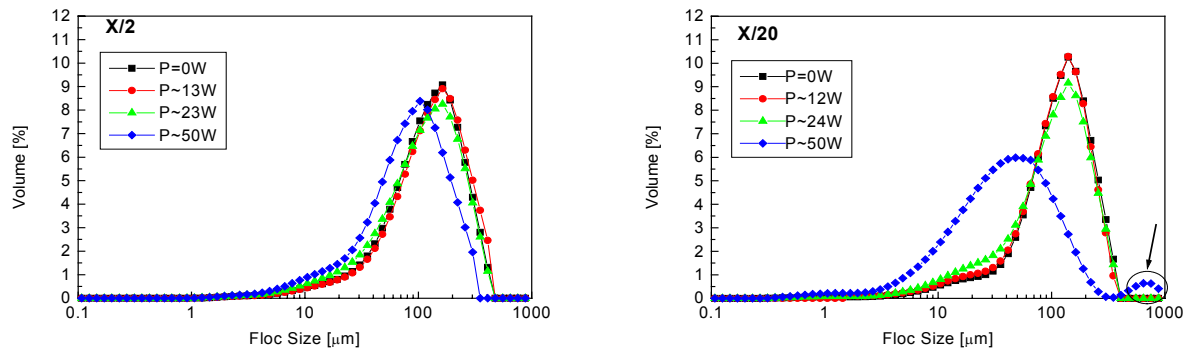


Figure 3.17 Influence of the sonication power (P) on FSD at different sludge concentrations: X/2 (left – Setup1) and X/20 (right – Setup 2). Sonication time: T = 4 min. The oval mark in the left figure (X/20) indicates the presence of the bubbles air in the system.

The influence of sonication time was investigated under high sonication power (~50 W). Difficulties in maintaining a constant sonication power were recorded especially for the experiment performed by using Setup1. It was found that sonication power changed with the position of the sonicator tip in the vessel and also with decreasing sludge volume. For a concentration of X/20 the sonication had a stronger and faster break-up effect compared to the case of high concentrations (X/2; X/4), where due to the high in-vessel concentration the reflocculation process may occur as well (Figure 3.18). Moreover, for high sludge concentrations it seems necessary that sonication is applied for longer times to obtain a significant break-up effect. In this case, the risk to produce serious bacterial cell damage increases as well.

A second peak in large size classes was observed for low concentrations (<X/8) when high sonication power was applied (oval mark in Figure 3.17-right and Figure 3.18-right). This is clearly shown also in Figure 3.19 when a constant sonication power (50 W) and time (4 min) are used for different sludge concentrations. This phenomenon may be due to air bubbles generated by sonication. It is assumed that at high concentration, the collision rate between the bubbles and the flocs is higher and the bubbles collapse in the vessel, whereas at low concentrations this may happen rarely. This phenomenon is seen as well in the experiments performed for investigating the time effect (Figure 3.18-right) where the volume contribution of the second peak increased in time as well. This gave an indication that the formed bubbles could attach on the sizing device flow-through cell and accumulate in time. The hypothesis was confirmed by visual observations of the MastersizerS flow cell during an experiment specifically performed for checking the bubble formation.

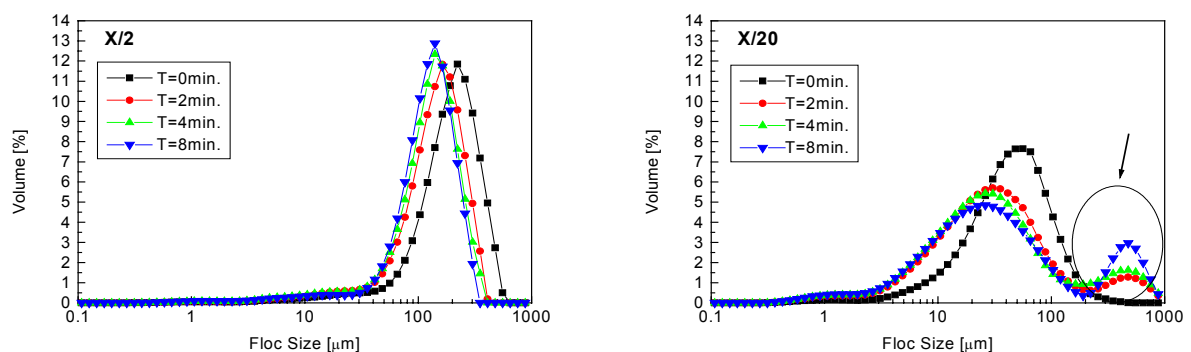


Figure 3.18 Influence of the sonication time (T) on FSD at different sludge concentrations: X/2 (left- Setup1) and X/20 (right- Setup2). Sonication power: P~50W. Oval mark indicates the air bubbles.

A broader size distribution was obtained especially at lower concentrations (Figure 3.19) suggesting a local breakage effect of sonication.

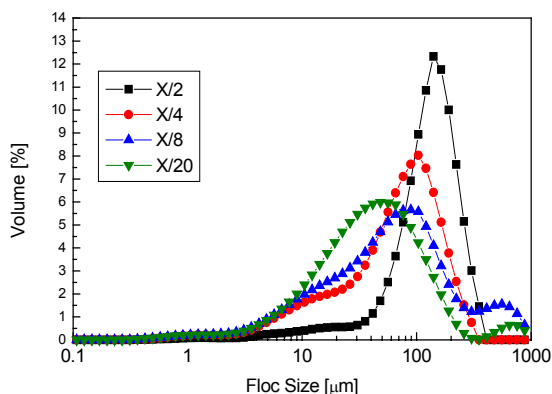


Figure 3.19 The FSD obtained for different activated sludge concentrations. Sonication characteristics: P~50W and T=4min.

In addition to the bubble formation, another major drawback of the sonication was the heating effect, which created difficulties in controlling the temperature in the reactor. An increase in temperature of about 3-4°C was recorded when 50 W sonication was applied in the vessel for 4 min.

To conclude, in-situ sonication does not represent a good approach for studying the deflocculation dynamics.

3.4.4. Influence of dilution

Since large quantities of water are required for performing the in-tube dilution, the possibility of using deionised water was investigated and compared with the effect created by using filtered effluent (0.45 µm). Zita and Hermansson (1994) showed that by treating the sludge with deionised water a strong floc dissociation may be produced. The experiments performed with deionised water showed that in-tube dilution of the sludge with deionised water produced a deflocculation effect indicated by the shift of the FSD to a smaller floc size range as compared with the one performed with filtered effluent (Figure 3.20).

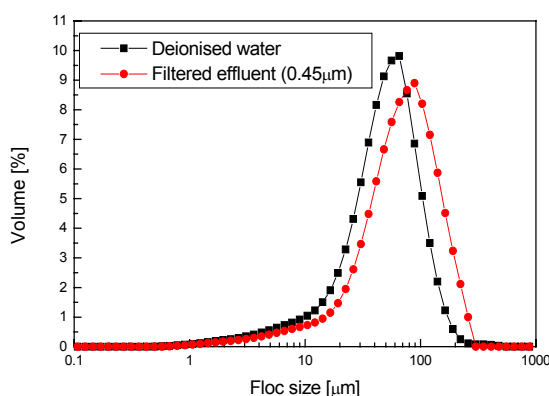


Figure 3.20 The effect of dilution water on FSD by using Setup 2 (continuous recycle) and no sonication. Mixing: 60 rpm and flow rate: 3 ml/s.

A separate experiment was performed in order to check as well the (de)floculation behaviour of a sludge sample diluted with deionised water, as compared to the one diluted with filtered effluent. To perform these experiments, a small amount of sludge (25 ml) was added to 800 ml dilution water. An automatic wet sample dispersion unit MSX17 (Malvern, UK) was used as flocculation reactor. This unit allows to control the flow rate, mixing speed as well as the sonication power which in this case is generated via the unit walls and leads to a uniform sonication in the reactor. The minimum mixing intensity found to be necessary for keeping the flocs in suspension was 210 rpm and the flow rate was set at 3 ml/s.

Before starting to record the FSD, the sludge samples were mixed and pumped at a constant flow for 30 min. to reach steady state. Identical sludge treatment was applied for both performed experiments and the same sludge sample was used. In the first 10 min. the steady state distribution of the floc was recorded. Next, sonication was applied for 10 min at 35 W. Finally, the initial conditions were reimposed for another 10 min. As shown in Figure 3.21, the mass mean diameter of the sludge sample diluted with deionised water was significantly smaller as compared to the one recorded by using filtered effluent for dilution. Moreover, for the sludge diluted with deionised water, the sonication effect was less and just a slight reflocculation tendency was observed after sonication. In agreement with this observation, Mikkelsen et al. (1996) demonstrated that diluting the sludge with deionised water led to an increase of the surface charge density and shear sensitivity due to the desorption of cations and to the reduction of the ionic strength.

It is therefore suggested that the dilution medium is of high importance for a good interpretation of the results. Changing of the sludge water will lead to a destabilization of the flocs, which may react in a different way to the operational conditions.

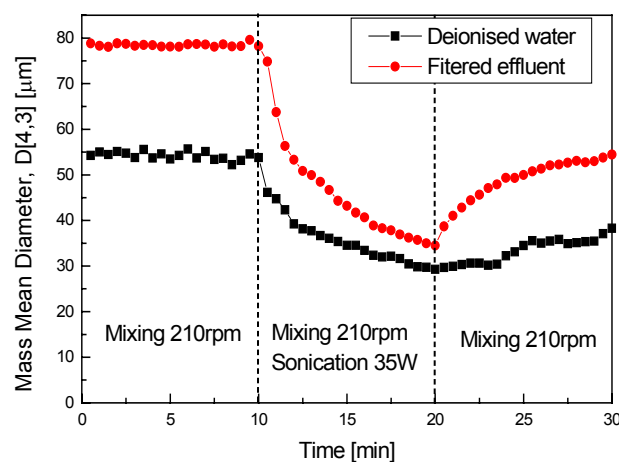


Figure 3.21 The influence of dilution water on sludge breakage and aggregation.

3.4.5. Influence of the setup components

The influence of the tubes length (total length 40 and 60 cm) on the FSD has been studied since it was visually observed that small aggregates were formed inside the tubes connecting the sizing device, especially at high sludge concentration. The length of the tubes before dilution was 20 cm and 40 cm, respectively. Figure 3.22 shows the PSD obtained under the same experimental conditions (Setup 1; X/2) by varying only the tube length. It is concluded that flocculation indeed occurred in the tubes. Hence, tubing should be as short as possible to minimise this effect and to maximise the representativity of the measurement. Moreover, it seems that the place where in-line dilution is performed is very important, too. To avoid

flocculation in the tubes, the dilution should be performed close to the place of sampling. The pump used for in-line dilution may have as well an important impact on the observed flocculation in the tube due to the shear forces exerted on the pumped sludge since pulsations at the dilution point have been observed. Hence, a dosing pump (Group D, Seepex GmbH, Germany) was further considered when building the experimental flocculation setup. It allows to work with small flow rates at high accuracy, low fluctuations (<1%) and low shear.

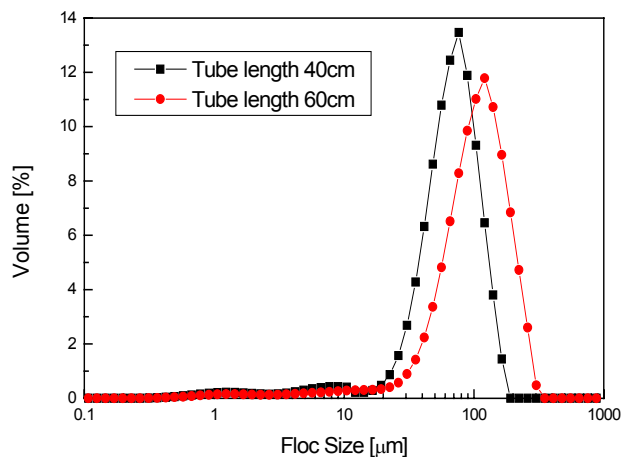


Figure 3.22 Tube length influence on the FSD measured by using Setup 1. Mixing: 60 rpm; flow rate: 3ml/s and no sonication.

For the purpose of checking the influence of the tubes connector on the FSD the sludge sample was pumped to the MastersizerS by using two tubes joined together by means of a tube connector (T-part). Since the only difference in the experimental configuration shown in Setup 2 is the T-part, discrepancies in FSD's are assumed to be due to the latter. Even if some small differences were observed on the recorded FSD, it may be concluded that this does not have a noticeable influence on the FSD (Figure 3.23).

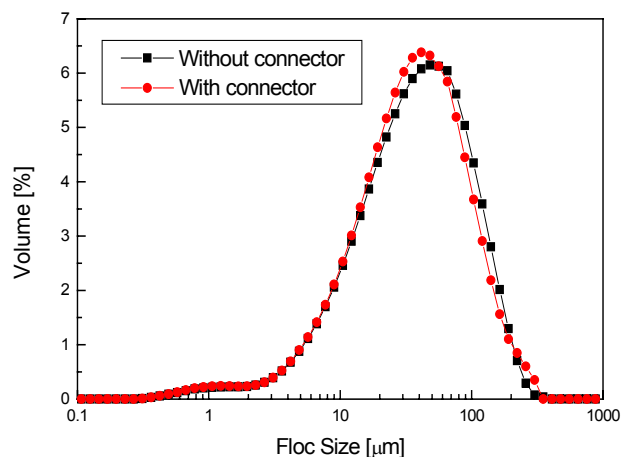


Figure 3.23 Tubes connector influence on FSD measured by using Setup2. Mixing: 60 rpm; flow rate: 3ml/s and no sonication.

3.4.6. Conclusions

To summarize, the obtained results show the necessity to find optimal experimental conditions for a correct evaluation of FSD dynamics. The following experimental conditions are important in developing a good experimental technique for on-line quantification of the floc size dynamics in a relatively large sample volume and for different sludge concentrations in the vessel:

- Mixing was found to be the optimum solution for creating floc breakage and aggregation. An alternative method, investigated for purposely disturbing the flocs was in-situ sonication by using a sonication tip. Several disadvantages were found when this method was considered. Due to these, sonicating a large volume of highly concentrated sludge was found not to be a good solution for disturbing the flocs at least not with a sonicator tip and consequently, this method is not appropriate to be used for the purpose of the present study. The main drawbacks of the sonication found are:
 - High sonication power (~50 W) and longer time (more than 4 min) should be applied for obtaining a significant disturbing effect. This may lead to significant cell lysis (Biggs, 2000).
 - The sonication effect was largely dependent on the sludge concentration in the vessel. For high sludge concentrations the disrupting effect of sonication was minimised due to the high reflocculation rate. Moreover, at low sludge concentrations, small bubbles formed and attached on the flow through cell of sizing device, which led to a detection of a ghost peak situated in the large size classes.
 - The sonication effect was mostly local and a very broad FSD was recorded.
 - An increase of the temperature in the vessel was registered due to the sonication, which makes the temperature control in the vessel impossible.
- Long tubes create in-line flocculation. Further, the tube connecting the reactor with the sizing device should be as short as possible. Moreover, to avoid flocculation in the tubes the in-line dilution should take place close to the sampling point and another pump which creates less pulsations on the flow must be considered.
- The tube connectors (T-part) do not have an important influence on the FSD.

3.5. From spherical particles to activated sludge distribution - Simultaneous investigation by different techniques

The floc size and size distribution have often been reported in literature as outcome of a particular measurement technique and less importance has been given to the influence of the measurement technique on the results. Since the various measuring devices are based on a broad range of measurement principles, it is expected that different results are obtained. Moreover, for the case of activated sludge, due to the biological fragile and irregular structure of the flocs, the results may often lead to a misinterpretation of the data. Therefore, a systematic investigation of the activated sludge FSD obtained from several instruments with different working principles is required. The results are compared and the performance of each technique is critically assessed.

As discussed earlier in this chapter the particles size measurement most often starts from the approximation of spherical shape particles. Because of this, the size measurement of particles with irregular shape can sometimes be subject to measurement errors (Naito et al., 1998).

Moreover, it was shown that the sample dilution represents one of the major drawbacks of all three sizing devices considered in this research.

This section aims at finding the optimum dilution range appropriate to be used for all considered devices. Moreover, the influence of the particles shape on the obtained size distributions measured by using different techniques is evaluated and the results are compared against each other in order to gain insight in the FSD characteristics, as well as to detect the limitations of each measurement technique. To reach this purpose simultaneous measurement of differently sized and shaped particles were performed: spherical glass bead particle size distributions are compared with those provided by irregular shape inorganic particles and finally the distributions obtained for activated sludge flocs are presented and evaluated statistically.

3.5.1. Materials and methods

Samples

Glass beads

Solid glass beads were selected for evaluating the size distributions in a larger size range. The glass beads are perfectly spherical with a smooth, shiny surface and insoluble in water (Figure 3.24). Two different samples were analysed, corresponding to a size range of 44 μm and less (AQ 313) and 149 – 250 μm (AC) respectively (Microperl®, Sovitec-Glaverbel, Belgium). The particles were characterised by a density between 2460 – 2490 kg/m^3 and a refractive index of 1.515 (Technical data, Glaverbel, Belgium).

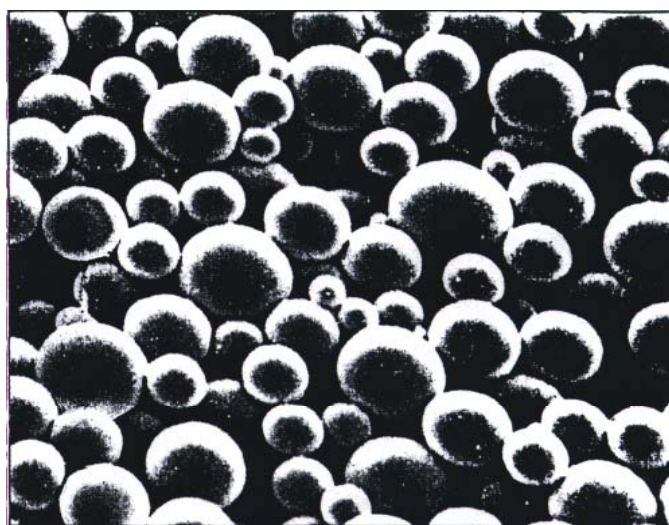


Figure 3.24 Microscopic observation of glass beads AQ313 (diameter from 25 to 40 μm) (Microperl®, Sovitec-Glaverbel, Belgium).

Sand particles

For evaluating the shape effect, two types of irregular sand particles were used, namely Sikron®M400 (mass median diameter $D_{50}=7 \mu\text{m}$) and Milisil®M4 ($D_{50} = 49 \mu\text{m}$) (Sibelco, Belgium). The particles are selected silica sand (SiO_2) and have a bulk density of 850 kg/m^3 (Sikron®M400) and respectively 1150 kg/m^3 (Milisil®M4). The refractive index of the particles was 1.55 (Sibelco, 2004).

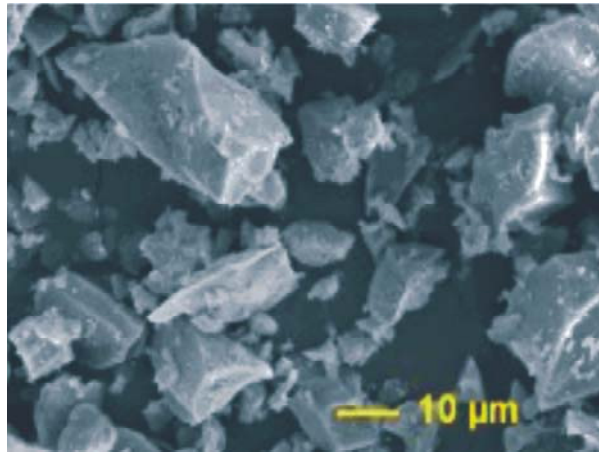


Figure 3.25 Microscopic observation of sand particles (Milisil ®M4; Sibelco, 2004).

Activated sludge

The activated sludge samples have been collected from a pilot-scale SBR. Three experiments were performed over a period of 4 months. During this period the sludge characteristics changed as observed microscopically and by the measurements of floc size and settling properties. For the latter, the sludge volume index (SVI) showed values of 469 ml/g; 131 ml/g and 256 ml/g respectively. The analysed samples will be further referred to as S1, S2, S3 for an easier comparison.

3.5.1.2. The experimental setup

In order to perform the experiments the sizing devices (MastersizerS, CIS-100 and IMAN) were coupled in series as shown in Figure 3.26. Since, the CIS-100 has two measurement channels based on different analysing principle, for convenience the image analysis channel will be further referred as SHAPE and those based on time-of-transitions will be named TOT. The experiments have been conducted by using an MSX17 (Malvern, UK) automated wet sample dispersion unit as reaction vessel. A flow rate of 3 ml/s and a mixing speed of 210 rpm were used in all the experiments. From the dispersion unit, the samples were passed to the MastersizerS, CIS-100 and IMAN to finally return to the reaction vessel. In this way, the variations that can occur due to sample preparation and manipulation were avoided.

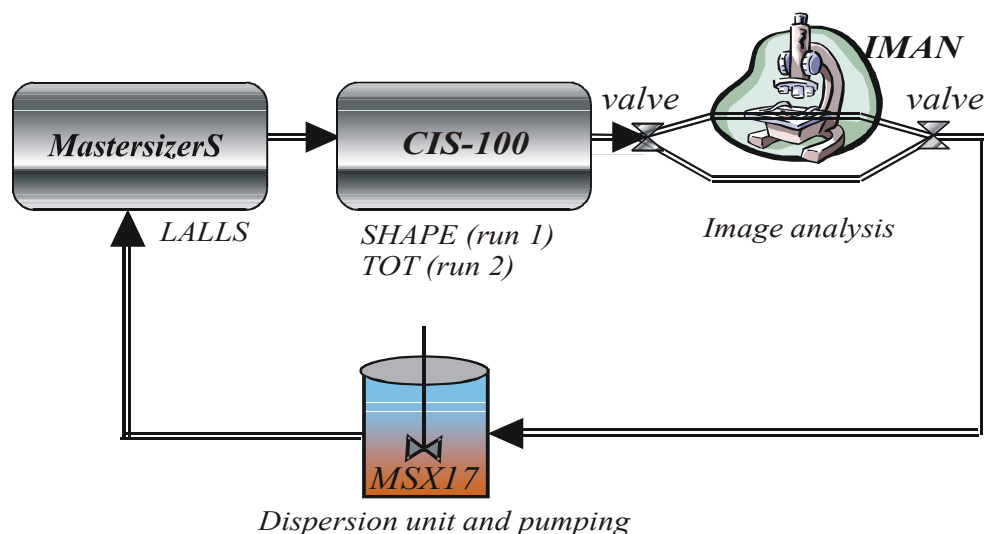


Figure 3.26 The experimental set-up used for on-line particle size distribution measurements.

3.5.1.3. Experimental procedure

For each analysed sample two experiments were performed in order to investigate both available measurement channels provided by the CIS-100 device. In the first experiment, the on-line size distributions were recorded successively from MastersizerS, SHAPE and IMAN. By maintaining the same sample in the dispersion unit MSX17, a second experimental run was possible. The FSD were then recorded from MastersizerS, TOT and IMAN. For each experiment the devices were programmed in order to allow repetitive measurements for a given time period. This procedure was preferred since it allowed to verify the reproducibility of the results. Given the different nature of each of the samples different treatment and analysing procedures were applied depending on the purpose of the study (dilution requirement evaluation or shape influence). Since two image analysis systems were used the results are presented and interpreted as a function of the surface equivalent spherical diameter (d_s) defined as a diameter of a sphere having the same surface area (A) as the particle, which was calculated in the same way by both used software as given by equation (3.21).

$$d_s = \sqrt{\frac{A}{\pi}} \quad (3.21)$$

Devices dilution requirement

The devices dilution requirement was evaluated by using different concentrations of glass beads (44 μm and less) dispersed in 1 l deionised water. Different amounts of glass beads were selected on a logarithmic scale in order to obtain 10 different concentrations between 0.2 g/l and 20 g/l. The analysis sequence and device settings are presented in Table 3.6. The experiments started from the lowest considered concentration (0.2 g glass beads in 1 l deionised water) and successive experiments were performed by addition of a supplementary quantity of glass beads.

Table 3.6 The analysis sequence and devices settings for dilution requirement evaluation.

Device	Lens/size range [μm]	Acquisition time [min]		Measurement sequence	
		Run 1	Run 2	Run 1	Run 2
MastersizeS	300RF/0.05-900	5	5	1 meas. every 30 s	1 meas. every 30 s
CIS-100 (SHAPE)	CW/2-150	5	-	10 000 particles	-
CIS-100 (TOT)	A/0.1-300	-	5	-	1 meas. every 30 s
IMAN	4x/15-4000	5	5	1 image every 15 s (valves stopped 10 s)	1 image every 15 s (valves stopped 10 s)

Shape effect evaluation

The sample concentration was set as function of the optimum dilution range found to be suitable for all investigated techniques. This was controlled by fixing the obscuration level of the MastersizerS at 15-20 %, which was found to correspond to an optimal or near optimal dilution ratio for all devices used. The dilution was performed by using deionised water except for the case of activated sludge in which filtered effluent (0.45 μm) was used. Each experiment had an acquisition time of 15 min and the same measurements sequence as described before was used. The devices size range was adapted function of the analysed particles size as given in Table 3.7.

Table 3.7 The size detection range used for each device.

Device	Small size particles (sand-M400)		Large size particles (glass beads, sand M4, activated sludge)	
	Optical lens	Size range	Optical lens	Size range
MastersizerS	300RF	0.05-900 μm	300RF	0.05-900 μm
CIS-100(SHAPE)	CW	2-150 μm	DW	10-600 μm
CIS-100(TOT)	A	0.1-300 μm	B	2-600 μm
IMAN	4x	15 –4000 μm	4x	15 –4000 μm

The experiments started when a steady state size distribution was recorded for more than 10 min. During this time the sample was recirculated through the devices' flow cells. This is an important issue to be considered especially for the case of activated sludge where flocs can easily be disturbed under the imposed conditions and therefore a steady state floc size is necessary to be achieved. The results were evaluated as averages of the steady state distributions measured. For the MastersizerS and IMAN two experiments were performed each time and the average distribution of each of the two experiments was calculated as well.

3.5.2. Evaluation of devices dilution requirement concentration influence

An increasing glass beads (44 μm and less) concentration was used for evaluating the devices dilution requirement. The obtained cumulative volume distributions are presented in Figure 3.27.

A first point to consider is that the IMAN results showed a slight overestimation of the size. This may be due to the relatively limited size detection range of the device for smaller particles. Hence, the small particles were not able to completely obscure a single pixel (1 pixel = 5.81 μm) and were not counted. However, it may be possible as well that the particles agglomerated inside the flow through cell connected to the microscope and therefore gave an overestimation of the size. It is believed that this eventually happened when the valves interrupted the flow for acquiring an image since it was observed that due to their sphericity and smooth surface the glass beads came easier in contact. This was also favoured by the horizontal positioning of the cell on the microscope.

The results provided by the MastersizerS and CIS-100 yielded similar distribution at low concentrations (0.2-0.928 g/l). When the glass beads concentration increased (SNF decreased from 1 to 0.96), TOT showed a tendency to form a second mode in the volume distribution located in a larger size range. It is possible that due to the increase of the concentration two very close particles were measured as a bigger transparent one. The second mode becomes more significant for concentrations higher than 4.309 g/l. A rapid increase of the S.N.F. from 0.96 to 0.57 was observed. Meanwhile, the S.D.U. increased from 639 to 3 255. These values indicate that the sample was overconcentrated. From the same concentration, it was also noticed that the MastersizerS devices showed a broader distribution with a slight tendency to form a second mode in the smaller size classes probably due to the multiple scattering phenomena. Indeed, the recorded obscuration levels increased significantly (higher than 30 %). For concentrations higher than 4.309 g/l image analysis methods (IMAN and SHAPE) were not possible to be applied since the light was completely obscured by particles. Similar phenomena occurred also in the MastersizerS and TOT when 20 g/l concentration was measured. The distributions recorded with MastersizerS and TOT at a concentration of 11.99 g/l showed a very similar trend with the one obtained at 7.188 g/l and are not shown in Figure 3.27.

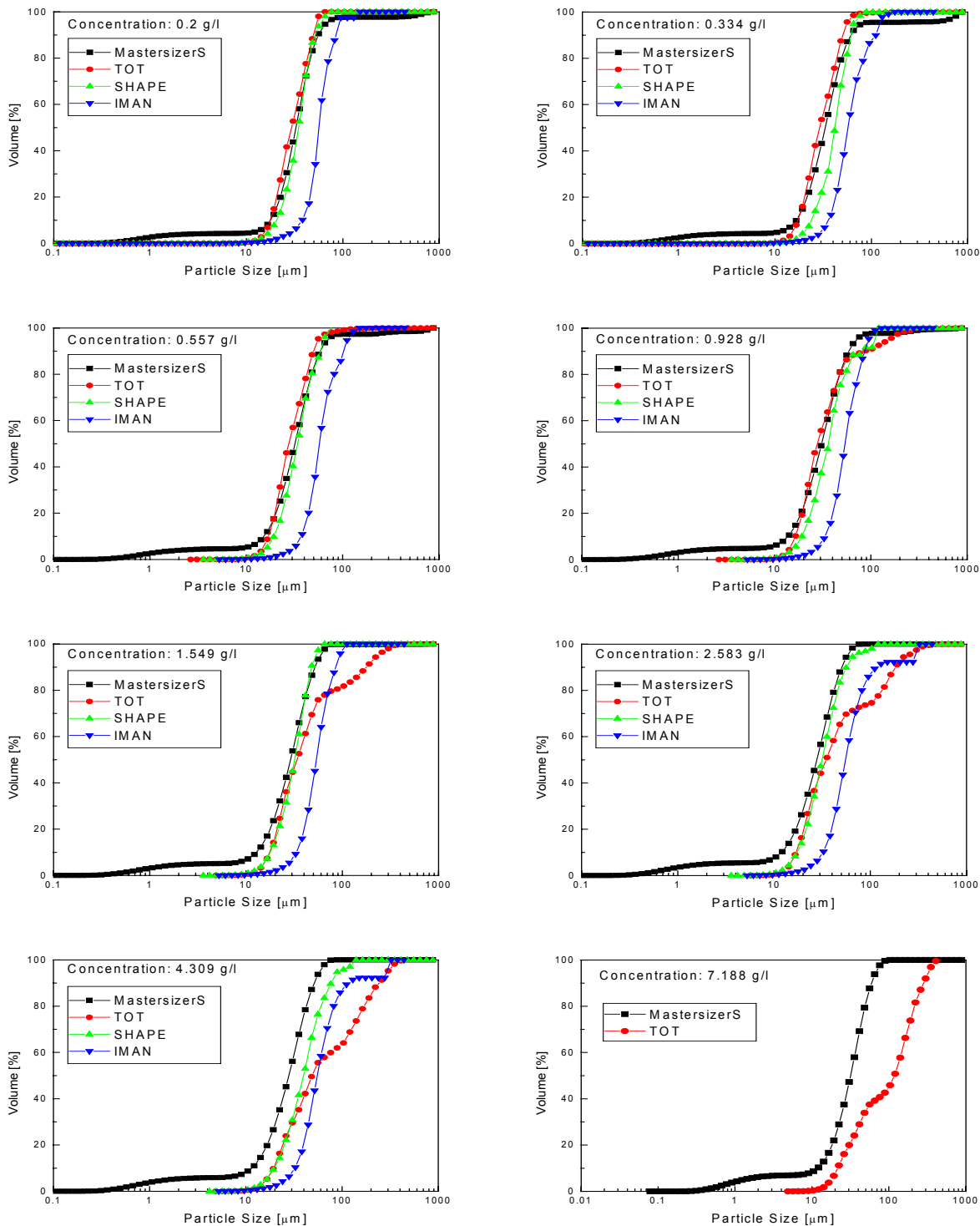


Figure 3.27 The volume based cumulative particle size distribution measured for different glass bead (44 μm and less) concentrations measured by using the sizing devices coupled in series.

It may therefore be concluded that the devices operate with similar dilution requirements, allowing to perform simultaneous measurements with all devices. However, small concentrations are preferred. Consequently, performing the measurements in the optimal range of concentration as given by the devices will allow to easily set the necessary sample dilution levels. As an example, it was observed that an obscuration level between 15-25 % of MastersizerS gives suitable sample concentration for all considered devices.

3.5.3. Effect of particle shape on the particle size distribution

The effect of particle shape on the obtained particle size distributions is discussed for the experiments performed with glass beads, sand particles and activated sludge. The results are evaluated only by taking into account the volume based distributions as given or calculated from the measurements performed by each considered device. However, the effect produced by the results transformation by using the spherical shape assumption are evaluated as well for the case of the activated sludge samples.

Spherical particles (glass beads) distributions

Very similar volume based cumulative distributions were measured by all devices for glass beads (Figure 3.28).

For small sizes (44 μm & less) (Figure 3.28-left), as observed before IMAN showed a tendency to overestimate the size. The MastersizerS gave a broader distribution in the small size range as compared with TOT and SHAPE. This may be due to the differences in the size detection range between the used devices. However, except for IMAN, the other devices predicted very similar glass bead size distributions.

For larger particles (149-255 μm) (Figure 3.28-right) the drawback of size limitation is avoided and the volume based cumulative distributions given by all devices are in a good agreement.

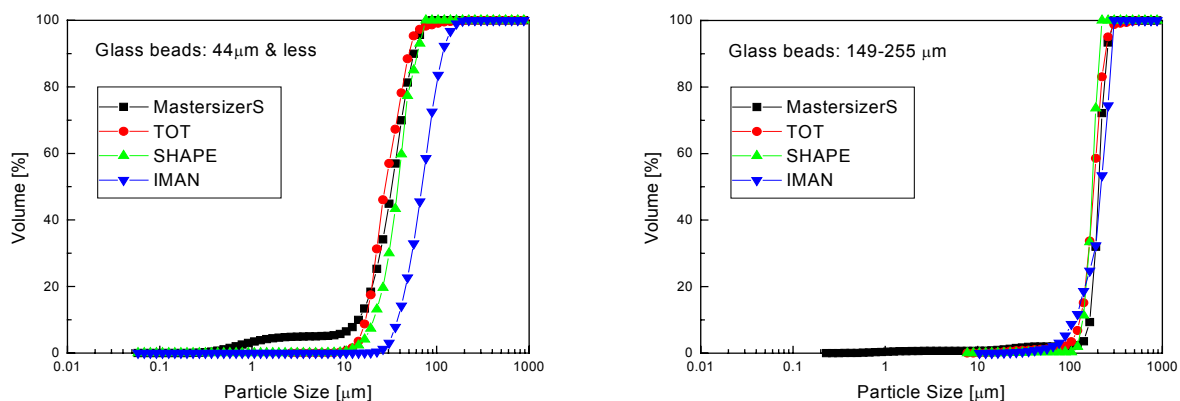


Figure 3.28 The volume based cumulative distributions of glass beads 44 μm & less (left) and 149–255 μm (right) measured with the sizing devices coupled in series.

It may therefore be concluded that for the case of spherically shaped particles the measurements results by different devices are in agreement with each other and generate rather similar size distributions. Moreover, the similarity between the distributions gives an indication that the time sequence chosen for recording the distributions gives sufficiently accurate results even for the counting techniques which usually require longer measurement times for generating statistically correct distributions.

Irregular particle (sand) distributions

Results obtained for irregular sand particles are shown Figure 3.29. A similar trend of the results given by the devices was observed for both investigated samples.

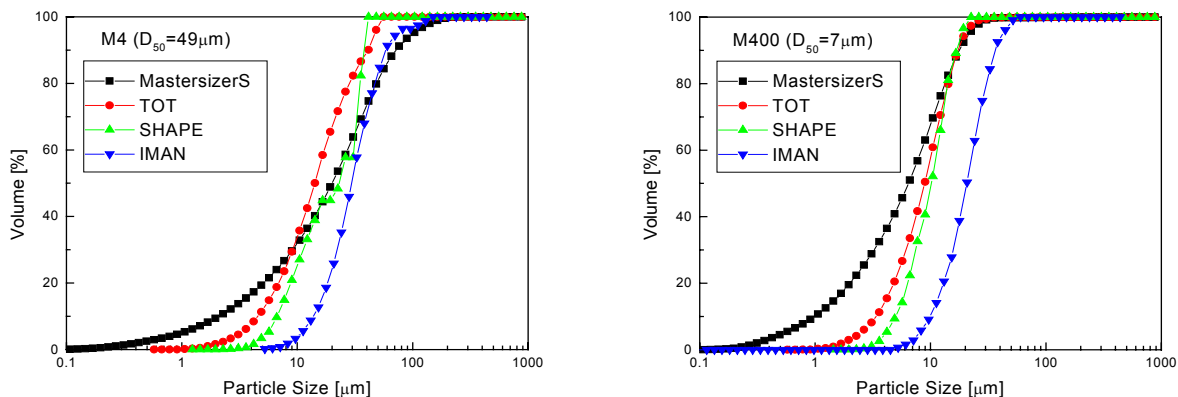


Figure 3.29 The volume based cumulative distributions of the sand samples: M400 ($D_{50}=7\ \mu\text{m}$ - left) and M4 ($D_{50}=49\ \mu\text{m}$ - right) measured with different devices coupled in series.

The MastersizerS results indicated a wider distribution compared to other techniques. This broadening of the distribution is assumed to be due to the irregular shape of the particles since the particles are measured over all orientations. Similar results regarding the effect of shape on laser diffraction devices are reported by Naito et al. (1998) and Bowen (2002).

By comparing the volume based distributions of the sand samples measured with the MastersizerS it was observed that the distribution obtained for M4 samples was broader than the distribution obtained for M400. An evaluation of the shape factor (SF) as given by the SHAPE technique (equation (3.22)) showed that the M4 sample contained a larger number of irregular shape particles as given by the broad range of shape factor values (Figure 3.30 right) as compared with those of M400 (Figure 3.30 left).

$$SF = \frac{4\pi A}{P^2} \quad (3.22)$$

where: A is particle surface area and P is the particle diameter.

This suggests that the broadening of the distribution given by the laser diffraction techniques increase with an increase of the deviation of the particles' shape from a sphere. Similar observations were reported also by Xu and Guida (2002).

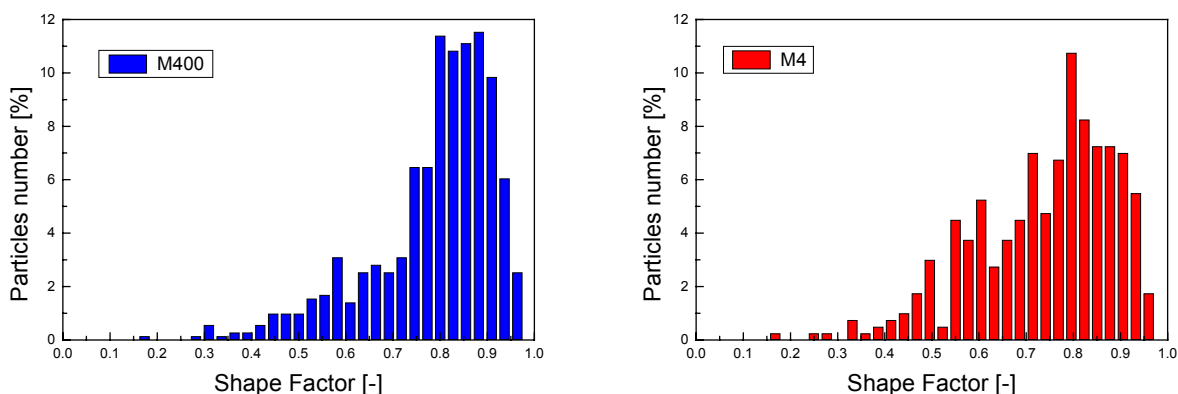


Figure 3.30 The shape factor of the sand particles as measured by SHAPE M400 ($D_{50}=7\ \mu\text{m}$ - left) and M4 ($D_{50}=49\ \mu\text{m}$ - right).

The distributions measured by using TOT and SHAPE showed similar trends while IMAN showed the same slight tendency to overestimate the size especially for M400 sample. The effect of the particles shape on the measured particles size distribution is less observed as compared to the results obtained for MasterzireS. This may be due to the conversion of the results from number to volume in which larger particles have more influence in determining the distribution.

Naito et al. (1998) reported a lower influence of the shape factors on the obtained distributions measured by using the TOT method. It is believed that this is due to the random orientation of the particles in the dispersion medium. This hypothesis may however be valid only for the case in which the particles do not have large irregularities in their shape.

3.5.3.3. Activated sludge floc size distributions

The shape effect of the activated sludge flocs on the obtained size distributions was evaluated after reaching a steady state in the flocculation. The volume distributions obtained from the sizing techniques showed a similar trend as those obtained for the sand particles (Figure 3.31). The MastersizerS showed a less broad distribution, which may give an indication of a narrower shape factor values as compared with the one observed for the large sand particles. This is confirmed by shape factor evaluation by using the SHAPE technique (Figure 3.32).

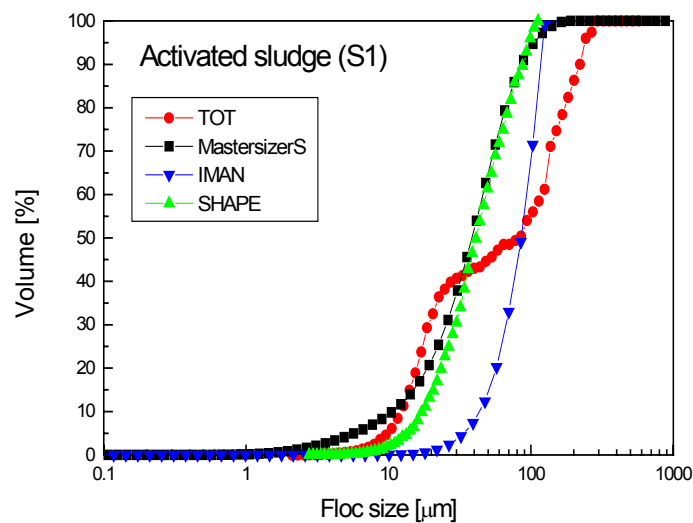


Figure 3.31 The volume based cumulative distributions of activated sludge samples (S1): initial steady state measured with different devices coupled in series.

TOT results showed again a bimodal volume based distribution due to its transparency checking feature which has a large influence on the transformed volume distributions. However, since the second peak was observed as well when spherical particles were analysed it may be considered that its occurrence is not due to the floc shape influence.

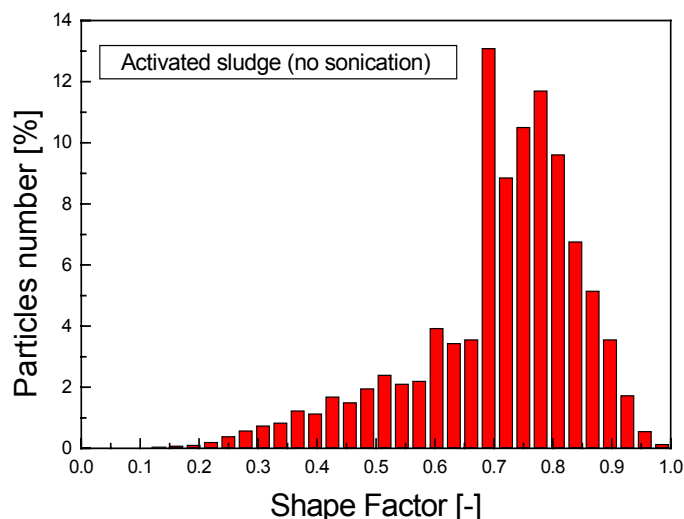


Figure 3.32 The shape factor of the activated sludge flocs as measured by SHAPE technique.

3.5.3.3. Shape effect on particle size distribution - devices comparison

In order to allow a general comparison of the results obtained for particles with different shape the span function was used. It gives an indication of the distribution width, which is independent of the median size (Motta et al., 2001) and may be calculated by using the following formula:

$$Span = \frac{D(v,90) - D(v,10)}{D(v,50)} \quad (3.23)$$

where: $D(v,10)$; $D(v,50)$ and $D(v,90)$ are the volume-based average diameters that represent 10%; 50% and respectively 90% of the particles size.

All devices showed narrow distributions and rather similar span values when glass beads (GB44 and GB150) were analysed (Figure 3.33). For irregular sand particles (M400 and M4) MastersizerS showed the wider distribution as compared with the other devices. The very high span values measured by MastersizerS for the sand particles give an indication of the highly irregular particles' shape, especially for the M4 sample. The observed results are considered to be in agreement with the measured shape factor (Figure 3.30) and indicate a direct relationship between the particles shape and the broadening of the distributions measured by the MastersizerS. For the case of the activated sludge samples (S1, S2, S3) for which a narrower range of the shape factor was observed (Figure 3.32) a decrease of the span value was obtained.

The narrower distributions and very close span values obtained for the techniques based on image analysis (IMAN and SHAPE) indicate less influence of the particles shape on the distributions generated as function of the equivalent spherical diameter.

A broader distribution was measured by TOT for sand particles as compared with image analysis, while the trend in span values was very similar to those of MastersizerS. Consequently, even if less observed, shape may have as well a influence on the distributions measured with TOT method. However, due to the bimodal volume-based distributions generated by TOT for the activated sludge it is difficult to quantify the shape effect in this case.

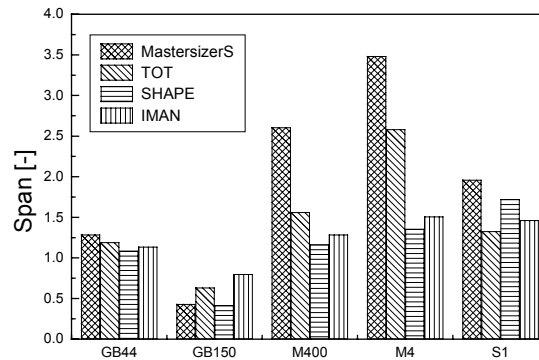


Figure 3.33 Effect of the particle shape evaluated function of the distributions span (GB44 – glass beads (44 μm & less); GB150 – glass beads (149-255 μm); M400 – sand particles ($\sim 7 \mu\text{m}$); M4 – sand particles ($\sim 49 \mu\text{m}$); S1 – activated sludge samples).

3.4.3.4. Conclusions

The effect of the particles' shape on the size distributions generated by various devices was analysed in this section. For spherical particles it was found that all devices generated similar and rather accurate results. The MastersizerS showed a higher dependency on the particles shape. A direct relationship between the increasing particle irregularities as measured by the shape factor and the broadening of the MastersizerS distribution was found.

The techniques based on image analysis showed a less significant effect of the particles' shape when the distributions were analysed as function of the equivalent spherical diameter. This may be attributed to the measurement principle of the image analysis, which only allows a 2D visualisation of the particles. Therefore, some spatial details may be sometimes not correctly detected, due to the information loss associated with projecting a 3D object onto a 2D surface, as opposite to the volume based techniques, where the 3D details are accounted for (Pons et al.1999).

The TOT technique too, showed to be relatively sensitive to the particles' shape when sand particles were analysed but a validation of the observed trend could not be extended to the activated sludge samples due to the detection of fewer large particles, which had a significant influence on the volume based distributions.

Consequently, it is very important to investigate the effect produced by the results transformation on the obtained distributions. This will be discussed below.

3.5.4. Influence of devices measurement principle on activated sludge floc size distribution

The IMAN, SHAPE and TOT methods are all counting techniques, primarily yielding *number* distributions, whereas laser diffraction is an ensemble technique that is most sensitive towards the volume contribution of each size class, and as such primarily yields *volume* distributions. The obtained number- and volume-based distributions are the subject of the present investigations. The comparison starts with an interpretation of the observed results as they can be obtained directly from the devices and their transformations in number and volume distributions, based on the spherical shape assumption. Finally, statistical data analysis and comparison are carried out.

3.5.4.1. Experimental results transformation based on spherical shape assumption

The measurements performed over the four months period showed a rather consistent trend of the results given by the devices even if the sludge structure changed. Particularly, the MastersizerS and SHAPE devices yielded similar volume FSD's (Figure 3.34 a,c,e). IMAN had a slight tendency to overestimate the floc size (especially for the samples containing mainly small particles sized e.g. S1), whereas TOT showed a bimodal distribution. The latter may be due to the used measurement method, which, as discussed before, may treat two very close opaque particles as a bigger transparent one. By looking at the number distributions obtained from the TOT measurements it was observed that only a few particles have been detected in that higher range (Figure 3.34 b,d,f) and the results were in agreement with those obtained from SHAPE measurements. The number distributions generated by the MastersizerS were mainly located in the submicron region. These results are believed to be unrealistic, being caused by the irregular particles shape. On the other hand, the distributions generated by IMAN were shifted towards larger sizes, which can be explained by the limited size detection range of this method.

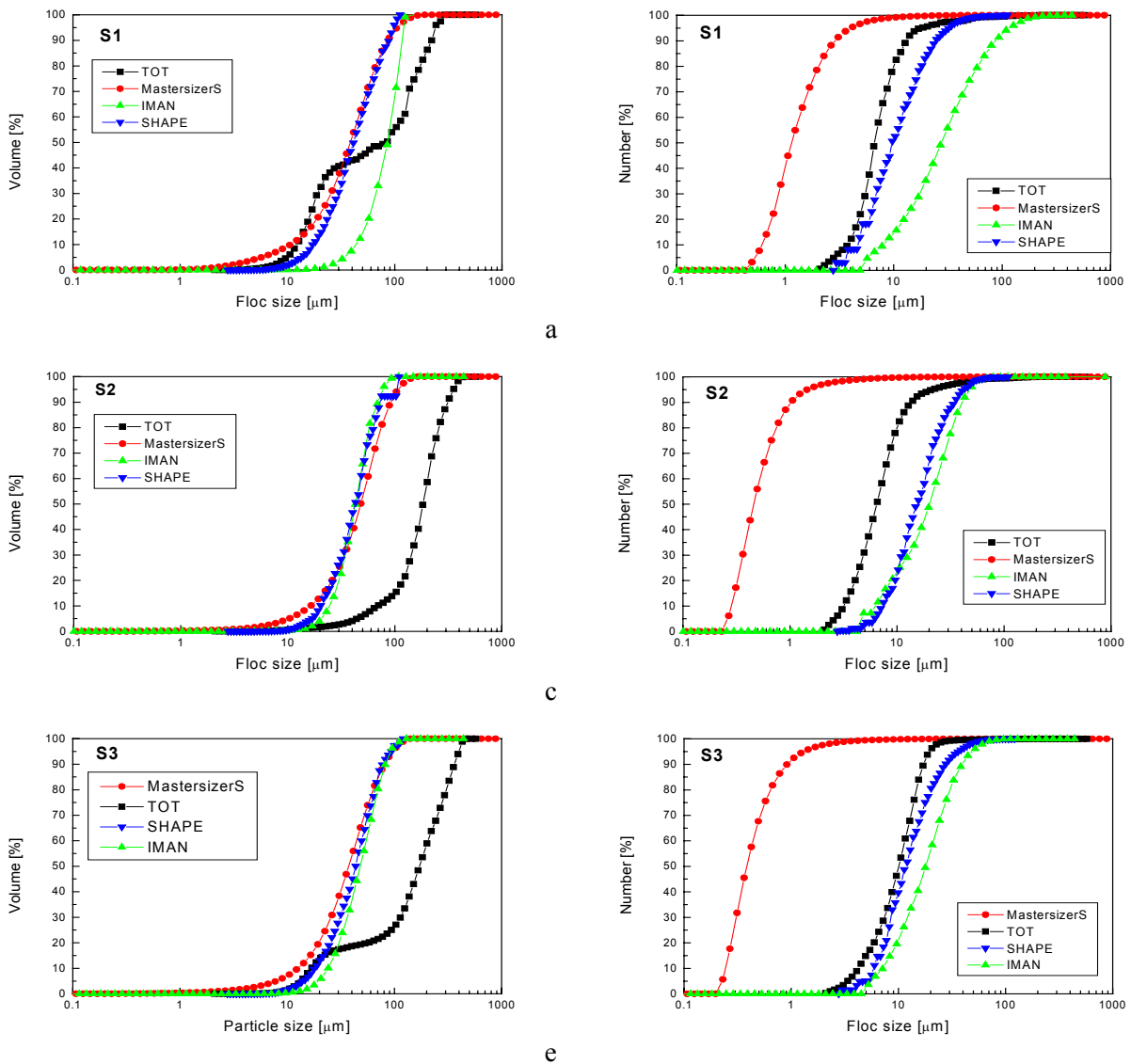


Figure 3.34 Comparison between volume (a,c,e) and number (b,d,f) cumulative distributions measured by using the sizing devices coupled in series for the three activated sludge samples (S1, S2, S3).

3.5.4.2. Log-normal distribution and results transformations

The activated sludge FSD is reported to be described well by a log-normal distribution (Li and Ganczarczyk, 1991; Barbusinski and Koscielniak; Wilén and Balmér, 1999; Biggs, 2000). Accordingly, this model was selected in the present work to fit the data. To allow for an easy comparison, the measured frequency distributions were first normalized. The log-normal distribution used for fitting the experimental distributions is given by equation (3.4).

Most of the experimental distributions fitted well to this log-normal distribution curve. However, a known problem when fitting the log-normal distribution to the whole size range is that it is difficult to choose the minimum and maximum size limits (Allen, 1997). Consequently, fitting with a log-normal distribution will give good agreement with the data in the middle of the distribution, whilst it may fail at each of the tails. In addition, due to the already existing differences between the size detection range of each device, fitting of the middle of the distribution is a good compromise for comparing the data. In most cases, the distributions were monomodal, which allowed to fit them to log-normal curves. However, the relatively broadened distributions observed especially for the MastersizerS are an indication of a possible bimodal distribution originating from monomodal distributions with largely overlapping tails. This fact can also be observed from the standard deviations obtained after fitting a log-normal distribution to the data. The geometric standard deviations from fitting the IMAN, SHAPE and TOT data were mainly between 0.35 μm and 0.60 μm , whereas those of the MastersizerS device were between 0.87 μm and 1.29 μm . Comparable geometric means were obtained when fitting SHAPE and TOT number distributions and SHAPE, TOT and MastersizerS volume distributions (Table 3.8). It should be mentioned that, since the volume-based distributions of the TOT yielded bimodal distributions, their fit with a log-normal distribution could not be reliably performed.

Table 3.8 The geometric mean obtained from fitting the results with the log-normal distribution (N = number based distribution, V = volume based distribution).

Sludge sample	$x_g N / x_g V$ (μm) (MastersizerS)	$x_g N / x_g V$ (μm) (TOT)	$x_g N / x_g V$ (μm) (SHAPE)	$x_g N / x_g V$ (μm) (IMAN)
S1	1.15/51.45	6.61/-	9.58/43.41	22.66/94.25
S2	0.45/54.8	7.09/-	15.46/43.63	18.81/45.69
S3	0.38/43.49	10.98/-	11.75/44.36	17.72/50.53

Since the geometric mean and the median of a log-normal distribution coincide, the distribution can be completely characterized by calculating its parameters according to Allen (1997):

$$x_g = x_{50} \quad (3.24)$$

$$\log \sigma_g = \log x_{84} - \log x_{50} = \log x_{50} - \log x_{16} = \log \sqrt{\frac{x_{84}}{x_{16}}} \quad (3.25)$$

where x_{16} , x_{50} and x_{84} are the particle sizes at 16 %, 50 % and 84 %, respectively and are extracted from the cumulative floc size distributions.

If a number distribution fits a log-normal distribution, then its transformation to volume distribution will result in another log-normal distribution (Allen, 1997), characterized by:

$$\sigma_g V = \sigma_g N \quad (3.26)$$

$$\ln x_g V = \ln x_g N + 3 \ln^2 \sigma_g \quad (3.27)$$

Equations (3.26) and (3.27) were applied to transform the TOT, SHAPE and IMAN fitted log-normal number distributions into log-normal volume distributions, which were then compared with original MastersizerS volume-based distributions. Similarly, the fitted log-normal

volume distributions from the MastersizerS were transformed into log-normal number distributions and compared with the number-based distributions measured by using the counting techniques. By performing these transformations, new values for the geometric standard deviation and geometric mean have been obtained (Table 3.9).

Table 3.9 The geometric mean and geometric standard deviation obtained from the transformation based on log-normal distribution.

Sample	MastersizerS		TOT		Shape		IMAN	
	σ_g (μm)	x_g N(μm)	σ_g (μm)	x_g V(μm)	σ_g (μm)	x_g V(μm)	σ_g (μm)	x_g V(μm)
S1	2.02	8.53	1.58	12.56	1.99	40.35	2.52	110.10
S2	1.89	14.13	1.71	15.53	1.78	41.47	2.15	119.25
S3	2.15	6.66	1.72	24.78	1.79	32.81	1.90	68.37

The number- and volume based cumulative distributions obtained from the log-normal distribution assumption are shown for each of the analysed sludge sample in Figure 3.35.

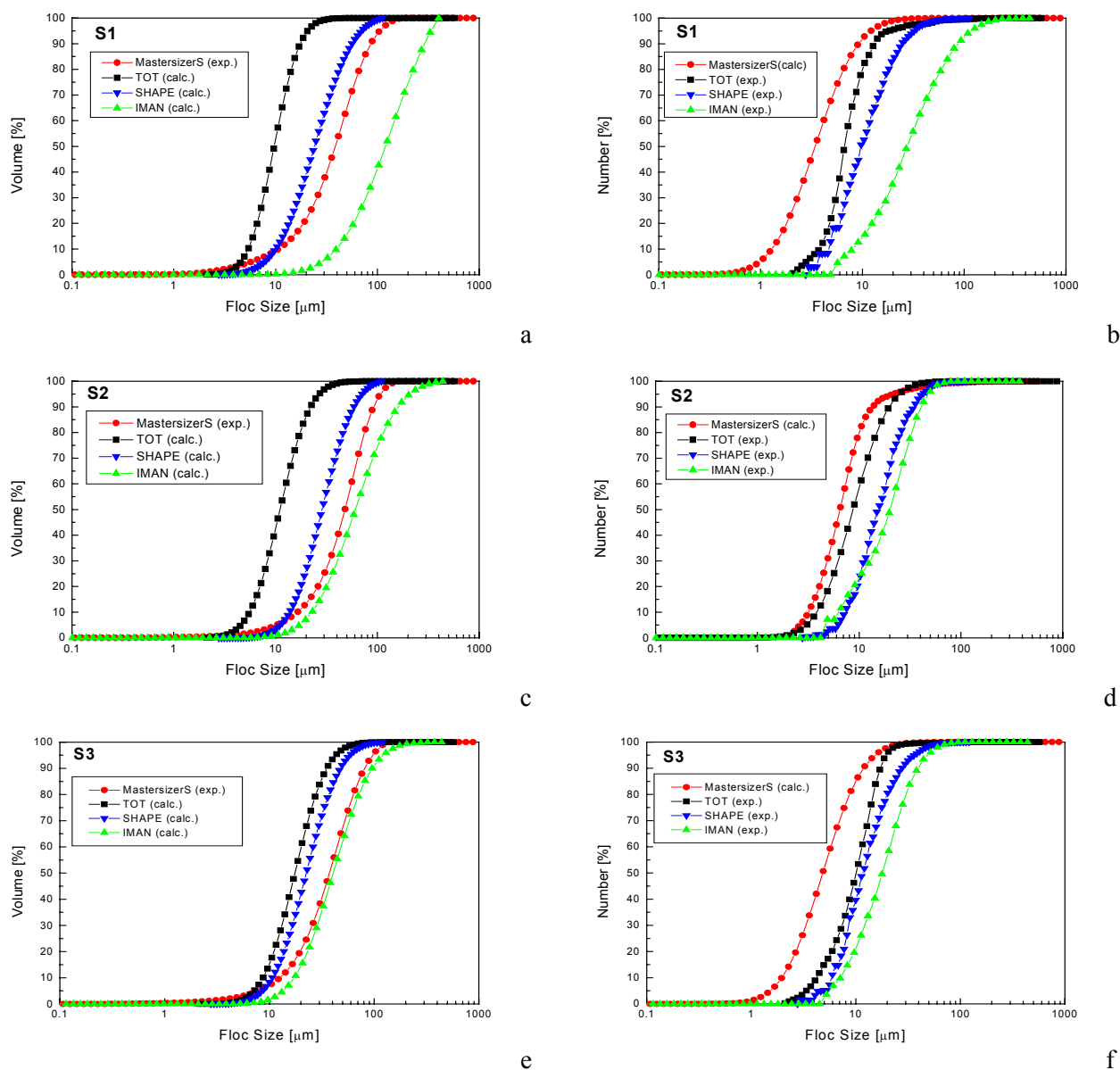


Figure 3.35 Log-normal volume (a,c,e) and number (b,d,f) distributions calculated from fitted log-normal number (a,c,e) and volume (b,d,f) distributions.

It was observed that for all analysed samples the volume distribution given by the MastersizerS showed a better correlation with the other devices calculated volume size distributions (Figure 3.35,a,c,e). This is mainly due to the fact that the few big size particles detected by the TOT method are not accounted for anymore in the log-normal volume distribution when this is calculated back from the fitted log-normal number distribution.

For the case in which the experimental number distributions of SHAPE, TOT and IMAN are compared with the calculated log-normal number distributions of the MastersizerS, the latter does no longer show the very large number in small particles and tends to agree better with the results obtained with the CIS-100 device (Figure 3.35,b).

Moreover, by using the average diameters a general comparison between the experimental distributions and those calculated based on the log-normal distribution assumption of the analysed sludge sample may be carried out.

Accordingly, when number-based average diameters $D(n,10)$; $D(n,50)$; $D(n,90)$ are compared (Figure 3.36) a similar trend of the generated results by the measurement techniques is observed. The tendency of IMAN to overestimate the size of particles is observed especially for sample S1. However, the techniques based on image analysis (IMAN and SHAPE) generally measured larger size as compared with the laser techniques (MastersizerS and TOT)

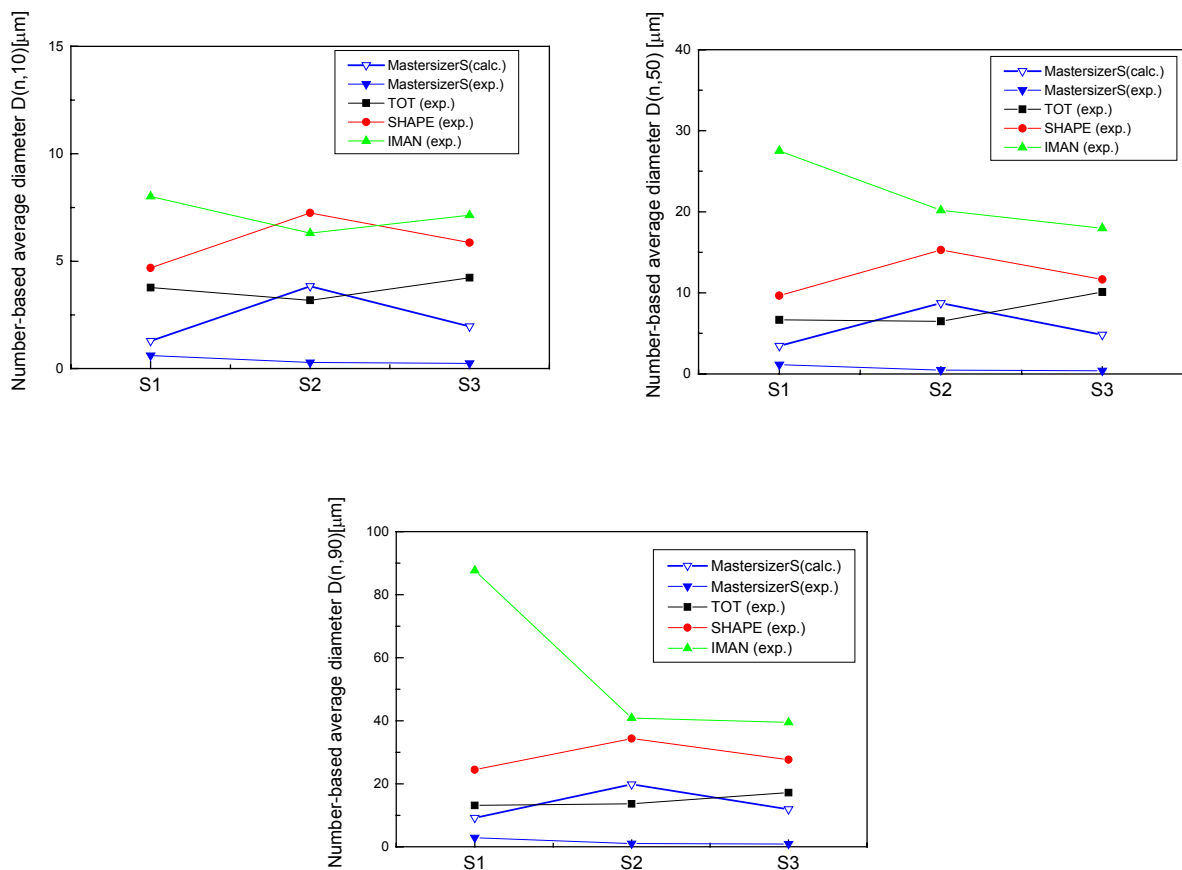


Figure 3.36 Number-based average diameters obtained experimentally and calculated from a log-normal distribution for the case of MastersizerS.

The TOT and SHAPE showed close number-based average diameters values, which indicate an agreement between the number-based distributions measured by those two devices. MastersizerS results predicted the smallest number-based average diameter values as directly

generated from the experimental results. When the results are calculated from the log-normal distribution, they showed values closer to those of TOT and SHAPE. A remarkable similarity was shown for the $D(n,90)$ obtained from TOT and MastersizerS calculated from the log-normal distribution. This gives an indication of the good prediction of the overall number distributions obtained by using the laser devices and especially in the larger size range. However, this is only valid for the log-normal distributions obtained from the MastersizerS where the long tail in the submicron range was not considered.

The volume-based average diameters ($D(v,10)$; $D(v,50)$ and $D(v,90)$) obtained directly from the experimental data (MastersizerS) are compared in Figure 3.36 with those transformed from number distributions based on the spherical shape assumption (TOT, SHAPE and IMAN) and log-normal distributions. A relatively good agreement between the results was seen especially for MastersizerS, SHAPE and the diameters calculated from the log-normal distribution for the case of TOT.

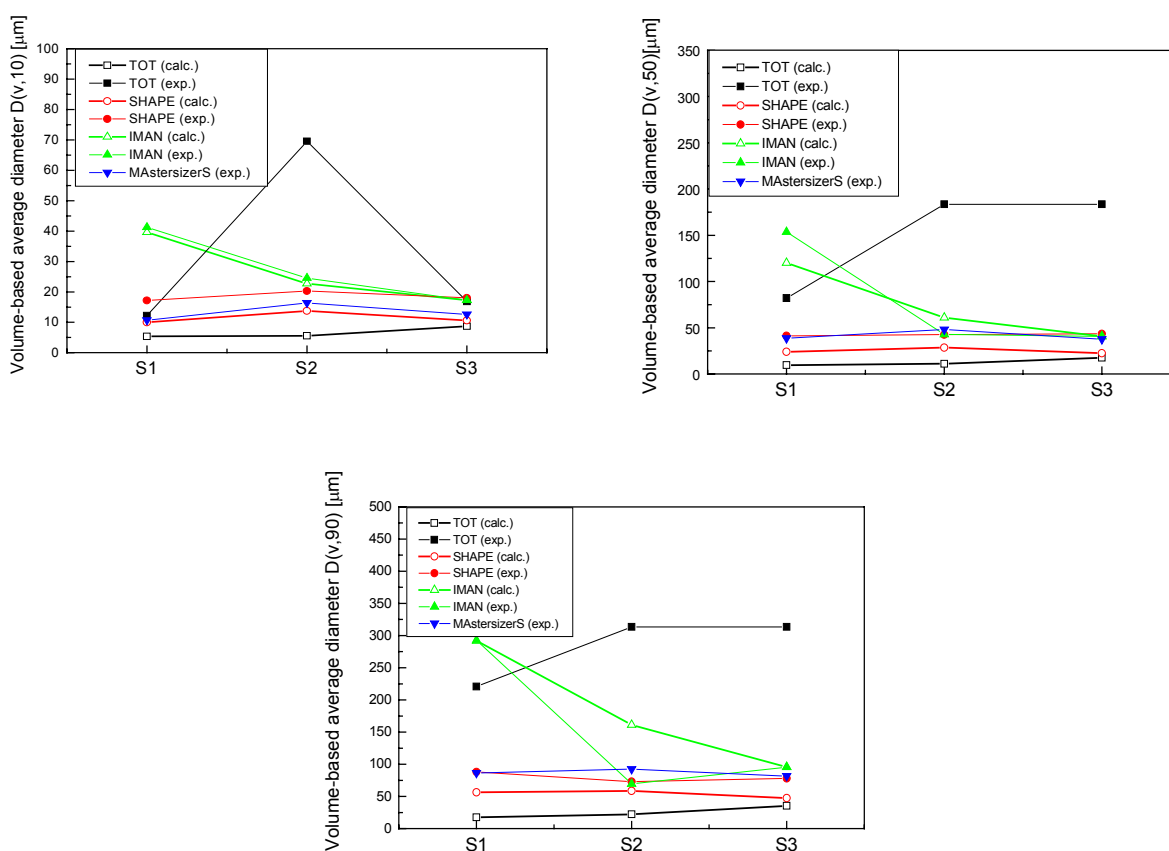


Figure 3.37 Volume-based average diameters obtained experimentally and calculated from a log-normal distribution for the case of number-based measurement techniques (TOT, SHAPE and IMAN).

4.5.4.3. Conclusions

The results showed that the MastersizerS and SHAPE devices yield similar volume weighted FSD's. In contrast, the IMAN slightly overestimated the floc size and TOT frequently showed a bimodal distribution. The number distributions from TOT, SHAPE, IMAN were in general in good agreement, while those generated by the MastersizerS were mainly located in the submicron range.

It may be concluded that the measurement principle (number or volume based) is of large importance for the correct interpretation of the data. Conversion of the results may be misleading and should be used with caution.

3.6. Fractal dimension measurement by using on-line techniques

As shown and discussed before in this chapter activated sludge flocs are often described by using the fractal concept. Depending on the measurement method different fractal dimensions may be calculated and used to characterize the fractal nature of the aggregates: D_3 (a three dimensional fractal dimension), D_2 (a two-dimensional fractal dimension) and D_1 (a one-dimensional fractal dimension) in which compact aggregates will have values of 1, 2 and 3 for linear, planar and respectively three-dimensional space. Fractional values measure the fractal dimension of an aggregate. Accordingly, any object found in a real physical process may have a mass fractal dimension $1 < D_f < 3$ (Bushell et al. 2002). High fractal values indicate compact aggregates whereas low values correspond to more 'loose' aggregates (Wilén et al., 2003).

In this section the fractal structure of the activated sludge is analysed as a function of the results given by the different sizing devices. The aim is to evaluate whether a possible link can be found between the floc structure as predicted by the different devices used as well as whenever the fractal dimension may be used for evaluating the structural changes of the flocs during the flocculation of the activated sludge.

For this purpose, a simple case will be analysed here for the measurements performed with activated sludge sample (S1) of which results are presented in Figure 3.34-a,b. For evaluating the possibility to predict the structural changes by using fractal dimension the effect of 5 min. sonication on the same sludge sample is considered (Figure 3.31). Moreover, the floc size dynamics and fractal dimension values recorded during a deflocculation – reflocculation process will be investigated as well.

3.6.1. Fractal dimension obtained by using MastersizerS device

The MastersizerS is one of the most often reported devices based on LALLS principle which is used for fractal dimension determination (Jin et al., 2003; Wilén et al., 2003). An intensive study regarding the possibility of using LALLS theory for describing the fractal dimension was carried out and is described in detail by Guan et al., (1998a), Waite (1999) and Bushell et al. (2002).

Basically, as summarized by Waite et al. (1998), the concept of fractal dimension determined by LALLS devices starts from the power law dependency between the total scattered intensity $I(q)$ and the magnitude of the wave vector (q) as shown in equation (3.28).

$$I(q) \propto q^{-dF} \quad (3.28)$$

where dF is the fractal dimension and the wave vector (q) is calculated by using the following formula:

$$q = |q| = (4\pi n_0 / \lambda) \sin(\theta/2) \quad (3.29)$$

where θ is the scattering angle, λ is the wavelength of the incident beam and n_0 is the refractive index of the medium.

For the case of analysing activated sludge samples by using MastersizerS the following issues should be taken into consideration. In analysis, a 300RF lens has been used for which

scattering angles for each of the 44 detectors are provided by Malvern Instruments Ltd (UK), known as "magic numbers". The device wavelength (λ) is 362.8nm and the refractive index of the dispersed medium which in this case was filtered effluent was considered as being equal with that of water (1.33) (Biggs, 1999).

Moreover, the equation (3.28) is supported by the Rayleigh-Gans-Debye approximation (RGD) which is valid only if the following conditions are satisfied:

$$|m - 1| \ll 1 \quad (3.30)$$

$$(4\pi a/\lambda)|m - 1| \ll 1 \quad (3.31)$$

where: a is the size of the scattering particle and m is the relative refractive index to the medium (n/n_0) of the particles.

Guan et al. (1998a) showed that for the case of activated sludge the first condition may be satisfied by assuming a refractive index of the particles (1.05) which was found to be specific for biological systems.

The second condition is apparently valid according to the RGB approximation for particle sizes less than 1 μm . However, Guan et al. (1998a) demonstrated that for the case of systems with low refractive index this assumption can be relaxed and showed the method applicability for relatively large flocs size ($\sim 100 \mu\text{m}$). Based on this assumption later work on fractal dimension determination for activated sludge by using LALLS was presented by Chaignon et al. (2002) and Wilén et al. (2003).

However, two other important criteria were indicated by Guan et al. (1998a). They should be satisfied in order to measure the fractal dimension from the scattering data.

The first criterion consists in the necessity to find a distinct power law behaviour of the scattering pattern which may be satisfied only if $1/R_g \ll q \ll 1/a$ where R_g is the radius of gyration that represents the standard deviation of the particles from their centre of mass (Waite et al., 1998). The fractal dimension is therefore calculated as a linear slope of a log-log plot between the light scattering intensity (I) and the wave vector (q).

The most controversial criterion is that related to the sample polydispersity effect, which must be negligible. Waite et al. (1999) argued that the polydispersity effect is insignificant for narrow distributions. This however, is not the case for the activated sludge floc size distributions. In this context, Biggs (2000) pointed out the importance of considering the polydispersity effect when sludge samples are measured and suggested that only a correct incorporation of this issue on the calculated fractal dimension may lead to a correct interpretation of the changes in fractal dimension that occur during flocculation.

This method was applied for the activated sludge samples with a size range up to 100-200 μm (Waite 1999; Wilén et al. 2003). Figure 3.38 shows the volume-based FSD recorded at the initial steady state and after 5 min. sonication. It may be observed that by sonication a shift of the distribution to the lower size ranges occurred.

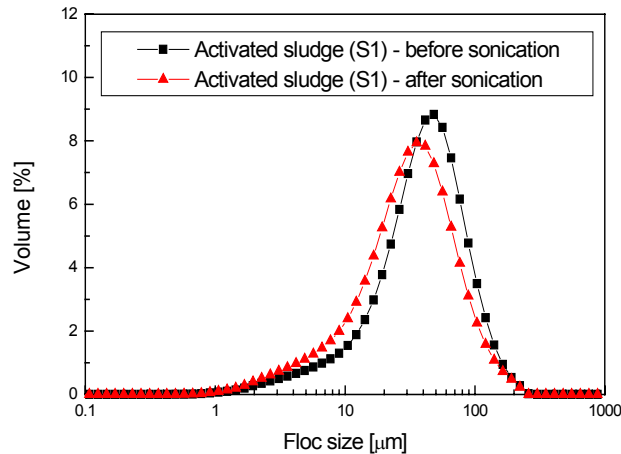


Figure 3.38 The volume based FSD of the activated sludge sample (S1) measured by using the MastersizerS technique before and after sludge sonication.

To calculate the fractal dimension the log-log plot of scattering intensity (I) as a function of the wave number (q) was used. Figure 3.39 illustrates an example of fractal dimension determination for one measurement performed at steady state flocculation with the activated sludge sample (S1).

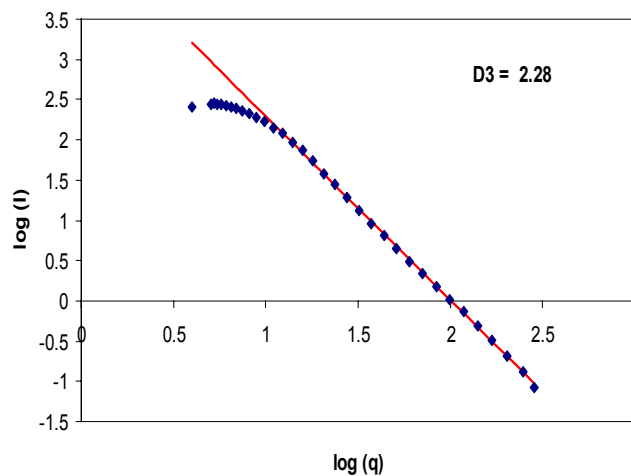


Figure 3.39 Example of calculating the fractal dimension by using MastersizerS for the activated sludge sample (S1) without sonication.

By calculating the average fractal dimension of the size distributions at steady state a value of $D_3 = 2.27 \pm 0.01$ was found. The steady state size distribution was characterised by a floc size mass mean diameter $D[4,3] = 44.46 \pm 0.45 \mu\text{m}$. When sonication was applied a decrease of the fractal value to $D_3 = 2.15 \pm 0.05$ occurred and the floc size $D[4,3] = 35.46 \pm 0.66 \mu\text{m}$.

The obtained values for the fractal dimension are in agreement with other reported values for activated sludge flocs. Accordingly, Guan et al. (1998a) reported fractal dimensions taking values from 2.04 up to 2.20 determined by using the same method.

It seems however, that the high energy imposed by sonication affected the internal structure of the flocs creating smaller aggregates but with a "looser" structure. It may be also that the polydispersity phenomena may have an influence on the obtained results as shown by Biggs (2000). Indeed, the obtained results are not always in agreement with the reported fractal dimensions when exposed to different shear conditions. In this sense, Zartarian et al. (1994) found that microfloc formation is characterised by a fractal dimension close to 3 and very dense aggregate formation. Therefore, the method used for the fractal dimension measurement and the nature of the analysed flocs may also be relevant.

However, before any conclusion, the fractal dimension results of the other techniques should be investigated as well.

3.6.2. Fractal dimension obtained by using TOT

A few methods are presented in literature to derive the fractal dimension of aggregates from a counting technique.

A first method presented by Jiang and Logan (1996) and Tang et al. (2001) is the so-called two-slope technique. According to this technique it is necessary to identify the portion of a size distribution that describes the same population of particles in terms of length or volume.

Another method, very similar with the previous one described by Li et al. (1998) and Serra and Logan (1999) was called particle concentration technique (PCT). The fractal dimension can be calculated from the same length and volume cumulative distributions obtained from different measurement techniques.

However, it is considered that for applying these methods a technique based on the Coulter principle is more suitable since it allows a direct relation between the number of the particles and their volume. Using TOT the volume is related to the measured chord length diameter and therefore the results obtained are related to different particles size classes which create difficulties in obtaining a direct correspondence between each analysed particle and its volume which is required for building an exact volume weighted cumulative distribution. Moreover, combining two techniques for determining the floc structural properties may be considered as being not suitable because fast structural changes may occur during the flocculation process when different external conditions such as sonication are applied. Therefore, a fractal dimension extracted by using the TOT method is not considered, further.

3.6.3. Fractal dimension by using the SHAPE method

The fractal dimension (D_f) may be derived directly from the image analysis software incorporated in the CIS-100 device. It is calculated from the relationship between the log of the perimeter against the log of the resolution.

A fractal dimension $D_f = 1.05 \pm 0.12$ was calculated for the activated sludge sample before sonication, while after sonication the fractal dimension became $D_f = 1.036 \pm 0.11$. The obtained values are very close to a fractal dimension of 1 which gives an indication of a regular perimeter. A slight decrease of the fractal value was observed when sonication was applied. It should be considered that in this case, in order to obtain a statistically significant size distribution, the short recording time steps as used for the MastersizerS could not be applied and the sonication was evaluated as a global effect occurring on the analysed sludge sample during 5 minutes sonication time.

3.6.4. Fractal dimension obtained from IMAN

By using image analysis technique a two-dimensional fractal dimension may be calculated since the obtained images are projected in a two-dimensional space. Several methods are reported in literature and may be used to obtain the fractal dimension from image analysis. Cousin and Ganczarczyk (1998) determined two fractal dimensions by using image analysis (Sierpinski and Boundary). The Sierpinski fractal dimension is typically used to quantify pore structure and distribution, while the boundary fractal dimension represents a measure of the roughness of the surface profile of the measured flocs. Grijspeerdt and Verstraete (1997) determined the fractal dimension by using the “mosaic amalgamation” algorithm. The most common technique is the box-counting method. Boxes of variable size (s), are placed over the object, and the number of boxes that contain portions of the object, $N(s)$, are counted (Russ, 1990). The fractal dimension (D_f) is calculated from:

$$N(s) \propto s^{-D_f} \quad (3.32)$$

However, for calculating these fractal dimensions the analysis of individual flocs is necessary. This may be performed when a sufficiently high magnification lens is used which allows the analysis of each individual floc. This method is difficult to be applied for the considered on-line image analysis system in which 4x magnification lens was used.

Therefore the perimeter based fractal dimension (D_p) method which allows a global overview of the floc dimensions obtained from the image analysis was used. In this case the particle perimeter (Pr) was related to the projected area of the flocs (A) by equation (3.33) (Spicer and Pratsinis, 1996).

$$A \propto Pr^{2/D_p} \quad (3.33)$$

The D_p may be related to the floc surface morphology and varies between 2 (a line) and 1 (the projected area of a solid sphere, a circle). Large values of D_p therefore represent open and irregular floc structure (Spicer and Pratsinis, 1996).

The fractal dimension was derived from the slope ($2/D_p$) of the log-log plot between perimeter and related projected area as illustrated in Figure 3.40. Accordingly, for the activated sludge sample (S1) the fractal dimension calculated from the IMAN data is $D_p = 1.22$ before sonication (Figure 3.40-left) and $D_p = 1.05$ after sonication (Figure 3.40-right). The obtained fractal dimension for the sludge before being supposed to the sonication is in good agreement with the results reported by Li and Ganczarczyk (1991) which found a $D_p = 1.13 - 1.22$

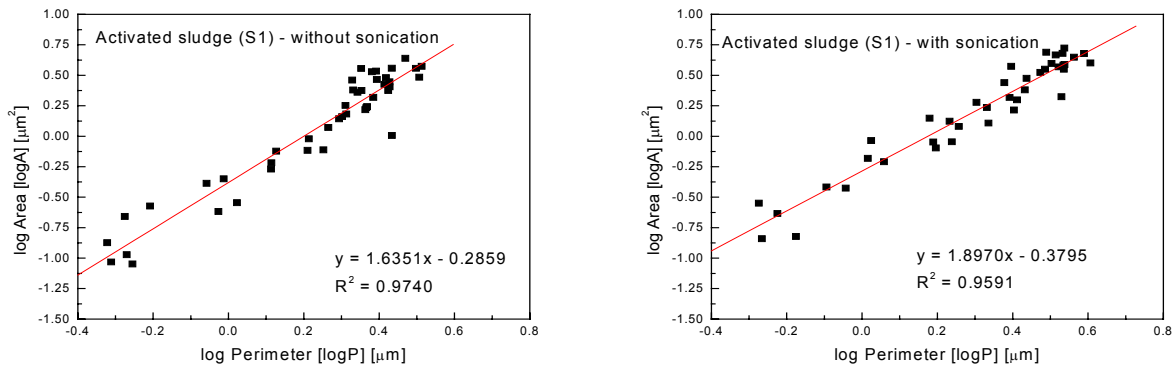


Figure 3.40 The fractal dimension (D_p) calculated for activated sludge sample (S1): without sonication (left) and with sonication (right).

Accordingly, the decrease of the fractal dimension D_p as observed by the IMAN technique gives an indication of compact flocs which are very close to those of a solid sphere. These results however contradict the results obtained with the MastersizerS and are more in agreement with the other reported literature data in which it is shown that under shear stress conditions small and compact aggregates are formed (Spicer and Pratsinis, 1996).

3.6.5. The dynamics in fractal dimension as recorded with MastersizerS

Due to the contradictory observations, another experiment was performed by using the MastersizerS. Accordingly, the fractal dimension was evaluated during a deflocculation-reflocculation experiment and compared with the mass mean diameter of the flocs. As observed before as well, sonication created a decrease of the fractal dimension, which as shown in Figure 3.41 has a similar trend with the decreasing floc size. After sonication a small reflocculation effect was observed in the floc size data. The restructuring effect is observed from the fractal dimension, which continues to decrease slightly especially in the first minutes after sonication. This is followed by a tendency to stabilise.

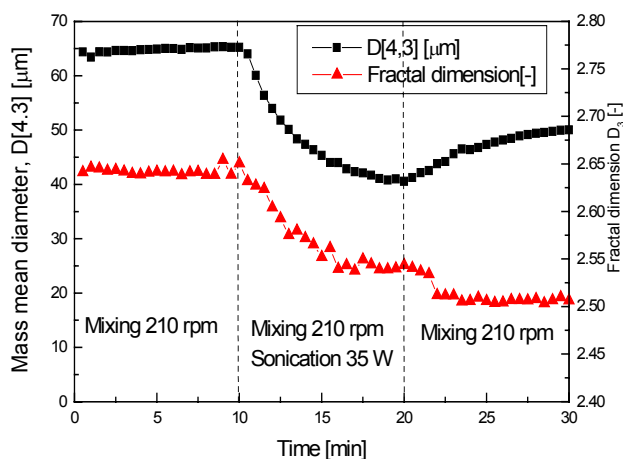


Figure 3.41 The evolution of fractal dimension and mass mean diameter for an experiment performed with an activated sludge sample.

By taking into account the previous results and the observed disagreement between the results predicted by different devices it seems that the MastersizerS is not well suited for the determination of the fractal dimension of the sonicated sludge and polydispersity phenomena may influence these results. According to Bushell et al. (2002), polydispersity can be observed by deviation of the power law at a higher q values. However, Figure 3.42 shows an example of two log-log plots obtained for the recorded data after 5 min. and respectively 10 min. sludge sonication in which no significant deviation from the power-law of the high q values, was observed which may sustain the polydispersity hypothesis.

Since contradictory results were observed at this stage it is difficult to find a right answer regarding the fractal dimension measurement as given by the evaluated techniques. It may be possible as well that the low magnification lens used for image analysis caused the method to be less sensitive for the correct evaluation of the particle perimeters, which were used for fractal evaluation.

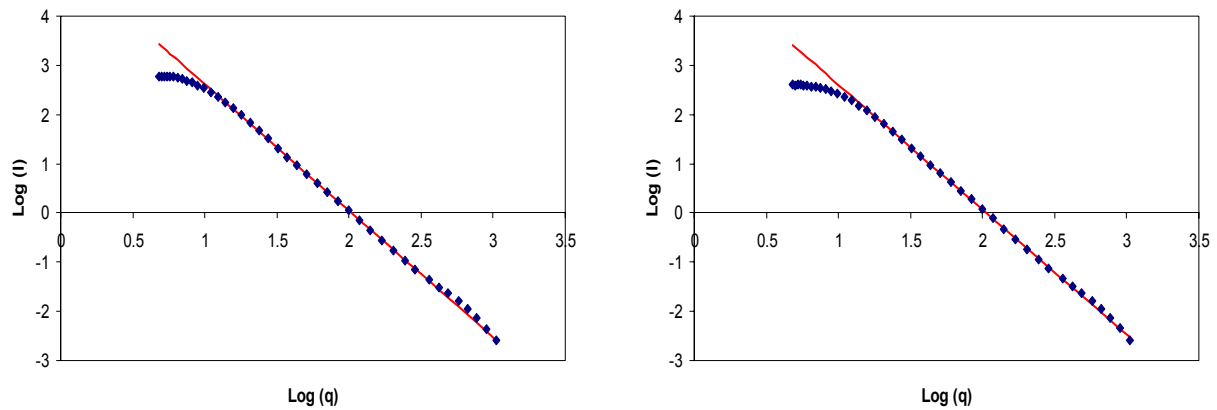


Figure 3.42 The log-log plot for the activated sludge sample analysed after 5 min. sonication (left) and 10 min. sonication (right).

Given that the sludge sonication method was found not to be suitable for the purpose of the present study, it was not used further and a systematic investigation of the observed phenomena was not performed. However this is highly recommended for future work. It is believed that studying the sonication effect on floc structural properties by using fractal dimensions measurements may give valuable insights into understanding the structural properties of the flocs.

It is concluded that the fractal dimension may only be used for evaluating the floc structural properties if some limitations imposed by the devices are respected. In this context the measured floc size is at high importance. For very large and open structure flocs the MastersizerS produces multiple scattering and self-interactions between the large aggregates occurred which may be detected by an excessive curvature of the log-log plot (Guan et al. 1998a). Moreover, the techniques based on image analysis may not be always fast enough for detecting the changes into the floc structure in very dynamic processes. This may also accentuate when large flocs are formed leading to very few flocs to be counted in each image. Very small flocs may be a restriction for the image analysis technique as well due to its limitations in the smaller size detection range. Therefore, the considered devices can not be used for the measurement of the fractal dimension of large or very small size aggregates.

3.7. Conclusions

It was shown in this chapter that for a correct evaluation of the morphological properties, and especially the floc size and size distribution measurements, it is important to establish a good experimental protocol in which the selection of the suitable device and the influence of the set-up components play an important role.

Accordingly, a MastersizerS and a CIS-100 (with two measurement channels, based on time of transition (TOT), and image analysis (SHAPE) principles), as well as an in house image analysis system (IMAN) have been selected and their performances and capabilities for activated sludge FSD were systematically evaluated and compared.

For selecting these devices, their relative wide size range measurements, limited chances of damaging the flocs during the measurements, on-line measurement abilities and similar sample dilution requirements were considered. However, a fact to accounted for from the beginning was their drawback in the measurement of small particles (down from 10 μm)

which are due to the measurement principle (requirement of the optical properties – MastersizerS) or the limited size detection range (IMAN).

Before evaluating and comparing the selected sizing devices capabilities, some features related to the experimental protocol and set-up components were evaluated in view of the development of a suitable on-line technique. The main conclusions revealed the following:

- For a large volume of samples (2 L and more), mixing is preferred over a sonication tip to disturb the flocs with the purpose of following the reflocculation process
- The tubes connecting the flocculation reactor with the sizing devices should be as short as possible and the in-line dilution should be performed as close as possible to the sampling point to avoid in-tube flocculation.

The sizing devices results were further evaluated by connecting the devices in series and performing on-line measurements.

A very important issue to consider when activated sludge floc size distributions are measured is the effect of the particles' shape on the results generated by the considered devices. To investigate the effect of shape, the activated sludge floc size distributions were evaluated and compared with the results obtained by using spherically shaped particles (glass beads) or irregularly shaped inorganic particles (sand). It was found that when spherically shape assumption is used for generating the results the most sensitive to the particles shape is the MastersizerS, which similar to all ensemble techniques, measures the particles over all their orientations, producing a broader distribution. The techniques based on image analysis (SHAPE and IMAN) were less sensitive to the particles shapes when the equivalent spherical diameter was used to generate the results. A shape effect on size distributions generated by using the TOT method was detected for sand particles. However, it was difficult to extend this conclusion to the activated sludge flocs due to the few large particles detected in the volume distributions, which affected the results interpretation.

Consequently, it was found that the measurement principle is of high importance for the correct interpretation of the results and their transformation can lead to a misinterpretation of the data.

Finally, the possibility to investigate the fractal dimension by using the selected devices was analysed. It was concluded that the fractal dimension can not be used for characterising very dynamic processes of the large size aggregates due to the limitations of the considered devices.

In summary, by coupling three sizing devices it was possible to comparatively measure the activated sludge floc size distributions, while eliminating variations in time due to sample preparation and manipulation. All techniques used turned out to be fast and reliable methods to quantify the floc size distribution under steady state conditions. The measurement results were often in agreement, and the methods complemented each other in terms of size range. However, when the focus is on monitoring flocculation dynamics, the techniques based on laser light scattering are more suited to follow the fast changes in floc size that may occur during the process. The counting devices suffer from the longer acquisition times needed. Since devices like the MastersizerS do not usually offer visual information, coupling them to an image analysis system allows a direct visual inspection of the process evolution, while a counting technique such as TOT is more accurate when the number distributions are of interest.

Monitoring of the activated sludge properties in a Sequencing Batch Reactor

4.1. Introduction

The effectiveness of the activated sludge process is, among others, subject to a good solid – liquid separation. The settling properties mainly depend on the flocs' morphological properties and the activated sludge microbial population. Several attempts have already been made to evaluate the settling and floc size and structural properties of activated sludge (Andreadakis, 1993; Wilén and Balmer, 1999; Dagot et al., 2000; Seka et al., 2001) or to monitor the population dynamics under stable environmental conditions (Fernandez et al. 1999; Kaewpipat and Grady, 2002). However, due to the high sensitivity of the microorganisms to environmental conditions, many characteristics of the biological treatment system remain poorly understood and therefore, difficult to interpret and to control.

Since the main purpose of this research is the evaluation of the effect of different physico-chemical parameters on the (de)floculation process it is of utmost importance to exclude as much as possible the variations that can occur in the investigated activated sludge properties. Hence, achieving a stable biological sludge to be used for experiments is required in this study. This chapter will deal with the breeding of this stable sludge and its monitoring.

It focuses on:

- A brief review of sludge stability and its evaluation procedures.
- A general presentation of the Sequencing Batch Reactor (SBR) set-up used for experimentations, including a description of the main parts and of the operating conditions.
- Both a long-term and a short-term monitoring of the SBR's activated sludge structural properties and of the population dynamics for the sludge stability evaluation.

4.2. Sludge stability evaluation

The primary goal of biological wastewater treatment is to sustain optimum reactor performance over a long-term period. Therefore, a stable reactor performance requires at least some degree of stability among the individual populations that constitute the microbial community in such bioreactors, but it also requires flexibility of this community to adapt to changing conditions. The main question is whether any functional stability implies a persistent microbial community and therefore, uniform activated sludge properties.

"Ecosystem" stability encompasses a broad spectrum of definitions, which resolve into two main groups: the measurable functional properties of the ecosystem and the population composition (Fernandez et al., 1999). Despite the importance of the microbial community in wastewater treatment, there is still a limited understanding of the relationship between microbial community and process functionality. Moreover, only a few attempts to evaluate the microbial community dynamics can be found in literature. In this context, Fernandez et al. (1999) found that an extremely dynamic community sustained the functional stability of the process. In contrast, long-term stable microbial communities were reported by LaPara et al. (2002) for operationally stable wastewater treatment plants. Moreover, Smith et al. (2003) observed a stable microbial community during normal operation conditions as well as during short-term process instabilities.

A first requirement for obtaining stable sludge properties and, especially, microbial community is to have a well controlled and stable activated sludge process. Good monitoring techniques are therefore essential to quantify and qualify the activated sludge settling properties as well as the structural properties and the dynamics of the microbial populations. This may provide insights in the relation between the microbial community changes and process performance.

In this study, a Sequencing Batch Reactor (SBR) process was evaluated in terms of its sludge settling properties (Sludge Volume Index - SVI), structural properties (floc size, size distribution and microscopy) and microbial community (Denaturing Gradient Gel Electrophoresis – DGGE).

4.2.1. Operation principle of the SBR technology

In its most basic form, a SBR system is simply a set of tanks that operate on a fill-and-draw basis. Due to its batch character, several SBR reactors are used in parallel with cycles shifted in time to ensure a "continuous" treatment of the incoming wastewater. A single-tank system is well suited for noncontinuous flows, especially those found in small communities and in many industries (Irvine and Busch, 1979).

The essential difference between the SBR and conventional continuous-flow activated sludge systems is that the SBR tank carries out many functions such as equalisation, aeration and sedimentation in a time rather than in a space sequence. In short, the SBR is best defined as a time-oriented and periodic process (Irvine and Ketchum, 1989).

Factors that enabled this technology's acceptance for wastewater treatment include the following (Wilderer et al., 2001):

- its simple automation;
- its operation can be easily modified to allow control over bacterial species that cause filamentous bulking, nutrient removal or the destruction of hazardous organics;
- the ability to select robust microbial communities that maintain high removal performances during periods of shock loads;
- the ability to adjust the time and magnitude of energy input, the fraction of each tank's volume used and the number of tanks placed into operation to meet the actual loading conditions.

SBRs are typically used for small flow rates and are very useful for areas where the available land is limited. Due to their great efficiency and flexibility, the SBRs are very appropriate to

treat different kinds of wastewater such as municipal, domestic, hypersaline, tannery, brewery, etc. under different conditions (Mace and Mata-Alvarez, 2002).

The operation of an SBR consists basically of the following steps: Idle, Fill, React, Settle and Draw (Figure 4.1). More than one operating strategy is possible during most of these steps (EPA, 1999).

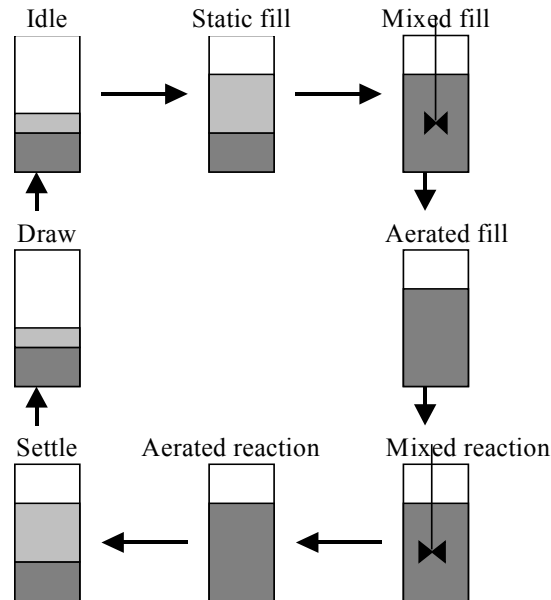


Figure 4.1 Schematic overview of the SBR operation cycle (adapted from Mace and Mata-Alvarez, 2002).

The *idle* step occurs between the *draw* and the *fill* phase in a multitank system. Purpose is to provide time for one reactor to complete its fill cycle before switching to another unit. Since idle is not a necessary step, it is sometime omitted. The length of the idle step varies depending on the influent flow-rate and the operating strategy. Mixing of the biomass and sludge wasting can also be performed during the *idle* step, depending on the operating conditions.

Influent wastewater is added to the reactor during the *fill* step. Depending on the operating strategy, three types of filling may be used: *static fill*, *mixed fill* or *aerated fill*.

- During the *static fill*, influent wastewater is added to the biomass already present in the SBR. *Static fill* is characterised by the absence of mixing or aeration, meaning that there will be a high substrate concentration when mixing starts. A high food to microorganisms (F:M) ratio creates an environment favourable for floc forming organisms versus filamentous organisms, which provide good settling characteristics for the sludge. *Static fill* may be compared to a "selector" compartment in a conventional activated sludge system to control the F:M ratio.
- *Mixed fill* is used when the added the influent is mixed with the biomass, which initiates biological reactions. During *mixed fill*, bacteria biologically degrade the organics and use residual oxygen or alternative electron acceptors, such as nitrate-nitrogen. Denitrification may occur under these anoxic conditions. Anaerobic conditions can also be achieved during the *mixing fill* phase. After the microorganisms have depleted the nitrate-nitrogen, sulphate becomes the electron acceptor.

- *Aerated fill* is characterised by aerating the content of the reactor to already begin the aerobic reactions that are normally completed in the react step and can therefore reduce the aeration time required in the react step.

The biological reactions are completed in the *react* step, in which *mixed react* and *aerated react* modes are available.

- During *aerated react*, the aerobic reactions possibly initialised during the *aerated fill* are completed and nitrification can be achieved.
- In the *mixed react* mode anoxic conditions are created to achieve denitrification. An anaerobic medium can be achieved as well in the *mixed react* mode enabling biological phosphorus removal.

Settle is typically provided under quiescent conditions in the SBR. In some cases, gentle mixing during the initial stages of settling may result in a clearer effluent and a more concentrated settled sludge, thanks to improved flocculator.

The *draw* step uses a decanter to remove the treated effluent, and its construction is the primary distinguishing factor between different SBR manufacturers. In general, there are floating and fixed decanters.

The number of processes and components together with the complexity of SBR hydraulics makes it impossible to come up with an accurate prediction of the effluent quality, without the use of appropriate modelling (Artan et al. 2002). For a systematic evaluation of the design and operating strategies and therefore for process optimisation, models reflecting microbial behavior with reasonable accuracy are regarded as valuable tools. In this sense, a calibrated activated sludge model is a good tool to evaluate numerous operation scenarios within a short time in order to upgrade the nutrient removal capacity of an SBR (Sin et al., 2004). For performing this, the model requires a good calibration methodology, which includes the use of knowledge of the influent wastewater, operating conditions and of the treatment system itself (Insel et al., 2004). The model-based interpretation of the system may then not only lead to a better understanding of the biological processes but also provide a way of selecting the most appropriate operating parameters.

4.2.2. Monitoring the SBR activated sludge properties

4.2.2.1. Settling properties – Sludge Volume index (SVI)

In practice, settling and separation properties are typically characterised by the SVI and the supernatant turbidity.

As shown in Chapter 2, the SVI is the most common way to evaluate how well a sludge settles and compacts, being widely accepted as a standard method (APHA, 1992) because of the simplicity of the analysis methodology. However, it is also a very controversial and non-specific variable, which may be influenced by a series of factors such as the structure of the flocs, suspended solids concentration, cylinder diameter and height of the settling column, temperature and stirring (Dick and Vesilind, 1969; Sezgin, 1982).

The floc characteristics that have been found to affect the SVI are the number and type of filamentous bacteria and/or zooglycal bacteria (Sezgin, 1982; Jin et al., 2003), the floc size and density for non-filamentous sludge (Andreadakis, 1993) and the amount of EPS in the sludge (Urbain et al., 1993).

4.2.2.2. Structural properties – Floc Size Distribution (FSD) and microscopical observations

As discussed in Chapter 3, floc size measurements represent a useful tool for the fast detection of operational changes. Moreover, monitoring the size of the flocs will allow for thorough understanding of the settling properties and of the process performance.

Microscopical evaluation is still the most used technique for analysing floc properties. Even if, for size measurements, this technique requires special attention and is time consuming since a large number of flocs should be analysed in order to have a statistically good evaluation, this technique remains very useful for a fast evaluation of the floc morphology.

4.2.2.3. Microbial community – Denaturing Gradient Gel Electrophoresis (DGGE)

During the last decade, modern analytical methods based on molecular microbiology were developed, allowing for a more comprehensive analysis of microbial communities. An overview of the mostly used molecular techniques available is given in Table 4.1.

Table 4.1 Overview of the molecular techniques used for investigation of microbial aggregates (adapted from Ranjard et al. (2000) and Wilderer et al. (2002)).

Method	Application*	Advantages	Limitations
PCR ¹ fragment cloning and functional gene libraries	D, PS	High phylogenetic resolution, required to design new gene probes and to identify new bacteria	Time consuming, expensive, PCR and cloning biases, not quantitative in view of community composition.
Genetic fingerprint techniques - depend on: -size (ARDRA ² , T-RFLP ³ , RISA ⁴ , RAPD ⁵) - sequence (DGGE ⁶ , TGGE ⁷)	D, PS	Inexpensive, high sample throughput	DNA extraction and PCR biases, not quantitative in view of community composition.
Fluorescent in situ hybridisation (FISH)	D, PS, A	Allows direct visualisation of the non-cultured species, can be directly combined with microautoradiography and microsensors	Adaptation of experimental protocols for some gram-positive bacteria; non-detectable inactive cells with low ribosome content; sample embedding required to preserve aggregate architecture.
FISH/fluorescent staining combined with confocal laser scanning microscopy (CLSM)/image analysis	A, D, PS	Quantitative analysis of population structure and/or floc architecture; non-invasive technique, amenable to automation	Expensive instrumentation, time consuming

*Estimation of microbial diversity (D); determination of microbial population structure and dynamics (PS), aggregate architecture (A).

¹PCR – Polymerase Chain Reaction; ²ARDRA – Amplified Ribosomal DNA Restriction Analysis; ³T-RFLP – Terminal Restriction Length Polymorphism; ⁴RISA – Ribosomal Intergenic Spacer Analysis; ⁵RAPD – Random Amplified Polymorphic DNA; ⁶DGGE – Denaturing Gradient Gel Electrophoresis; ⁷TGGE – Thermal Gradient Gel Electrophoresis.

The DGGE or related TGGE are among the most cited techniques in molecular ecology being a very efficient in detecting population changes with an emphasis on the stability and dynamics of microbial communities (Kaewpipat and Grady Jr., 2002; Boon et al., 2002; La Para et al., 2002).

Fingerprinting of complex bacterial communities by DGGE was first published by Muyzer et al. (1993). The technique allows the separation of DNA fragments of the same length but with different base pair composition. The separation is based on the decreased electrophoretic mobilities of partially melted double-stranded DNA molecules in polyacrylamide gels containing a linear gradient of DNA denaturants or a linear temperature gradient. This methodology allows a fast screening of multiple samples and gives additional information about changes within bacterial communities.

Even if DGGE and TGGE techniques have been shown to be powerful tools to analyse the dynamics of microbial community, they have some limitations in the analysis of community structures. The length of the DNA fragments that can be separated is limited to approximately 500 bp (base pairs). Small variations in the base pair composition are not always noticeable. Only the most dominant species (comprising at least 1% of the population) are visible on the DGGE gel (Seghers, 2004). Co-migration of different DNA fragments is possible, especially in complex communities, such as activated sludge samples, giving problems during the identification of certain individual bands. In this way, the main difficulty remains the "one band –one species" hypothesis.

Although the DGGE procedure is not perfect, it allows a rapid comparison of bacterial diversity in activated sludge as compared with other available molecular techniques. Due to this, it represents one of the best qualitative methods for monitoring the microbial community dynamics.

4.3. Construction and monitoring of a lab-scale SBR

4.3.1. Description of the set-up

In order to obtain stable sludge, an 80 l pilot-scale SBR for nitrogen and phosphorous removal was built. The SBR was inoculated with 40 l activated sludge from the Ossemeersen domestic wastewater treatment plant (Ghent, Belgium).

The SBR was built from PVC (ext. diameter = 0.4 m, wall thickness = 5 mm and height = 0.85 m). Basically, the SBR operated 4 cycles per day of 6 hours each. Each cycle contains 6 phases. A synthetic sewage was used as influent. For devices controlling and performing the on-line measurements the LabView 6.1 (NI, USA) was used.

The main components of the SBR are illustrated in Figure 4.2 and a schematic diagram of the SBR set-up is shown in Figure 4.3.

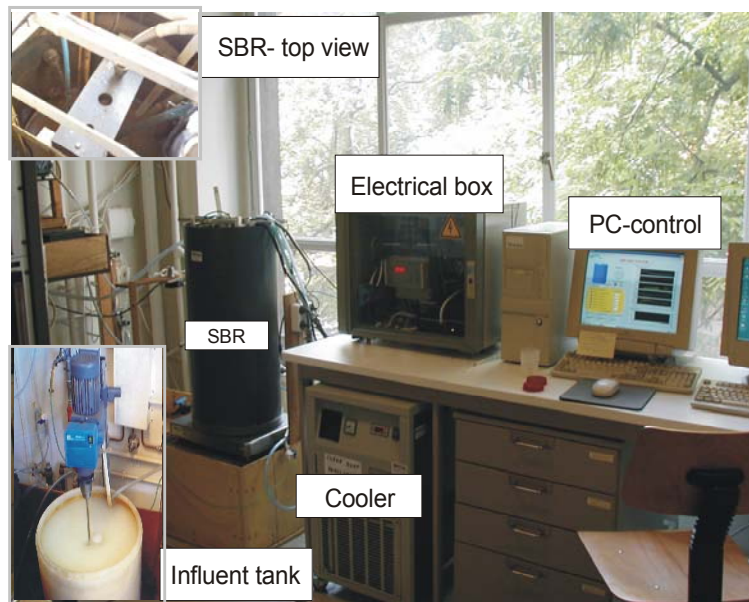


Figure 4.2 The SBR's main components

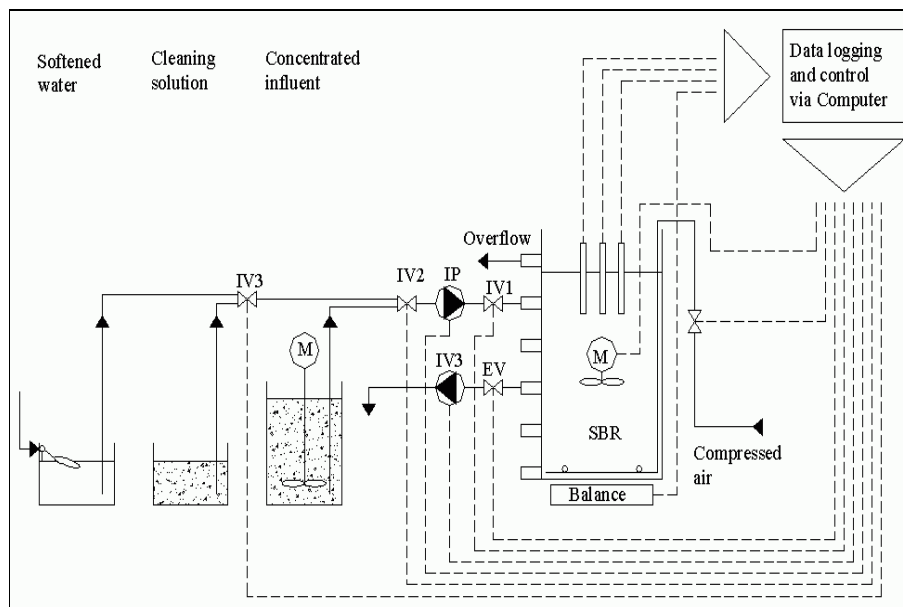


Figure 4.3 Schematic overview of the SBR pilot-plant (IV-influent valve; IP-influent pump; EP-effluent pump; EV-effluent valve; M-mixer).

4.3.1.1. Influent control set-up

A synthetic sewage which aims at mimicking real pre-settled domestic wastewater was used as influent (see section 4.3.2.1.). A 75L concentrated synthetic feed was prepared weekly. This procedure was preferred because it enabled to use a rather small volume of synthetic feed stock during one week and it minimised the influent preparation effort. The influent was diluted in-line with softened water using a dilution ratio influent : softened water = 1 : 20. A computer controlled pump 505U (Watson Marlow, Belgium) was used to generate the influent flow. Water was added by using a computer-controlled two-way pinch valve S307 02 (Sirai, Italy) and silicone tubing of 10 mm/12 mm (internal/external diameter). To prevent deterioration of the concentrated influent due to microbial growth, the concentrated sewage was stored in a tank at pH=3. This was found to be the best option among three methods,

which were investigated: refrigeration (4°C or lower), alkaline (pH>11) and acidic conditions (pH<3). Details regarding the influent stability and the methods used for its investigation can be found in Nopens et al. (2000). Continuous mixing of the influent was realised by using a propeller mixer RW28W (IKA, Germany) to avoid settling of the suspended matter. After completion of the filling phase the tubes connecting the influent tank to the SBR were cleaned with soft water in order to avoid a microbial growth inside the tubes. To perform the cleaning a two-way pinch valve S307 02 (Sirai, Italy) was used, which blocks the access of the cleaning water to the SBR. By using the same computer controlled pump 505U (Watson Marlow, Belgium) the water was pumped through the tubes and was wasted to a drain pipe.

4.3.1.2. On-line measurements and auxiliary devices

On-line measurements of dissolved oxygen (OxyGuard, Kelma, Belgium), pH (Mettler Toledo, Germany), oxidation-reduction potential (Mettler Toledo, Germany), temperature and conductivity (Yokogawa, Japan) were performed. Signal amplification and calibration was performed by using specific transmitters for each of the different sensors (OxyGuard transmitter (Elscolab, Belgium) for DO, Knick Stratos pH (Elscolab, Belgium) for pH, Knick Stratos ORP (Elscolab, Belgium) for oxidation-reduction potential and EXA SC400 (Elscolab, Belgium) for temperature and conductivity). The electrodes were placed in the SBR at approximately 10 cm below the minimum water level and fixed by using a PVC platform, which was placed on top of the reactor as shown in Figure 4.2 (denoted as SBR-top view). Aeration was supplied by compressed air (4 bar) and controlled on/off by an air valve (Burkert, Germany). The reactor weight that was used to control the volume was measured on-line by using an electronic balance Spider 1S (Mettler Toledo, Belgium)

4.3.1.3. Effluent and sludge control unit

A computer-controlled pump 605 Di (Watson Marlow, Belgium) at a flow rate of 2 l/min consequently drew activated sludge and effluent from the SBR by a one-way pinch valve S10602 (Sirai, Italy).

4.3.1.4. PC control and SBR VI's

All devices controlling the SBR setup and performing the on-line measurements of temperature, pH, DO, ORP, conductivity were connected to a PC-based data acquisition system. In this section, the specially developed program in LabView 6.1 (NI, USA) and the SBR process control and operation by using the PC are briefly described. Detailed information is given in Lee et al. (2003).

The SBR VI's front panel is shown in Figure 4.4. Overall, five sub-panels can be identified in the front panel:

- The first sub-panel visualises the status of the SBR reactor. The *STOP*-button allows to interrupt the program. The program can also be terminated by activating the safety level switch. If some water reaches a certain level in the security flooding basin built around the SBR, it closes an electrical circuit between two electrodes. In this case, all devices are switched off and the system will go to a continuous aeration state.
- The second sub-panel describes the phases of the SBR-cycle and their duration.
- The third sub-panel consists of the times reference. There is an indicator showing the number of cycles performed up to the moment. Furthermore, the time for

sampling sludge and effluent, the start time of the current cycle and the current time are specified.

- The fourth sub-panel contains the graphs for temperature, pH, ORP and conductivity together with their respective values indicator.
- In the last sub-panel, the oxygen control set-point can be fixed at a certain level. The oxygen profile of the current cycle is also displayed.

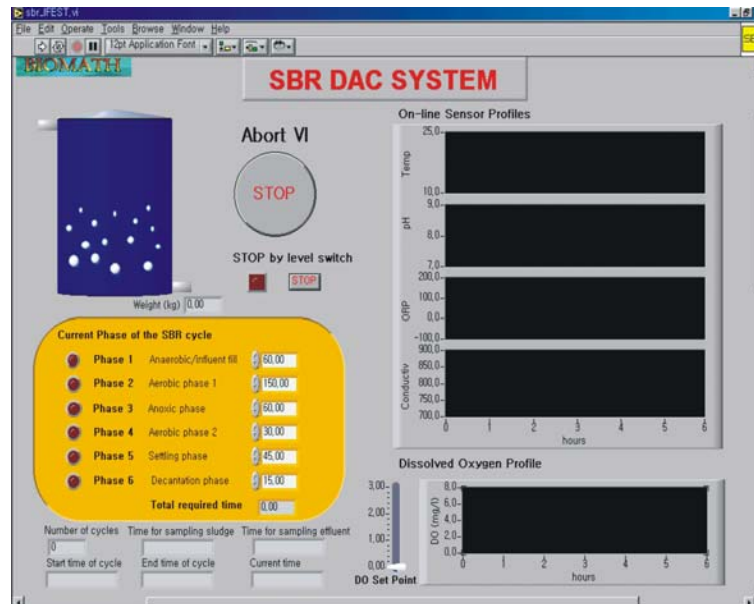


Figure 4.4 SBR VI's front panel.

4.3.2 Influent characteristics

4.3.2.1. Influent composition

As influent a synthetic medium was preferred over actual sewage for the following reasons:

- Constant, well-defined and easy to control composition.
- Easily available (there is no need to transport wastewater from a treatment plant on a daily basis).

The composition of the influent was based on the synthetic sewage "Synto" (Boeije et al., 1998) and was slightly modified to reduce costs. Its final composition is shown in Table 4.2. The influent has a ratio COD:N:P = 100:13.7:2.14. The measured BOD is 285 mg/l.

4.3.2.2. Influent cations composition

Due to its very important role in flocculation the cation concentrations present in the diluted influent have been analysed by using an atomic absorption method (VARIAN SpectrAA-800). Note that the high concentration of sodium ions is due to the softening of the water, which was used for influent dilution (Table 4.3).

Table 4.2 Synthetic influent composition.

Chemical compounds	Concentration [mg/l]	COD [mg/l]	N [mg/l]	P [mg/l]
Urea	91.74	23.22	42.81	0
NH ₄ Cl	12.75	0	3.52	0
o Na-acetate.3H ₂ O	131.64	79.37	0	0
Peptone	17.41	17.41	0.67	0
MgHPO ₄ .3H ₂ O	29.02	0	0	5.14
KH ₂ PO ₄	23.4	0	0	3.14
FeSO ₄ .7H ₂ O	5.80	0	0	0
Food ingredients				
Starch	122.00	122.00	0	0
Milk powder	116.19	116.19	6.95	1.14
Yeast	52.24	52.24	6.28	0
Soy oil	29.02	29.02	0	0
Trace metals		mg/l	mg metal /l	
Cr(NO ₃) ₃ .9H ₂ O	0.770	0.100		
CuCl ₂ .2H ₂ O	0.536	0.200		
MnSO ₄ .H ₂ O	0.108	0.035		
NiSO ₄ .6H ₂ O	0.336	0.075		
PbCl ₂	0.100	0.075		
ZnCl ₂	0.208	0.100		

Table 4.3 Cations concentration in diluted influent.

Cation	Concentration (mg/l)
Na ⁺	187.5±45.96
K ⁺	9.95±0.06
Ca ²⁺	3.13±0.01
Mg ²⁺	14.3±0.14
Fe ³⁺	2.47±0.03
Al ³⁺	<0.5

4.3.3. Description of the SBR cycle

As mentioned before, each SBR cycle had a duration of 6 hours; hence 4 cycles were performed each day. To enhance the COD and nutrients removal, the cycle was divided into six phases, which are summarised in Table 4.4. The system had a Hydraulic Retention Time (HRT) of 12 hours and a Sludge Retention Time (SRT) of 10 days. The nutrient removal performance of the SBR were 70% and 50% for Total Nitrogen and PO₄-P respectively (Sin et al., 2004).

Table 4.4 SBR reaction sequences for nutrient removal.

	Phase	Purpose	Duration (min)
1	Anaerobic + filling	P release, COD uptake	60
2	Aerobic 1	P uptake, nitrification, COD removal	150
3	Anoxic	Denitrification	60
4	Aerobic 2	Excess COD removal, N ₂ stripping	30
5	Settling	Settling	45
6	Decanting	Decanting	15

Phase 1

During the fill-phase 40 l of diluted influent was added to the biomass remaining in the reactor from the previous cycle. During this phase, agitation is provided by means of three multi-use mixing pumps (Project, Italy) placed at the bottom of the reactor. Since the mixed fill favours the mixing between the biomass and the organic influent, the biological reactions start at once. The microorganisms degrade the organic compounds using residual oxygen or an alternative electron acceptor such as nitrate. Hence, denitrification occurs. During the anaerobic phase (i.e. when all nitrate is removed), organisms absorb short-chain fatty acid and store them as polyhydroxybutyrate (PHB). The energy required to perform this is obtained from the decomposition of internally stored polyphosphates, thus releasing large amounts of soluble phosphates in the water (P release).

Phase 2

Reactions initiated during the fill-phase are completed during the reaction-phase. During the react-phase the aeration valve (Burkert, Germany) controls the air supply. DO control set-point was 2 mg/l. A perforated tube (12mm-internal/15mm-external diameter) is used as air diffuser. In this aerating phase COD removal, nitrification and P-uptake are achieved. The microorganisms convert the organic matter present in the influent into new cell mass, carbon dioxide, water and other end products, ammonium is converted into nitrate (nitrification) and the internally stored PHB is oxidised to produce energy for growth and polyphosphate (P-uptake).

Phase 3

In order to achieve denitrification, the aeration valve is switched off in order to obtain anoxic conditions in the reactor. In this phase, the mixing pumps are switched on to keep the sludge in suspension. Nitrogen removal is accomplished biologically by heterotrophic bacteria that use nitrate as electron acceptor.

Phase 4

The removal of excess COD and the stripping of the nitrogen gas produced by denitrification are achieved in the second aerobic and mixed phase. In this phase, 2 l of mixed liquor is wasted as well, in order to maintain a sludge age of 10 days in the reactor.

Phase 5-6

In the last two phases, the sludge is allowed to settle under quiescent conditions. During phase 6, 38 l of effluent is wasted from the SBR.

4.3.4. SBR monitoring

Samples of activated sludge and effluent were collected daily at the end of the second aerobic phase (phase 4) and during the decantation phase. The influent stability was also verified weekly by analysing the freshly prepared influent and the one prepared one week before. The samples were stored at 4°C before being analysed in order to keep their characteristics as constant as possible.

4.3.4.1. On-line SBR monitoring

The values of temperature, pH, DO, oxido-reduction potential, conductivity and reactor weight were measured continuously and were saved every minute in a text file. The weight of

the reactor was used as a control for the effluent draining and influent filling in order to have a good estimation of the SBR-volume. The DO signals were used to regulate aerators such that the desired dissolved oxygen level was maintained during the aerobic phases.

4.3.4.2. Off-line SBR monitoring

Intensive off-line monitoring of the SBR was performed to check the properties of the activated sludge, the effluent quality and the influent stability. An overview of the analyses as well as the measurement frequency is presented in Appendix 4.1. A brief description of the analytical methods used will be presented next.

Influent and effluent analysis

The analytical determination of the chemical components was in general performed using Dr. Lange Kits (Dr. Lange, Germany). The samples were measured by using a photo-spectrometer (Xion 5000, Dr. Lange, Germany). The parameters investigated are summarized in Appendix 4.2. The BOD measurements were performed using an OxiTop (WTW, Germany).

Sludge analysis

The methods used for investigating the activated sludge properties and characteristics are presented in this section. A systematic evaluation of the sludge properties was required as its stability represented the main purpose of building and monitoring the SBR. It was therefore necessary to set out a series of methods which would allow to detect changes into the sludge structural properties as well as to evaluate the microbial community evolution. A short description of each of the method used is given bellow:

1. Mixed Liquor Suspended Solids (MLSS) and Mixed Liquor Volatile Suspended Solids (MLVSS)

The MLSS of a well-mixed activated sludge sample, as well as the MLVSS measurements were performed according to Standard Methods (APHA, 1992).

2. Sludge volume index (SVI)

The SVI measures the settling characteristics of the sludge and represents the volume of settled sludge in milliliters occupied by 1 g of a suspension after 30 minutes settling. It is determined by taking 1 l of mixed liquor and allowing the sample to settle for 30 minutes in a graduated cylinder. The SVI was calculated with the following formula:

$$SVI [ml/g] = \frac{\text{Settle sludge volume (ml/l) after 30 min.} \cdot 1000}{MLSS (mg/l)} \quad (4.1)$$

3. Floc Size and Size Distribution Measurements

The monitoring of the floc size and the size distribution was performed by using the MastersizerS (Malvern, UK). The measurement principle as well as the advantages and drawbacks of this method were presented in detail in Chapter 3.

For experiments the 300RF lens corresponding to a size range of 0.05-900 μm was used. Fresh activated sludge samples collected directly from the SBR were analysed weekly. In order to obtain identical initial conditions 1 l of undiluted sludge was mixed for 30 minutes by using a SW6 flocculator (Stuart Scientific, USA) at 35 rpm. For analysis, a small volume of sludge (20-30 ml) was diluted with 1l of filtered effluent (0.45 μm). The sludge concentration

was controlled by fixing the obscuration level at 15 % in the Mastersizer software. Experiments have been conducted by using the MSX17 automated wet sample dispersion unit (Malvern, UK) at a flow rate of 3 ml/s and a mixing speed of 210 rpm. For deflocculation experiments the ultrasonic bath of the MSX17 automated wet sample dispersion unit was used at a power of 35 W.

4. Microscopical evaluation

The microscopical observations were performed by using an optical microscope Olympus CX40 (Olympus, Japan) equipped with an Ikegami ICD-46E video camera (Ikegami Electronics Inc., USA). A drop of mixed liquor was carefully deposited on a glass slide and covered with a cover slip before being observed through the microscope. The samples were examined by using 4x, 10x and 40x objectives. The images were recorded on a PC by using a frame grabber PCI – 1411 (NI, USA).

5. Microbial community dynamics

The microbial community dynamics were monitored by using the DGGE method. The experimental protocol is illustrated schematically in Figure 4.5 and consisted of the following steps:

DNA extraction and purification:

Two samples of activated sludge (2 ml) were collected weekly from the SBR and stored before analysing at -20°C. The total DNA was extracted from the sludge sample based on the extraction protocol as presented by Boon et al. (2000). A 100 µl aliquot of the crude extract was further purified using Wizard PCR preps (Promega, Madison, Wis.). The clean DNA was stored at -20°C.

PCR-DGGE analysis

The extracted DNA (1 µl) was amplified by PCR with the bacteria specific 16S rRNA forward primer P338f (5'-ACTCCTACGGGAGGCAGCAG-3') and the reverse primer P518r (5' -ATTACCGCGGCTGCTGG-3') based on a universally conserved region, as previously described by Muyzer et al, 1993. A GC-clamp of 40 bp was added to the forward primer. All PCR reactions were done with a 9600 thermal cycler (Perkin-Elmer, Norwalk, Connecticut). The PCR mastermix contained 0.5µM of each primer, 200µM of each deoxynucleoside triphosphate, 1.5mM MgCl₂, 10µl thermophilic DNA polymerase 10X reaction buffer, 2.5U of Taq DNA polymerase (Promega, Wisconsin), 400ng/µl of bovine serum albumin (Hoffman-La Roche, Switzerland) to a final volume of 100µl. DGGE was performed with the D Gene System (Bio-Rad, Hercules, CA). The electrophoresis was run for 16 h at 45 V on 6 % (wt/vol) polyacrylamide gel with a denaturing gradient ranging from 45 - 60 % (where 100 % denaturant contains 7 M urea and 40 % formamide). After electrophoresis the gels were stained with SYBR Green I nucleic acid gel stain (1:10000 dilution; FMC BioProducts, Rockland, Maine). The stained gel was immediately photographed on a UV transillumination table with a video camera module (Vilbert Lourmat, France). Subsequently, the matrix of similarities between the densitometric curves of the band patterns was calculated based on the Pearson product moment correlation coefficient with GelCompar 4.1 software package (Applied Maths, Belgium). Finally, the DGGE patterns were clustered using Ward's method (Ward, 1963). After cluster analysis, a dendrogram was obtained which visualizes the similarities of the different banding patterns of the DGGE.

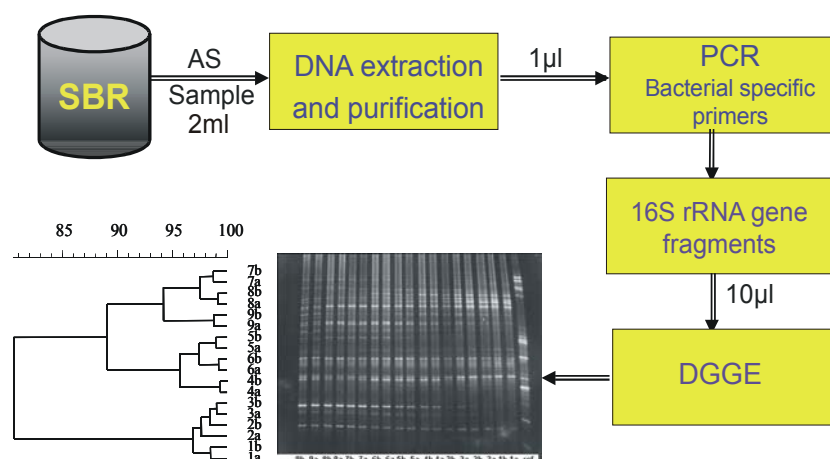


Figure 4.5 Overview of the methods used for DGGE analysis.

Sequencing of DGGE fragments

DNA fragments to be sequenced were cut from the DGGE gel, placed into sterile Eppendorf tubes containing 20 μl of sterilised water, and frozen at -20°C . Two microliters of the DNA diffused in water served as a template for PCR amplification. The amplified products were subjected to a second run of DGGE to confirm their electrophoretic mobility and were subsequently purified and sequenced by ITT Biotech (Bielefeld, Germany). The sequences were aligned with 16SrDNA sequences obtained from the National Centre for Biotechnology Information database using the BLAST 2.0 search algorithm (Altschul et al., 1997).

4.4. Evaluation of the SBR activated sludge stability

4.4.1. Long-term SBR monitoring

The SBR was operated and monitored over a period of two years before proceeding to the planned (de)floculation experiments. During this period, effort was put into maintaining the operating conditions as stable as possible, to avoid SBR failures or some other disturbances.

Accordingly, the changes in activated sludge settling properties (SVI), floc size and size distribution (FSD) and microbial community (DGGE) were monitored in the SBR from the starting-up day over a period of 227 days. The aim of this study was to investigate whether a link between these properties exists and also to evaluate whether the used methods will allow to detect the sludge stability. It has to be mentioned also that during this period, no major failures or other unexpected problems occurred in the SBR operation, which may have had a significant influence on the obtained results. The SBR nutrients removal abilities did not represent the focus of this research and therefore, data related to the effluent qualities are not presented here.

4.4.1.1. Floc size and size distribution

Floc size and size distribution measurements were performed weekly during only two periods. The first period covered days 1 to 70 (Figure 4.6, a), whereas the second period lasted from day 156 to 226 (Figure 2, b).

During the first 28 days, a monomodal distribution with a small decrease in floc size and a mass mean diameter ($D[4,3]$) showing a slight decrease from $35.12 \mu\text{m}$ to $32.04 \mu\text{m}$ was

observed. A high level of similarity in the FSD appeared between day 21 and day 28. From the 35th day on, a bimodal floc size distribution with a weak tendency to form larger flocs of approximately 400 μm was observed. This tendency became more pronounced in time (days 42 and 56) until again a monomodal distribution (day 63), this time with predominantly larger flocs, was obtained. The observed trend of the floc size distributions could be associated to a transient period of the microbial community to adapt to the new operating conditions. During the second period (Figure 4.6, b) a slight increasing trend in the floc size was observed. However, monomodal distributions were always obtained and the flocs were characterised by a mass mean diameter between 40 μm and 85 μm .

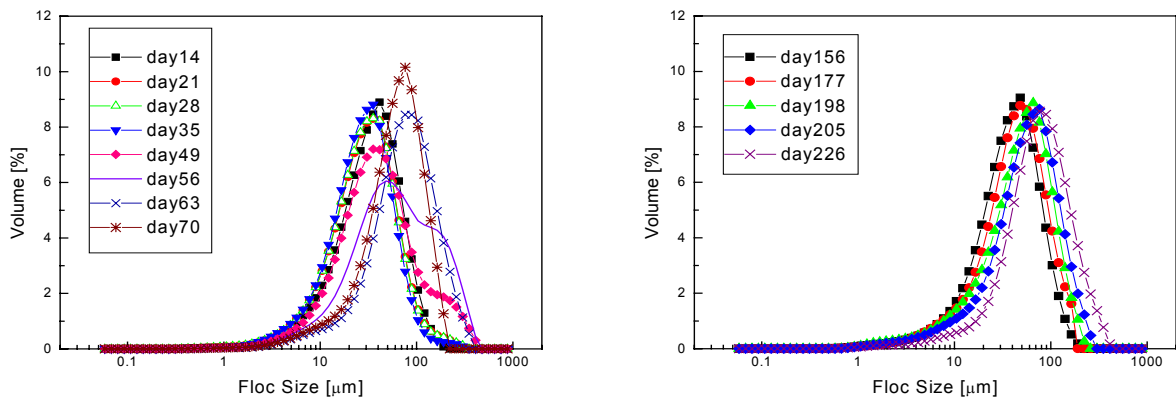


Figure 4.6 Floc size distribution evolution in time for days 1 to 70 (left) and 156-226 (right).

4.4.1.2. Evaluation between floc size and settling properties

For the two time periods considered it was observed that the SVI may be linked to the floc size measurements. During the first period i.e. days 1-70 (Figure 4.7 – left) the increase in mean floc size diameter correlated well with a decrease in the SVI (Figure 4.8 – left). In the second period i.e. days 156-226 (Figure 4.7– right) the increasing SVI correlated with an increase in mean floc size (Figure 4.7 and Figure 4.8 – right). However, no correlation between the activated sludge settling properties and floc size was found when the results for the complete monitored period were compared. These observations suggest that in general a correlation between floc size and settling properties is highly dependent of the type of microorganisms present in the floc structure. Also, the flocs' structural properties and especially the floc density may play an important role in interpreting the observed results.

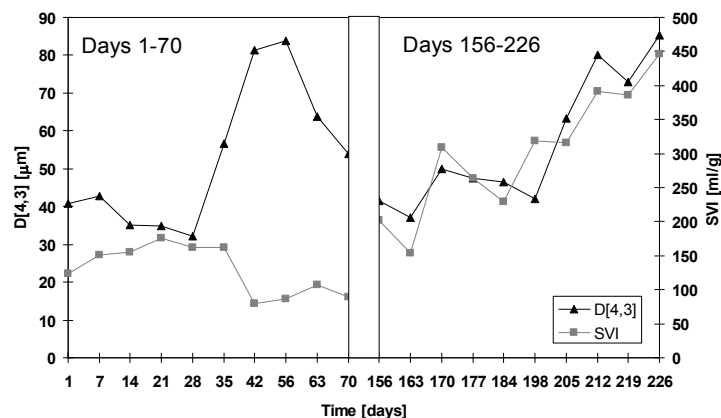


Figure 4.7 D[4,3] and SVI evolution for days 1-70 (left) and days 156-226 (right).

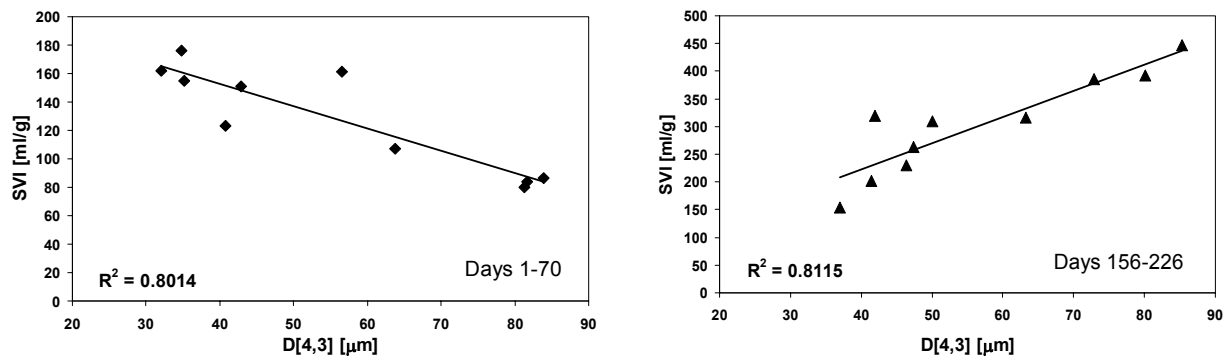


Figure 4.8 Observed correlation between D[4,3] and SVI. Days 1-70 (left) and days 156-226 (right) .

Microscopic examination of the sludge during the experimental period showed that filamentous organisms were less present in the sludge for the first 91 days. The flocs showed to be small, weak and nearly spherical, especially in the first 30 days. This may be due to the acclimatisation period of the sludge to the new experimental conditions, manifesting a stress factor on the floc structure. In time, the flocs evolved to a larger size, compact structure and presented a more rounded shape. A highly turbid supernatant characterised the first monitored 91 days, which together with the performed microscopical evaluation provided an indication of the presence of pinpoint flocs in the system. During the first 91 days, the SVI measurements revealed good settling properties. Since no significant variations in the sludge concentrations were observed (Figure 4.9) it may be assumed that the SVI was primarily influenced by the floc structural properties and especially by the floc size (Figure 4.8). The very few filamentous organisms observed microscopically, together with the floc size and SVI measurements for the first 91 days suggested that the flocs predominantly consisted of floc-forming bacteria.

Starting from day 91, microscopic observations revealed a small increase in the number of filamentous bacteria. The filaments were mostly attached to the flocs and showed to be rather short and thin. The amount of filamentous microorganisms present in the activated sludge were investigated by using the filament index (FI) introduced by Eikelboom (2000). According to this method the filament index is rated on a scale from 0 to 5, where a filament index of 0 corresponds to absence of the filaments and 5 corresponds to an excessive number. A filament index between FI=1 and FI=2 (Eikelboom, 2000) characterised the filament amount during this period. The flocs were larger and more irregular in shape as compared to the previous period. No significant change in SVI was seen between day 91 and 126 and the settling experiments showed a good and fast sludge sedimentation and less turbid effluent. Due to the lack of data on floc size measurements for this period, a comparison between SVI and floc size was not possible. Similar to Jenkins' (1993) description of the *ideal* floc, the above observations indicated that during this period filamentous organisms and floc-forming bacteria grew in balance.

From day 126, microscopic observations indicated an increase in the number in filaments and also of the attached ciliates and rotifers (FI= 4-5). During the same period, foam was formed on top of the reactor. The decreasing trend observed for SVI between days 154 – 161 and days 184-191, respectively (Figure 4.9) is associated with an increase in sludge concentration. The continuous growth of filamentous organisms may explain the increasing trend observed for floc size and SVI (Figure 4.8 –right).

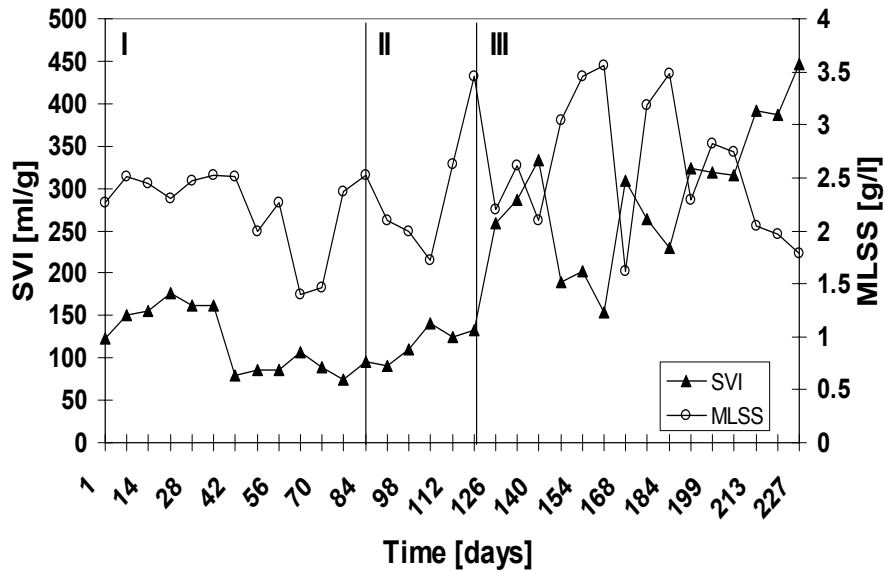


Figure 4.9 SVI and MLSS evolutions over 227 days.

Three distinct stages were observed: I – predominant floc-forming bacteria; II – equilibrium between floc-forming and filamentous bacteria; III – predominant filamentous bacteria.

Kaewipat and Grady (2001) reported similar evolutions in the floc structure when two lab-scale reactors were monitored. As observed microscopically, only few filamentous microorganisms were present in the first 100 days from the start-up of the reactors. An increasing number of filaments, which finally led to filamentous bulking, occurred from day 140 on.

The above observations allow to conclude that three distinct stages existed in the evolution of the floc structural properties. The first one corresponded to the predominant presence of floc-forming bacteria. The second stage was a short period (days 91-126) in which the filaments started to grow, but a balance between floc-forming and filamentous bacteria still resulted in good settling properties. Finally, in the third stage bulking occurred, which was associated with the presence of a large number of filamentous organisms.

4.4.1.3. (De)flocculation ability of the flocs

The flocs' capability to break-up and aggregate was investigated as well. In each test, after 10 minutes of continuous mixing (210 rpm), the sludge was subjected to a disrupting effect by using a sonication bath for another 10 minutes. Hereafter, the initial conditions were imposed again and the flocs' reflocculation ability was followed for other 10 minutes. (De)flocculation studies showed a distinct difference in the activated sludge behaviour as function of their structural properties. It could be noticed that sonication caused a stronger deflocculation for larger flocs containing filaments (Figure 4.10, days 202 and 219) as compared to the sludge samples analysed during the transient period after the start-up of the SBR (Figure 4.10, days 14 and 35). Moreover, a faster reflocculation occurred for the flocs containing filaments, whereas non-filamentous flocs reflocculated only slightly.

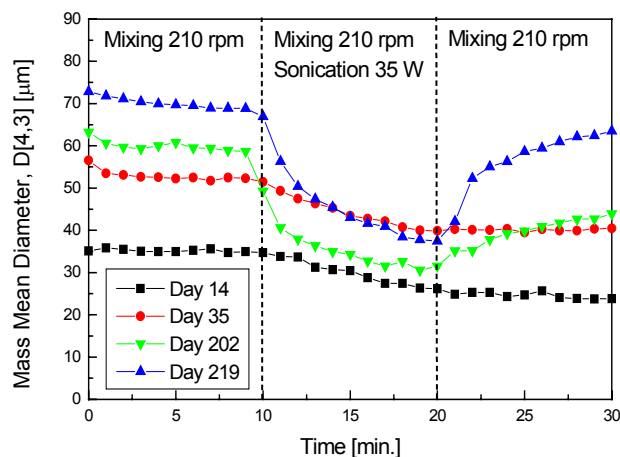


Figure 4.10 Mean diameter evolutions during deflocculation and reflocculation experiments.

It has been shown by Sezgin et al. (1978) that, depending on the quantity of filamentous microorganisms protruding from activated sludge flocs, different types of aggregates can be formed in the course of agglomeration. At a very low extend filament length, flocs approach each other to make particle-to-particle contact. As a result, compact and high density "floc-to-floc" aggregates are formed. When flocs have an extended filament length the first contact occurs between filaments and later filaments and flocs. As a result, "filament-to-filament" and "floc-to-filament" aggregates are formed. These aggregates are rather loose and have low densities. It was suggested that the filamentous organisms form a backbone within the floc onto which the floc-forming bacteria attach. Moreover, Parker et al. (1971) demonstrated that when the shear rate is increased, filament fracture may occur and the floc-forming bacteria may erode from the filamentous organism backbone. This may explain the observed flocculation behaviour of samples as investigated here. During the first mixing period a relatively steady-state size distribution was observed which indicates that rather stable size aggregates formed. By applying sonication, the flocs that contain filaments break-up rapidly due to filament fracture. Moreover, due to the weak and highly irregular structure of the flocs, surface erosion may occur as well, increasing the number of primary particles in the system. When the original mixing is reimposed, reflocculation occurs but this is not completely reversible and smaller aggregates size are recorded. Similar behaviour for metal hydroxide flocs was reported by Duan and Gregory (2003) and could be attributed to sweep flocculation. They found that floc re-growth was not reversible and the degree of recovery decreased for longer breakage times. It was suggested that the breakage of metal hydroxide flocs involved rupture of chemical bonds that inhibit them to reform. Investigating the breakage and aggregation abilities of the activated sludge flocs Biggs (2000) showed that the shear rate history is important as well. Long-term high shear rate produced an irreversible floc restructuring while a high shear rate applied for a very short time showed a reversible floc re-growth. Therefore, it may be suggested that due to the high shear rate conditions, a rupture of the filaments and a possible damage of the EPS occurred which does not allow the flocs to re-grow to the initial size.

In contrast, the rather small "floc-to-floc" aggregates formed in the first monitored period were much more resistant to the imposed shear rate conditions and the breakage effect was less pronounced. However, since almost no floc re-aggregation was observed, it is believed that the absence of the filaments and the rupture of the polymer bridge bounds played an important role in the observed behaviour.

4.4.1.4. Microbial community dynamics

Sampling effect

In order to investigate the effect of the sampling and storage procedure on the microbial community, the samples variability was first evaluated. To achieve this goal, nine duplicate samples collected in succession over a one month period were taken during the sludge wasting phase and stored at -20°C before analysis. Results showed that duplicates yielded the same DGGE-patterns, which clustered always together with high similarity (Figure 4.11). This suggested a homogenous community within the sample and also demonstrated that further analysis of duplicates would not be necessary. Similar conclusions were drawn by Curtis and Craine (1998) for replicate samples collected from a full scale plant.

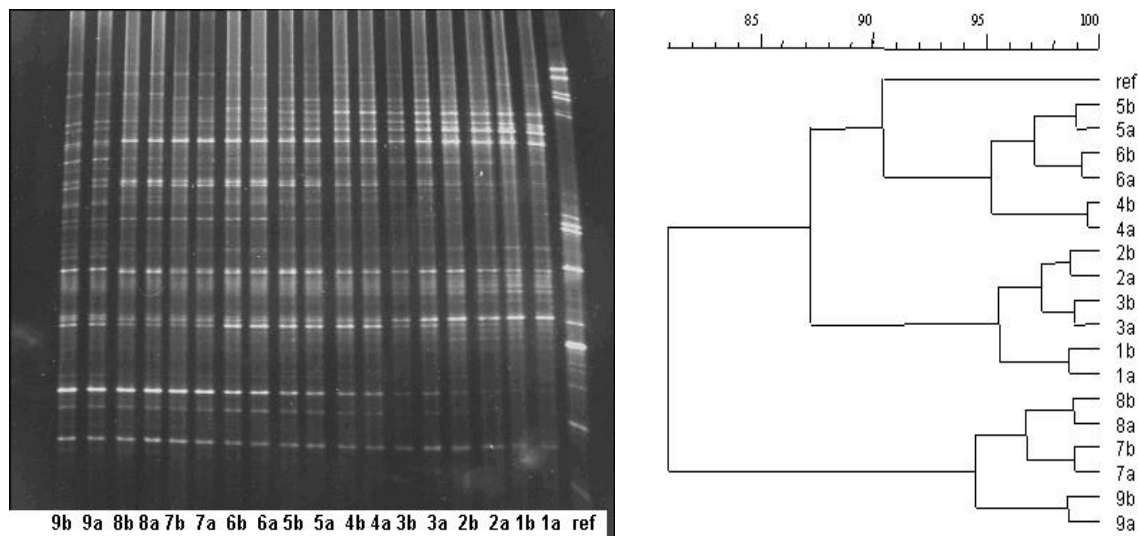


Figure 4.11 DGGE profile for replicate samples (left) and corresponding cluster analysis (right).

Long-term (227 days) monitoring of the population dynamics

The DGGE patterns of the sludge samples taken during the monitored period were compared and analysed by cluster analysis, revealing 3 major groups (Figure 4.12).

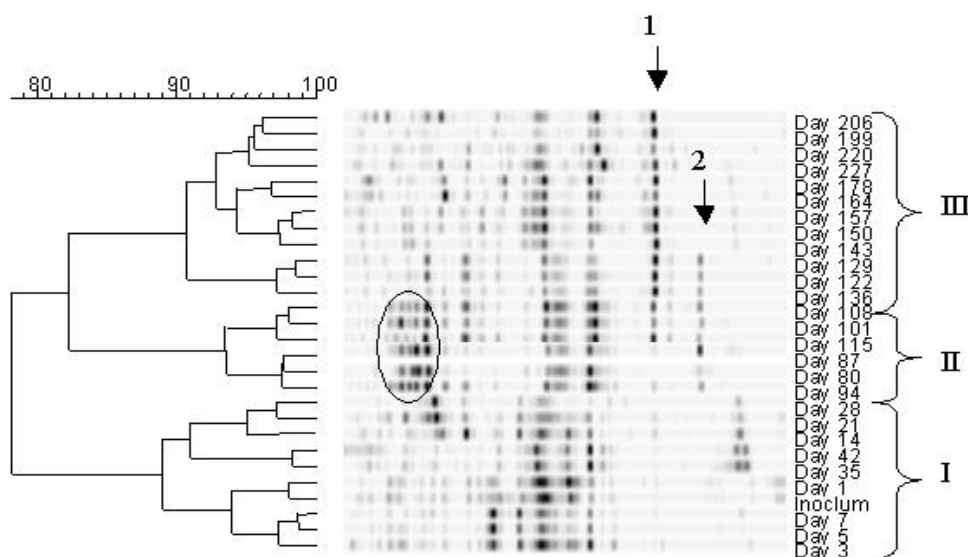


Figure 4.12 DGGE profiles (right) at different time periods and cluster analysis (left).

The first group (I) corresponded to the first 42 days. The inoculum was characterised by two dominant bands, which were already present in the first operating day of the SBR. During the first week (days 3-5-7) some new ribotypes appeared in the patterns and the two original bands became less dominant. The patterns of the next 35 days evolved into separate clusters with highly diversified ribotypes appearing on day 14. A high similarity was observed between days 21-28 and days 35-42, which clustered together. When comparing the floc size with these DGGE results, it was observed that the changes of the community structure were correlated with the FSD evolution. In Figure 4.6,a the FSD of day 14 looked very different from those of days 21 and 28, which presented a rather similar size distribution. Similarly, the FSD of day 14 is different from those of days 35 and 42, corresponding to the moment when large particles started to form. This first major group could be assigned to the period of adaptation of the community to the SBR conditions, where new populations became dominant and others disappeared from the pattern. In agreement with Boon et al. (2000) and Muthumbi et al. (2001), the bands in the inoculum sludge were significantly different from those of all other samples. The structural properties' evaluation revealed dominant floc-forming bacteria during this period and showed quite dynamic changes in the floc size.

The microbial communities further evolved rather dynamically. In the second major period (Figure 4.12, II), the appearance of diverse populations was observed (oval mark in Figure 4.12). The large diversity observed in this period coincided well with the period where structural properties exhibited a good balance between filamentous and floc-forming bacteria. During this period, two new ribotypes became visible as well (arrows 1 and 2 in Figure 4.12).

The third major cluster (Figure 4.12, III) started in the period when filamentous bacteria became abundant. During this period the bands at the top of the gel, as well as the band indicated by arrow 2 disappeared again (day 143). The band patterns of the last 28 days (days 199-227) clustered together with a higher degree of similarity as compared with other similar long periods. This slight tendency was, however, for the first time observed during the monitored period. The band indicated by arrow 1 also became brighter, indicating that the corresponding organisms seemed to be adapted very well to the SBR conditions because its presence was rather stable until the end of the monitored period. The corresponding species could be one of the developing filamentous organisms observed when structural properties were investigated. To validate this hypothesis, a sequencing of the DNA fragments of the ribotype marked with arrow 1 in Figure 4.12 was performed. Three band patterns corresponding with days 101, 150 and respectively 206 were analysed.

The sequences analysis indicated that the identified species belonged to the class of actinomycetes most closely related to the *Rhodococcus* (79% similarity). It is reported in many studies that actinomycetes can cause severe bulking and foaming in activated sludge plants (Davenport et al., 2000; Madoni et al., 2000; Boon et al., 2002). In this context, Boon et al. (2002) found a positive correlation between the SVI and the Shannon index of diversity of the actinomycetes, which allowed to conclude that they play an important role in sludge bulking occurrence.

Foaming is also often associated with the presence of mycolic acid-containing actinomycetes (Mori et al., 1988; Francis et al., 1997; Davenport et al., 2000). These are classified in the *Mycobacterium* complex, a suprageneric group that forms a distinct phyletic line (Ruimy et al., 1994) and contains the genera *Corynebacterium*, *Tsukamurella*, *Mycobacterium*, *Gordona*, *Rhodococcus* and *Nocardia* (Francis et al., 1997).

It is therefore concluded that the observed dominant species are filamentous branched species, which may be responsible for the observed sludge bulking and foaming effects at the end of the monitoring period.

The results suggested a dynamic bacterial community during the first 227 days. The stable operating conditions of the SBR did not imply stability in floc structure and microbial community. A similar finding was presented by Fernandez et al. (1999), who showed an extremely dynamic microbial community for a period of 2 years under stable operating conditions.

It was shown here that long-term monitoring of the SBR revealed a highly dynamic microbial population. It appeared necessary to evaluate the process and microbial community evolution on a shorter time scale as well in order to detect if the stability of the biological sludge can be obtained.

4.4.2. Short-term SBR monitoring

Short-term stable sludge properties were often observed during the SBR monitoring. This occurred especially when no failures were recorded in the process operation. Short term microbial community stability is often reported in other studies as well. In this context, LaPara et al., (2002) observed 87 days of a stable microbial community that occurred in operationally stable wastewater treatment reactors, whereas Smith et al. (2003) mentioned a microbial community stability for 37 days.

4.4.2.1. Short-term SBR monitoring under stable operation conditions

Figure 4.13 shows the cluster analysis performed to evaluate the microbial community during a one-month monitoring study of the SBR. During this period as well as in the month preceding this investigation, the SBR operated stably and no failures or other incidents were recorded. A very high degree of similarity was observed between samples collected during April 2-April 14 and April 21- April 30 respectively. During one month, however, two distinct clusters were observed which clustered together with 96% similarity, suggesting that some minor changes occurred. However, these were not highly significant. The microbial community may therefore be considered as rather stable during this one month period.

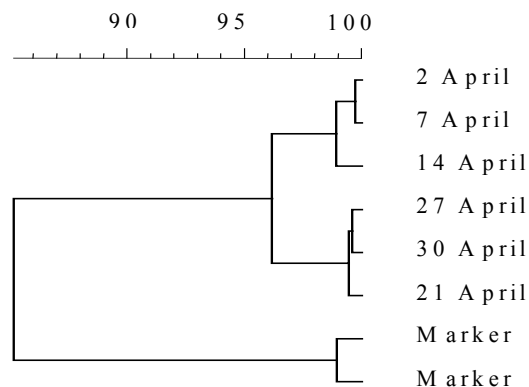


Figure 4.13 Cluster analysis performed on DGGE data for a one month SBR monitoring period under stable SBR operating conditions.

4.4.2.2. Short-term SBR monitoring under unstable operating conditions

It should be expected that a possible SBR operating problem could occur during the flocculation experimental period (its purpose will be detailed in Chapter 5), which may affect the reproducibility of the results. Such possible scenario was investigated on a short-term time scale in the SBR by changing the operating temperature. According to Wilén (1999), the temperature affects both the metabolic activity of the microorganisms and the physical

properties of the activated sludge. Moreover, Krishna and van Loosdrecht (1999) found that the SVI increased with increasing temperature at the same time as the production of storage polymers in the sludge (PHB) decreased, which could affect the kinetic selection of certain microorganisms such as filamentous bacteria and *Zoogloea* bacteria. It was also shown that the amount of EPS increased at elevated temperatures. It may therefore be considered that a change of the temperature could be an important factor which may lead to system disturbances.

Monitoring started at day 576, when the SBR was operated at 15°C for more than 3 months and the process was characterised by high SVI values and filamentous bulking. The microscopical analysis showed a large number of robust filaments and a large amount of attached ciliates and rotifers (Figure 4.14). On day 583 the cooling system was switched to 20°C and the SBR was operated at this temperature for a period of 1 month (3xSRT). The monitoring was performed by using the same method as described before.

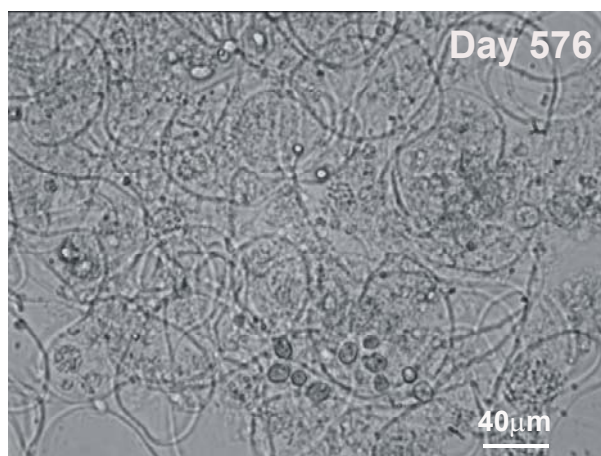


Figure 4.14 Microscopical observations of the activated sludge (day 576).

Floc size and size distribution

The floc size measurements performed over the monitored period showed a slight decreasing effect on the floc size (Figure 4.15). However, the large flocs size seemed to be less affected by the temperature changes and the observed differences are too small to consider them as significant.

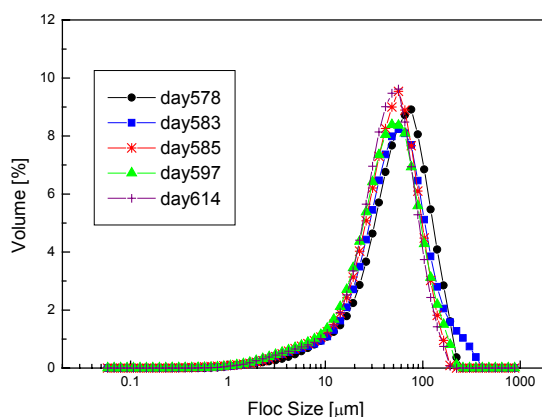


Figure 4.15 Floc size distribution during short-term SBR monitoring.

Settling properties

The settling properties of the sludge were investigated in terms of the SVI. As mentioned before, filamentous bulking phenomena characterized the process when the monitoring started. The SVI measurements performed before and after the temperature changes showed that SVI and the MLSS values remained in the same range for the entire monitored period.

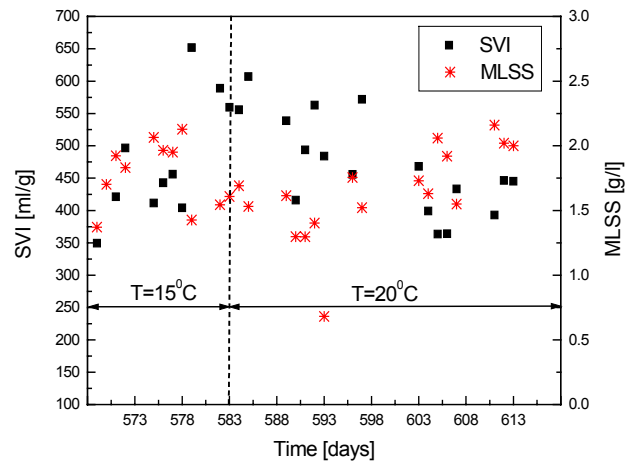


Figure 4.16. SVI and MLSS evolution over 40 days SBR monitoring.

Microbial community dynamics

Three major clusters were observed by analysing the DGGE profiles. The change of temperature at day 583 especially showed changes in the species dominance as illustrated by the first two clusters (Figure 4.17 –1,2). A high species dominance is observed at day 586, which shows lower similarity compared to the other sample patterns which clustered following the chronological order of the samples. Days 614 and 616 formed another cluster with less similarity as compared to the previous days. It is observed that another species becomes more dominant while some of them disappeared or showed a weaker presence. It may therefore be concluded that the microbial community reacted slowly to the changes that occurred in the operational conditions due to the temperature change and a shift in the populations became only visible after approximately 31 days.



Figure 4.17 Short term microbial community monitoring: cluster analysis (left) and DGGE profile (right).

The short-term evaluation of the temperature effect on the sludge properties showed that the microbial community was faster affected by the temperature, as compared to sludge settling and structural properties. It may therefore be concluded that any possible perturbation, which eventually occurs in the reactor, should be avoided as much as possible to obtain a stable microbial community. However, the presented evaluation was just a particular case and it

could happen that different reactor failures and/or changes of the operational conditions may create a different response of the flocs physical, chemical and biological properties. In this context, Eichner et al, (1999) showed a complete breakdown of the community structure after phenol shock loads. Furthermore, LaPara et al., (2002) found that the functional stability of reactors were maintained in response to varying influent characteristics by a microbial community that adapted its structure to sustain an effluent of high quality.

4.4.3. Conclusions

The method proposed in this study to monitor the properties of the activated sludge in an SBR is believed to be a good procedure to find a link between changes in the activated sludge settling properties, the floc structure and the microbial community dynamics. This contributes to a better understanding of the process performance and helps to detect when stable sludge properties are obtained in the reactor.

Long-term monitoring of the SBR revealed a dynamic microbial community, which was found to correlate well with the observations recorded in sludge structural and settling properties.

Short-term stability of the sludge properties and microbial community may be obtained. However, any reactor failure or change of the operating conditions should be avoided since they may induce different degrees of perturbation in the reactor.

With respect to the planned flocculation experiments (Chapter 5), achieving stable sludge is an essential condition which can be fulfilled only by keeping stable operating conditions in the reactor for a long time and try to make the experimental period to be as short as possible.

Methodology for experimental design and analysis

5.1. Introduction

Modelling the activated sludge process requires an understanding of many physical properties of the biological flocs as well as of the influence of process conditions. Insufficient insight in the impact of these conditions makes that models frequently lump them together and ignore the effect of different changing conditions on important phenomena such as settling, particles aggregation and breakage, sludge dewatering and compaction, etc. This is the reason why, as a first step towards the development of a good flocculation process, it is necessary to screen out the most important parameters and investigate their influence.

The elaboration of the experimental technique and the experimental protocol as well as of an experimental design in view of to the purpose of the study will be presented in this chapter. Two main issues are described and discussed:

- Developing an experimental set-up in which the flocculation experiments can be performed under controlled operating conditions;
- Elaborating on the experimental design and the experimental protocol to be followed when performing the experiments.

5.2. Experimental layout

The influence of physical and chemical parameters on the (de)flocculation process was investigated in a specially designed flocculation set-up (FlocUNIT). This set-up permits long-term flocculation experiments and allows to control conditions such as pH, conductivity, temperature, dissolved oxygen (DO) concentration and mixing intensity. By connecting the FlocUNIT to three sizing devices coupled in series: MastersizerS (Malvern Instruments, UK); CIS-100 (Ankersmid, Belgium) and IMAN software (LabView, NI, USA) an on-line evaluation of the dynamics of floc size and structural properties becomes possible.

5.2.1. Experimental set-up

A general overview of the set-up is shown in Figure 5.1. Detailed information regarding the set-up development and functionality can be found in Govoreanu et al. (2003). The operating procedure basically consisted in filling the reaction vessel with activated sludge from the SBR (as presented in Chapter 4). The imposed experimental conditions are maintained by specific sensors and transmitters. During an experiment, sludge is constantly withdrawn from the reaction vessel and analysed by the different sizing devices (Figure 5.2). The entire system is controlled by LabView 6.i (NI, USA). In order to perform size measurements, low concentration samples are necessary as shown in Chapter 3. Consequently, the activated sludge should be diluted before being analysed and for dilution filtered effluent (0.45µm) was

used in order to minimise the changes in the flocs structure. Dilution was realised in-line by using a dosing pump (Group D, Seepex GmbH, Germany), which allows a small flow rate with high accuracy, low fluctuations (<1%) and low shear. A second dosing-pump (Group D, Seepex GmbH, Germany) was used to achieve the required flow (3 ml/s, Biggs, 2000) to perform the flocs sizing measurement. This type of pump was preferred over peristaltic pumps since it gives more stable flows. After the measurements the diluted sludge was collected in a waste tank. The floc size and size distributions as well as pH, DO, temperature, mixing intensity and conductivity, were recorded on-line as the activated sludge underwent (de)flocculation. Off-line analysis of the activated sludge settling properties (SVI), zeta potential, cations concentrations (Na^+ , Ca^{2+} , K^+), supernatant turbidity were performed prior and after the (de)flocculation experiments for process performance evaluation.

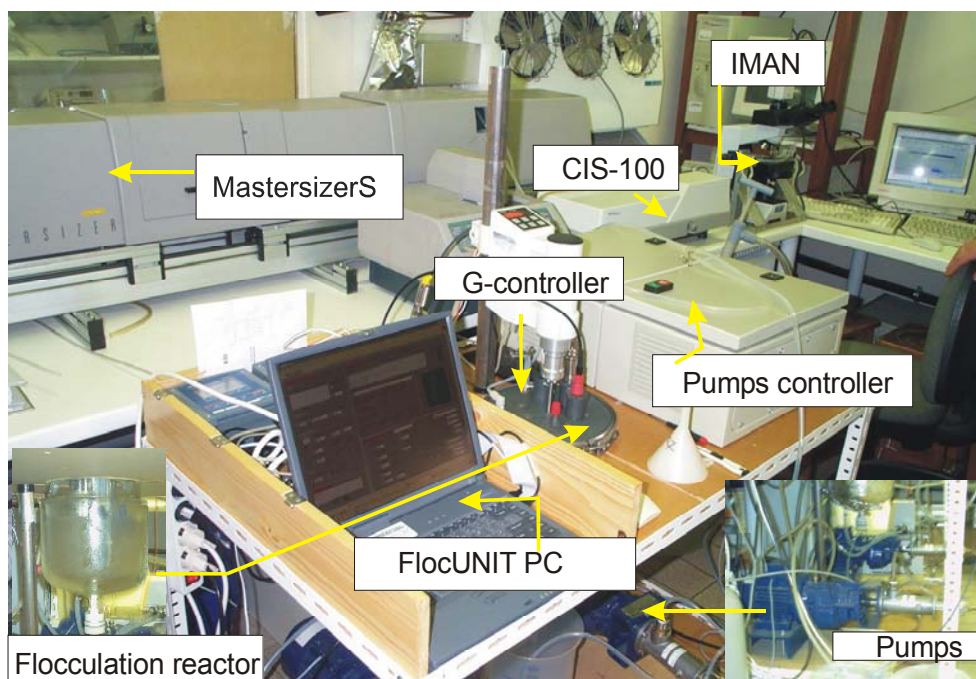


Figure 5.1 The FlocUNIT experimental set-up.

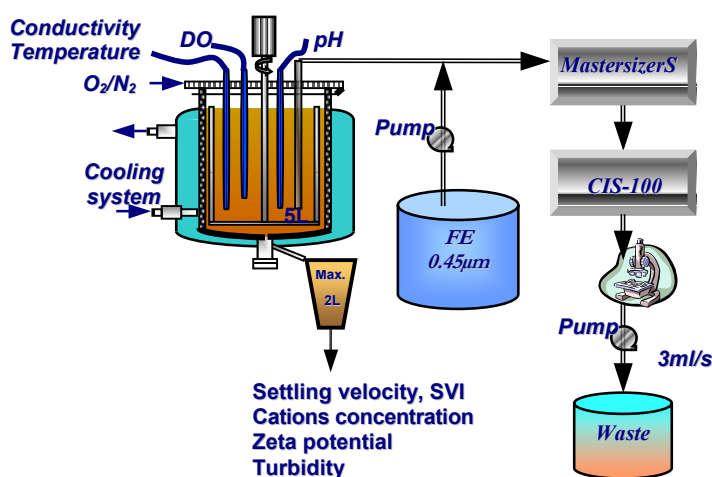


Figure 5.2 Scheme of the FlocUNIT experimental set-up (FE –filtered effluent - 0.45 μm).

The activated sludge (de)flocculation dynamics was investigated in a 5 l reaction vessel (Isotherm TRGN 7392 - Figure 5.3). Near the vessel wall and connected to the vessel cover

four baffles were placed to obtain homogenous mixing. Around the baffles silicone tubes (9/11 mm) were located in order to allow oxygen or nitrogen to diffuse through and ensure the desired DO level in the vessel without creating bubbles as these would cause supplementary shear and eventually affect the floc size measurement (Devisscher *et al.*, 1998). The shape of the mixing blade and its dimensions are given in Figure 5.3. It was specially constructed to allow a uniform mixing in the vessel and also to not interfere with the other sensors which were placed in the vessel in between the rotating mixer blades. A double wall allows to control the temperature in the vessel.

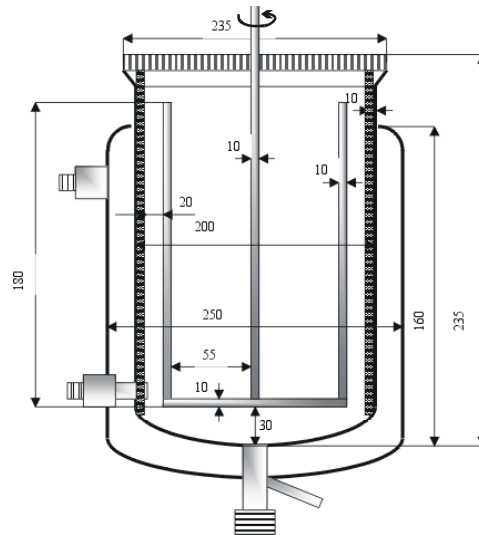


Figure 5.3. Flocculation vessel.

5.2.2. On-line control and data logging

All devices controlling the FlocUNIT set-up (Figure 5.4) were connected to a PC-based data acquisition system (DAQ-system). For data acquisition, a DAQCard-1200 (NI, USA) and a multifunction PCMCIA 232 DAQ-card (NI, USA) to extend the serial ports of the connected portable computer were used and a special VI (Virtual Instrument) was developed in LabView (NI, USA) for automatic control of the FlocUNIT set-up.

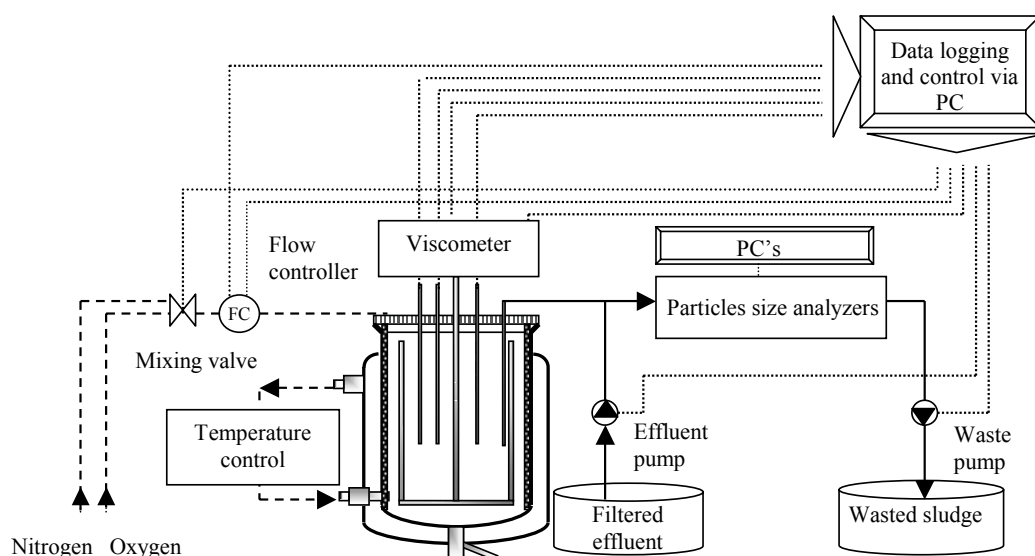


Figure 5.4. Main FlocUNIT set-up connections.

The tasks of the programmed VI were to control the FlocUNIT during an experiment, in particular to maintain the imposed physical and chemical conditions in the vessel, to control the pumps and the valve and to log data. The front panel of the MAIN VI consisted of four parts: *Experiment configuration*, *Program status*, *Experiment status* and *Device configuration* (Figure 5.5). The main VI contained some subVI's, which allowed to control the different parts and equipments of the set-up. Below, more information is provided on the monitoring and control of mixing intensity, DO, conductivity, temperature, pH and floc size.

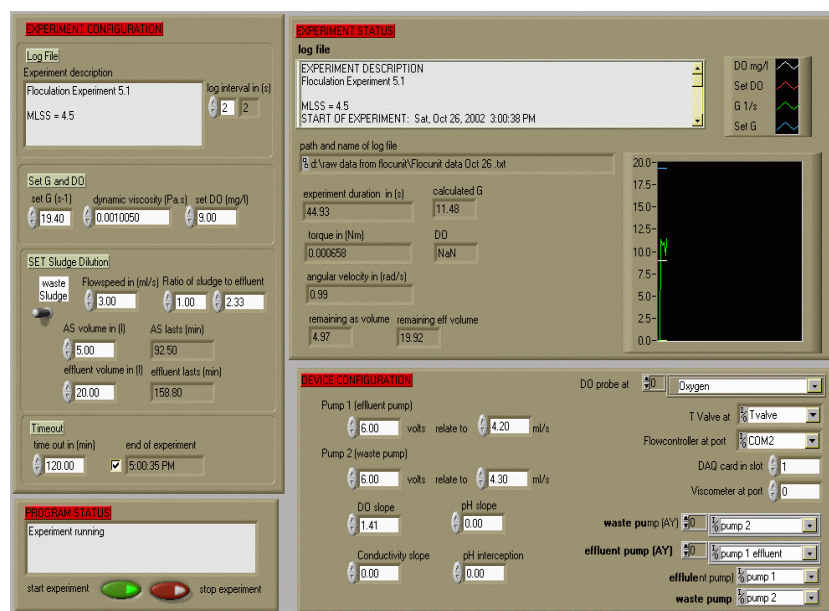


Figure 5.5 Front panel of the MAIN VI .

5.2.2.1. Mixing control

The aim of the mixing control is to keep the shear rate, in terms of the square root mean velocity gradient G , constant during an experiment. G describes the specific power input per unit volume of liquid and it is a quantitative measure of shear imposed to a liquid. In order to generate a constant G in the vessel, a viscometer (VT550, Haake GmbH, Germany) was used. This device can use any geometry of mixing blade at ten discrete rotation speeds and measure the torque experienced while mixing the liquid. With these two features, viscometers are generally used to determine the viscosity of a liquid, for given specific parameters of the stirrer. If the viscosity of a liquid is known, the device can be used to maintain a constant G in a vessel by using the average energy dissipation.

To describe the shear rate within an agitated system the formula introduced by Camp & Stein (1943) was used:

$$G = \sqrt{\frac{\varepsilon}{\nu}} \quad (5.1)$$

where: ν (Pa.s) is the kinematic viscosity of the suspending fluid and ε (m^2/s^3) is the mean energy dissipation per unit mass, which is defined by Chin *et al.* (1998) as:

$$\varepsilon = \frac{P}{\rho V} \quad (5.2)$$

where: P (W) power dissipation; V (m^3) is the volume of the suspension and ρ (kg/m^3) is the density of the suspension.

Based on Parker et al. (1970) who showed that viscosity did not change as a result of the presence of mixed liquor solids during turbulent mixing, the kinematic viscosity was assumed to be the absolute viscosity of water at the temperature measured in the reactor.

The power dissipation P (W), was calculated by using a formula given by Cooke *et al.* (2001):

$$P = 2\pi N_a T_a \quad (5.3)$$

where: N_a (s^{-1}) is the agitation speed and T_a (N.m) the torque.

Preliminary experiments showed that, on average, a velocity gradient of $G = 15 s^{-1}$ (21 rpm) was the minimum shear needed to keep the solids in suspension and, therefore, to provide a representative sample for floc size analysis. The maximum shear that could be achieved with the device was found to be around $G = 200 s^{-1}$ (151 rpm).

5.2.2.2. Dissolved oxygen (DO) control

The purpose of the oxygen control was to maintain a constant oxygen level in the vessel. The oxygen level was changed by introducing pure oxygen or pure nitrogen in the vessel. To raise the oxygen in the vessel O_2 -gas was supplied through the permeable silicon tube, from where the gas diffuses into the liquid in a bubble-less manner (Devisscher *et al.*, 1998). To decrease the oxygen level, N_2 -gas is used in a similar way. The dissolved oxygen concentration in the vessel was monitored by using an oxygen probe (InPro 6000, Mettler Toledo, Belgium) connected to a transmitter (Knick-Stratos 2401Oxy, Elscolab, Belgium). Pure oxygen was preferred over compressed air due to the resulting faster response.

The tubes coming from the O_2 -bottle and the N_2 -bottle were connected to a 3-way-mixing valve (TYP 0330 E, Bürkert GmbH, Germany). Depending on the status of the valve either oxygen or nitrogen is able to pass through. The outlet of the mixing valve is connected to a mass flow controller (Mass Flow Controller 5850S, Brooks Instruments B.V., NL) to control the gases flow and the pressure in the silicon tube. The mass flow controller is linked to the computer by a RS-232C serial connection. For communication the mass flow controller uses the HARTTM protocol (Brooks Instruments manual, 1994). In order to speed up the process and reach the required DO level in the vessel faster the head space of the vessel (between the liquid and the cover) was filled with gas (oxygen or nitrogen, as function of the requested DO value). The oxygen control is schematically shown in Figure 5.6.

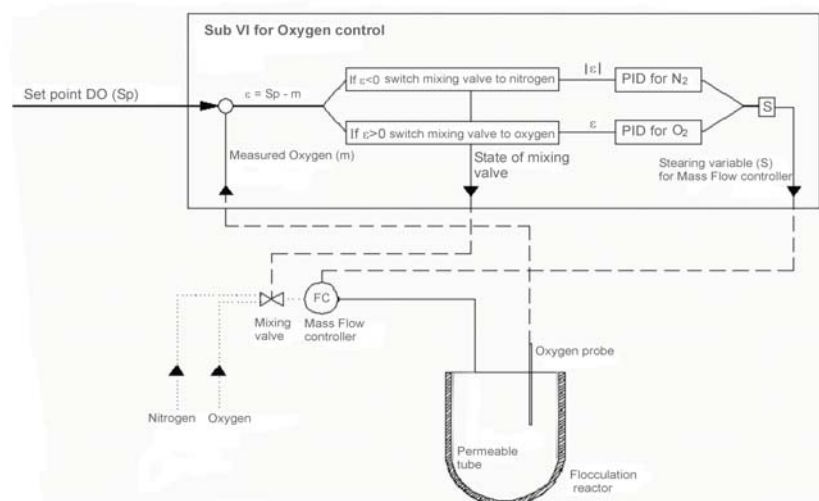


Figure 5.6 Overview of the oxygen control.

The measured DO value was used by the Sub VI to determine whether oxygen or nitrogen needs to be added. The signal is further used to adjust the gas mass flow rate (separate for the two gases) by a PID controller.

The equation for the PID controller is shown below:

$$S = P \cdot \varepsilon + I \int \varepsilon \cdot dt + D \frac{d\varepsilon}{dt} \quad (5.4)$$

where: S is the output variable used by the control device, P is the proportional part, I is the integral portion and D is the derivative part.

The basic working principle consisted in specifying the desired set point for oxygen in the oxygen control subVI. Using the PID controller the subVI then determines whether nitrogen or oxygen is required and also the amount of gas that should be introduced in the vessel. Since the dissolving behaviour of oxygen and nitrogen in activated sludge differ, different values of P , I and D contributions for oxygen and nitrogen were chosen. The PID controller determines a steering variable, S , which is sent to the flow controller (equation (5.4)). The value of the steering variable, S , ranges from 0 to 1 l/min. For values larger than 1 l/min the pressure in the permeable tube becomes too high and the tube would explode. The front panel of the Sub VI is shown in Figure 5.7.

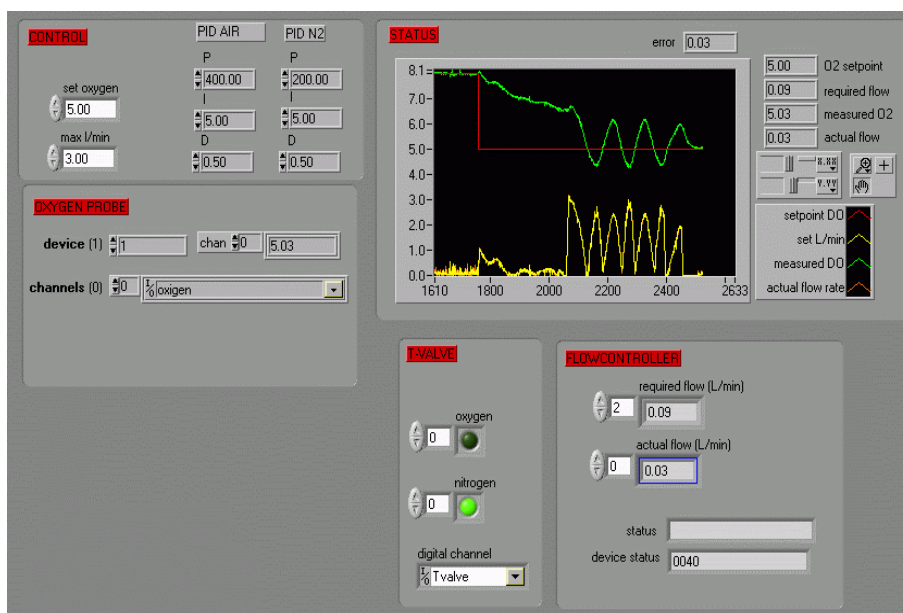


Figure 5.7 Front panel subVI's for Oxygen Control.

5.2.2.3. Conductivity measurement and temperature control

A convenient way to measure the total dissolved solids (TDS) is to test the sample's conductivity. For its measurement, a conductivity sensor (Kemotron 9222, Elscolab, Belgium) connected to a transmitter (Knick-Protos 73LF, Elscolab, Belgium) that allowed a simultaneous measurement of both conductivity and temperature was used.

The reaction vessel had a double wall, in which cooled water recirculated from a cooling system (Lauda RE 307, Germany).

5.2.2.4. pH measurements

During the flocculation experiments the pH was monitored in the reaction vessel using a pH probe (Xerolyt HA-405 DXK S8 225, Mettler Toledo, Belgium) and transmitter (Knick-Stratos 2401pH, Elscolab, Belgium).

5.2.2.5. Floc size and size distribution

The measurement principles of the used sizing devices have already been presented and discussed in Chapter 3. The technical details and methods used for the measurement of the floc size and size distribution are summarised in Table 5.1.

Table 5.1 The measurements settings performed for sizing devices.

Device	Measurement principle	Optical lens	Detection range	Measurement sequence
MastersizerS	Laser diffraction/ Fraunhofer theory	1000	4 – 3500 μm	1 measurement every 30 s
CIS-100	Time-of-transition/ Special mode	B	10 – 3600 μm	1 measurement every 30 s
IMAN	Image analysis	4x	15 – 4000 μm	1 image every 30 s

5.2.3. Off-line measurements

To evaluate the effect of the controlled conditions on the flocculation process, a series of variables were analysed before and after the flocculation experiments.

5.2.3.1. Supernatant turbidity and total suspended solids concentration

The initial and final supernatant turbidity were measured after 30 minutes sludge settling by using a HI93703 turbidity meter (Hanna Instruments, UK). The total suspended solids (TSS) concentration of the supernatant was measured according to Standard Methods (APHA, 1992). For analysis, the same samples as for the turbidity measurement were used.

5.2.3.2. Settling properties

The activated sludge settling properties, investigated as sludge volume index (SVI), were analysed before and after the flocculation experiments by using the method described in Chapter 4, section 4.3.4.2.

5.2.3.3. Zeta potential

The zeta potential is a measure of the electrostatic interaction between individual particles, and it is particularly important for dispersions containing particles less than 30 microns in size. The zeta potential of the supernatant after 45 minutes of settling was determined by using a Zetasizer IIc (Malvern, UK) as described by Van der Meeren et al. (2004).

5.3. Experimental design

5.3.1. Background

Traditional Design Of Experiment (DOE) techniques suggest to preliminary select a large number of independent variables (*factors*), to explain the behaviour of a set of dependent variables (*responses*). The relative importance of each of these factors on the response(s) under investigation should be assessed by performing a first order DOE with the purpose of

screening for the least important factors based on statistical indicators. It is subsequently followed by their removal from the initial set of factors, which is thus reduced to a restricted set of more important factors. The reduction of the number of factors that are simultaneously considered in a designed experiment is a prerequisite to limit the work to a reasonable number of experiments (under the particular circumstances basically imposed by the complexity of the response model to be built afterwards).

The screening step is not absolutely necessary in a DOE methodology. Its execution may be replaced by prior knowledge, or experimental evidence that some factors have a determining role in a particular process, requiring them to be included in the set of variables to be considered. In this study, the set of factors was restricted based on the following observations:

- There is abundant literature in which the effect of a number of factors is discussed and it is widely acknowledged that they may influence the dynamics of the flocculation process. Still, sometimes, their role in the flocculation process is subject to controversy.
- The selected factors are among those that are easily controllable in a laboratory environment.
- The number of experiments to be performed, including the ones of screening phase, must be kept to a minimum; this constraint is dictated by the necessity of having a similar sludge for the entire duration of the experiment.

With these remarks in place, the most important factors to be considered in the experimental design are:

- Average velocity gradient (G)
- DO concentration (DO)
- Calcium addition (Ca)
- Temperature (T)
- Sludge concentration (X)

The following variables were considered as responses:

1. **Mass mean size diameters** as reported by the sizing devices. Dynamics of these size indicators can be time-monitored, therefore allowing to construct initial-process responses, steady-state responses and to monitor their time evolution, thanks to the on-line capabilities of the devices. The mass mean size diameters were chosen as a cumulative evaluation of the recorded floc size distributions (FSD) since it was necessary for the design purpose to find a parameter, which can give an indication of the whole distribution.
2. The effect of the considered set of factors on **SVI** was analysed off-line. These experiments consist of a comparison between initial activated sludge settling properties (before starting the experiment) and sludge settling properties after performing the experiment.
3. The **zeta potential**, **supernatant turbidity** and **suspended solids concentration** were checked before and after the flocculation experiment takes place.
4. The **conductivity** and **pH** were monitored on-line during the experiments.

5.3.2. Time development of a measurement cycle

Details concerning the time development of a single measurement cycle will be given in this section. A brief discussion is necessary to motivate the methodology and for the further

subdivision of the complete set of factors over the overall study period. The method of programming the experiments will also be outlined. It represents the best compromise between the statistical recipes that accompany a designed experiment and the constraints of the setup.

The steps followed when performing a “single-point” measurement cycle (1 experiment) are:

1. Fill the 5 l - reaction vessel with activated sludge of the requested concentration. The activated sludge was collected during two SBR cycles and kept aerated for 6 hours before the experiments started. In order to reach a certain sludge concentration, the activated sludge was diluted with filtered effluent (0.45 μm) or concentrated by eliminating the necessary supernatant volume. To carry out this adjustment, a time t_0 is allocated. During this time the off-line initial analysis is performed, too.
2. Set the conditions in the vessel to obtain an initial steady state flocculation. Identical settings were used for all experiments. Calcium is not added at this stage since it represents a factor that cannot be adjusted (reduced) during an experiment. The same holds for the sludge concentration. The time t_1 to reach the desired preliminary conditions in the vessel (particularly T and DO) may vary and depends, for instance, on the sludge concentration and environmental temperature. During this period only the on-line responses from the conductivity, pH, DO and viscometer are recorded. The dynamics of floc size and size distribution was not monitored since the time t_2 varied as function of the imposed conditions and a size monitoring during this period would result in a significant consumption of the sludge sample from the reactor.
3. Measure the initial conditions effect on floc size and size distribution for a time $t_2=10$ min.
4. Set the factor values corresponding to the current design point, except for calcium addition. The time t_3 required to reach the imposed experimental values in the reactor can fluctuate again, from a few seconds up to a few hours, and the floc sizing measurements are not performed during this period.
5. Measurement of the design points effect without calcium addition for a time $t_4=10$ min.
6. Addition of the requested calcium concentration. This takes a time t_5 , which is approximately 30 s. During the addition process the sizing devices are recording.
7. Measurement of design points effect on the flocculation dynamics until steady state is reached or the volume of sludge in the vessel is lower than 2 l, for a time t_6 ($30 \text{ min} < t_6 < 6 \text{ hours}$).

Figure 5.8 schematically illustrate the experimental time evolution used for all experiments.

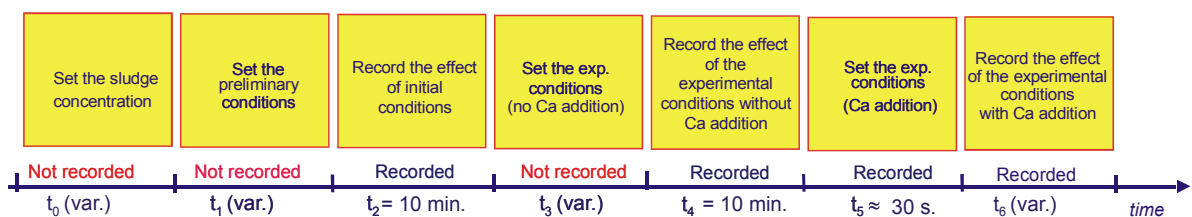


Figure 5.8 The time scale evolution of an experiment.

The above experimental protocol has been constructed on the basis of the accumulated practical expertise and in view of making a compromise between an accurate observation of the flocculation dynamics and the time needed to reach the design values in the vessel. The first issue to be considered was the volume of sample, consumed during one experiment since the analysed samples cannot be returned into the vessel due to the in-line dilution. The sample volume in the FlocUNIT allowed for an experiment taking between 30 minutes and 6 hours depending on the initial sludge concentration in the vessel. Furthermore, the time to achieve the setpoint values for temperature and dissolved oxygen can change a lot from one experiment to another. Hence, any recording of floc sizes during this transition period were not considered. Another limitation originates from the fact that the sludge concentration should have from the beginning the value given by the design since any additional concentration or dilution of the sample was difficult to control afterwards. Moreover, once a cation concentration was added, the considered sample cannot be measured at a lower concentration. Eventually, a higher concentration can be set. Finally, the G parameter can be modified “instantly”. The sizing devices are able to provide a measured data set at every 30 seconds and so, during steps 3 and respectively 5, 6 and 7 the floc size and size distribution were recorded with a known frequency.

5.3.3. DOE considerations: working methodology and experimental matrix

In this section, the design study is discussed: once the data are collected, these should be analysed and interpreted accordingly. It is therefore required that a decision is made on the models used for interpreting the data. In fact, this decision back-propagates and imposes the design scheme.

5.3.3.1. Design properties, response models and experimental effort

The aim is to build empirical models of the set of considered responses and eventually use it for predicting optimal operating conditions. This requires at least a second-order model, which means an experiment in which each factor takes at least three levels. An important attribute of a DOE that allows to unambiguously determine the response model coefficients is the *orthogonality* of the design. This guarantees a nonsingular design matrix and furthermore, the model coefficients have minimal variance.

It is also desirable that the design is *rotatable* (or nearly rotatable), which guarantees that the variance of the model response in any point of the design space is a function of the design-space distance only, and not of the direction. In other words, all directions are equally important and the quality of the model estimate is the same at any point situated on a hypersphere centred around the design-space central point. The centre of the experimental region is called central point, and the corresponding values of the factors are referred as nominal values. An important class of rotatable designs that allows for 2nd-order *response surface models* (RSM) are the so-called *central-composite designs* (CCD), in fact an augmented design resulting from a *factorial part* and an *axial part*. The rotatability is achieved when the axial distance α (i.e. the distance between an edge on a design axis and the centre point of the design) takes a particular value, dependent on the dimensionality of the design space. First-order designs have the great property that orthogonal designs are also rotatable and reciprocally (Myers, 1976).

Unfortunately, this equivalency is lost for higher order designs, as is the case in this experiment. However, there is a solution, rooting in the fact that adding a centerpoint experiment to an already rotatable design does not affect its rotatability. Instead, it affects the orthogonality, and a rotatable design can be made (nearly) orthogonal with the addition of a certain number of centerpoint experiments, depending on the dimensionality of the design

space. Therefore, the number of experiments that is needed to perform the design is $2^n + 2n + k$, where n is the number of factors, k is the number of centerpoint experiments, 2^n is the factorial number of experiments and $2n$ is the axial number of experiments. Table 5.2 illustrates that the addition of a single factor to the design set leads to an exponential increase of the number of experiments that are necessary for completing the design (Myers, 1976).

Table 5.2 Experimental effort for performing an orthogonal and rotatable CCD.

Factors	Exp. Total	Exp. Fact. Part (2^n)	Exp. Axial Part ($2n$)	Centerpoints (k)	Axial distance, α
2	16	4	4	8	1.414
3	23	8	6	9	1.682
4	36	16	8	12	2.000
5	59	32	10	17	2.378

An important (statistical) aspect concerns randomisation of the experiments, which minimises the influence of nuisance variables, ensures a uniform noise level, etc. The experiments have accounted for all these facts, but also had to considered the setup limitations. An important condition for the overall quality of the study is the stability of sludge samples properties. It has to be mentioned that *failing to achieve a sufficiently stable sludge can compromise the design entirely*. Therefore, as shown in Chapter 4 it is of utmost importance that the total time for performing the complete design of the experiment should be minimised as much as possible.

According to Table 5.2, it turns out that a number of 59 experiments is needed for a 5-factors experiment, if a second-order RSM is considered. This experimental effort is too large to be dealt with due to the constraints raised by the sludge stability. Therefore, the design was reduced to a number of 36 experiments only. This goal may be achieved at the price of having *confounding effects*, while still maintaining the important attributes discussed above. Important to note is that this cost is not too high if the confounding effects do not occur between linear and second-order terms themselves, but only for higher order terms. This is the case with a so-called *Resolution V* design, which has the following properties (Myers, 1976):

- It consists of one-half of a full-factorial design (1/2 fractional factorial design), augmented with an axial part, and a number of central points to maintain the rotatability and the orthogonality of the design.
- Does not confound main effects with two-factor interactions.
- Does not confound two-factor interactions with each other.
- Does confound two-factor interactions with three-factor interactions and the main effects with fourth-order interactions.
- The total number of experiments is now reduced to $2^{n-1} + 2n + k'$, where k' is the new number of central point experiments to be performed (10, in this case). Compared to the complete design it is thus reduced with $2^{n-1} + (k - k')$ experiments. Hence, a number of 23 experiments could be saved by using this design. The value of α that is needed to preserve the rotatability is 2.

In order to minimise the time-confounding effect, the experiments were performed in the optimal order, as resulting after minimization of the correlation between the time effect and main effects of the factors. This order is listed in Appendix 5.2.

5.3.3.2. Range selection for the different factors

Average velocity gradient: As already mentioned in this chapter the average velocity gradient range was selected as function of the limitations given by the vessel geometry and the mixing device. In this regard, preliminary tests showed that the minimum mixing intensity to keep the sludge in suspension was 15 s^{-1} . Instead, it was found that 200 s^{-1} was the maximum intensity supported by the mixing engine. This range was considered large enough since literature data showed G values for wastewater treatment processes between 20 s^{-1} and 200 s^{-1} (Tchobanoglous and Burton, 1991; Galil et al. 1991). As the range is quite large, the minimal, maximal and central points, have been calculated on a logarithmic scale.

Sludge concentration: The sludge concentration effect is often directly linked to the ability of sludge to settle. At a sufficiently high sludge concentration, hindered settling dominates the settling process. At low sludge concentration, discrete and flocculant settling, which are influenced by the individual floc properties (size, density, permeability), occurs. A sludge concentration range between 0.1 g/l and 4 g/l was considered in this study. The design values were calculated on a logarithmic scale in order to have a more balanced sampling of the lower concentrations.

Dissolved Oxygen: According to Ganczarczyk (1983), a dissolved oxygen concentration of 1 to 2 mg/l is sufficient for aerobic activated sludge treatment. In this study, the dissolved oxygen concentration limits have been set between anaerobic conditions ($\text{DO}=0 \text{ g/l}$) and an aerobic level at $\text{DO}=4 \text{ g/l}$. The intermediate value was chosen on a linear scale.

Temperature: Temperature was varied between 5°C and 25°C with the intermediate values imposed on 10°C , 15°C and 20°C . These values were chosen as being the most frequently found for domestic wastewater treatment for regions with temperate climate.

Calcium concentration: A consensus exists between all mechanisms available and the beneficial effect of calcium in flocculation is well recognised. Moreover, as shown in Chapter 4 the calcium concentration in the SBR feed is very low with a monovalent (M) to divalent (D) cations ratio of: $\text{M} (\text{Na}^+, \text{K}^+): \text{D} (\text{Ca}^{2+}, \text{Mg}^{2+}) \cong 14:1$ ($8\text{-}9 \text{ meq/l Na}^+$). The calcium concentrations considered in the design were calculated by taking into account the available studies (Higgins and Novak, 1997a) which demonstrate that a sodium to divalent cations ratio larger than approximately 2 would produce a deterioration of settling properties. Moreover, Cousin and Ganczarczyk (1998) observed that at the same sodium concentration the calcium effect varies as function of its concentration. It was shown that a $\text{Ca}^{2+}:\text{Na}^+$ ratio larger than one is recommended to improve the flocculation properties. By taking these studies into account the central point of the design was decided to be close to a ratio $\text{Ca}^{2+}:\text{Na}^+ = 1.5:1$ and go higher to a ratio $\text{Ca}^{2+}:\text{Na}^+ = 3:1$ ($\text{Ca}^{2+}=24\text{meq/l}$). Calcium was added as $\text{CaCl}_2 \cdot 2\text{H}_2\text{O}$ dissolved into 50ml filtered effluent.

5.3.3.3. Factors normalisation

It should be taken into account that different factors have different units and orders of magnitude. From a numerical viewpoint, a DOE should always be performed in a normalised factor space. In this respect, it was fixed that each factor varies in a range $[-1;+1]$, and the linear mapping of the true value to the normalised counterpart is given by:

$$\varphi_{lin}(F) = \frac{F - F_{0,lin}}{\Delta F_{lin}} \quad (5.5)$$

$$F_{0,lin} = \frac{F_{min} + F_{max}}{2} \quad (5.6)$$

$$\Delta F_{lin} = \frac{F_{max} - F_{min}}{2} \quad (5.7)$$

where F is any factor for which the normalisation type is chosen as linear and F_0 is the nominal (or centerpoint value) of that factor.

Notice that due to α values larger than unity, the axial points actually fall outside the interval, e.g.

$$F_{\alpha} = \alpha * \frac{(F_{max} - F_{min})}{2} + F_0 = \frac{(\alpha + 1) * F_{max} + (\alpha - 1) * F_{min}}{2} > F_{max} \quad (5.8)$$

The logarithmic mapping of the true values to normalised values is:

$$\Phi_{log}(F) = \frac{\log(F/F_{0,log})}{\log(\Delta F_{log})} \quad (5.9)$$

$$F_{0,log} = \sqrt{F_{min} * F_{max}} \quad (5.10)$$

$$\Delta F_{log} = \sqrt{\frac{F_{max}}{F_{min}}} \quad (5.11)$$

Again, F is a factor for which the normalisation type is chosen as logarithmic.

The relations used to calculate the design points of each of the considered factors are presented in Appendix 5.1. The unnormalized factors range is presented in Table 5.3. In Table 5.3 the five factors were coded and normalized by using equation (5.5) (for the linear scale) and equation (5.9) (for the logarithmic scale) as follows:

Temperature, T [°C]:

$$x_1 = T = \frac{T - 15}{5} \quad (5.12)$$

Average velocity gradient, G [s⁻¹]:

$$x_2 = G = \frac{\lg(G/\sqrt{29*105})}{\lg(\sqrt{105/29})} = \frac{\lg(G/55)}{0.28} \quad (5.13)$$

Calcium concentration, Ca [meq/l]:

$$x_3 = Ca = \frac{Ca - 12}{6} \quad (5.14)$$

Dissolved oxygen, DO [mg/l]:

$$x_4 = DO = \frac{DO - 2}{1} \quad (5.15)$$

Activated sludge concentration, X [g/l]:

$$x_5 = X = \frac{\lg(X/\sqrt{0.25*1.59})}{\lg(\sqrt{1.59/0.25})} = \frac{\lg(X/0.63)}{0.40} \quad (5.16)$$

Table 5.3 Factors range and nominal values.

Factors	Normalisation type	Minimum (-1)	Maximum (1)	Nominal (0)	Minimum Axial (-2)	Maximum Axial (2)
Temperature, T [C]	linear	10	20	15	5	25
Average velocity gradient, G [1/s]	logarithmic	29	105	55	15	200
Calcium addition, Ca [meq/l]	linear	6	18	12	0	24
Dissolved Oxygen, DO [mg/l]	linear	1	3	2	0	4
Sludge concentration, X [g/l]	logarithmic	0.25	1.59	0.63	0.1	4

Following the proposed experimental design and by taking into account the above discussed working methodology the complete time scale evolution, which was followed in all the experiments performed is shown in Figure 5.9.

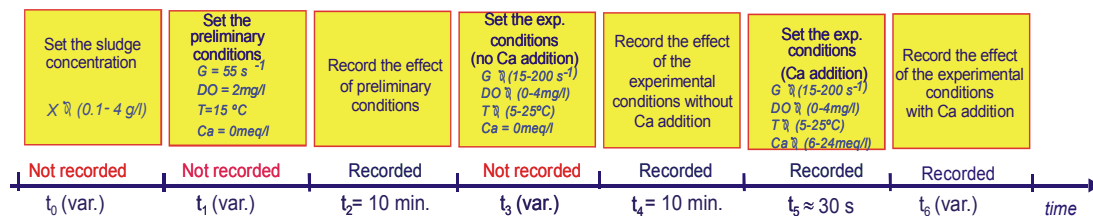


Figure 5.9. The time scale evolution of an experiment.

The experimental design matrix, in terms of coded (normalized) variables, together with the chronological order of the experiments, which minimises the time confounding effect is shown in Appendix 5.2.

5.4. Fundamentals of the Response Surface Methodology (RSM)

Response Surface Methodology (RSM) has been intensively developed in the '50's as a framework for solving problems in the area of chemical engineering. Myers et al. (1989) defined it as follow "Response Surface Methodology is a collection of tools in design or data analysis that enhances the exploration of a region of design variables in one or more dimensions". It consists of a series of steps eventually answering questions like "Where to experiment?", "How much to experiment?", "What to do with the experimental data?". The former questions are subject to DOE, which was described before in this chapter. The latter is

mainly concerned with RSM techniques, which in turn consists of two steps: model synthesis and model analysis.

In this section, the main steps that are used in building an empirical model are briefly reviewed. The outcome of any experiment is subject to measurement errors, and these errors have to be dealt with using statistical tools. Commonly, regression analysis is the statistical tool employed for quantifying polynomial models, for which the minimisation of the sum-of-square errors is adopted as the objective for the determination of the model parameters. The model error is then divided on statistical grounds in pure error, inherent to the experiment, and lack-of-fit error, which reflects the inability of the proposed model to describe the system under consideration.

1. *Evaluation of the response model associated with the experimental design carried out assuming a Resolution V quadratic model.*

The basic steps in constructing a linear model are outlined as follows: there is a dependent variable y (response) that depends on a set of independent variables x_1, x_2, \dots, x_n (factors), $y=g(x_1, x_2, \dots, x_n)=g(\mathbf{x})$ where g is an unknown smooth continuous function and $\mathbf{x}=(x_1, \dots, x_n)^T$ is the vector of factors. Note that, from a numerical point of view it may be convenient that $x_i, i=1 \dots n$ are scaled variables. Then, a response surface is a function $f(\mathbf{c}, \mathbf{x})$ that approximates the true unknown function:

$$y = f(x_1, x_2, \dots, x_n) + \varepsilon_m \quad (5.17)$$

where ε_m is the model error and f is a linear function with respect to the model parameters $\mathbf{c}=(c_1, \dots, c_p)^T$:

$$f = \sum_{j=1}^p c_j F_j(x_1, x_2, \dots, x_n) = \mathbf{f}^T(\mathbf{x})\mathbf{c} \quad (5.18)$$

and $f(\mathbf{x})=(F_1(\mathbf{x}), \dots, F_p(\mathbf{x}))^T$. The parameters c_j have to be estimated from the experimental data, usually based on the least squares method, as already mentioned before.

Some assumptions concerning the error, ε , have to be made, too. Thus, the model error is assumed to have a zero mean and a constant variance σ^2 . Moreover, the errors are independent and normally distributed.

Supposing that a number m of experiments $(t_k, \mathbf{s}_k^T)=(t_k, s_{1k}, \dots, s_{nk})$, $k=1 \dots m$, $m > p$ have been performed, the least squares estimator is:

$$\hat{\mathbf{c}} = (F^T F)^{-1} F^T \mathbf{t} \quad (5.19)$$

under the assumption that $F^T F$ is non-singular, where $F=(\mathbf{f}^T(\mathbf{s}_1), \dots, \mathbf{f}^T(\mathbf{s}_m))^T$ is the experimental or design matrix and $\mathbf{t} = (t_1, \dots, t_m)^T$. By inserting equation (5.19) in equation (5.18) it is now straightforward that at any \mathbf{x} , the predicted value of the response is:

$$\hat{y}(x) = \mathbf{f}^T(\mathbf{x})\hat{\mathbf{c}} = \mathbf{f}^T(\mathbf{x})(F^T F)^{-1} F^T \mathbf{t} \quad (5.20)$$

The steps followed to evaluate the influence of the considered factors on the obtained responses are described below.

2. *Statistical analysis of the obtained model by ANOVA and regression coefficients*

The statistical analysis of the model (equation (5.20)) is performed using Analysis of Variance (ANOVA) and F -test statistics for the determination of the relevance of the model terms. For statistical reasons, a good measure of the quality of the fit should be expressed in

terms of the mean of sum of squares (MS). The following formula are implemented in Matlab for the calculation of the statistical indicators:

$$F = MS_{reg} / MS_{res} \quad (5.21)$$

where: $F = F\text{-ratio}$ which represents a statistical indicator of the model fit, MS_{reg} and MS_{res} are the regression mean of sum of squares, residual mean of squares, given by the following equations:

$$MS_{reg} = SS_{reg} / df_{reg} \quad (5.22)$$

$$MS_{res} = SS_{res} / df_{res} \quad (5.23)$$

where: SS are sum-of-squares and df are degrees of freedom, calculated as follows:

$$SS_{reg} = \sum_{i=1}^m (\hat{R}_i - \bar{R})^2 \quad (5.24)$$

$$SS_{res} = \sum_{i=1}^m (R_i - \hat{R}_i)^2 \quad (5.25)$$

$$df_{reg} = p - 1 \quad (5.26)$$

$$df_{res} = m - p - 2 \quad (5.27)$$

where: p – number of terms (including the free term), m – number of data points ; and $m-p-2$ is the number of degrees of freedom available for error analysis (m and p have the same meaning as in step 1).

The probability value, $p\text{-value}$, gives the probability of finding by chance an $F\text{-ratio}$ as large as or larger than the one observed. Small $F\text{-ratios}$ are associated with large $p\text{-values}$ and occur with models that do not explain a significant fraction of the variation in the response. In this case, the hypothesis that there is no need for this model is accepted. By contrast, large $F\text{-ratios}$ (small $p\text{-values}$) indicate that the difference between the residuals with and without the model is larger than could be expected by chance. The smaller the $p\text{-value}$ the stronger is the indication that there is a relation between the set of variables and the response. Hence, if the probability is smaller than the pre-set significance level, e.g. if $p\text{-value} < 0.05$, the model is assumed to explain a significant amount of the variation present in the data, or in short, "the model is (statistically) significant".

The quantitative measures of the model performance were estimated by using regression parameters. In this respect, the multiple correlation coefficient R^2 represents the fraction of the total variation explained by the model:

$$R^2 = \frac{SS_{reg}}{SS_{total}} = 1 - \frac{SS_{res}}{SS_{total}}; \quad 0 \leq R^2 \leq 1 \quad (5.28)$$

Furthermore, the adjusted R^2 (R^2_{adj}) penalises models with unnecessary extra model parameters:

$$R^2_{adj} = 1 - \left(1 - R^2\right) \frac{m - 1}{m - p + 1}; \quad -\infty \leq R^2_{adj} \leq R^2 \leq 1 \quad (5.29)$$

As a last performance parameter, the root mean square error (RMSE) indicates the standard deviation of the spread around the model. It can be regarded as the experimental error (reproducibility). It should be neither much higher (lack-of-fit) nor much smaller (overfit) than the empirical estimate, possibly known from previous experience.

3. Identification and analysis of the stationary points of the fitted surfaces and analysis of the RSM in the box-constrained design space

This step is carried out using standard analysis of the RSM curves where, after the determination of the stationary points, each RSM is reduced to its canonical form, which allows to determine the nature of these points. In the next paragraphs, the definition of these terms and the steps required for their determination are briefly reviewed.

The goal of the determination of the stationary points is to estimate the conditions on the factors (x_1, x_2, \dots, x_k) , which maximise or minimise the response R . The stationary point of the response function is the point for which the derivative with respect to the independent variables is zero.

For a second-order polynomial model the fitted response surface \hat{R} , is written as:

$$\hat{R} = b_0 + \sum_j b_j x_j + \sum_{m < j} \sum b_{jm} x_j x_m + \sum_j b_{jj} x_j^2 \quad (5.30)$$

Note that the coefficients $b_0, b_j, b_{jm}, b_{jj}, (j, m = 1, \dots, k)$ correspond to the elements of the coefficients \mathbf{c} in the general model equation (5.18).

In matrix notation, the fitted second-order function from equation (5.30) is written as:

$$\hat{R} = b_0 + \mathbf{x}^T \mathbf{b} + \mathbf{x}^T B \mathbf{x} \quad (5.31)$$

where:

$$\mathbf{x} = \begin{bmatrix} x_1 \\ x_2 \\ \dots \\ x_k \end{bmatrix}, \quad \mathbf{b} = \begin{bmatrix} b_1 \\ b_2 \\ \dots \\ b_k \end{bmatrix}, \quad B = \begin{bmatrix} b_{11} & b_{12}/2 & \dots & b_{1k}/2 \\ & b_{22} & \dots & b_{2k}/2 \\ & & \dots & \dots \\ & & & \dots & b_{k-1,k}/2 \\ sym & & & & b_{kk} \end{bmatrix}$$

The $\mathbf{x}^T \mathbf{b}$ term in equation (5.31) gives the first order contribution to the response function, whereas the term $\mathbf{x}^T B \mathbf{x}$ gives the quadratic contribution. The latter term contains terms involving the mixed quadratic coefficients b_{ij} ($i \neq j$) and the pure quadratic coefficients b_{ii} . The maximum/minimum, if it exists, will be a set of conditions on (x_1, x_2, \dots, x_k) such that the first derivatives with respect to each variable are simultaneously zero. This value, say $\mathbf{x}_0^T = [x_{1,0}, x_{2,0}, \dots, x_{k,0}]$ is the stationary point of the fitted surface. The stationary point is very useful for describing the response surface system. The derivative of equation (5.31) with respect to the vector \mathbf{x} , equated to 0, gives:

$$\frac{\partial \hat{R}}{\partial \mathbf{x}} = \frac{\partial}{\partial \mathbf{x}} [b_0 + \mathbf{x}^T \mathbf{b} + \mathbf{x}^T B \mathbf{x}] = 0 \quad (5.32)$$

Solving for \mathbf{x} , the stationary point \mathbf{x}_0 becomes:

$$\mathbf{x}_0 = -B^{-1} \mathbf{b} / 2 \quad (5.33)$$

The response computed by using the equation (5.33) can be:

- a point at which the fitted surface attains a maximum,
- a point at which the fitted surface attains a minimum,
- a saddle point of the fitted surface.

If the stationary point is a maximum, moving away from \mathbf{x}_0 results in a decrease in response. If \mathbf{x}_0 is a minimum, a corresponding increase would result. However, in the case of a saddle point, one may get an increase or a decrease in response when one moves away from the stationary point depending of the taken direction. In the theory of real functions of a single variable, the nature of the stationary point is found by looking at the sign of the second derivative, calculated at the stationary point. For a second-order polynomial function (e.g. the RSM, in this case) of multiple variables, however, the nature of the stationary point is investigated by using the canonical form, which may be written as:

$$\hat{R} = \hat{R}_0 + \lambda_1 w_1^2 + \lambda_2 w_2^2 + \dots + \lambda_k w_k^2 \tag{5.34}$$

where \hat{R}_0 is the estimated response at the stationary point $\mathbf{x}_0 = -B^{-1}\mathbf{b}/2$, and λ_i are characteristic roots of the matrix B .

The reduction of the response surface to its canonical form is called canonical analysis. In order to determine the nature of the stationary point, the sign and the magnitude of the λ 's have to be investigated. More precisely, if all λ 's are negative, a move in any direction from the stationary point results in a decrease in the response. Therefore, the stationary point represents a point of maximum response for the fitted surface. On the other hand, if all λ 's are positive, the stationary point is a minimum of the fitted surface. In the case when the λ 's differ in sign, the stationary point is a saddle point. If one or more of the λ values is near zero or considerably smaller in magnitude than the others, a type of ridge response system is indicated. Possible situations of the nature of the stationary point are schematically drawn in Figure 5.10.

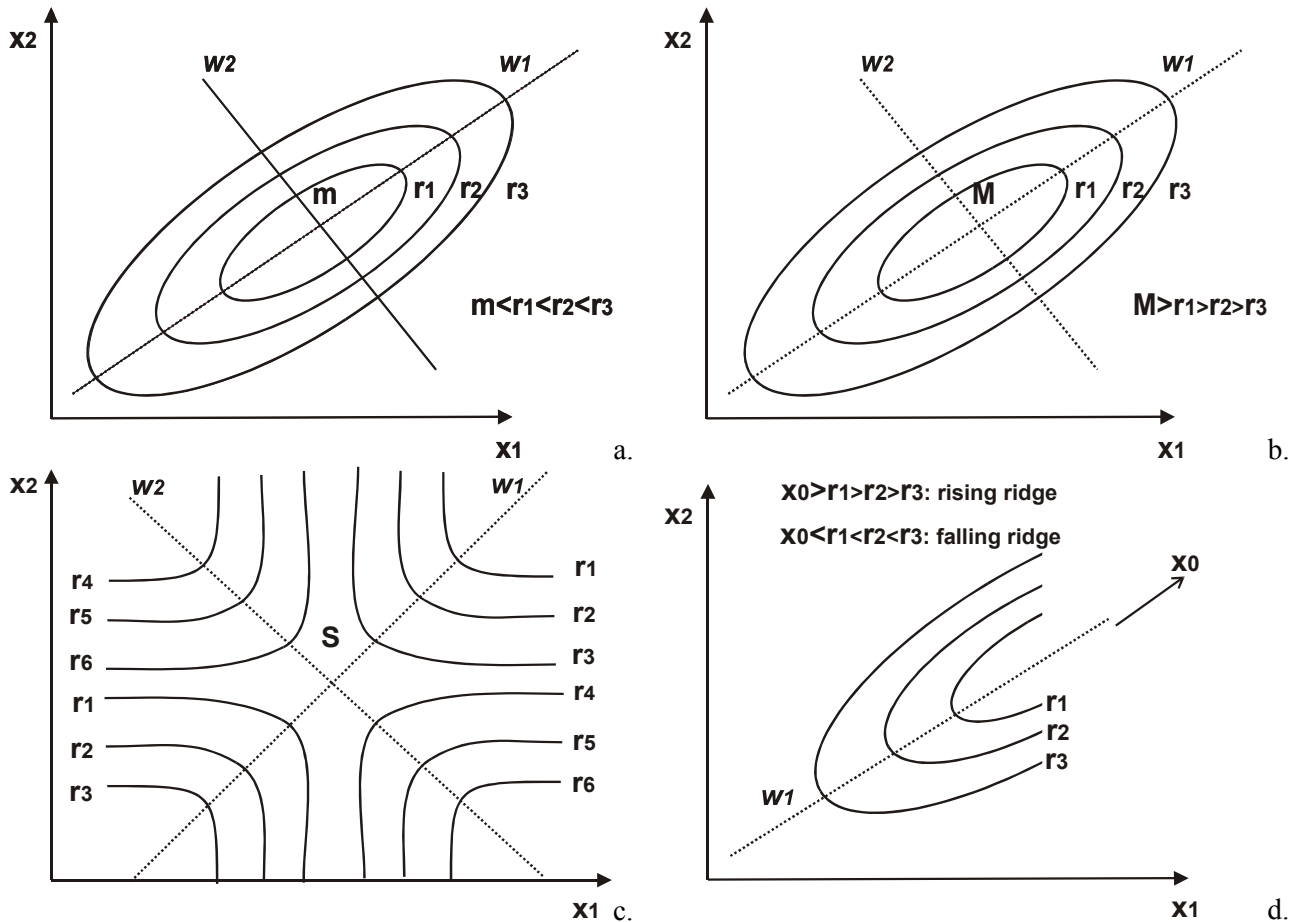


Figure 5.10 Nature of stationary point in a fitted surface: a. minimum; b. maximum; c. saddle; d. ridge.

4. Statistical model identification and the corresponding model simplification.

The Akaike Information Criterion (AIC) is a popular method for comparing the adequacy of multiple, possibly non-nested models and being used for simplifying the derived models, wherever possible. It represents a measure of the goodness of fit plus a penalty of each parameter used. This generic function calculates the Akaike information criterion for one or several fitted model objects for which a log-likelihood value can be obtained, according to the formula:

$$AIC = -\log(\text{likelihood}) + n_{par} \quad (5.35)$$

where n_{par} represents the number of parameters in the fitted model. Then first term in equation (5.35) is a measure of the goodness of fit, whereas the second adds a penalty for increasing model complexity. The smaller the AIC, the better the model is. In order to simplify a model based on the AIC, the following procedure is used: a model with a large number of parameters is used as the initial model. Each model term is sequentially "skipped" from the current model, and the AIC is calculated. The term that gives the largest decrease in the AIC is selected for removal. This procedure is repeated with the new model, which is simplified until no significant decrease of the AIC is possible any more. The model simplification using the AIC was carried out using a program written in the S-Plus software package.

5. Optimisation of the operating point

In general, an optimisation problem may be formulated as minimization of an objective function. The objective function may be defined depending on the particularities of the optimisation problem. The optimal point(s) are searched in a parameters space, possibly being subject to several constraints. The simplest constraints are of the box-type, which specify a limited interval of allowed values for each factor. This type of constraints should be naturally imposed on the response models, which are constructed by making use of knowledge gathered in a box-like subspace. Additionally several other constraints may be imposed, and these can be divided into equality or inequality constraints.

One simple definition of the objective function (OF), implemented with the present RSM set of routines is:

$$OF = \sum_{j=1}^{N_{res}} tw_j \cdot (R_j(\mathbf{x}) - T_j)^2 + \sum_{j=1}^{N_{res}} sw_j \cdot \sum_{i=1}^{N_{fac}} \left(\frac{\partial R_j(\mathbf{x})}{\partial x_i} \right)^2 \quad (5.36)$$

The first term of the objective function contains the weighted sum of targets. This has an absolute minimum of zero if, and only if, $R_j(\mathbf{x}) = T_j$, for all the responses $j=1, \dots, N_{res}$. If one response is more important than the others, a higher target weight tw_j may be assigned to it. The second part is related to the sensitivity and minimizes the curvature. It reaches a global minimum of zero, if all the responses are at their stationary points (not necessarily extrema!). It basically says that when the sensitivity is smallest, the response is most stable (or has least variations) at small fluctuations of the factors values around the sensitivity-optimal point. Sensitivity weights sw_j may be assigned to each response, to discriminate between more important and less important response sensitivities.

It should be noticed that all responses requirements are collected in just one single objective function. This means that after the optimisation it might be possible that individual response specifications (i.e. targets and/or sensitivities) are not reached, but when combined altogether, the imposed conditions result in a minimal OF . It should also be remarked that the optimal points found are local optima rather than global, and there may be one or more such optima,

belonging to a countable or uncountable set of solutions. This peculiar feature of the optimal points is intrinsically related to the nature of the optimisation algorithms.

5.5. Conclusions

In this chapter a detailed description of the experimental technique and of the protocol used for the quantification of the flocculation process dynamics was presented. An on-line measurement technique methodology was developed and its main characteristics were discussed.

Elements of design of experiments theory were reviewed, tailored on the particular problem of concern in the thesis. A number of five relevant factors (temperature, average velocity gradient, dissolved oxygen concentration, sludge concentration and calcium addition), was selected and proper experimental ranges and normalisation scales for the purpose of numerical stability were discussed. Time budget limitations imposed a Resolution V design, which allowed for a five-factors experimental design. This maintains the properties of orthogonality and (near-) rotatability, required for a robust second-order model building. It resulted in a total of 36 experiments. The Resolution V design consists in a one-half fractional factorial design, augmented with an axial design with a parameter $\alpha = 2$, and 10 central points.

Furthermore, an account of the response surface model building was given. A survey of some parameters, useful for the assessment of the statistical quality of the model, followed. A standard methodology for the analysis of the RSM was discussed, with emphasis on the procedure for the identification of the stationary point and its nature. The Akaike Information Criterion (AIC) for model simplification was also briefly discussed.

Finally, the framework for an optimisation methodology was defined, by setting up a properly defined objective function, able to incorporate target as well as sensitivity contributions of a considered set of model responses.

All techniques and procedures used for model building and analysis described in this Chapter were implemented in two Matlab programs (except for AIC, see previous section) and were intensively used to analyse and interpret the experimental data, collected by carrying out the above mentioned five-factors design. The results are discussed at length in the following two Chapters.

The influence of different physical and chemical parameters on the (de)flocculation dynamics

6.1. Introduction

Activated sludge flocculation depends on many parameters such as: shear rate, cations concentration, temperature, pH, oxygen concentration, organic load, etc. These parameters may affect the structural and biological properties of the activated sludge flocs creating an improvement or a degradation of process performance.

In this chapter, the effect the five considered factors (average velocity gradient, calcium addition, temperature, dissolved oxygen concentration and activated sludge concentration) on floc size dynamics is analysed and discussed. As described in Chapter 5, to allow a correct interpretation of the effect of these factors, the biological and structural variations in the activated sludge need to be avoided as much as possible during the experimental periods. The activated sludge samples from the SBR, which was operated and monitored as described in Chapter 4, have been used to obtain "stable sludge". The main points that are tackled in this chapter are:

- Evaluating the microbial community and the activated sludge properties from a stability point of view.
- Investigating the effect of the physical and chemical parameters on the (de)flocculation dynamics by on-line monitoring of the floc size and size distributions.

6.2. Evaluation of the SBR's activated sludge properties during the experimental period

Achieving sludge stability during the experimental period was an essential condition for the proposed DOE. Working with a biologically unstable system would introduce additional difficulties in data interpretation as it may significantly affect the obtained design responses.

The biological and structural properties of activated sludge from the SBR have been investigated in terms of microbial community and structural properties by using the methods described in Chapter 4. In the same chapter, it was shown that for long-term monitoring the microbial population in the SBR was very dynamic and that it was almost impossible to obtain a biologically stable sludge. It was also observed that the microbial community was highly sensitive to the operating problems that occurred during the monitoring period. However, short-term evaluations showed a relatively stable microbial community. It was therefore necessary to avoid any perturbation that could occur in the SBR operation. To do so,

performing the flocculation experiments in a short time period was essential. In this sense, the experiments were performed within 36 days and were only started when stability in the SBR functionality had been achieved for a longer period (more than 3 months).

6.2.1. Microbial community

In order to examine the temporal change of the bacterial community structure, a DGGE analysis of 16S rRNA genes was used as described earlier in Chapter 4.

Figure 6.1 shows the evolution of the microbial community during the experimental period. A direct visualisation of the two performed gels suggests that a very diverse microorganisms population is present in the SBR activated sludge. This is illustrated by the large number of band patterns. More importantly, the band patterns show a high degree of similarity between the samples, suggesting no significant changes into the microbial community during the monitored period.

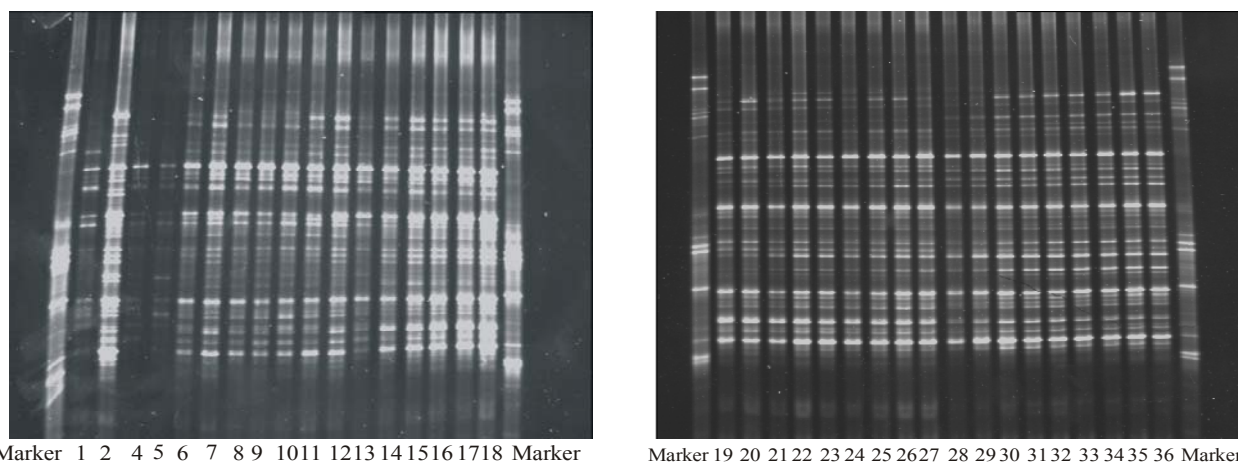


Figure 6.1. DGGE profiles for samples collected during the experimental period (the numbers correspond to the experiment number and represent the chronological experimental order)

For a precise evaluation, the cluster analysis of the DGGE patterns was performed (Figure 6.2-left). A relatively high similarity level between the samples can be observed as well. However, three major clusters are distinguished. The first cluster contains the band patterns of the markers, which were necessary to compare the two different DGGE gels. The two other clusters correspond respectively to the two analysed DGGE gels. It can be observed that no interactions between samples from different gels take place. It is therefore assumed that the observed differences are mainly due to the clustering method, which is based on image analysis and hence, very sensitive to different degrees of grey levels analysis. This hypothesis is confirmed by the relatively low similarity observed between the markers since the samples coming from the same DGGE gel clustered together with a high degree of similarity as compared with the markers. A separate analysis of each DGGE gel (Figure 6.2 – right) shows that the most dominant species are present during the whole period. Small changes in time are however observed especially with respect to in the dominance of the species and not in their dynamics.

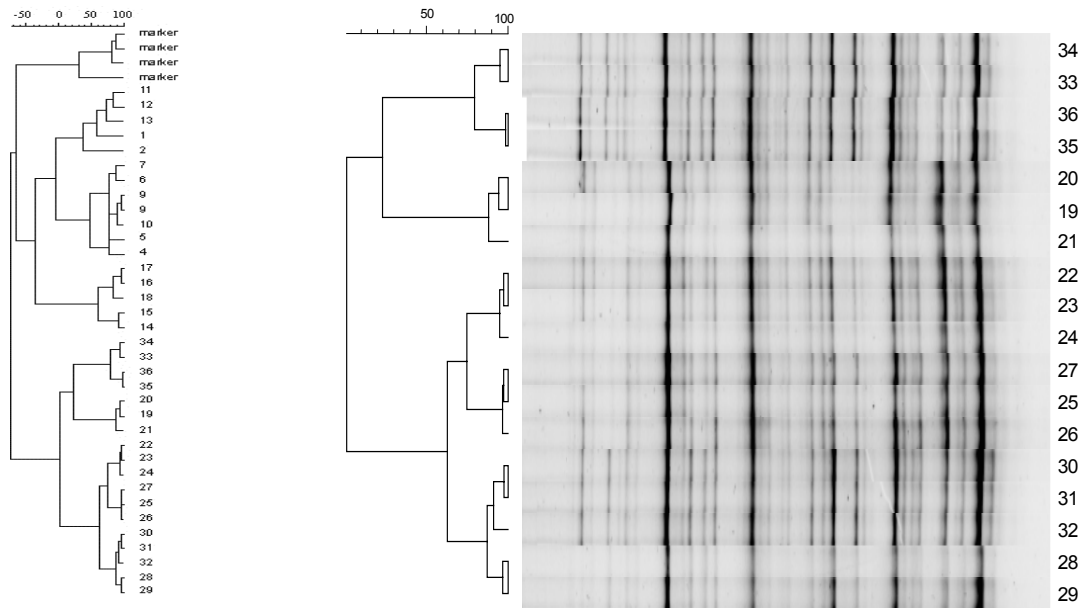


Figure 6.2. Cluster analysis of the DGGE patterns corresponding to all performed experiments (left) and the cluster analysis and DGGE patterns corresponding to the second DGGE gel (experiments 19-36) (right)

6.2.2. Activated sludge structural properties

As discussed in Chapter 4, a link between the sludge settling properties, floc size distribution and microbial community evolution was found for long term monitoring of the SBR activated sludge. Based on this information, the stability of the sludge during the flocculation experiments was further investigated.

The floc size and size distribution were examined over the measurement period by comparing the results obtained when preliminary conditions were imposed in the reactor ($G = 55\text{s}^{-1}$; $\text{DO} = 2\text{mg/l}$; $X = 0.63\text{g/l}$; $T = 15^\circ\text{C}$ and $\text{Ca} = 0\text{meq/l}$).

The cumulative distributions recorded over the experimental period showed that no trend was observed in the FSD evolution (Figure 6.3). The floc size measurements showed a mass mean diameter of the flocs between $300\text{-}450\mu\text{m}$, which indicates the presence of relatively large flocs in the activated sludge samples.

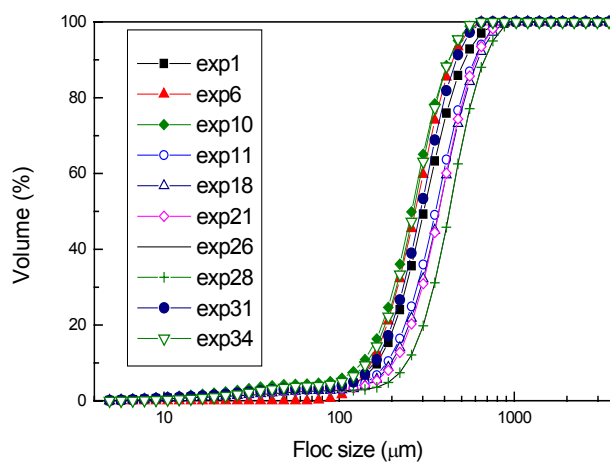


Figure 6.3. Cumulative size distributions recorded during the experimental period when the preliminary conditions were imposed into the flocculation reactor

As a confirmation, daily microscopic observations showed no major changes of the floc structure. The flocs were mostly characterised by a compact structure and had rounded to angular shapes (Figure 6.4.). The presence of some protozoa (ciliates) and metazoa (rotifers, nematodes and worms) in the activated sludge samples was also observed. The ciliates were attached to the flocs whereas the others were mostly moving freely in the water between the flocs. Attached ciliates, according to Jenkins (1993), are generally a sign of stable activated sludge operation.

For the entire experimental period the number of filaments present in the activated sludge samples were quantified to correspond to a filament index $FI=2$ evaluated according to the Eikelboom (2000) scale and the observed filaments were in general thin. For this filament index value the negative effect of this amount of filaments on the settling properties can be considered as minor (Eikelboom, 2000).

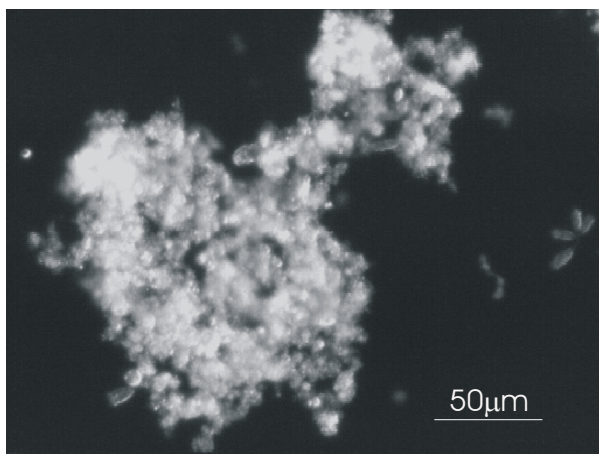


Figure 6.4 Image of an activated sludge floc acquired by using an optical microscope CX40 (Olympus, Japan) (10x)

To complete the overview of the process stability, the sludge SVI was investigated as well (Figure 6.5). No specific trend reflecting possible changes in the settling properties during the monitoring period was observed. However, the slightly elevated values of the SVI (average $SVI = 191.79 \pm 31.98$ ml/g) are in agreement with other structural properties of the analysed sludge samples.

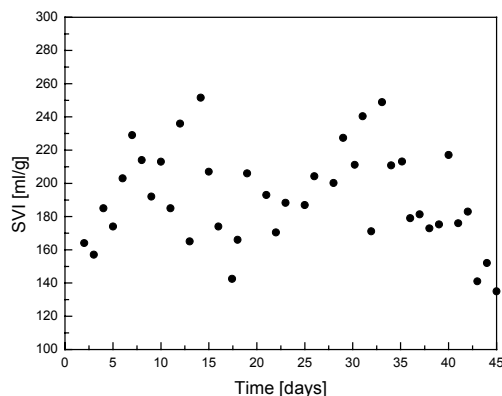


Figure 6.5. The SVI over the experimental period

6.2.3. Conclusions

By investigating the sludge structural and settling properties, as well as the population dynamics, it was observed that no significant changes in the floc properties occurred during the experimental period. It may therefore be considered that the possible changes of the initial characteristics of the sludge samples were weak and the sludge was rather stable during the experimentation period, especially with respect to the biological properties. This observation satisfies the essential condition required by the proposed DOE and allows to compare and interpret the effect that different physical and chemical parameters play on flocculation for the considered sludge samples.

6.3. Quantification of the influence of different factors on the (de)flocculation dynamics

Before proceeding with the overall analysis of the experimental design it is useful to look at the effect of the individual factors on the (de)flocculation dynamics. Among the 36 experiments performed only the minimum and maximum axial design points of each factor and 10 repetitive central design point experiments will be taken into consideration and discussed here. The experiments performed on minimal and maximal factorial design points were difficult to be interpreted as more than one parameter was varied at a time and then the coupled effects of more than one factor must be considered. These will be considered later on, by using the response surface methodology approach. Since the time of performing the measurements varied from one experiment to another as function of the sludge concentration in the vessel, only the first 75 minutes were considered in the data analysis. It was observed that after this time most of the floc size distributions tended to be steady state.

6.3.1. The effect of average velocity gradient (G)

Under turbulent conditions, deflocculation generally occurs causing an increase of the micro-sized primary particles and thus, negatively affecting the efficiency of the solid/liquid separation process by increasing the supernatant turbidity (Mikkelsen and Keiding, 1999). At low turbulence level the flocs tend to flocculate and to form bigger aggregates, which can settle easier. Of major importance is to investigate the capabilities of the flocs to break-up and aggregate since these are the two most important mechanisms responsible for floc formation.

The floc size dynamics in the FlocUNIT were investigated during all 36 experiments performed. To avoid multiple factors interactions, the G effect is quantified only for the experiments performed at the lowest value ($G=15\text{ s}^{-1}$), the highest value ($G=200\text{ s}^{-1}$) and in the central point, corresponding to a value of $G=55\text{ s}^{-1}$.

In all presented results the sludge concentration in the FlocUNIT was set to $X=0.63\text{ g/l}$ and diluted in-line with the filtered effluent until the requested concentration range for the sizing devices was reached ($\approx 0.1\text{ g/l}$). The other parameters were kept constant at their nominal values as given by the design scheme.

To record the floc size dynamics, the sample was subjected to identical conditions for all experiments ($G = 55\text{ s}^{-1}$, $T = 15^\circ\text{C}$, $\text{DO} = 2\text{ mg/l}$, $X = 0.63\text{ g/l}$, $\text{Ca}^{2+} = 0\text{ meq/l}$) during the first 10 minutes. For the next 10 minutes the effect of changing G to the nominal experimental value was recorded by the sizing devices and from time $t_5 = 20\text{ min}$ (Figure 5.11) the calcium was added to the system.

6.3.1.1. *MastersizerS data*

Figure 6.6 illustrates the volume-based mass mean diameter ($D[4,3]$) as it has been recorded by using the MastersizerS.

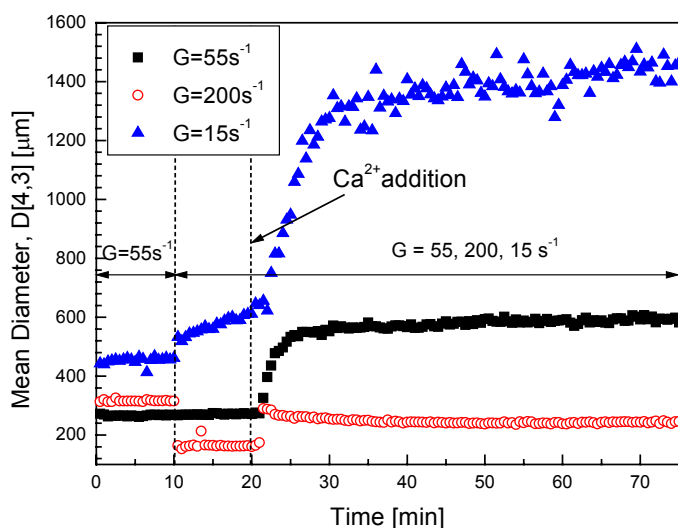


Figure 6.6. Average velocity gradient influence on the floc size dynamics measured with the MastersizerS device

As already discussed (Figure 6.3) small variations were observed in the initial floc size recorded under similar operations conditions. It is assumed however that these will not have a significant impact on the observed behaviour of the flocs when different average velocity gradient values were imposed.

$$G = 200 \text{ s}^{-1}$$

For $G=200 \text{ s}^{-1}$ an almost instant ($\sim 30 \text{ s}$) flocs breakup occurred with a decrease in the mean diameter from $316.38 \pm 2.97 \text{ }\mu\text{m}$ to $165.27 \pm 11.65 \text{ }\mu\text{m}$. The calcium addition created a partial reflocculation of the flocs. In the first few minutes after calcium addition a slight tendency to form somewhat larger flocs was observed, but very quickly a steady state floc size was reached with the average mean diameter $D[4,3]=245.99 \pm 8.81 \text{ }\mu\text{m}$.

Biggs (2000) quantified the regrowth behaviour of flocs after breakage by using the so-called recovery factor. For the analysed case, it was observed that calcium addition created a partial restructuring effect of the flocs even under high mixing intensity conditions. The recovery factor (RF) was used here to calculate the ability of the flocs to regrow after calcium addition. The recovery factor is defined as:

$$RF = \frac{(d_3 - d_2)}{(d_1 - d_2)} * 100 \quad (6.1)$$

where: d_1 - floc size before average velocity gradient is increased ($d_1 = 316.38 \pm 2.97 \text{ }\mu\text{m}$);

d_2 - floc size after average velocity gradient is increased ($d_2 = 165.27 \pm 11.65 \text{ }\mu\text{m}$);

d_3 - floc size after calcium addition ($d_3 = 245.99 \pm 8.81 \text{ }\mu\text{m}$)

A recovery factor of 53.41% was found suggesting a high affinity of the flocs for aggregation in the presence of calcium even when a high degree of turbulence was applied. Hence, floc

breakage and aggregation can occur simultaneously. However, an equilibrium in floc size was quickly reached, which is believed to be related to the strength of the flocs and occurs when the shear rate equals the floc strength.

$$G = 55 \text{ s}^{-1}$$

For $G=55 \text{ s}^{-1}$ the first 20 minutes showed a very small flocculation effect, which occurred by keeping the conditions in the vessel constant. The calcium addition, however, created a fast increase in the floc size for approximately 15 minutes. After this time, a slow continuation of flocculation with a slope similar to the one observed before calcium addition was obtained (Figure 6.7). Such a trend was also observed by Biggs (2000) concluding that the steady-state floc size has not been reached within the duration of the experiment. The observed slow increase in floc size suggests that the effect of calcium is limited to the fast increase in floc size observed during the first 15 minutes after calcium addition. The slow flocculation that occurred afterwards is attributed to the imposed conditions in the vessel and especially due to the G value which may be clearly observed from the almost identically slope values calculated for the observed flocculation trend before and after calcium addition (Figure 6.7).

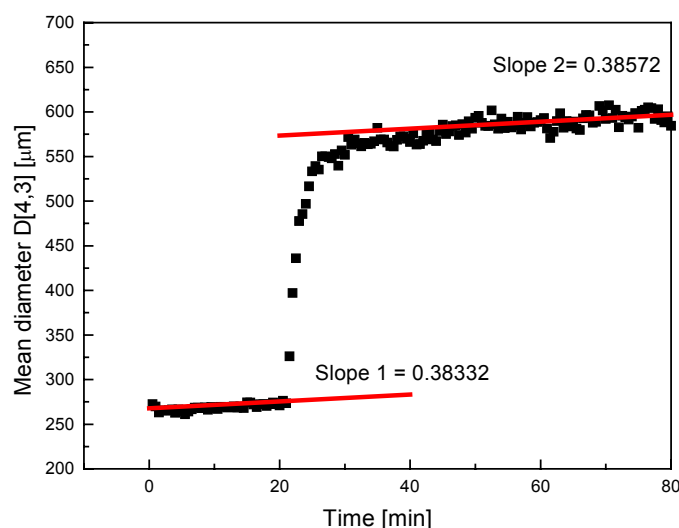


Figure 6.7. Quantification of the flocculation trend observed before and after calcium addition for an experiment performed for the design central point ($G=55\text{s}^{-1}$)

$$G = 15 \text{ s}^{-1}$$

At $G=15 \text{ s}^{-1}$ a continuous tendency of increasing floc size was observed for the recorded 10 minutes without calcium addition. Low mixing intensities together with calcium addition created very large flocs with the mass mean diameter increasing from $453.06 \pm 11.67 \mu\text{m}$ to $1415.7 \pm 46.65 \mu\text{m}$. As for the case of $G = 55 \text{ s}^{-1}$ the flocculation trend was observed as well before and after calcium addition but this time it seems to be more evident (Figure 6.6). Accordingly, it is clearly seen that small G values favour the flocs aggregation process.

To explain the floc breakage mechanism in turbulent flow the floc size is often evaluated relative to the Kolmogorov microscale. The Kolmogorov microscale describes the size of eddies formed as a result of the power input to a fluid and is calculated using the average turbulent dissipation rate (ϵ) and the kinematic viscosity of the system ($\nu=1.139\text{e}^{-6}\text{m}^2/\text{s}$ at 15°C) as given by equation (6.2).

$$\eta = \left(\frac{v^3}{\varepsilon} \right)^{\frac{1}{4}} \quad (6.2)$$

According to Thomas et al. (1999) for flocs smaller than the Kolmogorov microscale viscous forces predominate and erode the surface of the flocs. For the flocs larger than the Kolmogorov microscale floc fracture occurs as a result of dynamic pressure. The values of the η calculated for the G values imposed in these experiments as compared with the volume-based average diameters representing 10%, 50% and respectively 90% of the particles size is presented in Figure 6.8. The average diameters were calculated as average of 10 minutes measurements when different values of G were imposed and before calcium addition.

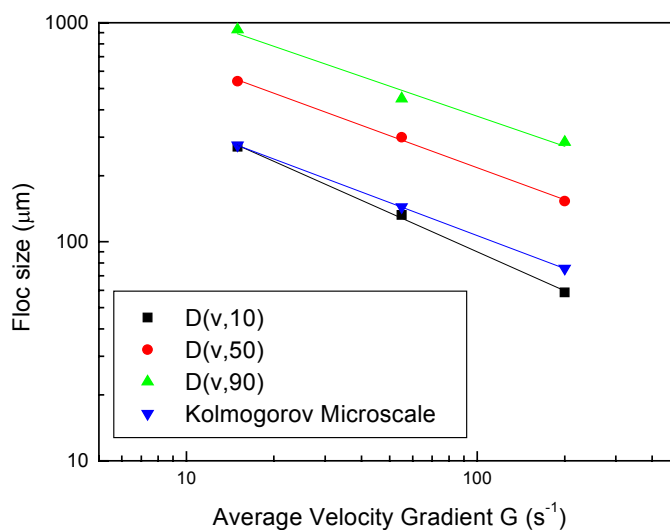


Figure 6.8 Volume based average diameters ($D(v,10)$; $D(v,50)$ and $D(v,90)$) function of the different average velocity gradient values and Kolmogorov Microscale

Figure 6.8 shows that only approximately 10% of the flocs size are smaller than Kolmogorov microscale. It may therefore be assumed that the fracture is the dominant breakage mechanism of the flocs.

6.3.1.2. *Image analysis data*

An evaluation of the above results was also possible by a direct visualisation of the floc size dynamics under the microscope. This was done automatically by using IMAN as previously described in Chapter 3. Figure 6.9 shows the floc size evolution under the effect of G. When average velocity gradient increased from 55 s^{-1} to 200 s^{-1} (Figure 6.9– top) the formed flocs becomes smaller, which is in agreement with the floc size evolution recorded with MastersizerS. By decreasing the average velocity gradient from 55 s^{-1} to 15 s^{-1} (Figure 6.9 – bottom) the formation of very large flocs was observed.

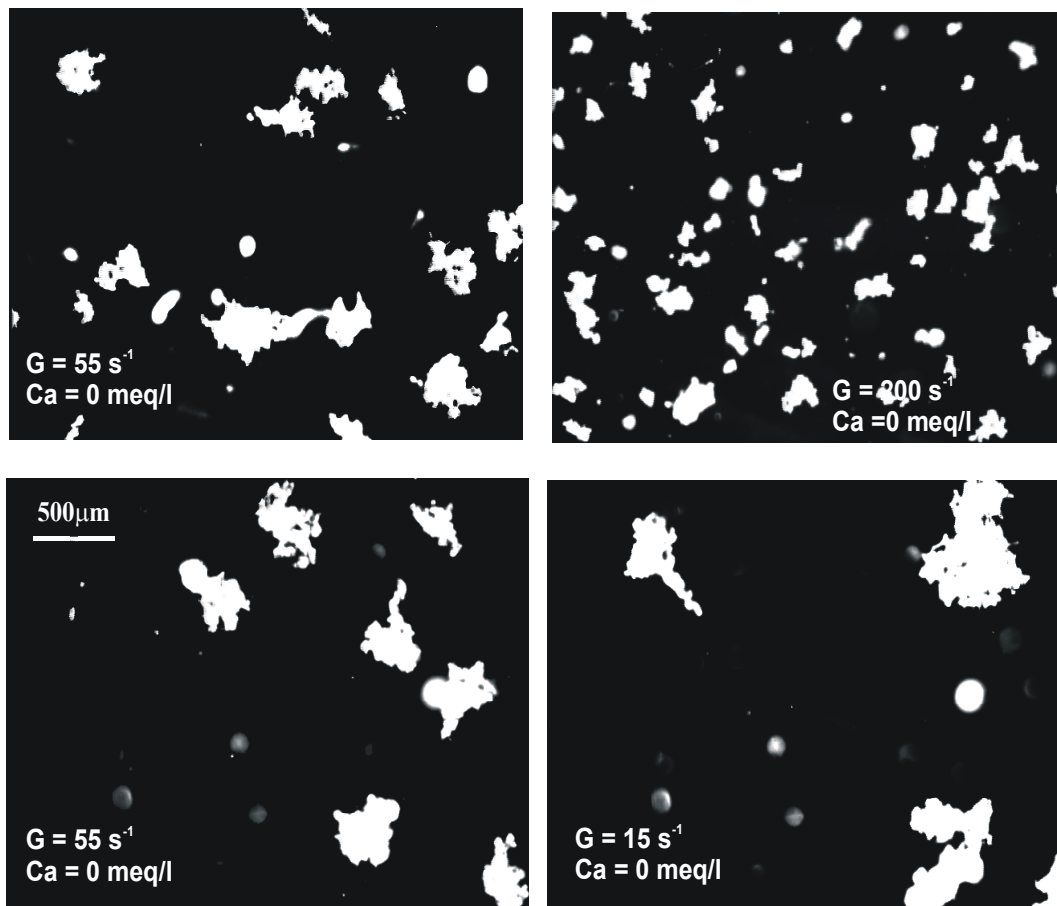


Figure 6.9. Microscopical evaluation of the average velocity gradient effect on flocs by using IMAN. The effect of increasing G is shown at the top (from 55s^{-1} – left to 200s^{-1} -right). Bottom G decrease from 55s^{-1} (left) to 15s^{-1} (right).

6.3.1.3. CIS-100 data

The TOT method was used as discussed in Chapter 3 to evaluate the floc number dynamics. Figure 6.10 shows the absolute number of flocs counted for each measurement by using the same time step as for the data collected with MastersizerS.

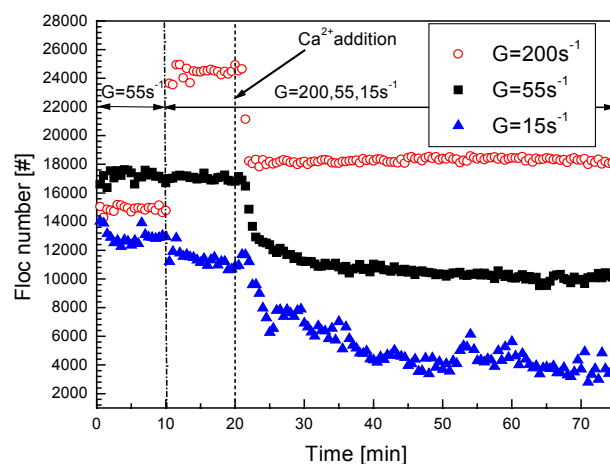


Figure 6.10. The floc number dynamics as function of the different average velocity gradient conditions. Results obtained with the CIS-100 device (TOT method)

Comparison with Figure 6.6 indicates that the floc number dynamics shows a good correlation with the floc size dynamics. These observations confirm that the floc number concentration decreases with increasing floc size. A similar trend was observed by Wahlberg et al. (1994) by investigating the changes in supernatant turbidity over time as flocculation took place. The similarity in results obtained with the different sizing devices provides a strong confirmation of the correctness of the results and also of the devices' capability to detect the fast changes that occur in floc size as the process proceeds.

6.3.1.4. *Floc size distribution*

It is of high interest to have not only a global evaluation of the floc size dynamics but to look at the floc size distribution itself as well, as it can give more insights in the particles frequency in each size class. To illustrate this, the experiments performed at $G = 200 \text{ s}^{-1}$ have been selected as an example, since in this case both aggregation and breakage phenomena were recorded. Therefore, by looking to the FSD it becomes possible to observe the disturbing and restructuring process of the flocs as it occurs in different size classes.

Figure 6.11 shows the average velocity gradient effect on the volume-based FSD. In general (Figure 6.11-left), the FSD shows that the large particles have the highest volume contribution, which shifts to smaller floc size when G increases to 200 s^{-1} . Flocs reaggregated when calcium was added.

Investigation of the evolution of the small size range particles represents an important step in the understanding of the flocculation mechanisms and the effectiveness of the clarification step. A detailed look at the small size classes evolution (Figure 6.11-right) shows a very broad floc size distribution with a tendency to form a three-modal distribution. The major volume contribution was observed for particles larger than $100 \mu\text{m}$. A significant contribution was also given by the flocs of $10\text{-}100 \mu\text{m}$. This is in agreement with Parker et al. (1971) who found a very wide size range of particles from $10 \mu\text{m}$ up to $5000 \mu\text{m}$ which were classified as flocs, and a very narrow band of primary particles of $0.5\text{-}5 \mu\text{m}$. The latter size range is however, difficult to be correctly evaluated due to limitations of the device in measurement of small particles (see Chapter 3).

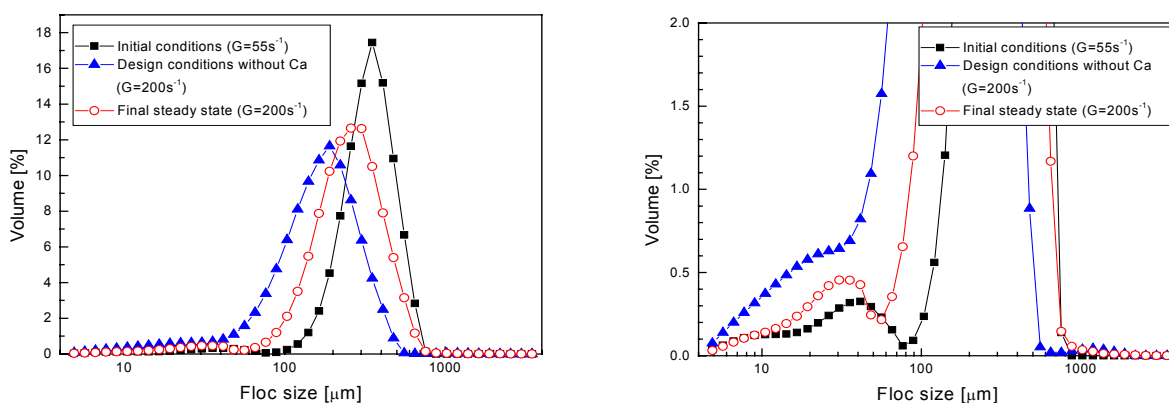


Figure 6.11. The volume-based floc size distribution (FSD) for the experiment performed at $G=200 \text{ s}^{-1}$ (left) and a detailed view of the small size particles evolution during the same experiments (right). Experiments were recorded with Mastersizer S.

When number distributions obtained with the CIS-100 device are evaluated, tri-modal distributions have been observed as well (Figure 6.12). Again, due to the limited size detection range of the device, flocs smaller than $10 \mu\text{m}$ could not be quantified. Also, a slight

increase in the size range was observed which is due to the different measurement principles as discussed in Chapter 3.

Figure 6.12 shows that the larger size flocs have the highest sensitivity to shear. In this respect, Jorand et al. (1995) suggested a structural floc model, which contains three structural levels i.e. microflocs (2.5 μm), secondary particles (13 μm) linked together by exopolymers and forming tertiary structures having a mass mean diameter of 125 μm . The later particles are the most sensitive to the shear forces. Even though differences in floc size occurred due to the different treatment procedure, the observed results show a noticeable agreement with the structural model of Jorand et al. (1995). As shown in Figure 6.12 (right) the number of the large flocs reduced significantly at high average velocity gradient. Addition of calcium reinforces the flocs' structure, showing an almost reversible regrowth effect of the middle size floc range and also the reformation of the larger flocs.

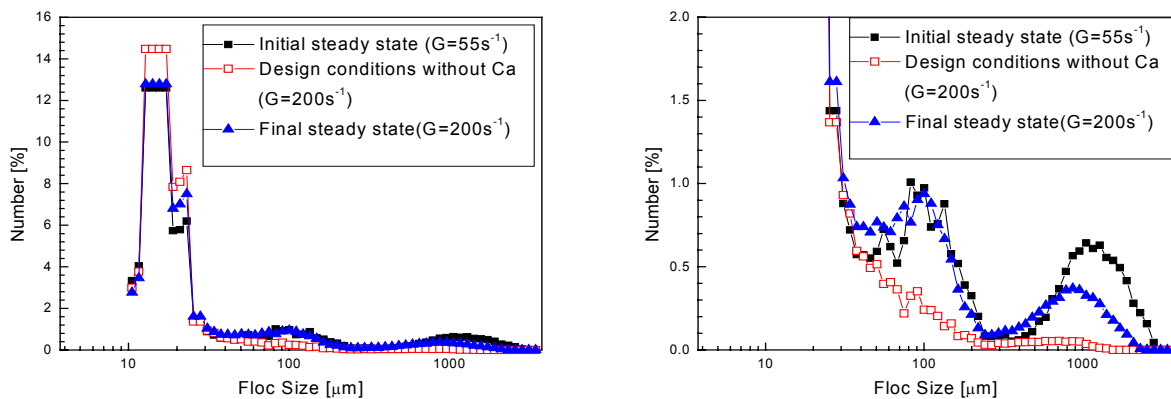


Figure 6.12. The number-based floc size distribution for the experiment performed at $G=200 \text{ s}^{-1}$ (left) and a detailed view (right) of the small size particles evolution during the same experiments. Measurements were recorded with CIS-100.

6.3.1.5. Conclusions

The effect of average velocity gradient on the flocculation dynamics was investigated in this section. Increasing the average velocity gradient resulted in a decrease in floc size and increased the rate at which the steady-state floc size distributions are reached. Calcium addition at high average velocity gradient reinforced the floc structure allowing the flocs to reaggregate. A restructuring factor of 53.41% was found.

At middle and low average velocity gradient values (55 s^{-1} and respectively 15 s^{-1}) the aggregation process dominated, creating a continuously increasing trend in the floc size. Again calcium addition had a beneficial effect, showing a very large floc size formation at a low average velocity gradient.

It was found that the particle number concentration decreased with increasing floc sizes. Different techniques were used for quantifying the flocculation. The techniques showed to be fast enough and complemented each other very well, providing an accurate overview of the floc size dynamics as well as a visual examination, thanks to the automatic image analysis system.

6.3.2. Activated sludge concentration

The effect of the activated sludge concentration on floc size dynamics was evaluated for the design axial points and compared with the central point experiment. Accordingly, the results of a sludge concentration of 0.1 g/l, 0.63 g/l and 4 g/l will be further described in this paragraph. The other operational conditions were kept constant at the nominal value given by the central point design ($G = 55 \text{ s}^{-1}$, $T=15^\circ\text{C}$, $\text{Ca} = 12 \text{ meq/l}$, $\text{DO} = 2 \text{ mg/l}$).

The sludge concentration has a less significant effect on the floc size dynamics (Figure 6.13) in comparison with the fast increase in floc size created by calcium addition or with the breakage and aggregation effects created by average velocity gradient variation. Due to this, the obtained results will only be briefly shown and discussed. A detail evaluation as that performed for the average velocity gradient was considered not to be relevant.

At a sludge concentration of 0.1 g/l, the experiments were performed by recirculating the sludge into the reactor since this concentration corresponded to the required dilution level of the sizing devices. This approach was adopted because wasting the sludge at this low concentration only allows a very short experiment time (less than 20 min.) due to the fast consumption of the sludge.

Under stable initial conditions at low sludge concentration (0.1 g/l), a slight and permanent decrease of the flocs mass mean diameter was observed. This observed breakage effect is assumed to be due to the supplementary stress created by the recirculation. A similar behaviour was observed on the floc numbers counted with the CIS-100 (Figure 6.14).

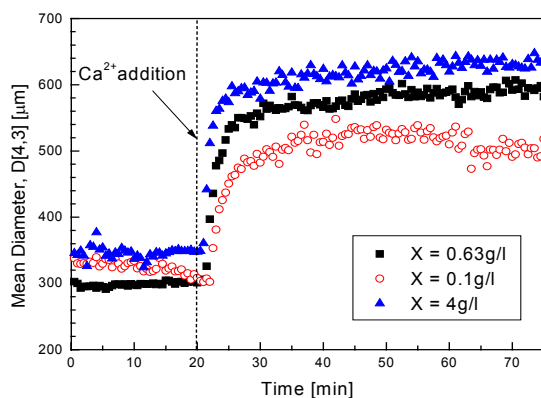


Figure 6.13. The effect of activated sludge concentration on floc size dynamics. Measurements performed with MastersizerS

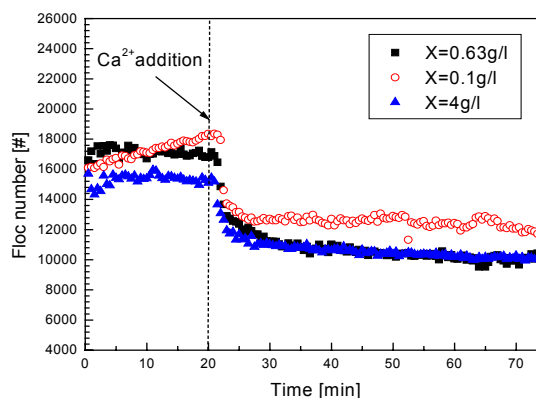


Figure 6.14. The flocs number dynamics function of activated sludge concentration. Measurements performed with CIS-100

A similar decreasing tendency in floc size was also observed after the direct effect of calcium addition had vanished (Figure 6.15). Examining the floc number evolution (Figure 6.14) the disturbing effect is less pronounced. It is therefore hypothesised that since the variations observed in the floc size were relatively small, the changes in particles numbers were less pronounced as well. Accordingly, due to the very limited counting time (30 s) it may be that not enough particles were counted to generate very precise results. This may explain as well why the number dynamics trend showed very close results for $X = 0.63 \text{ g/l}$ and $X = 4 \text{ g/l}$. When the results obtained with the CIS-100 were transformed to volume distributions the decreasing trend of the mass mean diameter can be clearly observed (Figure 6.16) and is in agreement with the trend indicated by MastersizerS (Figure 6.15).

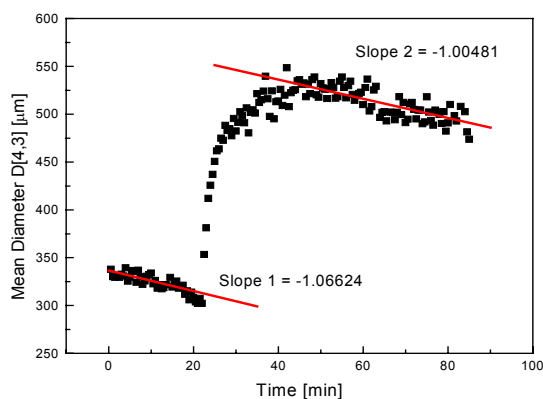


Figure 6.15. The disturbance effect created by recirculation of sludge in the reactor. Measurements performed with MastersizerS

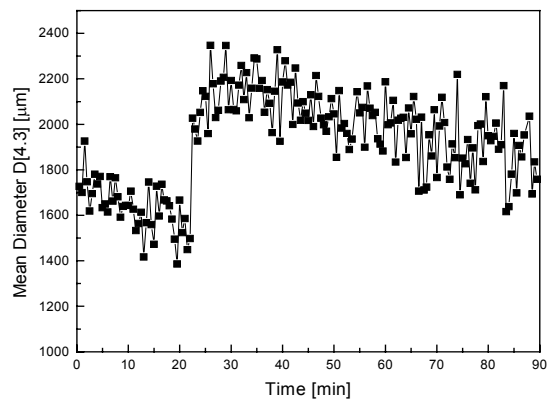


Figure 6.16. The disturbance effect created by recirculation of sludge in the reactor. Measurements performed with CIS-100

It should be mentioned that the disturbing effect produced by recirculation was not observed in the previous experiments performed with smaller sample volumes and for smaller floc sizes. Moreover, for a similar experiment Biggs (2000) did not report any disturbances created by sludge recirculation. Consequently, it seems that the experimental conditions and floc size may have a contribution to the observed phenomena as well.

The experiments performed at higher solids concentration ($X = 0.63$ g/l and $X = 4$ g/l) indicated a similar behaviour of the floc size. However, a tendency to form larger floc sizes at higher sludge concentrations ($X = 4$ g/l) was observed. This is consistent with De Clercq (2003) who observed that the higher flocculation rate occurred in secondary settling tanks at increased sludge concentration. Calcium addition led to a very closed size range for both investigated sludge concentrations. This can be seen as a saturation effect of the calcium leading to the maximum floc size that can be reached for the imposed conditions in the vessel.

In summary, the activated sludge concentration showed a less significant effect on the floc size as compared with other factors such as average velocity gradient and calcium addition. A tendency to form larger flocs at higher solids concentration was observed. Moreover, the collision rate between the particles increased with sludge concentration creating a faster reaching of equilibrium between aggregation and breakage rate. However, due to the limited number of experiments taken into consideration, a complete evaluation of the sludge concentration effect and its relation with other sludge properties will be further evaluated by analysing the complete experimental design.

6.3.3. Calcium concentration

The effect of the addition of 12 meq/l and 24 meq/l calcium on floc size is quantified in this paragraph and compared with the activated sludge flocculation behaviour when no calcium was added in the reactor. The other factors were kept constant at the values corresponding to the central point of the DOE.

As shown in Figure 6.17, the addition of calcium had a very fast floc aggregation effect. For the highest calcium concentration ($Ca = 24$ meq/l), the size of the flocs increased almost instantaneously indicating a very fast aggregation process. Apparently, as the flocs size increased, breakage became dominant and the floc size stabilized. It was observed that the increase in floc size was not directly proportional with the amount of calcium added to the system and the flocs tend to stabilise at a relatively similar size range (589.77 ± 7.97 µm for 12 meq/l Ca^{2+} and 623.18 ± 8.28 µm for 24 meq/l Ca^{2+}). It is hypothesised that the flocs were

saturated with calcium ions at a certain level. The observed behaviour of the sludge may also be related to the flocs' strength, which can reach a maximum floc size under the imposed conditions in the vessel.

However, looking at the trend of the floc size dynamics, two distinct processes seemed to take place. The first is a rapid process (2-3 minutes) in which the flocs responded quickly to the changes in operational conditions and this is directly proportional with the rate of influence that especially calcium addition has. The second is a slow (tens of minutes) process in which the flocs start to adapt to the new operational conditions and the tendency is that flocs become stronger and increase in size. A similar behaviour in floc size dynamics was observed by Biggs et al. (2000). For the experiment performed without calcium addition, the fast process does not take place and just the slight aggregation trend is visible. As shown in section 6.3.1. this trend is mostly due to the imposed average velocity gradient ($G=55 \text{ s}^{-1}$), which facilitates the aggregation process.

A good correspondence between the floc size dynamics recorded by using MastersizerS (Figure 6.17) and the total number of flocs counted by the CIS-100 device (Figure 6.18) was observed again.

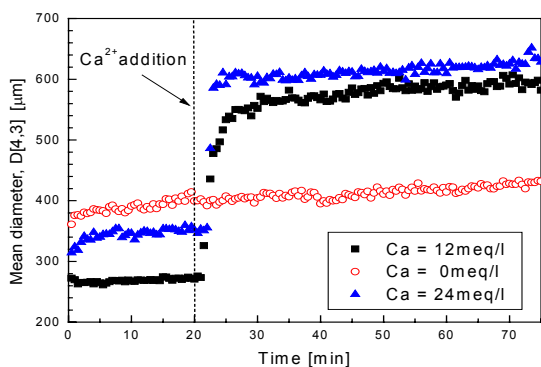


Figure 6.17. The influence of calcium on floc size dynamics. Measurements performed with MastersizerS

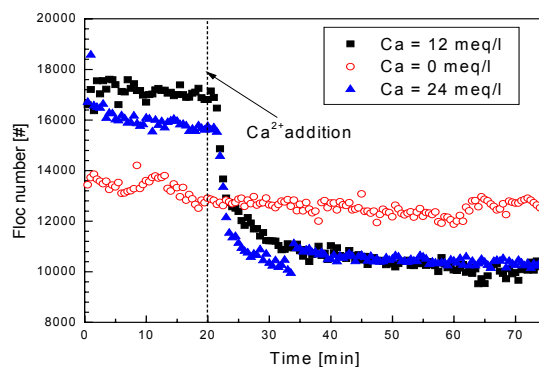


Figure 6.18. The flocs number dynamics as function of calcium addition. Measurements performed with CIS-100

From the volume-based floc size distributions recorded during the experiments performed without calcium addition (Figure 6.19) and with 24 meq/l Ca^{2+} (Figure 6.20) it can be clearly seen that calcium produced a complete shift of the distribution towards larger floc sizes.

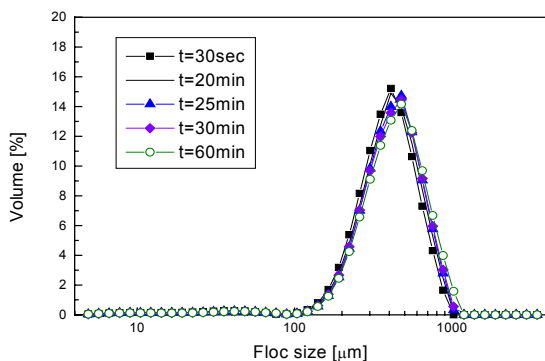


Figure 6.19. The floc size distribution evolution for the flocculation experiment without calcium addition. Measurements performed with MastersizerS

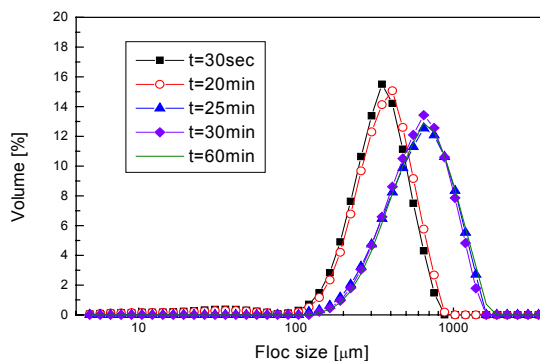


Figure 6.20. The floc size distribution evolution for the addition of $\text{Ca} = 24 \text{ meq/l}$. Measurements performed with MastersizerS

6.3.3.1. The calcium effect on different activated sludge samples

The effect of cations on bioflocculation is widely discussed and interpreted in literature. Sustaining the DCB mechanisms, the research studies performed by Novak and his collaborators (Higgins and Novak, 1997- a,b,c; Novak et al., 1998; Sudhir and Novak, 2001) showed that for optimal process performance in terms of activated sludge settling and dewatering, a ratio of sodium to divalent cations smaller than approximately two is desirable. Moreover, the same authors showed that even if a small short-term improvement was observed in settling characteristics of the sludge after cations addition, an effective process could only be obtained by cation additions in the feed. However, Novak et al. (1999) mentioned that batch tests do not provide a realistic view on the effect of cations in the influent and that for a more precise evaluation of the cation effect on activated sludge the cations must be considered individually. The short-term effect of increased calcium concentrations (up to 10 meq/l) on the physical structure of activated sludge flocs was studied by Cousin and Ganczarzyk (1999). A ratio $\text{Ca}^{2+}:\text{Na}^+ \geq 1$ created an increase of the floc size while for a ratio $\text{Ca}^{2+}:\text{Na}^+ < 1$ the calcium addition caused sludge deflocculation with significantly more smaller size flocs.

It is, however, concluded that a balance between monovalent and divalent cations and especially between calcium and sodium ions present into the system is highly important for good process performance. Since in all experiments performed with SBR sludge the flocculation effect created by calcium addition was significant, it may be of interest to compare these results with those obtained when another sludge sample characterized by a different cations $\text{Ca}^{2+}:\text{Na}^+$ ratio was used.

Accordingly, a supplementary experiment with a sludge sample taken from the Ossemeersen Wastewater Treatment Plant (WWTP) located in Ghent, Belgium was performed. The experimental conditions were identical to the central point experiment in which 12 meq/l Ca^{2+} was added after 20 minutes of recording the initial floc size evolution. The effect of calcium on floc size clearly showed that for this WWTP sludge sample calcium addition did not have the same fast increase in floc size (Figure 6.21). However, a small increasing trend in floc size is observed corresponding with the slow process observed for the SBR sludge and which is believed to be mostly due to the conditions imposed in the vessel.

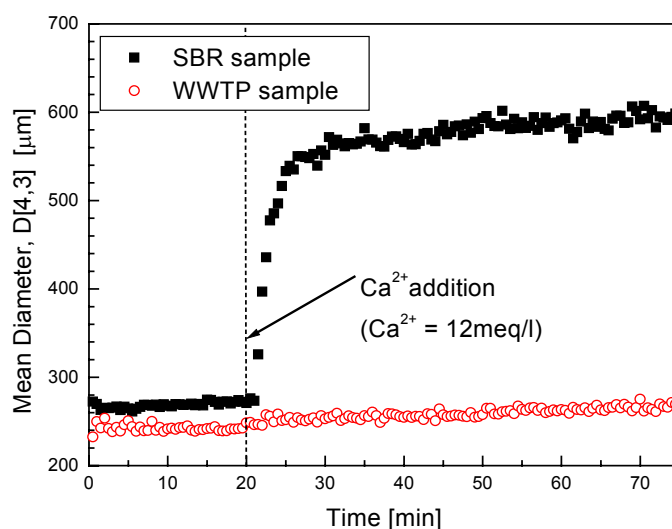


Figure 6.21. The effect of calcium addition on floc size dynamics for different activated sludge samples

In addition to the measurements performed with the MastersizerS, the microscopical observations recorded by using IMAN showed the same effects. For the SBR sludge a visible increase in the floc size is observed (Figure 6.23 -top). The sludge sample from the WWTP did not show much difference in floc size before and after the calcium addition (Figure 6.23 -bottom).

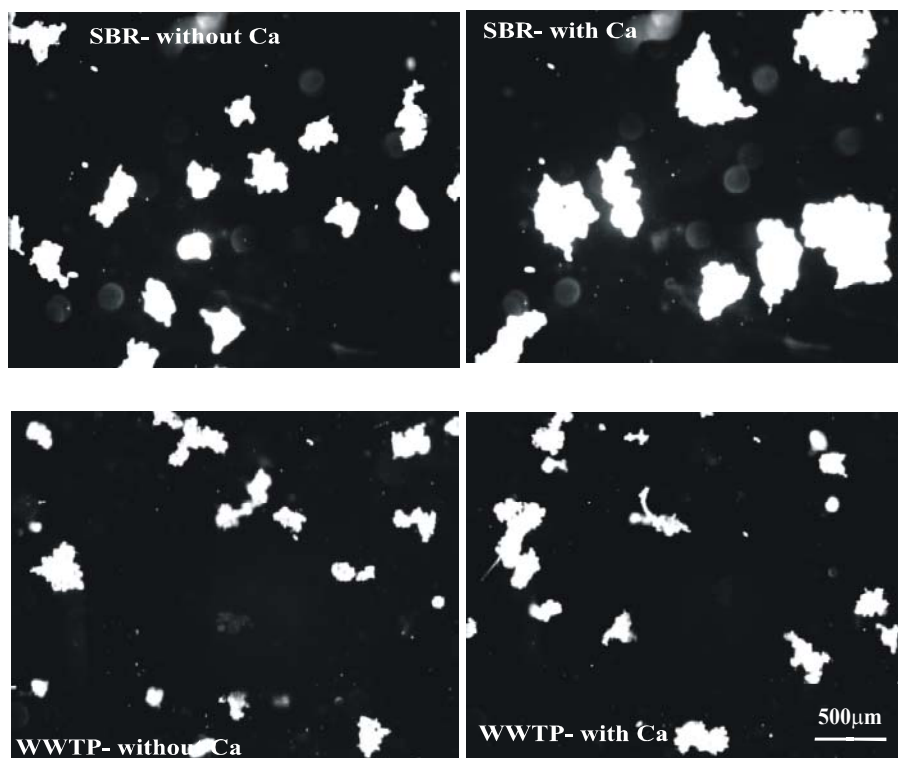


Figure 6.22. Microscopical evaluation of the calcium addition effect for sludge samples from the SBR (top) and the WWTP (bottom)

The observed difference in effect of calcium on flocculation can possibly be explained by the difference in initial cation content of the sludge samples. The SBR sludge sample contains a very little calcium and has an excessively high sodium content giving a very low ratio $\text{Ca}^{2+}:\text{Na}^+ = 0.0167$. By contrast, the sludge sample from the Ossemeersen WWTP contained higher calcium concentration with ratio $\text{Ca}^{2+}:\text{Na}^+ = 0.4944$ (Table 6.1).

Table 6.1. Initial cation concentrations for different sludge samples

SBR				Ossemeersen WWTP			
Ca^{2+} (meq/l)	Na^+ (meq/l)	K^+ (meq/l)	$\text{Ca}^{2+}:\text{Na}^+$	Ca^{2+} (meq/l)	Na^+ (meq/l)	K^+ (meq/l)	$\text{Ca}^{2+}:\text{Na}^+$
0.1562	9.3351	0.2543	0.0167	2.6153	5.2890	0.6082	0.4944

The low calcium content of the SBR sludge could explain the high affinity of this sludge sample for calcium and the fast and important increase in floc size. On the contrary, for the case of the Ossemeersen WWTP sludge sample a saturation with calcium ions apparently occurred and any calcium addition did not create any supplementary effect.

To further evaluate the effect of calcium addition on the process performance for the two considered sludges, the zeta potential, the SVI and the supernatant suspended solids concentration were compared (Table 6.2). It is seen for the SBR sludge sample that calcium

addition created a significant process improvement. In contrast, for the WWTP sludge sample no major changes occurred in its characteristics.

Table 6.2. Supernatant and sludge characteristics before and after the flocculation experiment

Parameter	SBR		Ossemeersen WWTP	
	Initial	Final	Initial	Final
Zeta Potential (mV)	-23	-2	-14	-11
SVI (ml/g)	172.72	117.77	82.83	81.32
Supernatant SS (g/l)	0.0405	0.0193	0.0292	0.0275

By investigating the calcium effect on flocculation dynamics the behaviour was observed to depend on the initial cation content of the sludge. It is therefore important to choose the most appropriate cation, which may create a fast improvement of the process. Since at this stage only the calcium addition was investigated it is hard to conclude whether the addition of a monovalent cation will create the same effect. It is also suggested that there is a saturation level of the solution with respect to the calcium ions. Any further addition will be regarded as an excess and will not create an improvement of the flocculation properties.

6.3.3.2. Evaluation of the calcium dynamics by using t_{95}

As mentioned above two different processes could be observed in the floc size dynamics when calcium was added to the system.

- A fast size-increasing process, which is assumed to be mainly due to the calcium added.
- A slow process which in most of the cases was found to show the same rate as in the period before the calcium addition.

In order to quantify the calcium effect, the fast process is further investigated. However, it should not be completely neglected that the other considered factors may also affect this process dynamics. To quantify this fast process, the time in which the floc size reached 95% of the final steady state size was used. The final steady state is taken into consideration here as being the size in which the fast process virtually vanishes and the trend of the floc size dynamics is similar with the one observed before calcium addition.

In the evaluation of the calcium effect the average velocity gradient also showed to have a strong influence. Two distinct floc size dynamics have been observed after calcium addition depending on the imposed average velocity gradient. For relatively low average velocity gradients (15 s^{-1} ; 29 s^{-1} and 55 s^{-1}) the floc size dynamics showed an exponential trend which may be described by a first order process (Figure 6.23 -left). For high average velocity gradients (105 s^{-1} and 200 s^{-1}), the process seemed to be much more complex and difficult to be described by a first order process. Comparing the floc size trend observed before and after calcium addition it can be seen that the fast aggregation process is followed by a slight deflocculation process of the flocs formed due to the calcium addition (Figure 6.23-right the circled region) until an equilibrium between aggregation and breakage is achieved in the reactor and the floc size reaches steady state.

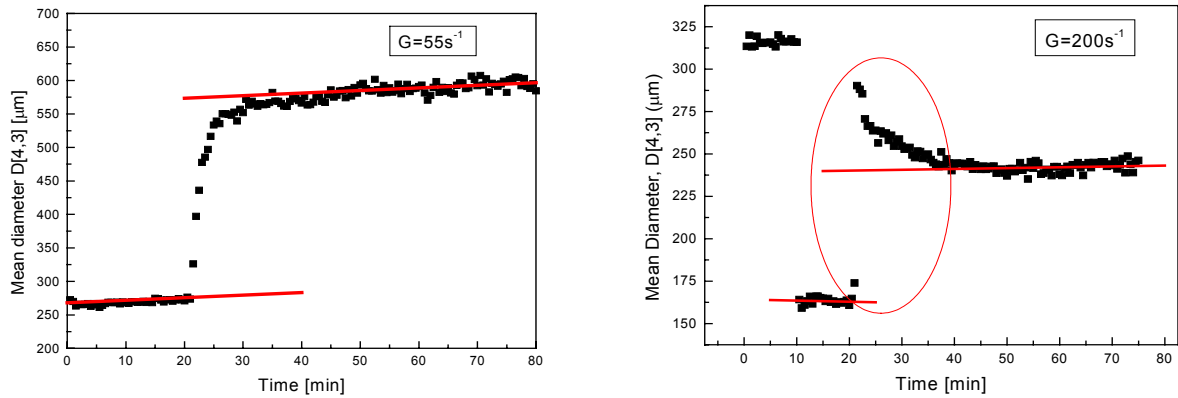


Figure 6.23 The calcium addition effect at $G = 55 \text{ s}^{-1}$ (left) and $G = 200 \text{ s}^{-1}$ (right)

Calcium effect (t_{95}) at low average velocity gradient values

For the case of the distributions showing an exponential trend, equation (6.3) was used to evaluate the characteristic time (t_{95}).

$$X(t) = X_0 + (X_f - X_0) \left[1 - e^{-\alpha(t-t_0)} \right] \quad (6.3)$$

where: $X(t)$ is the floc size at time t ; X_0 is the floc size at the initial time t_0 and X_f is the floc size at final time t_f calculated from the initial and final limit conditions as presented in equation (6.4) and equation (6.5). α is the inverse time constant of the process and is extracted by least square fitting.

$$t = t_0 \Rightarrow X(t_0) = X_0 \quad (6.4)$$

$$t = \infty \Rightarrow X(t) = X_f \quad (6.5)$$

The code of the Matlab program used for calculating t_{95} is listed in Appendix 6.1. From equation (6.3) the t_{95} parameter is extracted by imposing the following condition:

$$X(t_{95}) = 0.95 * (X_f - X_0) \quad (6.6)$$

An example of fitting the exponential equation to experimental data obtained from a central point experiment is given in Figure 6.24. The slow flocculation trend observed in the floc size dynamics was not considered for t_{95} evaluation since, as shown before, it doesn't represent a direct consequence of calcium addition and occurs probably due to the low average velocity gradient conditions.

Calcium effect (t_{95}) at high average velocity gradient values

For the cases in which calcium was added under high average velocity gradient conditions, the time constant of the process is very short and cannot be reliably captured by the measuring frequency (30 s) used in the experiments. Consequently, the fast effect of calcium addition is simply represented by a step change ($\Delta X = X_t - X_0$) of the mean diameter $D[4,3]$, as in equation (6.7).

$$\begin{aligned}
 X(t) &= X_0, \quad t < t_0 \\
 X(t) &= X_1 + (X_f - X_1) \left[1 - e^{-\alpha(t-t_0)} \right], \quad t \geq t_0
 \end{aligned}
 \tag{6.7}$$

where X_f is the floc size at the time when the maximum floc size after the calcium addition is reached.

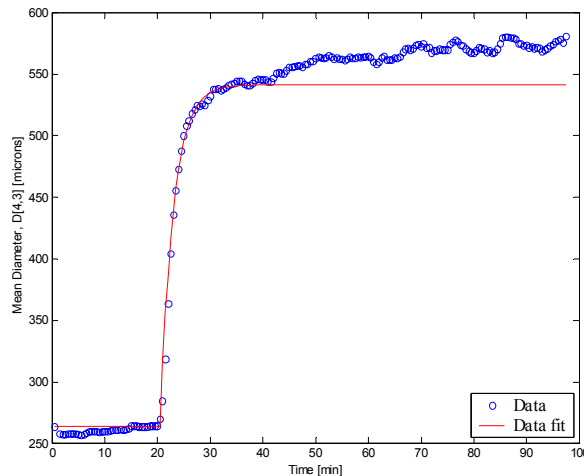


Figure 6.24 t_{95} evaluation for an experiment performed according to the central point design ($G = 55 \text{ s}^{-1}$; $X = 0.63 \text{ g/l}$; $T = 15^\circ\text{C}$; $\text{DO} = 2 \text{ mg/l}$; $\text{Ca}^{2+} = 12 \text{ meq/l}$)

In this case, t_{95} represents the time after which the mean diameter has returned 95% of the overshoot over the steady-state diameter.

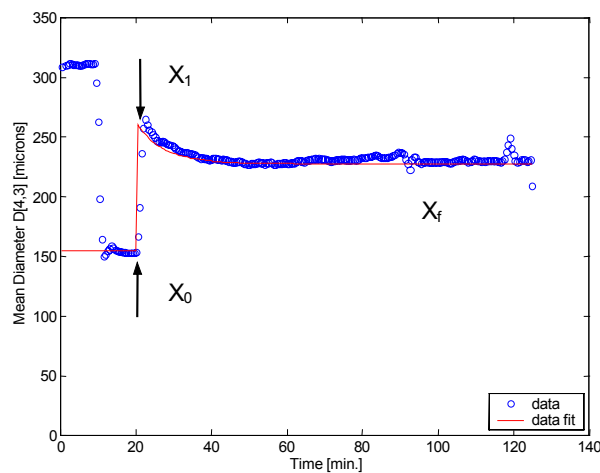


Figure 6.25 t_{95} evaluation for an experiment performed under high average velocity gradient ($G = 200 \text{ s}^{-1}$, $X = 0.63 \text{ g/l}$; $T = 15^\circ\text{C}$, $\text{DO} = 2 \text{ mg/l}$, $\text{Ca}^{2+} = 12 \text{ meq/l}$)

When t_{95} was evaluated for the experiments performed at low average velocity gradient, it can be clearly seen that the flocculation rate increased with the amount of calcium added (Figure 6.26). It should be noticed that the other imposed factors may play a role on the dynamics as well and this can explain the observed scatter among the t_{95} . However, an evaluation of the dependency of t_{95} to the other factors showed no clear correlation suggesting that the fast process was only dependent on the calcium addition into the system.

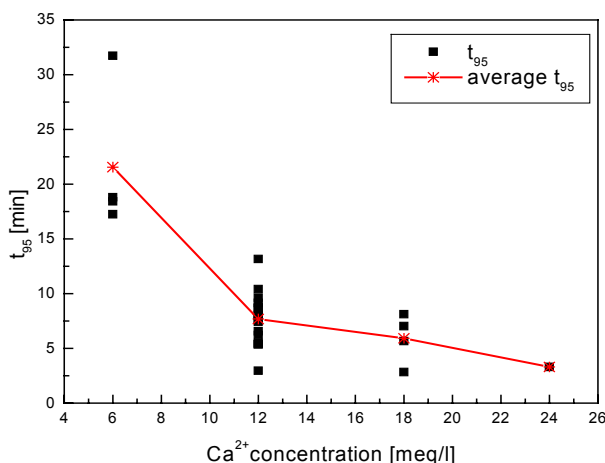


Figure 6.26 The effect of calcium addition on the flocculation process at low average velocity gradient, evaluated by t_{95}

When the effect of calcium was investigated for high average velocity gradient values, the t_{95} values are very close to each other and the floc size changes which occur due to the calcium addition are in the order of a few minutes (2-3 minutes). The calculated values for t_{95} are listed in Table 6.3.

Table 6.3 t_{95} values obtained for the experiments performed at high average velocity gradient values

T (°C)	G (s ⁻¹)	Ca ²⁺ (meq/l)	DO (mg/l)	X (g/l)	t_{95} (min)
15	200	12	2	0.63	23.096
10	105	6	3	1.59	26.461
10	105	18	1	1.59	22.6
20	105	18	3	1.59	22.37
20	105	6	3	0.25	23.723
10	105	18	3	0.25	22.717
20	105	6	1	1.59	25.155
20	105	18	1	0.25	22.504
10	105	6	1	0.25	24.563

To conclude, a direct relationship between the time in which the fast aggregation process occurs and the amount of calcium added was found. Even if the increase in the final floc size was found to be not proportional to the calcium concentration the process dynamics seems to be directly related to the amount of calcium ions added into the system.

Finally, since two distinct floc size dynamics have been observed for calcium addition mainly depending on the imposed average velocity gradient values, a complete evaluation of the calcium effect, expressed as t_{95} , was difficult and therefore the conclusions should be restricted to the two observed cases.

6.3.4. Temperature

The effect of temperature on floc size dynamics was evaluated for a temperature range between 5°C and 25°C. In this paragraph, the floc size dynamics are investigated by considering the effect of the extreme temperatures (5°C and 25°C) as well as of a temperature of 15°C, which corresponds to the operational temperature of the SBR.

A floc size larger than the initial floc size was observed for the lowest temperature (5°C). At this temperature flocculation after calcium addition (Figure 6.27) continues for the entire measurement period. In contrast, the aggregation effect created by the calcium addition was followed by only a slight deflocculation tendency at 25°C. Moreover, the process dynamics showed that a faster aggregation due to calcium addition occurred for the experiment performed at 15°C ($t_{95}=7$ min). For the other temperatures the calcium addition resulted in a slower effect, with $t_{95}=13$ min at 25°C and 35 min at 5°C.

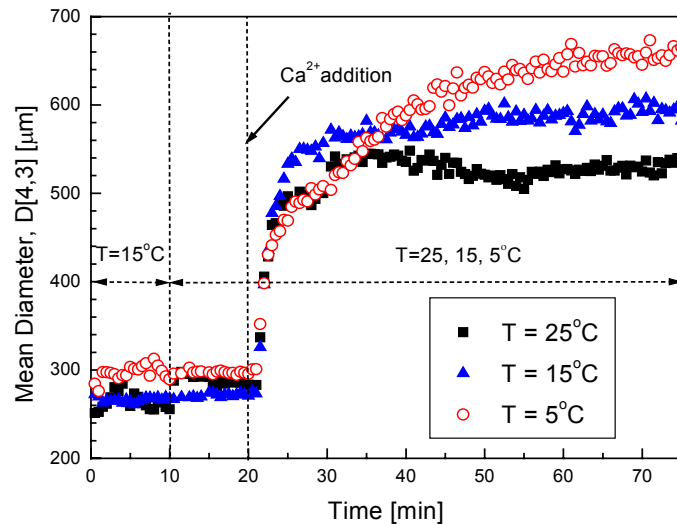


Figure 6.27. Temperature effect on activated sludge floc dynamics

A second experiment was performed in order to confirm the observed trend in floc size at different temperatures. It consisted in successive variations of temperature in the reactor while keeping the other parameters constant ($X = 0.63$ g/l; $G = 55$ s⁻¹ and DO = 2 mg/l). To avoid possible interactions, calcium was not added in this experiment. The evolution of the floc size was measured for 10 minutes for each of the cases (Figure 6.28). About 1 hour waiting time was used to reach the requested temperature in the vessel.

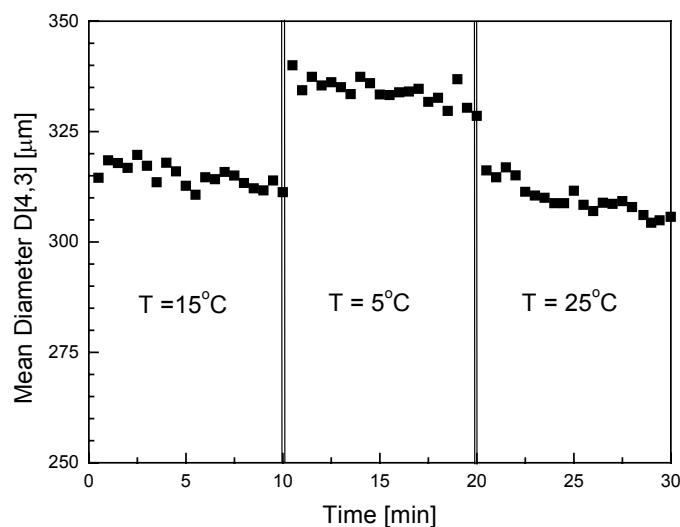


Figure 6.28. The effect of temperature on the floc size dynamics

Again, an increase in floc size was observed when the temperature inside the reactor was decreased to 5°C. Consistent with the Figure 6.27, a deflocculation effect was observed when the temperature was increased to 25°C.

Two hypotheses may explain the observed behaviour of the activated sludge at different temperatures.

The first hypothesis is related to a changes in viscosity. Changes in temperature may affect particles transport processes or particles collision rates due to viscosity changes, which affect the mixing energy in the reactor. When temperature increases, viscosity decreases, which may improve mixing. Looking at the average velocity gradient and shear rate history recorded in the log file with a frequency interval of about 17 s, only small differences have been observed among the average velocity gradient values recorded during the three experiments performed. The average velocity gradient values have been found to be: $G = 51.7 \text{ s}^{-1}$ ($T = 5^\circ\text{C}$); $G = 53.58 \text{ s}^{-1}$ ($T = 15^\circ\text{C}$) and $G = 54.20 \text{ s}^{-1}$ ($T = 25^\circ\text{C}$) respectively. The recorded differences between the applied average velocity gradient may be considered too small to explain the observed behaviour. In this context, Duan and Gregory (2003) mentioned that in case of the coagulation of hydrolysing metal salts in water, the system chemistry is more important and the different coagulation behaviours observed at 20°C and 5°C were related more to the floc strength and not to the turbulent flow field characteristics. Therefore, in the second hypothesis, the physico-chemical properties of the flocs as well as the biological activity were considered to explain the observed behaviour.

According to Wilén (1999), the activated sludge responds differently to various temperatures and this is function of the temperature at which the sludge was acclimatised.

In a similar context, Eikelboom (2000) showed that every microorganism has a specific temperature range for their growth and no growth is possible above the maximum temperature or below the minimum temperature. However, within this range the microbial activity and the growth rate increase as the temperature rises until the maximum is reached, after which the activity is reduced rapidly at further increase of the temperature. This may explain the faster aggregation effect observed due to the calcium addition, occurred at 15°C which represent the operating temperature of the SBR. However, it may be that the microbial growth and activity was still active when the temperature was lowered.

By contrast, Wilén (1999) reported that there is a clear short-term effect of temperature on the floc strength. It was suggested that the floc stability decreases at lower temperatures because the biochemical reaction rates are slower and thereby, also the production of EPS. Decreasing the floc stability may induce deflocculation via the flocs erosion process. However, this is not in agreement with the increases into the floc size observed for two of the experiments performed. Considering these observations to explained the observed floc size behaviour at lowering the temperature, its suggests that the microbial activity decreases gradually, being highly active in the beginning and trying to protect against the temperature shock effect. It is possible that during this period EPS are still produced, helping the flocs to aggregate and form the observed larger flocs. The slower aggregation effect and the capability of the flocs to form cation bridges when calcium was added to the system may explain the observed microbial activity behaviour. However, this fact represents just a hypothesis and needs to be validated by investigating the microbial community behaviour and the EPS production.

Studies performed at higher temperature showed that an increase of the temperature could affect the physical properties of the EPS (Sutherland, 1988) and for temperature variations from 20°C to 35°C the microbial community reacted selectively to the temperature changes (Pansward et al. 2003). Moreover, long-term monitoring of the effect of increasing

temperature by Krishna and van Loosdrecht (1999) revealed larger flocs and better settling properties of the sludge operated at 15-20°C as compared to 25°C. When the short-term effect of temperature was investigated by Wilén (1999) it was found that the activated sludge deflocculated substantially more than at lower temperature. This was also observed here when the reactor was operated at 25°C. Accordingly, the deflocculation effect observed when the temperature was increased to 25°C may indicate that the temperature reduced substantially the microbial activity of the microorganisms presents in the floc structure and therefore inhibited the microbial growth.

However, all the given explanations are just hypothesis which may possible explain the observed behaviour and should be considered accordingly. It seems that a high importance for explaining the short-term effect of temperature on flocculation dynamic is to consider and evaluate the microbial activity with a special emphasis on EPS production.

6.3.5. Dissolved oxygen concentration

The effect of the dissolved oxygen concentration on activated sludge flocculation was investigated by imposing different oxygen concentrations in the vessel. The experiments showed a very small difference between the floc size evolutions and especially the ultimate size reached (Figure 6.29). Apparently, at higher oxygen concentration (4 g/l) the calcium addition created a faster increase in the floc size in comparison with DO = 2 g/l. The slowest dynamics occurred under anaerobic conditions (DO = 0 g/l). This can be related to the microbial activity which depends on the dissolved oxygen concentration.

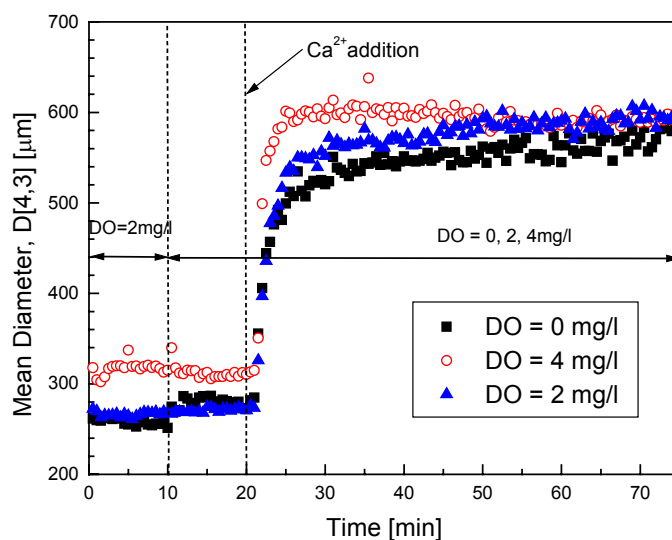


Figure 6.29. The dissolved oxygen concentration effect on floc size dynamics

Similar to the case of temperature, the short-term effect of dissolved oxygen was evaluated in another separate experiment. The imposed conditions in the vessel were kept at the values corresponding to the central point design ($X = 0.63$ g/l; $T = 15^{\circ}\text{C}$; $G = 55$ s⁻¹) and the dissolved concentration in the vessel was set at 0 mg/l, 2 mg/l and 4 mg/l. In this experiment no calcium was added to the reactor.

Figure 6.30 shows a slight decrease in floc size with average mass mean diameters of 347.37 ± 13.39 μm (DO = 2 mg/l); 332.45 ± 3.71 μm (DO = 4 mg/l) and 321.71 ± 2.91 μm (DO = 0 mg/l) respectively. It has to be mentioned that around 1 hour was needed to reach a steady dissolved oxygen concentration; the transient effect was not recorded. It is therefore assumed

that the observed slight decrease in floc size is mainly due to the disturbances to which the microbial flocs were subjected during the variation of the DO.

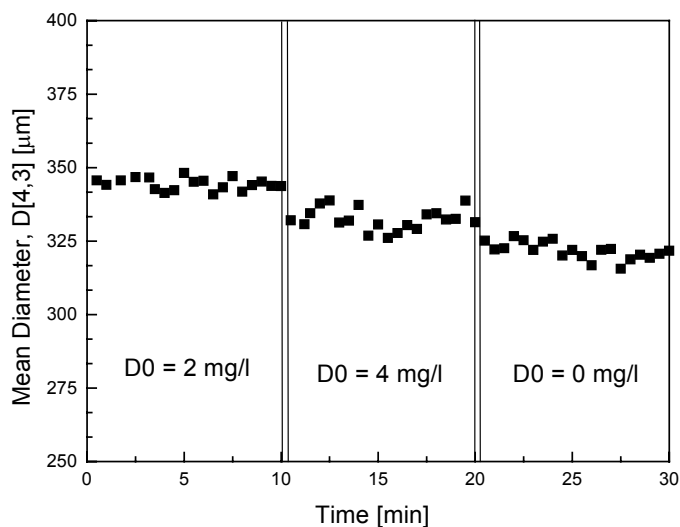


Figure 6.30. The effect of dissolved oxygen concentration on floc size. Short-term evaluation.

To summarise, the short-term changes in DO did not significantly affect the floc sizes. However, small disturbances created by the changes of the dissolved oxygen concentration was observed for the case in which calcium was not added to the system. Addition of calcium generated larger and stronger flocs, which were less sensitive to the DO variations.

6.3.6. Conclusions

The effect of several physical and chemical parameters on the floc size dynamics has been investigated on-line by using different sizing devices coupled in series. The main conclusions that can be drawn from these investigations are:

- The techniques used for quantifying the flocculation were shown to be fast enough to detect the changes in floc size during the (de)flocculation process. By using different measurement principles, a complete evaluation of the changes in numbers and volumes of the flocs as well as a direct visualisation of flocs were possible. Moreover, the highly similar floc size dynamics recorded by all devices represented a good validation of the correctness of the recorded results.
- Among the five investigated factors, the most significant effects on the floc size were due to the average velocity gradient and the calcium addition.
- At high average velocity gradient values, very fast floc breakage phenomena occurred. However, the calcium addition reinforced the floc structure allowing the flocs to reaggregate. A floc restructuring factor of 53.41% indicated the strong ability of the flocs to reflocculate. On the contrary, at low average velocity gradient values, floc aggregation dominated and resulted in slightly but continuously increasing floc size.
- The SBR activated sludge samples showed a high affinity for calcium ions, resulting in a fast increase of their size. It was found that the response of the activated sludge sample to batch-addition of calcium is highly dependent of the initial calcium content of the sludge. Moreover, at large calcium additions, a faster aggregation process was observed which led to an equilibrium floc size that was

increasing (but not directly proportional) with the amount of calcium added to the system. This indicates that the sludge reached a saturation level.

- At higher solids concentration a tendency to form larger flocs was observed. However, the activated sludge concentration showed a less significant effect on the floc size dynamics than calcium addition.
- Larger floc sizes were observed when the temperature in the reactor was decreased from 25°C to 5°C. It seems that the temperature at which the sludge was acclimatized played an important role on the process dynamics, showing a faster aggregation rate when calcium was added into the system at higher temperature. Several hypotheses were considered in order to explain the observed behaviour. It seems that the most important cause is related to the microbial activity, which react different to the temperature changes. When temperature was increased to 25°C a deflocculation effect occurred in time. Again, a comparison with the available literature studies led to conclude that the microbial activity and EPS production is highly influenced by the changing in temperature even when only short-term investigations are performed. However, the effect of short-term temperature variations on the floc size dynamics is difficult to explain with the available data and more investigations considering also the microbial activity and EPS are required.
- Short-term changes in the dissolved oxygen concentration did not affect the larger floc size and the observed dynamics were similar for the experiments performed at different dissolved oxygen concentrations.

Study of the influence of physical and chemical factors on the (de)floculation process by using the DOE and RSM

7.1. Introduction

During the flocculation process, many factors can interact and influence it at the same time. However, by performing experiments in a conventional way, the effect of just one factor at a time is investigated. This may depend on the values of the other independent factors. Evaluation of joint effects of more factors becomes possible thanks to the features of the DOE and RSM approaches described in Chapter 5.

Therefore, the effect of the considered design factors on a set of responses is investigated in this chapter. The considered responses are evaluated using a quadratic polynomial model, which is constructed from the experimental data. The interaction effects (up to the second order) between all five physical-chemical factors considered in the proposed DOE on the responses are quantified as well. Furthermore, identification of the set of experimental conditions that optimise the responses according to some optimisation criteria is possible (provided such a set exists). Knowledge of the responses as polynomial functions of all considered factors is very useful in gaining insights into the activated sludge flocculation process.

It should be mentioned that some experimental errors occurred when imposing the factor values resulting from the experimental design. These errors are related to the finite precision in controlling some factor values and actually led to small differences in the design points, as compared to the “theoretical” values, resulting from the requirements discussed in Chapter 5. A direct consequence of these small deviations from the values mentioned in Table A7-1 is that the orthogonality of the design is slightly affected, a fact that is not a major issue for this analysis, as long as the matrix $F^T F$ remains nonsingular.

According to the experimental procedure, the flocculation process was evaluated between two distinct steady conditions. The first refers to the analyses performed when the preliminary conditions were imposed to the sludge sample, as explained in section 5.3.2. The second refers to the end of each flocculation experiment. However, even if theoretically the initial state should give very similar results for all considered experiments, it was observed that this was not always the case. Particularly, some differences were recorded due to difference in sludge concentration, which had to be set prior to the experiment to the specific design point value. Moreover, the sampling and measurement procedure may have had an influence on the measured results. Therefore, in evaluating the factors influence, two models were each time evaluated and compared as well. One takes into consideration the response as the difference between the final and initial response values, whereas the second evaluates only the final response values. In this way, a closer monitoring of the possible experimental errors is achieved, which is helpful in validation of the model's predictions.

In this chapter, the joint effect of five considered factors (average velocity gradient (G), sludge concentration (X), calcium concentration (Ca), temperature (T) and dissolved oxygen concentration (DO)) on a set of seven flocculation process responses (floc size (D[4,3]), sludge volume index (SVI), zeta potential (ζ), supernatant total suspended solids concentration (TSS), supernatant turbidity, pH and conductivity) is investigated.

The steps followed¹ for evaluating the influence of the considered factors on the obtained responses are:

- 1 Evaluation of the response models from the experimental design data (corresponding to a Resolution V design). The response models are quadratic and include all main effects, all second-order interactions (higher order interactions cannot be estimated due to the design resolution), as well as purely quadratic terms.
- 2 Statistical analysis of the obtained model by using ANOVA and regression coefficients.
- 3 Identification and analysis of the nature of the stationary points of the fitted surfaces and analysis of the RSM in the box-constrained design space.
- 4 Statistical model identification, using the Akaike Information Criterion (AIC), and the corresponding model simplification.
- 5 Optimisation of the operating point based on specified optimisation criteria of a relevant (sub)set of responses, selected from the whole set of analysed responses.

7.2. Floc size

It was demonstrated before that on-line monitoring of the floc size and FSD, enables a fast detection of the floc size changes when imposing different environmental conditions in the FlocUNIT. Hence, a direct quantification of the development of the (de)flocculation processes becomes possible. It was however difficult to evaluate the effect that the variation of more than one or all the considered design factors would have on the floc size. Therefore, this investigation is carried out in this section by using the DOE and RSM approaches. To this end, the floc size response is evaluated as function of the quadratic polynomial model constructed from the experimental data. The aim is to quantify the effect of interactions between all five considered factors on the floc size.

7.2.1. $\Delta D[4,3]$

In this section the average mass mean diameter D[4,3] was considered as a design response. The difference between the final average size D[4,3]_f obtained when the imposed factors created a relatively steady state floc size distribution and the initial steady average size D[4,3]_i recorded as the effect of the preliminary conditions imposed in the vessel is denoted as $\Delta D[4,3]$ and is further analysed here. Figure 7.1 illustrates the way in which $\Delta D[4,3]$ was calculated.

The algorithms presented in Chapter 5 are used to evaluate and to analyse the quadratic model.

¹ The response model building, analysis and optimisation have been implemented in Matlab. The implementation mainly follows the methodology described in Myers (1976). The statistical model identification has been carried out using an S-Plus routine.

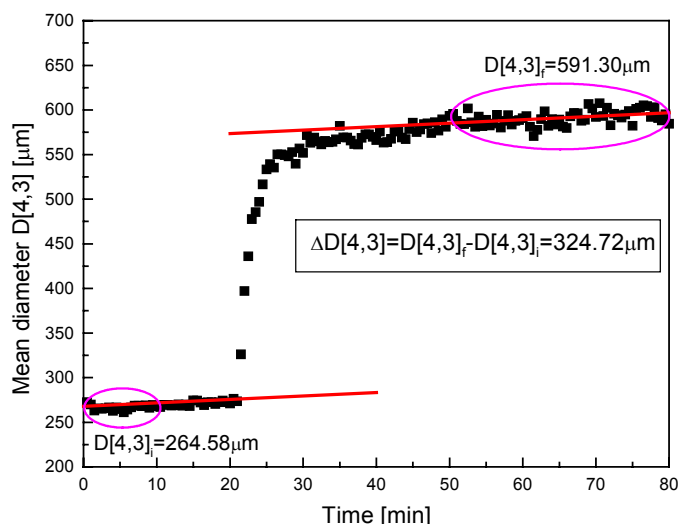


Figure 7.1 The floc size response evaluated as the difference between the final average $D[4,3]_f$ and initial average $D[4,3]_i$, i.e. $\Delta D[4,3]$.

Statistical analysis

Since the response model is constructed in a normalised factors space, all factor variations are within the same size intervals. Therefore, the most important contributions can be immediately identified by investigating the absolute value of the model coefficients. The bar plot in Figure 7.2, allows a quick screening of the importance of each model term.

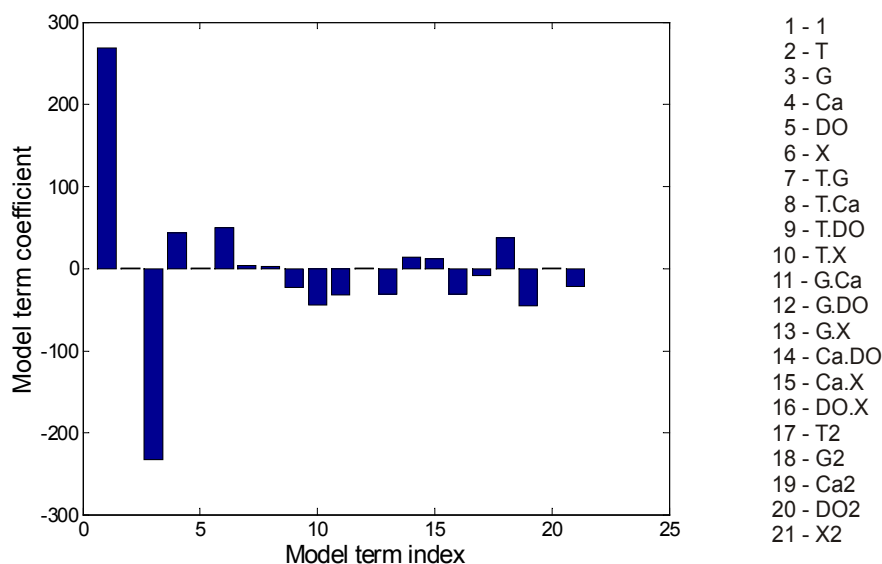


Figure 7.2 Contribution of the model terms to the floc size response. The numbers in the right side column corresponds to the model term index (x-axis), whereas the (response surface) model term coefficients (y-axis) multiplied the corresponding model terms from the right side column. The model terms corresponds to the normalized factors. The factors symbols are defined in Table 5.3.

It may already be noticed that the highest contribution is given by the linear contribution in G, an increase of which determines a decrease in the response, since it has a negative coefficient. However, the quadratic term in G acts in the opposite direction and the net effect is to

"soften" to some extent the linear contribution of G. Moreover, the interactions of G with other factors determine a complex variation of the response with G, which can be fully determined, depending on particular conditions.

Temperature (T) and dissolved oxygen concentration (DO) showed the lowest influence on the response, which suggests that these parameters should be rather regarded as introducing "second order" effects on the response.

The statistical evaluation of the model by using ANOVA yielded an F-ratio = 21.69 with a corresponding P-value = $1.093e-7$ (Appendix 7.2). The small P-value indicated that the selected model was relevant for the considered data set. Moreover, the lack-of-fit error had an F-ratio = 0.97 and P-value = 0.48, indicating that there is no significant lack-of-fit error in the model. Details regarding the performed statistical analysis are presented in Appendix 7.2.

The ability of the proposed model to correctly describe the response variation with the selected set of factors is illustrated in the scatter plot of Figure 7.3, where the response values predicted by the model are plotted against the measured data. The corresponding regression coefficient R^2 resulted to be 0.97, which is very close to the value of 1, of a perfect match. The statistical significance of the model is indirectly suggested by the adjusted regression coefficient, which penalizes the model complexity. This has a value, $R^2_{adj} = 0.92$ which is again a very good result, close to the ideal value of 1. Furthermore, the root mean square error of the model is 62.01. This is to a large extent determined by the replicated runs in the central point and is relatively small, if one accounts for the variation range of the response itself, which is in the order of 1000 μm . The relative RMS error is $\sim 60 \cdot 100 / 1000 \% \cong 6 \%$.

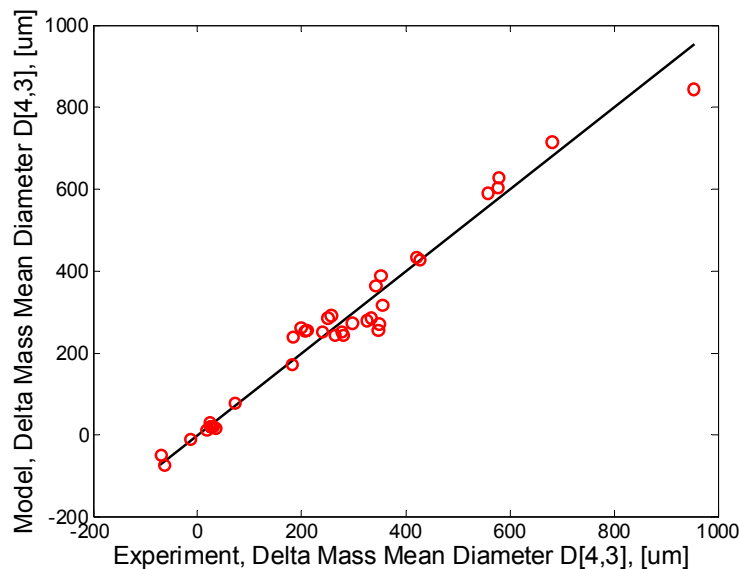


Figure 7.3. Model vs. experiment scatter plot.

Identification and analysis of the stationary point

The stationary point was calculated using the theory of the second-order response surface models as described previously in Chapter 5. For the response discussed here, the stationary point is listed in Table 7.1. The model value of the response at the stationary point is -131.15 μm .

Table 7.1 The model terms values calculated at the stationary point.

Factor	Stationary point (scaled)	Stationary point (unscaled)
T	-2.7712	1.1442
G	3.6726	586.01
Ca	-0.8101	7.1393
DO	-1.0488	0.9512
X	1.9189	3.7200

The canonical form of the response (Myers, 1976) is given by:

$$\hat{R}(\Delta D[4,3]) = -131.15 - 53.795w_1^2 - 42.739w_2^2 + 4.3956w_3^2 + 9.3271w_4^2 + 45.392w_5^2 \quad (7.1)$$

The coefficients of the canonical variables w_j , which have both positive and negative values, allowed to conclude that the stationary point is a saddle point. The canonical variables w_j are obtained from the original variables x_j by using the following transformation:

$$w = M^T \cdot (x - x_0) = \begin{bmatrix} -0.34247 & -0.40742 & 0.71419 & 0.43617 & -0.12807 \\ 0.05769 & -0.22487 & -0.27224 & 0.00685 & -0.93378 \\ 0.73799 & -0.64042 & 0.07548 & -0.09033 & 0.17715 \\ -0.30539 & -0.20977 & 0.26684 & -0.88812 & -0.05266 \\ -0.49142 & -0.57385 & -0.58216 & 0.11310 & 0.27838 \end{bmatrix} \begin{bmatrix} T + 2.7712 \\ G - 3.6726 \\ Ca + 0.8101 \\ DO + 1.0488 \\ X - 1.9189 \end{bmatrix} \quad (7.2)$$

where \mathbf{M} is the canonical transformation matrix. The transformed variables w_i define directions in the factors space which should be followed in order to achieve an increase (if the corresponding coefficient in the canonical form is positive) or decrease (if the corresponding coefficient is negative) of the response value.

Examination of equation (7.1) reveals that a decrease in the estimated mass mean diameter occurs upon moving away from the stationary point along the w_1 and w_2 axes. However, the estimated mass mean diameter increases when one moves along w_3 , w_4 and w_5 .

A plot of the response as function of the DO and Ca factors is shown in Figure 7.4. The remaining factors have been fixed at the values corresponding to the stationary point. It should be noticed that, for the saddle point, both an increase and decrease of the response are possible, depending on the direction of movement (Figure 7.4-right).

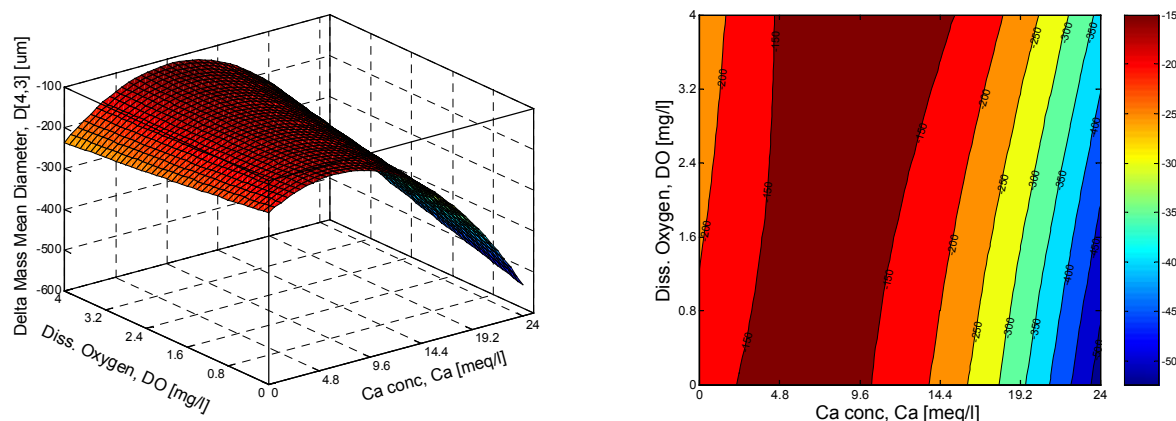


Figure 7.4 Saddle point in the fitted surface for the $\Delta D[4,3]$ function of the DO and Ca concentration. The other factors retain the corresponding stationary point values. Fitted 3D surface (left) and the surface contour plot (right).

It should be noticed that the stationary point is situated outside the experimentation window, for both temperature and average velocity gradient. Therefore, the result should be considered with caution, as it is not a good practice to trust results extrapolated significantly outside the investigation domain. According to the theory of experimental design and response surface methodology, a new experimental design should be carried out in a region containing the stationary point, if this would correspond to an experimentally "interesting" point. This is not the case here since interest exists in a point that maximises the response, while the stationary point is merely a saddle point of a surface that has no finite extreme. Moreover, the selected factors space with this experiment is wide enough to cover physically realistic values. Therefore, for the experimental region considered, the response has the characteristics of a ridge surface and it is of more practical interest to perform a constrained optimisation, where lower and upper box constraints are imposed upon the factors. These constraints are set to -2 for the lower bound, and to $+2$ for the upper bound, respectively, in a scaled factor space.

In the next step of the analysis, an attempt to determine optimal operational conditions is carried out. To this end, the steps in the optimisation procedure described in Chapter 5 are followed. For this case, it is of interest to find the factor values that maximise the $\Delta D[4,3]$. This objective is based on the consideration that larger flocs settle faster, although it is well-known that this also depends on the floc's structural properties. As discussed before, there is no absolute maximum. However, conclusions about the model can be drawn in the constrained region. The constrained optimisation therefore is discussed further.

Apart from elimination unphysical conditions, e.g. negative DO, Ca or X concentrations, it is important to find the maximum imposing the constraints that no factor exceeds the boundaries of the experimental region. Given the way in which the optimisation algorithm is implemented, a "target" optimisation method was used, where the target is set to a limit sufficiently high as compared to the expected range of maximum. This can be easily determined from a few model evaluations, or from the model vs. response plot (Figure 7.3). Precisely, the target was set to $\Delta D[4,3] = 2000 \mu\text{m}$. By setting any other target value higher than $2000 \mu\text{m}$ the same maximum value was found.

A local optimisation algorithm minimises the squared deviation of the model response from the target. This means that, depending on the initialisation point of the algorithm, more than one solution might be possible. Indeed, two optimal points were found as summarised in Table 7.2. Four constraints are active, three of which (T, G, X) at the same values, whereas the fourth (DO) sweeps from one side of the box to the other. Only one factor (Ca) has a value inside the optimisation interval.

Table 7.2 Optimisation parameters for maximum response.

Response $\Delta D[4,3]$ (μm)	1269.3			1260.5		
	Active constrains	Scaled value	Unscaled value	Active constrains	Scaled value	Unscaled value
T	yes	-2	5	yes	-2	5
G	yes	-2	15	yes	-2	15
Ca	-	1.6892	22.135	-	1.0891	18.535
DO	yes	2	4	yes	-2	0
X	yes	2	4	yes	2	4

It is observed that both T and G correspond to their minimal constraints, i.e. they should be maintained as low as possible to obtain a maximum floc size. Indeed, a high sludge concentration favours the formation of a larger floc size. Note that the dissolved oxygen is of

smaller importance for maximizing the floc size. This can be clearly seen when the contours plot of Figure 7.5 is examined.

The two optima are located, one on the bottom (horizontal) DO line, one on the top DO line. In fact, the projection of the response in the (Ca, DO) space behaves as a near-stationary ridge surface, for which the sensitivity of the response with Ca variation is much more pronounced as compared with that of the DO. Therefore, by changing the Ca concentration a little, the effect of the DO may be fully compensated.

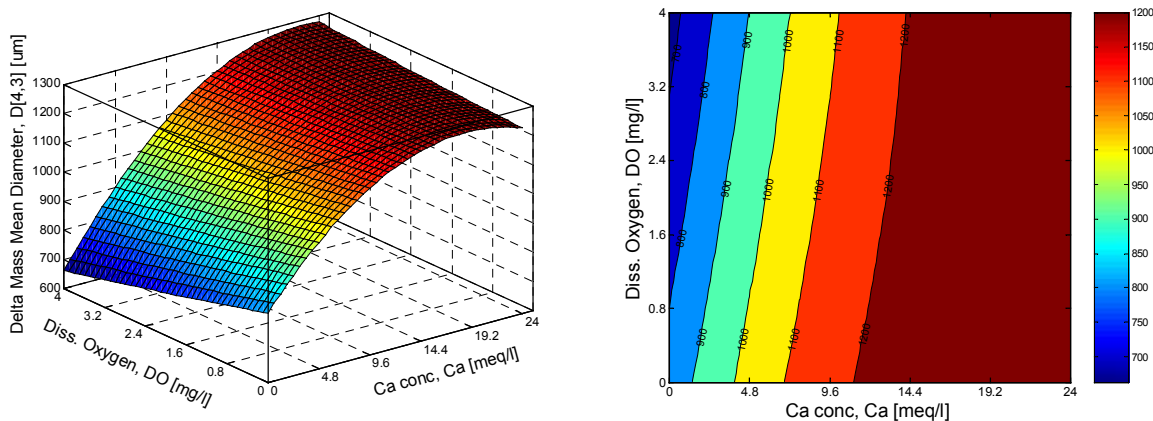


Figure 7.5 $\Delta D[4,3]$ as function of the DO and Ca concentration. The other factors were set at their optimal values ($T = 5^{\circ}\text{C}$; $G = 15 \text{ s}^{-1}$ and $X = 4 \text{ g/l}$).

Model simplification

Since not all model terms have a comparable contribution to the floc size response, a model simplification was carried out by using AIC. The simplification procedure is explained in Chapter 5. For comparison reasons, the model simplification was performed by using the values of normalised and unnormalised factors. For the case of unnormalised factors, the average velocity gradient and sludge concentration values must be first logarithmed, according to the design settings. For the normalised model, the logarithmic transformation is already included in the normalisation, as detailed in the Chapter 5.

Equation (7.3) shows the simplified model obtained by using normalised values of the factors:

$$\begin{aligned}
 R(\Delta D[4.3]) = & 265.1291 - 3.4055 \cdot T - 231.4861 \cdot G + 45.7473 \cdot Ca + 0.9053 \cdot DO \\
 & + 51.1049 \cdot X - 41.0257 \cdot T \cdot X - 31.8686 \cdot G \cdot Ca - 30.8686 \cdot G \cdot X \\
 & - 31.9097 \cdot DO \cdot X + 36.1675 \cdot G^2 - 45.3132 \cdot Ca^2 - 22.7091 \cdot X^2
 \end{aligned} \quad (7.3)$$

whereas the model obtained with unnormalised factors is given by:

$$\begin{aligned}
 R(\Delta D[4.3]) = & 659.476 - 4.7728 \cdot T_u - 2268.515 \cdot \log(G_u) + 70.946 \cdot Ca_u - 15.007 \cdot DO_u \\
 & + 1006.507 \cdot \log(X_u) - 20.425 \cdot T_u \cdot \log(X_u) - 19.010 \cdot \log(G_u) \cdot Ca_u \\
 & - 270.090 \cdot \log(G_u) \cdot \log(X_u) - 79.431 \cdot DO_u \cdot \log(X_u) \\
 & + 463.318 \cdot \log^2(G_u) - 1.2587 \cdot Ca_u^2 - 140.7134 \cdot \log^2(X_u)
 \end{aligned} \quad (7.4)$$

The subscript u has been added to emphasize that the true unscaled value is used in the model, as opposite to the case of normalized (scaled) variables, shown in equation (7.3). It may be observed that in this case both simplified models give the same model terms contributions for the cases in which normalised and unnormalised factor's values have been used. In the forthcoming analysis, normalised models will be used, since a model analysis with normalised terms is very useful, due to the equalisation of the factors ranges, enforced by normalisation.

7.2.2. Final $D[4,3]_f$

The average initial floc size ($D[4,3]_i$) measured at the initial conditions showed some small variations, which mainly occurred due to the deviations in the sludge concentration that had to be set at the design values. Consequently, there are two analysis options, namely to investigate the final value of the average floc size, $D[4,3]_f$, or the difference between the final value and the initial one, each of them with pro's and con's. However, in some situations this is not a critical issue, as revealed by the short comparison presented next: the generalised (7.5) as well as the simplified (7.6) second order polynomial RSM's of the final average floc size resulted to be:

$$\begin{aligned}
 R(D[4.3]_f) = & 609.06 - 2.12 \cdot T - 236.48 \cdot G + 47.81 \cdot Ca + 12.96 \cdot DO + 58.97 \cdot X \\
 & + 2.86 \cdot T \cdot G + 11.83 \cdot T \cdot Ca - 10.78 \cdot T \cdot DO - 56.43 \cdot T \cdot X \\
 & - 24.71 \cdot G \cdot Ca + 8.24 \cdot G \cdot DO - 57.01 \cdot G \cdot X + 45.29 \cdot Ca \cdot DO \\
 & + 18.82 \cdot Ca \cdot X - 38.49 \cdot DO \cdot X - 16.52 \cdot T^2 + 54.25 \cdot G^2 \\
 & - 32.97 \cdot Ca^2 - 5.75 \cdot DO^2 - 27.82 \cdot X^2
 \end{aligned} \tag{7.5}$$

and

$$\begin{aligned}
 R(D[4.3]_f) = & 595.14 - 4.78 \cdot T - 234.21 \cdot G + 51.94 \cdot Ca + 11.31 \cdot DO \\
 & + 59.44 \cdot X - 55.38 \cdot T \cdot X - 56.26 \cdot G \cdot X + 42.80 \cdot Ca \cdot DO \\
 & - 38.82 \cdot DO \cdot X + 53.53 \cdot G^2 - 32.44 \cdot Ca^2 - 28.18 \cdot X^2
 \end{aligned} \tag{7.6}$$

respectively, where the same AIC procedure was used to reduce the model complexity.

A very good statistical accuracy of the model was found also for this case (Figure 7.6). The detailed statistical analysis, the stationary point and model optimisation are presented in Appendix 7.2.

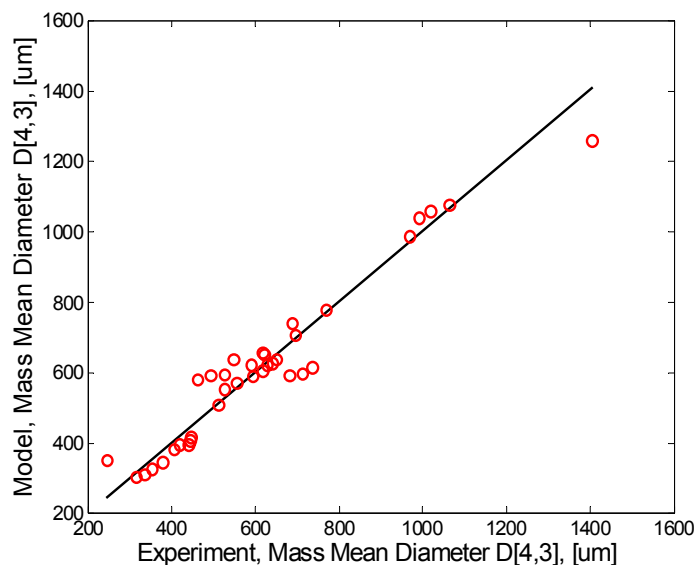


Figure 7.6 Model vs experiment for the $D[4,3]_f$.

The simplified model of the final average floc size is similar to that of the variation of the average floc size, in both the model terms that are still present in the model, as well as in the values of their corresponding coefficients. There is only some relatively minor difference,

where a two-factor interaction between G and Ca in equation (7.3) is "replaced" by that of Ca and DO (equation (7.5)).

This similarity suggests that the initial value of the average floc size has only a minor influence on the description of the flocculation process. However, this conclusion cannot be generalised and, depending on situation, it may apply or not.

Average velocity gradient influence

In section 6.3.1, the average velocity gradient was found to have one of the strongest influences on the floc size as well as on the floc size dynamics. In literature (Galil et al. 1991; Biggs, 2000) many attempts have been made to study the influence of average velocity gradient on flocculation process and consequently on floc size. Parker et al. (1972) showed that a power-law relationship exists between the maximum stable floc size (d_s) and the average shear rate:

$$d_s = CG^{-n} \quad (7.7)$$

where C is the floc strength component and n is an exponent expressing the floc size stability.

In order to check the correspondence of the RSM model with the one proposed by Parker, the generalised model from equation (7.5) was considered. The model was analysed for the case in which all other factors take the central point design values. In this way, on the normalised scale the factors values will be: $T=0$; $Ca=0$; $DO=0$ and $X=0$ and the model becomes:

$$R(D[4.3]_f) = 609.06 - 236.48 \cdot G + 54.25 \cdot G^2 \quad (7.8)$$

Figure 7.7 illustrates that the RSM model is consistent with the model proposed by Parker. Moreover, both models reproduce the experimental data with accuracy. Moreover, for the case of the RSM model, the standard deviation of the experimental data as compared with the model prediction are within the RMS errors calculated for this model (RMS Err: 91.43).

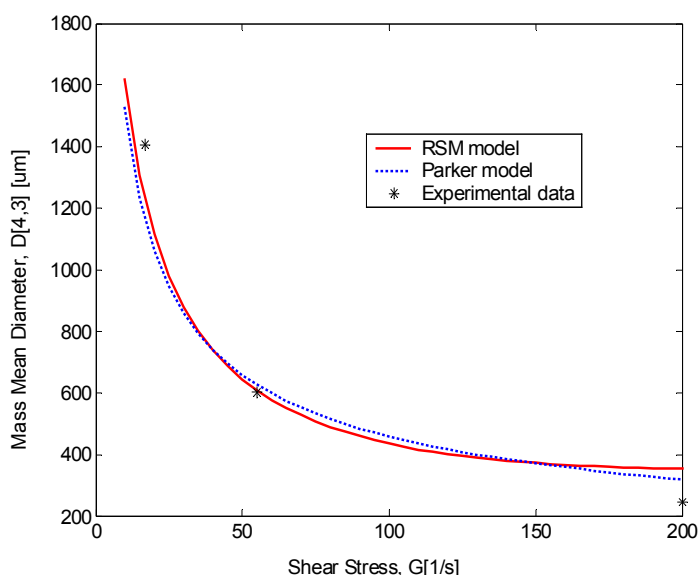


Figure 7.7 RSM model vs. Parker model and experimental data.

Fitting the Parker model to the RSM model, equation (7.9) was found to describe the Parker model for the sludge sample analysed in this case.

$$D[4,3]_s = 4888G^{-0.5138} \quad (7.9)$$

The power-law relationship between the floc size and the average velocity gradient has been confirmed by a series of studies. Parker et al. (1972), Galil et al. (1991), Biggs (2000) found n values ranging from 0.17 to 0.71. Note that these values depend on the flocs structural properties, which may lead to different responses to the average velocity gradient. Galil et al. (1991) found the same exponent (n) when different floc dimensions from the same sludge sample were investigated indicating that the response of flocs to shear was similar.

7.2.3. Conclusions

The analysis of the floc size by using the mass mean diameters ($\Delta D[4,3]$ and $D[4,3]_f$) by means of DOE and RSM revealed the following:

- With good accuracy, the variation of the response on the different environmental conditions could be reproduced with a second-order polynomial model. The analysis of the constructed model allowed to gain a global insight on the effect of all factors.
- The average velocity gradient has the strongest effect on the floc size and the dissolved oxygen concentration is the least important factor.
- There is no optimal condition for maximising the floc size, when all the factors are allowed to vary on the real physical axis. However, optimal conditions could be found when the constraints are imposed on factors. This situation allowed to find an optimum corresponding to minimal average velocity gradient and temperature. Further, higher sludge concentrations favour the formation of large flocs. These observations are in agreement with the observed floc size dynamics investigated in Chapter 6.
- The effect of DO can be fully compensated by slight variations of the Ca concentration, which makes the DO not really important for inducing optimal operation conditions for increasing the floc size under short term.
- A simplified model has been derived, based on the Akaike Information Criterion, which allowed to delimitate the valid region of the model.
- By considering just the final mass mean diameter $D[4,3]_f$ as response a similar empirical model with comparable values of the model coefficients and a similar simplified model were obtained. This shows that the observed variations of the initial floc size observed did not significantly affect the model obtained.
- The RSM model obtained for the floc size at steady state ($D[4,3]_f$) was found to be consistent with a power-law relationship proposed in the literature. Both models describe the experimental data with enough accuracy.

7.3. Sludge Volume Index (SVI)

As shown in section 4.2.2.1, the most commonly used measure for the activated sludge settling properties in practice is the sludge volume index (SVI). Any variations in this index reflect the biological responses to environmental factors, i.e. sludge loading, wastewater constituents, nutrients demand, etc. The large number of these potentially important influencing factors makes it difficult to predict the SVI. The SVI generally varies in the range

of 40 to 300 ml/g and a well settling sludge shows an SVI of less than 150 ml/g (Ganczarczyk, 1983). A low SVI generally indicates a well flocculated sludge with good settling properties. As the floc size and its structural properties influence the SVI, it is important to know the relationship as this may be used for process optimisation.

7.3.1. Δ SVI

As for the case of the floc size, the SVI was also evaluated as the difference between the SVI determined after and prior to the flocculation process, i.e. Δ SVI. Hence, negative values for Δ SVI indicate an improvement of the settling properties. As before it may also be of interest to model the final SVI as function of the different imposed environmental conditions.

Statistical analysis

Firstly, the Δ SVI will be discussed. The model coefficients and the statistical parameters for the evaluation of the coefficients are presented in Appendix 7.3.

From the bar plot of the model coefficients (Figure 7.8) it can be seen that it is rather difficult to identify the model coefficients with the most significant contribution to the response. It seems that the most relevant are the first order terms of DO and X which shows that a decrease of their values will result in a decrease of the response. Still, it is difficult to draw a conclusion since the difference between these two terms and the other terms is relatively small. It is therefore necessary to investigate the model fit to the experimental data and to proceed further with the model simplification procedure to draw quantitative conclusions concerning the model and its relevant terms for the considered response.

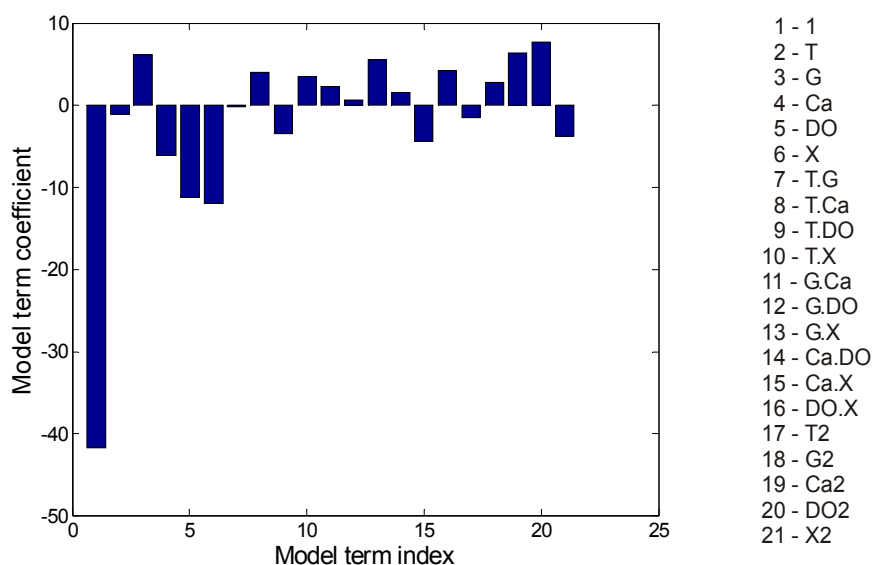


Figure 7.8 Relative contribution of model terms to Δ SVI response.

The ANOVA statistical analysis and the model regression quality are presented in Appendix 7.3. The relatively small F-ratio = 1.54, associated with a P-value = 0.19 indicates that the model does not entirely explain the variation of the response. Moreover, the P-value = 0.00001 calculated for the lack-of-fit shows that lack-of-fit is significant with a probability of 95%.

In Figure 7.9 the response values predicted by the model are plotted against the values obtained from the experiments.

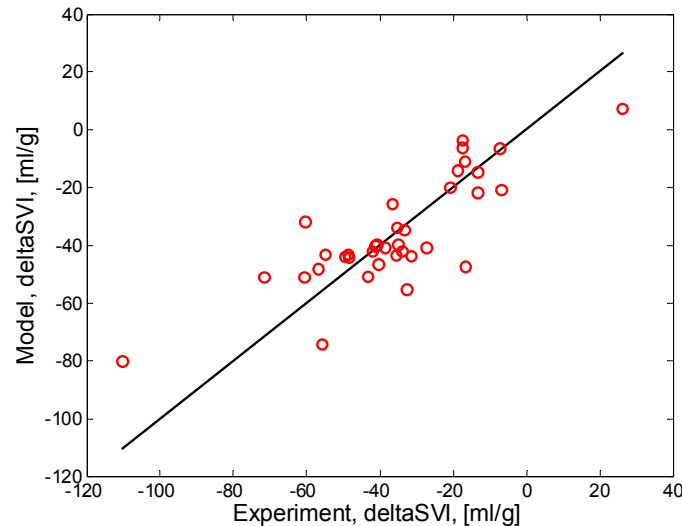


Figure 7.9 Δ SVI values predicted by the model vs experimental values.

The regression coefficient was calculated to be $R^2=0.6721$ which indicates a rather modest fit. The adjusted regression coefficient, which penalises the model for unnecessary terms showed a low value of 0.2349. This indicates that there might be model terms that do not really contribute to the response values.

Identification and analysis of the stationary point

The calculated values of the factors at the stationary point for the Δ SVI response are listed in Table 7.3. The model value at the stationary point is Δ SVI = -27.274 ml/g. It should be noticed that the stationary point is located outside the experimental interval for temperature (T) and sludge concentration (X). Moreover, the values indicated at the stationary point show a negative value for the temperature and very low activated sludge concentration; hence, they are not practically applicable.

Table 7.3 The stationary points for the model factors

Factor	Stationary point (scaled)	Stationary point (unscaled)
T	-3.27	-1.35
G	0.89	97.83
Ca	0.46	14.74
DO	0.54	2.54
X	-2.37	0.07

The canonical form obtained by calculating the characteristic roots (λ) is given by

$$\hat{R}(\Delta SVI) = -27.274 - 6.7259w_1^2 - 1.0030w_2^2 + 3.6397w_3^2 + 7.2108w_4^2 + 8.5067w_5^2 \quad (7.10)$$

Since the calculated characteristic roots (λ) show both negative and positive values it may be concluded that the stationary point is a saddle point. To perform the response optimisation one should consider that a decrease in the response value corresponds to an improvement of the settling process. In this context a target value of -200ml/g was initially fixed, thus forcing the optimisation routine to search for the minimum. An optimal minimal value response was found to have a value of Δ SVI = -153.03 ml/g. Random changes of the initialisation point inside the experimental region did not change the optimal response value. It can thus be expected that there is only one optimum in the optimisation box considered (the experimental

region). The optimal operating conditions obtained for the minimum response are presented in Table 7.4.

Table 7.4 Optimal factor values required for obtaining a maximum decrease of SVI

Response Δ SVI (ml/g)	-153.03		
Factor	Active constraints	Scaled value	Unscaled value
T	yes	-2	5
G	yes	-2	15
Ca	yes	2	24
DO	-	0.394	1.6057
X	yes	2	4

Four constraints were found active during the optimisation process. Two correspond to the minimal values of the temperature (T) and average velocity gradient (G). By contrast, high values for calcium (Ca) and sludge concentration (X) are required for minimising the response. DO is the only factor located inside the experimental region. Similar to the floc size low temperature and average velocity gradient values as well as high sludge and calcium concentrations favour the process efficiency, i.e. improve the settling properties. It may therefore be concluded that larger floc formation will also create an improvement of the settling properties.

To illustrate this, the average velocity gradient (G) and sludge concentration (X) were considered to illustrate the model response. Figure 7.10 shows the 3D plot and the contours plot on logarithmic scale, while fixing the other factors at the values corresponding to the constrained optimum (T = 5°C; Ca = 24 meq/l; DO = 1.6 mg/l). It is observed (Figure 7.10-right) that a decrease of the response value corresponds to an increase of the sludge concentration (X) and to a decrease of average velocity gradient (G). Accordingly, the model showed that the activated sludge sample treated during the flocculation experiments has a more effective settling for small average velocity gradient values and high sludge concentrations.

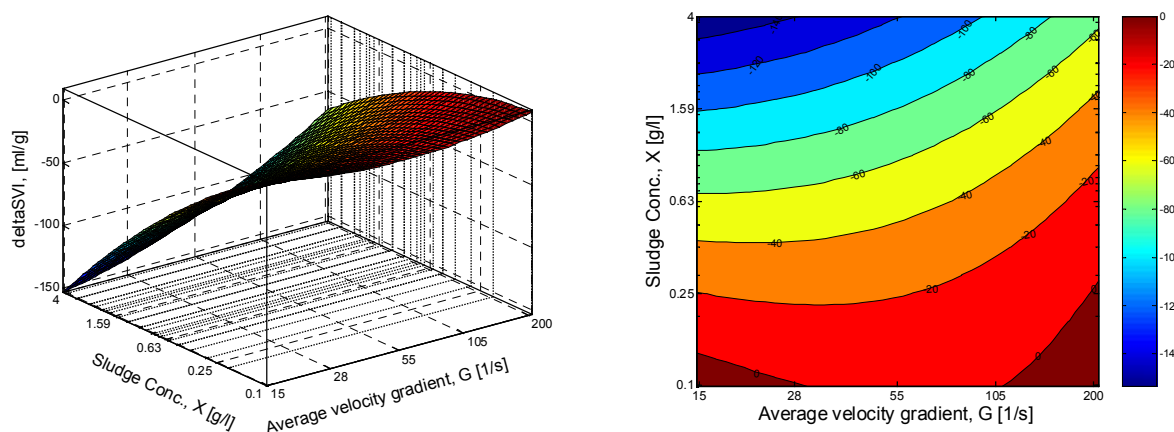


Figure 7.10 The Δ SVI variation as function of G and X where the rest of the factors were set at the optimal constrained values (T= 5°C; Ca = 24meq/l; DO = 1.6mg/l).

Model simplification

The model could be simplified to the form given by equation (7.11).

$$R(\Delta SVI) = -43.3676 + 6.2336 \cdot G - 6.2150 \cdot Ca - 11.5851 \cdot DO - 11.2447 \cdot X + 6.6108 \cdot Ca^2 + 7.4633 \cdot DO^2 \quad (7.11)$$

The simplified version of the model, which turns out to not contain any interaction term, can be easily exploited towards derivation of rules-of-thumb, allowing to quickly decide what operation should be performed in order to obtain a target decrease of the ΔSVI . Thus, from the differentiation of the response in equation (7.11) one finds:

$$\Delta R(\Delta SVI) = 6.2336 \cdot \Delta G - 11.2447 \cdot \Delta X + (13.222 \cdot Ca - 6.2150) \cdot \Delta Ca + (14.927 \cdot DO - 11.5851) \cdot \Delta DO \quad (7.12)$$

Accordingly, to obtain decrease of 1 unit response, $\Delta R(\Delta SVI)=-1$, by changing only one factor while the others are kept constant:

- irrespective of the current values of the factors, G should be decreased by about 0.16 log-normalised units or X should be increased by nearly 0.09 log-normalised units, i.e. $\Delta G|_{\Delta R(\Delta SVI)=-1} = -0.16$ or $\Delta X|_{\Delta R(\Delta SVI)=-1} = 0.09$.
- alternatively, depending on the current values of Ca and DO, one has to either change the added Ca by $1/(13.222 \cdot Ca - 6.215)$ lin-normalised Ca units or the DO lin-normalised concentration by $1/(14.927 \cdot DO - 11.5851)$ units. Depending on the values of Ca or DO, this change is either an increase (for $Ca > 0.47$ or $DO > 0.79$) or a decrease (in the opposite case). Concisely: $\Delta Ca|_{\Delta R(\Delta SVI)=-1} = \frac{1}{13.222(0.47 - Ca)}$, or $\Delta DO|_{\Delta R(\Delta SVI)=-1} = \frac{1}{14.927(0.79 - DO)}$.

For Ca and DO values close to the point where these determine a minimum for ΔSVI the response is most sensitive to X, followed by G. For values farther from the optimum, the situation reverses. These conclusions can be simply summarised in the plot of Figure 7.11, which shows the absolute values of the required normalised factor variations for a unit decrease of the response.

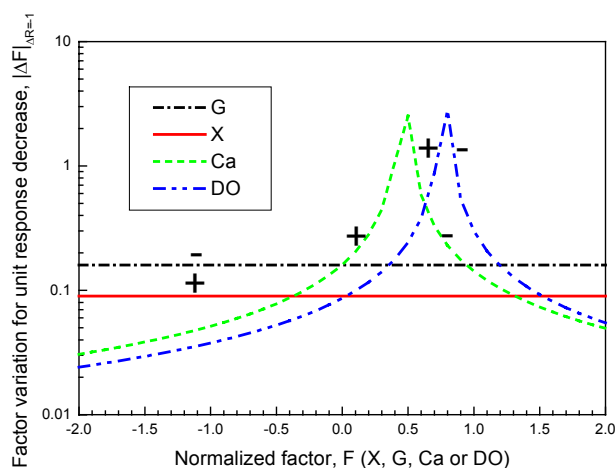


Figure 7.11 Absolute values of the normalised factor variation for a unit change in the response. The "+" sign indicates a positive variation (i.e. the factor variation is an increase), whereas the "-" sign indicates a negative variation w.r.t. the current values.

For instance, assuming that the current operating point in the normalized factor space is $(T,G,Ca,DO,X)=(0,0.2,-0.5,1,1)$, then, in order to decrease the SVI by one unit, the following alternative decisions can be made: reduce G by 0.16 units, increase Ca by 0.08 units, decrease DO by 0.32 units or increase X by 0.09 units. Here, all units are either lin or log normalised, according to the design settings. Consequently, it appears that the most effective decision is to increase the Ca concentration. It should be noticed that, depending on the current operation point, there may be situations when the mathematically most efficient decision does not correspond to a feasible operation from a physico-chemical point of view. For instance, assuming that the current Ca concentration would have been 1.5 instead of the considered value of -0.5 , while the other factors are at the same values. The new Ca change would now be a decrease of 0.07 units, which again points to Ca concentration change to decrease the SVI. However, Ca removal from the system is not an easy option, and therefore this factor should be eliminated from the list of available options, now reduced to X , G and DO . Hence, depending on the particular operating point in the factors space, it is possible to take the correct decision for process improvement.

7.3.2. Final SVI

For the sake of comparison the model obtained when only the final SVI is used was analysed as well. The second order polynomial model obtained in this case is:

$$\begin{aligned}
 R(SVI) = & 136.77 + 2.91 \cdot T + 3.99 \cdot G - 8.92 \cdot Ca + 4.38 \cdot DO - 1.47 \cdot X + 13.78 \cdot T \cdot G \\
 & - 17.05 \cdot T \cdot Ca - 2.14 \cdot T \cdot DO + 20.80 \cdot T \cdot X - 9.57 \cdot G \cdot Ca - 16.50 \cdot G \cdot DO \\
 & - 4.30 \cdot G \cdot X - 4.69 \cdot Ca \cdot DO - 11.14 \cdot Ca \cdot X - 5.80 \cdot DO \cdot X \\
 & + 7.19 \cdot T^2 + 0.89 \cdot G^2 + 11.68 \cdot Ca^2 + 0.27 \cdot DO^2 - 7.41 \cdot X^2
 \end{aligned}
 \tag{7.13}$$

Statistical analysis

The complete statistical examination of the obtained model is presented in Appendix 7.4. In comparison with the model obtained when ΔSVI , the model obtained final SVI showed a slightly worse fit (Figure 7.12) with the regression coefficients R^2 and R^2_{adj} equal to 0.5976 and 0.0611 respectively. Moreover, the model shows a high lack of fit with a p-value of only 0.00053.

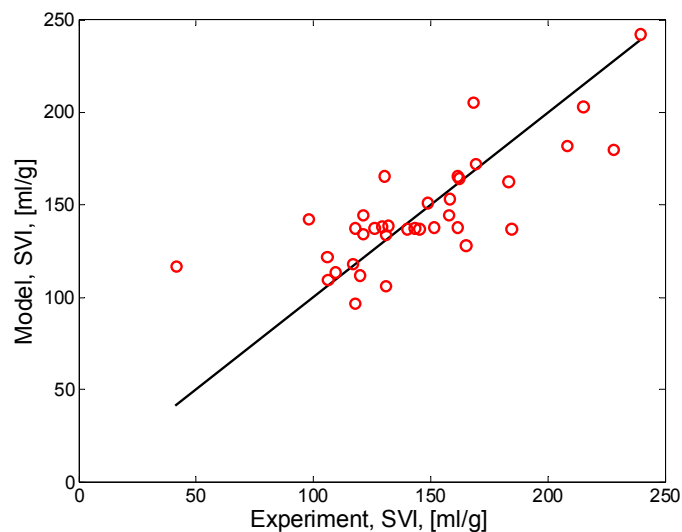


Figure 7.12 Model vs experiment for the SVI response.

Model simplification

In this case, the model simplification (equation (7.14)) indicates the dependency of SVI-final on the temperature as well. It shows a first-order effect as well as interactions with other factors. This was not identified by the Δ SVI.

$$R(SVI) = 138.45 + 3.41 \cdot T + 3.80 \cdot G - 9.03 \cdot Ca + 2.74 \cdot DO - 3.67 \cdot X + 12.80 \cdot T \cdot G - 16.76 \cdot T \cdot Ca + 20.47 \cdot T \cdot X - 15.28 \cdot G \cdot DO + 11.78 \cdot Ca^2 \quad (7.14)$$

According to Dick and Vesilind (1969), the SVI is influenced considerably by the temperature under which the tests are conducted, as would be expected due to the changes in viscosity. It is therefore suggested that the initial values of the SVI also play an important role for the obtained empirical model and those values present large fluctuations affecting the results. One possible reason of these fluctuations can be related to the temperature changes since this parameter could not be precisely evaluated when the tests were performed.

Moreover, the simplified final SVI model variation shows that the second order dependence of the DO vanished, as opposite to the simplified Δ SVI model.

Due to the obtained relatively large differences between the models, the optimisation process was performed by taking into account two possibilities. In the first case the target was fixed to SVI=130ml/g, which may be considered an optimal value for the settling properties (Table 7.5). In the second case, the aim was to find a possible minimum SVI value, within the box constraining the factors' space. To find the local minimum SVI value, the target was first fixed to SVI = -500ml/g.

Table 7.5 Factor values required to obtain an SVI=130ml/g

Response SVI (ml/g)	130		
Factor	Active constrains	Scaled value	Unscaled value
T	no	-0.997	13.853
G	no	0.787	34.615
Ca	no	0.163	19.105
DO	no	0.871	1.049
X	no	-0.057	1.384

Setting an optimisation target of 130 ml/g, with a given initial point, resulted in the operating conditions specified in Table 7.5. The results presented in Table 7.5 represent just an example since the corresponding objective function was near to 0 (within the algorithm tolerance) indicating that an exact solution was found. Since this is the solution of one single equation with five unknowns (the factors set), it is clear that it is not an unique solution, and setting the initial point to a different value would likely result in a different point. This non-uniqueness of the solution is also clearly visible in the contour plot of Figure 7.13, where, for fixed values of DO, T and Ca, the localization of the points with SVI = 130 ml/g is a curve in the (G,X) plane. By visual inspection, it is also clear that in the projected 2D subspace, the SVI value is quite insensitive to the value of the average velocity gradient. This conclusion is, however, not valid for all SVI values.

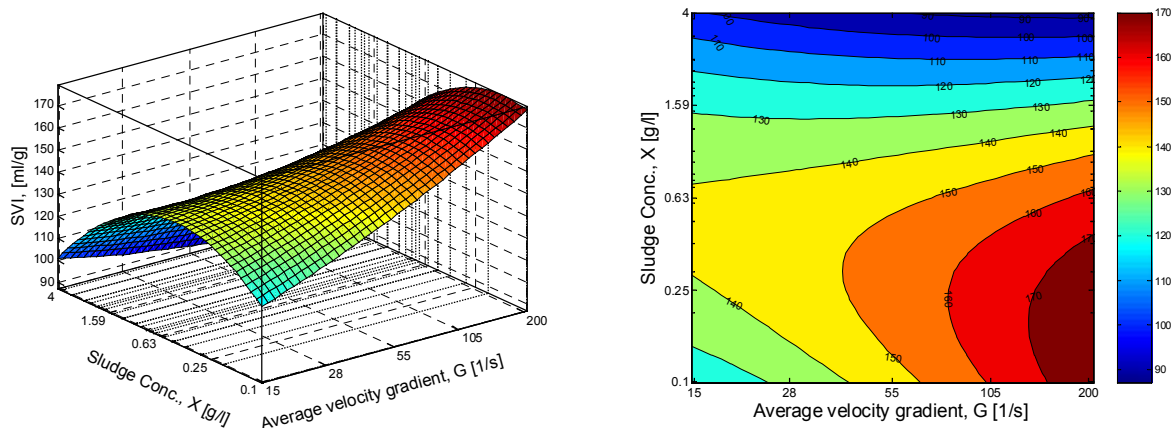


Figure 7.13 The SVI final dependence of G and X. The other values were set at the nominal values required for obtaining an SVI=130ml/g.

If the sludge concentration effect on the SVI is analysed at a given average velocity gradient value it can be observed that there is a sludge concentration interval for which SVI takes a high value (which is different function of the average velocity gradient value). Below and above this interval a decrease of the SVI value is observed. These observations agree with Bye and Dold (1998) who observed that for a given sludge sample, the SVI tends to be constant, with increasing concentration up to a certain value. At this point, there is a rapid increase in measured SVI with a further increase in concentration. The increase in SVI continues until a peak value is reached, after which the SVI begins to decrease with increasing solids concentration. However, as mentioned by Dick and Vesilind (1969) these observations are closely related to the measurement procedure of the SVI being considered as an artefact of cylinder diameter and does not occur necessarily in the full scale plant.

Depending of the imposed initialisation point and by taking into account that the stationary point is a saddle point two minimal values have been obtained when the minimum SVI was investigated for the experimental design window.

The first value indicated a negative value for the SVI, which does not make sense from a physical point of view and will not be taken into consideration. The second possible minimal value was found to be SVI=31.63ml/g which shows high sludge compactness for low temperature and average velocity gradient and high values of sludge concentration and dissolved oxygen. The only one factor which was found to not have an active constraint and give a value inside the experimental region was Ca=3.93mg/l.

Table 7.6 Factors values required for obtaining a maximum SVI.

Response SVI (ml/g)	31.63		
Factor	Active constrains	Scaled value	Unscaled value
T	yes	-2	5
G	yes	-2	15
Ca	no	-1.34	3.93
DO	yes	2	4
X	yes	2	4

It is however observed again that a minimal SVI value is obtained for the same low values of T and G and at high sludge concentration, being in agreement with the optimisation obtained when ΔSVI was considered as response. It is therefore suggested by both the considered

models that an increase of the applied average velocity gradient will determine an increase of the SVI values. Similar observations are reported by Galil et al. (1991) who observed that an increase of the shear indicated a poorer settling and thickening characteristics of the sludge, which were characterized by increasing SVI values.

7.3.3. Conclusions

The analysis of the effect created by the considered factors to the Δ SVI and final SVI values revealed less accurate empirical models characterized by a moderate fit to the experimental data. The observed difference between the models obtained when the change in SVI was considered showed a significant variability in the measured initial SVI, which may have affected the results.

However, both results indicated that average velocity gradient and sludge concentration are the most significant factors affecting the responses. The process optimisation in terms of minimizing the response showed that this would be achieved for low temperature and average velocity gradient values and for high sludge concentrations. The DO effect was found to be less significant.

It seems that a relationship between the floc size and SVI can be found since larger flocs formation occurred under the same operations conditions that were found to be responsible for minimizing the SVI. It confirms that large floc sizes will improve the settling properties of the sludge.

7.4. Zeta potential

As a result of the physico-chemical interactions between microorganisms (mainly bacteria), inorganic particles (silicates, calcium phosphate and iron oxides), exocellular polymers and multivalent cations, the activated sludge flocs are negatively charged (Urbain et al., 1993). If the amount of negative charge is large enough, small particles (colloids) will remain discrete, dispersed and in suspension. Reducing or eliminating the charge has the opposite effect and the colloids will gradually aggregate and settle. Fundamentally, the zeta potential is as important as particle size in determining the behaviour of particulate systems, especially of those in the colloidal range. Since the zeta potential depends on the charge on the particles' surface, as well as on the chemistry of the dispersing medium, the surface influences many of the properties of the colloids, including their stability and bulk rheology. In this way, the measurement of the zeta potential may give information regarding the colloids present in the supernatant. Liu and Fang (2003) showed that for different activated sludge samples the flocs and EPS carry a negative charge, with potential values ranging from -20 down to -30 mV. The link between zeta potential and the activated sludge flocculation process is often contradictory and its role in understanding the process performance is often not well understood. Indeed, Liao et al. (2001) found that there is no significant correlation between the SVI and the surface charge of the sludge. Urbain et al. (1993) further reported that activated sludge flocs with highly negative surface charge did not settle well. A dependency of the process performance in terms of charge neutralisation was often linked to the concentration of cations added during the process. Keiding and Nielsen (1997) observed that deflocculation occurred when some Ca was removed from the sludge. This was assumed to be due to the increase in negative charge by the zeta potential and not to a change in the double layer thickness, as suggested by Zita and Hermansson (1994).

7.4.1. $\Delta Zeta$

To evaluate the influence of the considered factors on the zeta potential, the $\Delta Zeta$ is considered here as response. This should give information regarding the effectiveness of the flocculation process in terms of colloids removal. As for the other responses, $\Delta Zeta$ is defined as the difference between the supernatant zeta potential measured before and after performing the flocculation experiments.

Statistical analysis

It may be observed (Figure 7.14) that the second order effects of calcium concentration and dissolved oxygen and the interaction between those two parameters as well as the mixed effect of G and X are the most significant model terms. These also show the smallest P-values, as shown in Appendix 7.4.

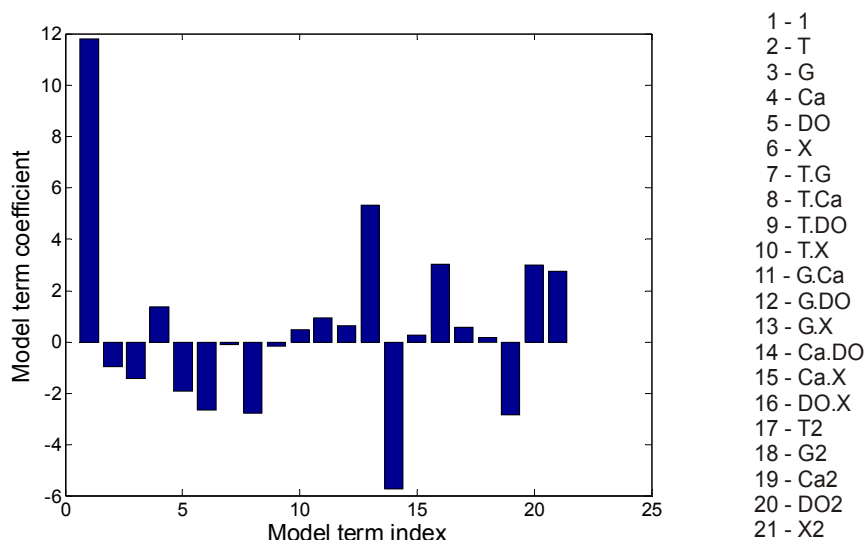


Figure 7.14 Model terms contribution to the $\Delta Zeta$ response.

Statistical analysis of the complete model (Appendix 7.4) reveals a P-value = 0.014, which indicates that with a probability of 95% the proposed model is able to describe the factors' effect on $\Delta Zeta$. The regression coefficient is $R^2 = 0.8054$ and indicates a rather good fit to the experimental data. The model versus experiment plot illustrating this good correspondence is shown in Figure 7.15.

Identification and analysis of the stationary point

The value of the response at the stationary point is $\Delta Zeta = 10.28$ mV and the values of the corresponding factors at the stationary point are presented in Table 7.7.

Table 7.7 The factors' value at the stationary point.

Factor	Stationary point (scaled)	Stationary point (unscaled)
T	0.547	17.74
G	0.148	60.72
Ca	-0.089	11.46
DO	0.081	2.08
X	0.236	0.78

The canonical form obtained by calculating the characteristic roots (λ) is given by

$$\hat{R}(\Delta Zeta) = 10.28 - 4.423w_1^2 - 1.468w_2^2 + 0.966w_3^2 + 3.366w_4^2 + 5.827w_5^2 \tag{7.15}$$

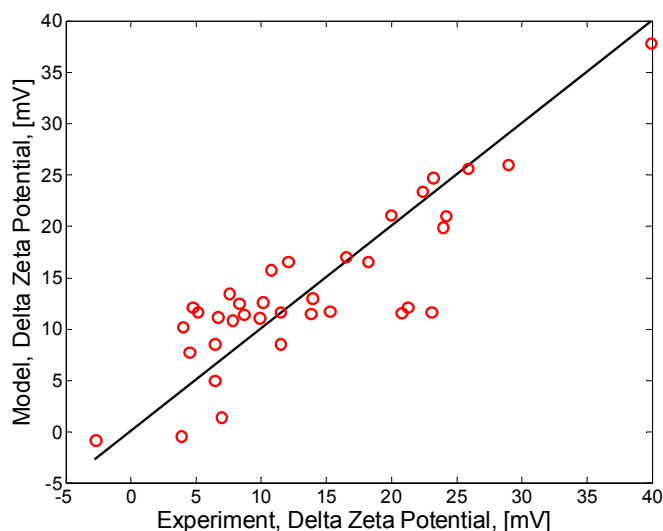


Figure 7.15 $\Delta Zeta$ values predicted by the model vs experimental values.

The canonical form shows both negative and positive values for the calculated characteristic roots indicating that the stationary point is a saddle point, which in this case is located inside the experimental region. An example of a fitted surface is given in Figure 7.16 where the response was plotted against calcium concentration (linear scale) and sludge concentration (logarithmic scale) by keeping the other factors at the stationary point values.

For response optimisation the following considerations should be taking into account:

- A positive $\Delta Zeta$ value would indicate that the final measured value was smaller than the initial one. This is based on the fact that the measured initial zeta potential showed that the particles in the supernatant were negatively charged with potential values between -18 mV and -30 mV.
- A value of $\Delta Zeta = 0$ shows a constant net charge
- A negative value of $\Delta Zeta$ will indicate an increase of negative charge particles after the flocculation process.

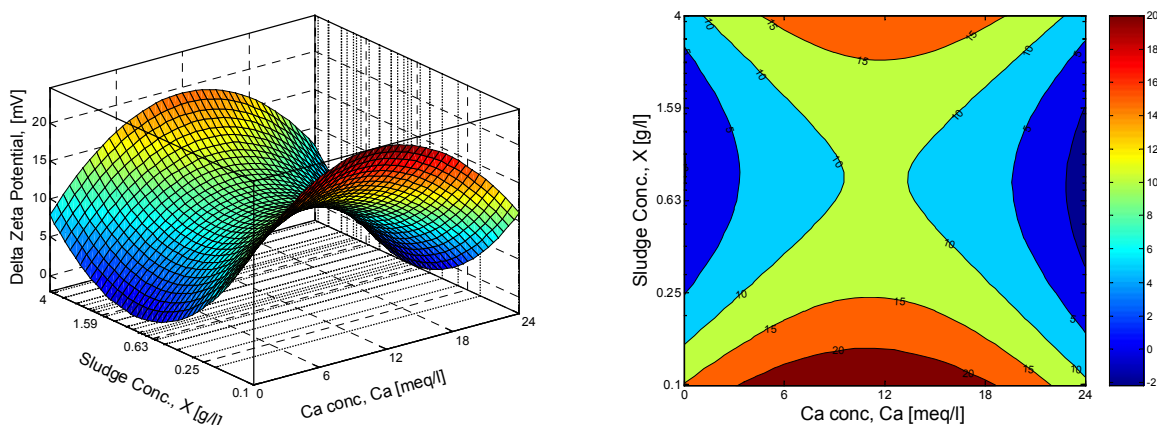


Figure 7.16 Saddle point on the fitted surface for $\Delta Zeta$ as function of Ca and X. The other factors were considered at the values of the stationary point.

It is also often assumed that a zeta potential at the isoelectric point (i.e. at zero zeta potential) or close to this point could represent an indication of optimal operating conditions (Bratby, 1983). Especially, the specific adsorption of ions on the particle surface, even at low concentrations, can have a significant effect on the zeta potential of the particles desorption. Ions can interact with charged surfaces in two distinct ways. Firstly, non-specific ion adsorption has no effect on the position of isoelectric point, but simply reduces the zeta potential. Secondly, specific ion adsorption has an the effect on the isoelectric point.

To performe the optimisation a positive value of $\Delta Zeta$ was chosen as the target. Depending on the starting point of the optimisation routine, two maximal values were obtained, corresponding to $\Delta Zeta = 117$ mV and $\Delta Zeta = 79$ mV (Table 7.8). These values are rather high and suggest a probable saturation of the solution with positive charges after flocculation.

Table 7.8 The operating conditions required to obtain the maximum $\Delta Zeta$.

$\Delta Zeta$ (mV)	117/79		
Factor	Active constrains	Scaled value	Unscaled value
T	yes	-2/2	5/25
G	yes	-2/2	15/200
Ca	yes	2/-2	24/0
DO	yes	-2/2	0/4
X	yes	-2/2	0.1/4

This is however questioned since experimentally, no positive values of the zeta potential were recorded even when high amounts of calcium ions were added to the system (Figure 7.17). It may be therefore considered that the operating conditions maximizing $\Delta Zeta$ were not reliably predicted.

Model simplification

The analysis of the simplified model showed relatively many relevant model terms (equation (7.16)), including e.g. all the first-order terms, some mixed effects and the second-order effect of Ca, DO and X. It is also difficult to predict from the simplified models, which are the most relevant model terms since all model coefficients have values in the same order of magnitude indicating that all terms are almost equally important. It may therefore be concluded from the simplified model that $\Delta Zeta$ shows a complex behaviour in which all factors play a role on the given response.

$$R(\Delta Zeta) = 11.81 - 1.11 \cdot T - 1.33 \cdot G + 1.20 \cdot Ca - 1.82 \cdot DO - 2.53 \cdot X - 2.83 \cdot T \cdot Ca + 5.25 \cdot G \cdot X - 5.74 \cdot Ca \cdot DO + 3.23 \cdot DO \cdot X - 2.85 \cdot Ca^2 + 3.25 \cdot DO^2 + 2.86 \cdot X^2 \quad (7.16)$$

7.4.2. Final Zeta Potential

Since the analysis of $\Delta Zeta$ showed a rather complex model in which almost all factors had a contribution to the response variation, it may be of interest to evaluate as well the model only considering the final value of the zeta potential.

The model obtained in this case has the form given by equation (7.17):

$$R(Zeta) = -6.97 + 1.80 \cdot T - 0.88 \cdot G + 1.41 \cdot Ca + 0.35 \cdot DO - 0.59 \cdot X + 0.62 \cdot T \cdot G - 1.30 \cdot T \cdot Ca - 0.06 \cdot T \cdot DO + 0.89 \cdot T \cdot X + 0.33 \cdot G \cdot Ca + 0.49 \cdot G \cdot DO + 0.45 \cdot G \cdot X + 0.15 \cdot Ca \cdot DO - 0.27 \cdot Ca \cdot X - 0.14 \cdot DO \cdot X + 0.45 \cdot T^2 - 0.37 \cdot G^2 - 1.18 \cdot Ca^2 + 0.96 \cdot DO^2 + 1.26 \cdot X^2 \quad (7.17)$$

Statistical analysis

The statistical analysis presented in Appendix 7.4 shows a less accurate model ($R^2=0.68124$) as compared to the model for $\Delta Zeta$. However, the P-value = 0.93293 obtained shows that there is no significant lack-of-fit for this model. The relatively low value of the regression coefficient is attributed to the large data scattering observed for the replicated central points experiments, characterised by a pure error with a mean-square of 14.403 (Figure 7.17).

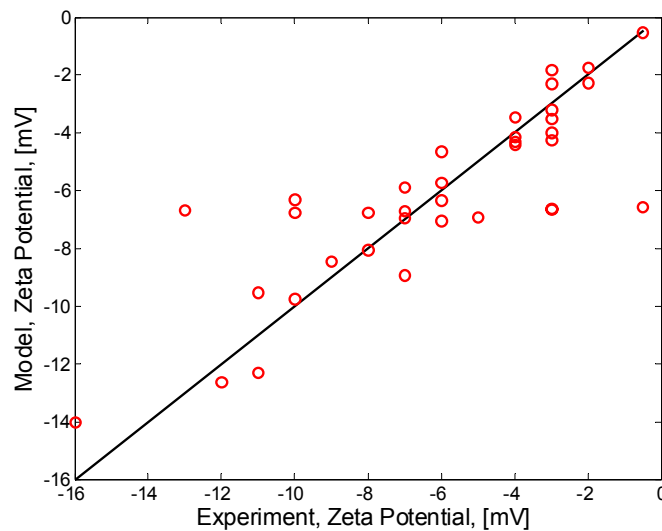


Figure 7.17 Model vs experiment for the Zeta response.

Model simplification

By simplifying the model (equation (7.18)), it is observed that the model was simplified more than the one corresponding to $\Delta Zeta$ due to its very low $R^2_{adj}=0.256$.

$$R(Zeta) = -6.86 + 1.79 \cdot T + 1.38 \cdot Ca - 1.28 \cdot T \cdot Ca - 1.18 \cdot Ca^2 + 0.99 \cdot DO^2 + 1.22 \cdot X^2 \quad (7.18)$$

The simplified model indicates that G does not have a significant effect on the final zeta potential values. Moreover, DO and X show a second order effect yielding minimum response values at $DO = 0$ and $X = 0$ on the normalised scale (corresponding to the real values of $DO = 2$ mg/l and $X = 0.63$ g/l). The predicted minima depend on the particular values of T and Ca.

Calcium addition showed the most complex effect, while temperature occurred as a linear effect (both main effect and interaction with Ca). This finding is in agreement with other data reported in literature (e.g. Keiding and Nielsen, 1997) where it has been concluded that calcium is one of the most important factors responsible for the charge neutralisation effect.

In order to evaluate the Ca effect in more detail, some physical limitations should be taken into consideration. It should be considered that normalised values smaller than -2 are physically impossible as it may represent negative concentrations of calcium. The coefficient of Ca^2 is negative, which means that the response has a maximum for a value $Ca=Ca_0$. For $Ca < Ca_0$ the response will increase with increasing Ca, whereas for $Ca > Ca_0$ the response decreases with increasing Ca. These considerations are valid when all the other factors are maintained constant. The model can be written as:

$$R(\text{Zeta}) = -1.18 \cdot Ca^2 + (1.38 - 1.28 \cdot T) \cdot Ca + (-6.86 + 1.79 \cdot T + 0.99 \cdot DO^2 + 1.22 \cdot X^2) \quad (7.19)$$

and the value of Ca_0 is:

$$Ca_0 = \frac{-1.38 + 1.28 \cdot T}{2 \cdot (-1.18)} = 0.58 - 0.54 \cdot T \quad (7.20)$$

From equation (7.20), it is observed that the value of Ca that maximises the zeta potential depends on the temperature. Fixing the temperature at a value $T = 0$ (normalised scale), the maximum response value occurs for a normalised calcium value $Ca_0 = 0.58$ ($Ca_0 = 15.48$ meq/l). From a physico-chemical viewpoint, a decrease of the absolute value of the zeta-potential with the Ca concentration is commonly reported (Keiding and Nielsen, 1997), eventually followed by a saturation when Ca reaches high concentration levels. Since for the ascendant part of the absolute value of the zeta potential (i.e. for $Ca > Ca_0$) as function of Ca concentration, the model and experiment agree well, the exact reason of this behaviour is not clear. A possible cause could be attributed to the measurements errors in the experimental design points, errors which also propagates into the model. As alternative possibilities, the charge neutralisation effects, often related to the formation of the bridging between cations and EPS or other particulate materials carrying negative charges, are not directly related to the amount of calcium added. It therefore appears that after the system reached a saturation level, a supplementary calcium addition will have a reverse effect on the zeta potential values. Mikkelsen and Keiding (2002) showed that the zeta potential increases in absolute value with an increasing content of the EPS and a stabilising effect in the floc structure occurred even if the zeta potential was high. Above the saturation level of the system with calcium ions, a release of the EPS or other charge destabilisation process may have eventually occurred. However, possible causes relating the direct effect of calcium on charge neutralization cannot be fully proved with the available data. This remains a possible topic for further research.

If all the factors (except $Ca=0.58$) are considered equal to zero on the normalised scale, then a response value evaluated to $Zeta = 0.40$ mV is obtained. Since the obtained zeta potential value corresponds to a nearly complete neutralization of the electrical charge, it may be considered that under the imposed (nominal) operating conditions the addition of 15.48 meq/l Ca^{2+} would represent the saturation level of the system with calcium ions. In agreement with, the floc size dynamics evaluated in section 6.3.3 revealed that an increasing of the calcium concentration in the system was not direct proportional with an increase of the floc size and a saturation level occurred, stabilising the flocs size. Therefore, the Zeta target of 0 mV is retained for process optimisation of a larger set of responses. However, the predicted dependence on the Ca addition showed that the charge neutralization is not uniquely determined by the Ca concentration alone, especially if the temperature approaches zero (scaled value) and therefore it may be possible that an optimum dose of calcium (to maximize zeta) would not necessarily correspond to a complete charge neutralization of the activated sludge. Similar observations were made by Mikkelsen and Keiding (2001) in their study of the optimal polymer dosage necessary for sludge dewatering.

7.4.3. Conclusions

A statistically satisfactory model was constructed for the case in which $\Delta Zeta$ was considered as response. The obtained model turned out to be rather complex, as most of the model terms survived the model simplification algorithm. However, the box constrained model maxima suggested that the supernatant was positively charged. This response did not correspond with

optimal operating conditions, i.e. reducing the amount of colloids in the supernatant for a more effective flocculation process.

When only the final zeta potential is considered instead, a more 'aggressive' model simplification was possible. The simplified model indicated a complex effect of Ca and showed that it is not the only factor being responsible for charge neutralisation. When the response variation was evaluated merely as a function of the calcium ions addition while keeping the other factors at the nominal values of the central point, it was observed that a calcium concentration of 15.48 meq/l yielded an almost complete charge neutralisation. However, under the same conditions a calcium addition over the saturation level was found to create an increase in the absolute value of the zeta potential. A precise cause of this behaviour can not be clearly deduced from this study.

From the obtained RSM models it seems difficult to find a link between the zeta potential variation as predicted by the models and the effectiveness of the flocculation process. It seems however that for this case the destabilization mechanisms which occur during the flocculation process are not mainly produced by charge effects and can not be described fully by using the zeta potential.

Although charge neutralisation may not be a requirement for the evaluation of the destabilisation process as observed for this particular case of the SBR sludge, the zeta potential can be used to improve the process relying on the calcium effect.

7.5. Turbidity

The supernatant turbidity represents a parameter that is often linked with the quality of the effluent and the effectiveness of the clarification step. Suspended matter giving rise to turbidity include bacteria, algae, viruses macromolecules and material derived from organic soil matter, mineral substances, many industrial pollutants and so on. Hence, it is evident that any decrease in turbidity involves the removal of a wide variety of substances. Turbidity measurements are however strongly influenced by the nature, size, concentration and refractive index of the particles.

In this section the turbidity will be evaluated as a response and the influence of the considered factors on the removal of suspended solids from the supernatant is investigated. Accordingly, similar to the other considered cases the Δ turbidity and final turbidity will be considered for evaluation.

7.5.1. Δ Turb

In this study, the turbidity of the supernatant was measured after 30 minutes of settling before and after the flocculation process. As a first variable the difference between the measured final supernatant turbidity after the flocculation and the initial supernatant turbidity, i.e. Δ Turb, was considered.

Statistical analysis

The coefficients of the model terms and their statistical analysis are presented in Appendix 7.5.

The obtained model showed that the coefficients values are all situated in the same range, which makes it difficult to evaluate the relevance of the terms. This can be clearly seen in the bar plot (Figure 7.18).

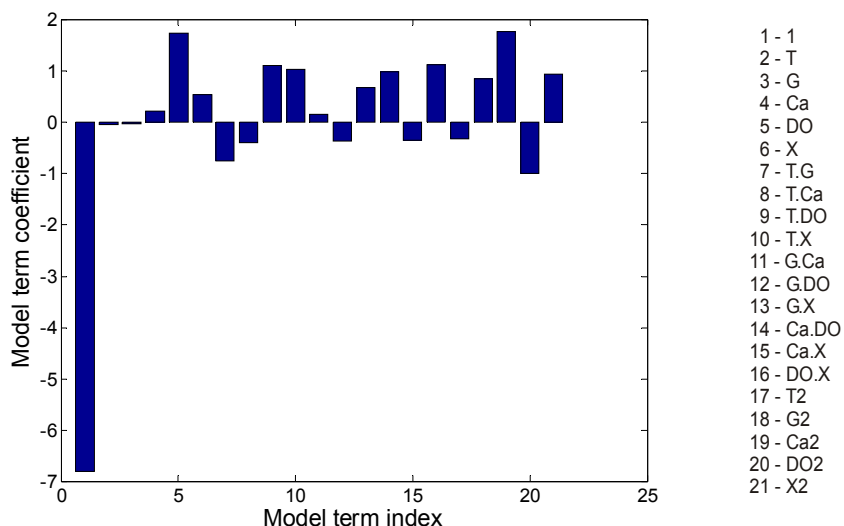


Figure 7.18 Model terms contribution to the Δ Turb response.

The model shows a rather bad fit ($R^2 = 0.33542$ and $R^2_{adj} = -0.55069$) corresponding to an inaccurate model (Figure 7.19). The very high P-value (0.97795) also indicates that the second-order polynomial model is not able to explain the response variation. Consequently, a full analysis of the obtained model is not recommended. The model versus errors plot in Figure 7.19 suggests a large measurement error in the central point of the experimental design as well as the presence of some outliers, which determined the poor model fit. Quantitatively, the ANOVA analysis indicated a mean square of the pure error of about 36, which is twice as large as the mean squared error of the entire regression.

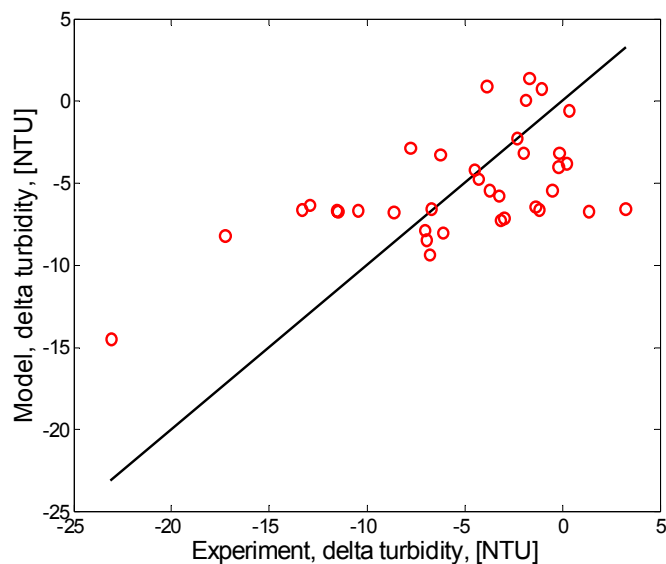


Figure 7.19 Δ Turb values predicted by the model vs experimental values.

Model simplification

When simplifying the model (equation (7.21)) it turned out that Δ Turb merely depends on the quadratic term of the sludge concentration:

$$R(\Delta Turb) = -6.48 + 1.84 \cdot X^2 \tag{7.21}$$

The simplified model suggests that there is a minimum response value, which can be obtained for $X = 0$ on the normalised scale. This suggests that, irrespectively of the other imposed conditions, the least turbid supernatant is obtained for $X=0.63\text{g/l}$ and for any other sludge concentration the supernatant turbidity will increase. This observation may not be valid in practise since it contradicts many of the studies performed in literature.

Moreover, the turbidity values are often linked to a series of other factors such as: dissolved oxygen concentration (Sürücü and Çetin, 1989; Rasmussen et al., 1994; Wilén, 1999), average velocity gradient (Mikkelsen and Keiding, 1999), temperature (Vogelaar et al., 2002); cation addition (Sanin and Vesilind, 2000; Bott and Love, 2002). However, the simplified model does not predict these dependences. Therefore, this response cannot be reliably investigated with the DOE/RSM techniques.

7.5.2. Final turbidity

The second order polynomial model obtained when the final turbidity (Turbidity) was considered is given by equation (7.22).

$$\begin{aligned}
 R(\text{Turbidity}) = & 5.54 - 1.89 \cdot T + 0.42 \cdot G - 0.17 \cdot Ca - 0.76 \cdot DO - 1.09 \cdot X + 0.01 \cdot T \cdot G \\
 & + 0.44 \cdot T \cdot Ca + 0.63 \cdot T \cdot DO - 0.02 \cdot T \cdot X - 1.28 \cdot G \cdot Ca + 1.29 \cdot G \cdot DO \\
 & + 1.39 \cdot G \cdot X - 0.35 \cdot Ca \cdot DO - 0.98 \cdot Ca \cdot X + 1.62 \cdot DO \cdot X \\
 & - 0.78 \cdot T^2 + 0.55 \cdot G^2 - 0.64 \cdot Ca^2 - 0.02 \cdot DO^2 - 0.80 \cdot X^2
 \end{aligned} \tag{7.22}$$

Statistical analysis

Statistical analysis revealed a better regression quality ($R^2 = 0.60429$ and $R^2_{\text{adj}} = 0.07668$) in comparison with ΔTurb , but still the model has a high P-value=0.4 which is too high for the model to be considered as good. Therefore, the statistical analysis of the models obtained in both considered cases (i.e. ΔTurb and Turbidity) suggests that the models cannot describe the response with enough accuracy. It seems therefore that the experimental errors played an important role in the precision of the results. However, the final turbidity response model will be shortly analysed, even though the results should be regarded with precaution.

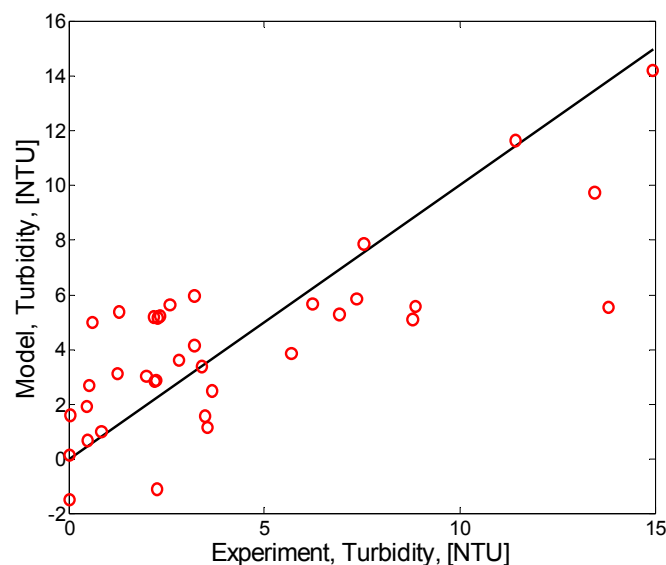


Figure 7.20. Model vs experiment fit for the final turbidity.

Identification and analysis of the stationary point

The value of the response at the stationary point is 11.23 NTU and the corresponding factors are presented in the following table:

Table 7.9 The stationary points for the model factors.

Factor	Stationary point (scaled)	Stationary point (unscaled)
T	-3.26	-1.32
G	2.54	283.66
Ca	-2.13	-0.77
DO	-3.69	-1.69
X	-0.85	0.28

The canonical form obtained by calculating the characteristic roots is given by equation (7.23) and indicates that the stationary point is a saddle point.

$$\hat{R}(\text{Turbidity}) = 11.23 - 1.45w_1^2 - 1.09w_2^2 - 0.70w_3^2 - 1.48w_4^2 + 1.71w_5^2 \quad (7.23)$$

For practical reasons, very low values of the final turbidity (close to 0) would indicate a good quality of the supernatant. So, the response optimisation is to find the operating conditions, i.e. factors, for which the response is minimised.

Hence, the target was set at Turbidity = 0 NTU. The optimisation algorithm returned an objective function value very close to zero, indicating that it is not possible to find a unique solution and that by setting the initial point to a different value another different point would be obtained.

A target value of 100 NTU gave two possible maximal values calculated for the constrained factors (Table 7.10).

Table 7.10 Operating conditions for obtaining a maximum value of final turbidity.

Response Turbidity(NTU)	19.82			10.26		
	Active constrains	Scaled value	Unscaled value	Active constrains	Scaled value	Unscaled value
Factor						
T	yes	-2	5	-	-1.59	7.04
G	yes	-2	15	yes	2	200
Ca	-	-0.252	10.48	-	-1.24	4.55
DO	yes	-2	0	yes	-2	0
X	yes	-2	0.1	-	-0.89	0.276

The results show that a turbidity of 10.26 NTU may be obtained at high average velocity gradient values and under anaerobic conditions. These observations are in agreement with Wilén (1999), who observed that the highest increase of effluent turbidity occurred under oxygen limitation and at higher shears. However, being not a singular value for the maximal turbidity, as shown in Table 7.10, a high turbidity (19.82 NTU) can also be obtained at low average velocity gradient values and under anaerobic conditions. In this case, it seems that a larger addition of calcium is required as compared to the case in which the final turbidity measures 10.26 NTU. It should be taken into account that both turbidity values are obtained for very low sludge concentrations and are probably due to the very low collision rate between the particles. This is in agreement with the investigations of the floc size at low sludge concentration, which showed a smaller flocculation effect (section 6.3.2.).

An example of a fitted surface by using the optimal values is given in Figure 7.21. It is observed that the variation of the response as function of Ca and X behaves as a rising ridge

that shows maximum turbidity values for low sludge concentrations and high concentrations of calcium. It is however observed that the calcium concentration becomes less important as the sludge concentration increases. It seems that the lowest turbidity values are obtained for a high sludge concentration.

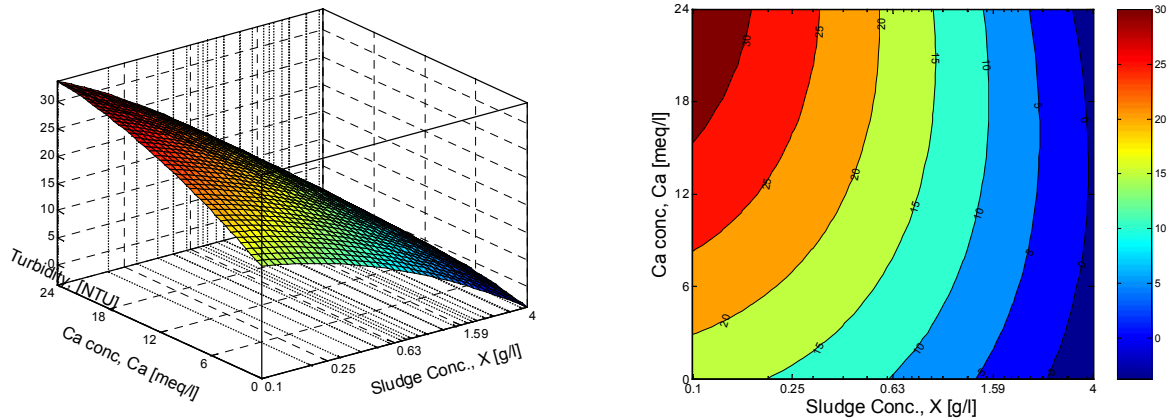


Figure 7.21 Final turbidity variations as function of Ca and X when the other factors were set at the values found for an optimal turbidity value of 19.82 NTU.

Model simplification

The simplified model does not show second-order contribution of the factors. The Ca effect seems to be insignificant as well, since all its terms were eliminated. However, according to Zita and Hermansson (1994) the supernatant turbidity depends of the ionic strength in the medium. Previous evaluations in this work (section 6.3.3. and respectively sections 7.2. and 7.4) also showed that Ca positively affects the floc size and supernatant zeta potential. These suggest a lower turbidity as a consequence, although the model shows the opposite, i.e. Ca has no effect. Further, according to the model, an increase of temperature would create a linear decrease of the response. The effect of G, DO and X showed to be dependent on the variation between these terms.

$$R(\text{Turbidity}) = 4.56 - 1.80 \cdot T + 0.41 \cdot G - 0.85 \cdot DO - 1.29 \cdot X + 1.46 \cdot G \cdot DO + 1.56 \cdot G \cdot X + 1.85 \cdot DO \cdot X \quad (7.24)$$

6.5.3. Conclusions

The evaluation of the supernatant turbidity revealed that the response cannot be reproduced with enough accuracy by a second-order polynomial model. The too large experimental errors may be the cause of the observed poor fit of the analysed models to the experimental data. Due to this, the evaluation of the factors' effect on the supernatant turbidity has to be interpreted with care.

For the case in which the final supernatant turbidity was considered as response, the model improved statistically but it still shows not to be a very good model to correctly evaluate the turbidity variation. According to the model predictions, anaerobic conditions and very low sludge concentrations are mainly responsible for high supernatant turbidities. It was also suggested that the Ca effect on the supernatant turbidity is relatively insignificant, which has not been supported by previous observations.

7.6. Supernatant suspended solids concentration

Taking into account that the response surface modelling of turbidity showed some lack-of-fit error, an evaluation of the supernatant total suspended solids (TSS) concentration may be an alternative approach.

7.6.1. ΔTSS

Statistical analysis

From the calculation of the model coefficients (Figure 7.22 and Appendix 7.6) it can be observed that most of the terms have a relevant contribution to the model.

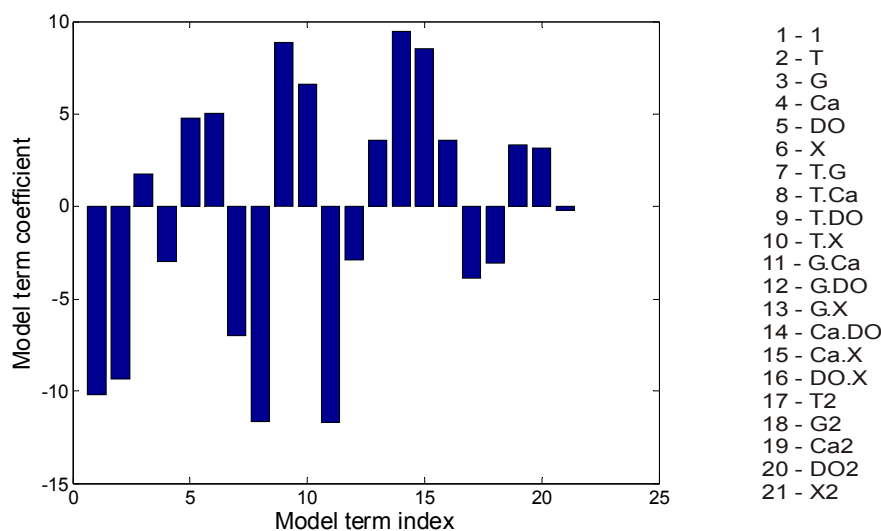


Figure 7.22 Contribution of the model terms to the ΔTSS response.

In Figure 7.23, the response values predicted by the model are plotted against the measured values. The corresponding regression coefficient was $R^2 = 0.7081$, which can be considered as satisfactory fit when accounting for the possible off-line sampling or experimental errors.

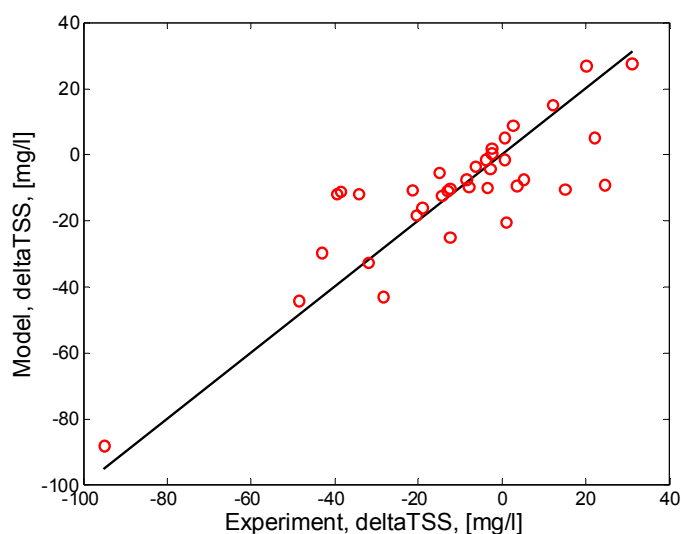


Figure 7.23. Model vs. experiment scatter plot.

Identification and analysis of the stationary point

The factor values corresponding to the stationary point are listed in Table 7.11. The model value of ΔTSS at the stationary point is -19.51 mg/l.

Table 7.11 Factor values for the stationary point.

Factor	Stationary point (scaled)	Stationary point (unscaled)
T	-0.1325	14.337
G	-2.6377	10.112
Ca	-0.5536	8.678
DO	2.1124	4.112
X	-5.3527	0.004

The canonical form is presented by equation (7.25). Its analysis shows that the stationary point is a saddle point situated outside the experimental region.

$$\hat{R}(\Delta TSS) = -19.51 - 14.41w_1^2 - 2.71w_2^2 + 0.37w_3^2 + 4.82w_4^2 + 11.22w_5^2 \quad (7.25)$$

To determine optimal operational conditions also should consider that highly negative values of ΔTSS will indicate a better removal of particles by sedimentation. It is therefore of interest to find the operating conditions that minimise the response.

Two optimal points were found by optimising the response, as summarised in Table 7.12. To obtain these two minimal response values, all factors were actively constrained. The two optima switch from one side of the experimental box to the other.

The values related to the minimal response indicate that for low values of temperature and average velocity gradient and high sludge and dissolved oxygen concentrations calcium addition does not improve supernatant quality. However, a second minimal value showed that when operating the reactor at low sludge concentrations, anaerobic conditions, high average velocity gradient and temperature, calcium is required to neutralise the large deflocculation effect created by the imposed conditions. In this case the cations bridging phenomenon occurs.

Table 7.12 Optimisation parameters for minimum response.

Response deltaTSS(mg/l)	-215.45			-297.10		
	Active constraints	Scaled value	Unscaled value	Active constraints	Scaled value	Unscaled value
T	yes	-2	5	yes	2	25
G	yes	-2	15	yes	2	200
Ca	yes	-2	0	yes	2	24
DO	yes	2	4	yes	-2	0
X	yes	2	4	yes	-2	0.01

An example of the response as function of G and Ca is given in Figure 7.24. It clearly shows that a minimum response is obtained by keeping both the average velocity gradient and Ca concentration as low as possible. The Figure 7.24 also indicates that by increasing the calcium concentration the response becomes less dependent on G.

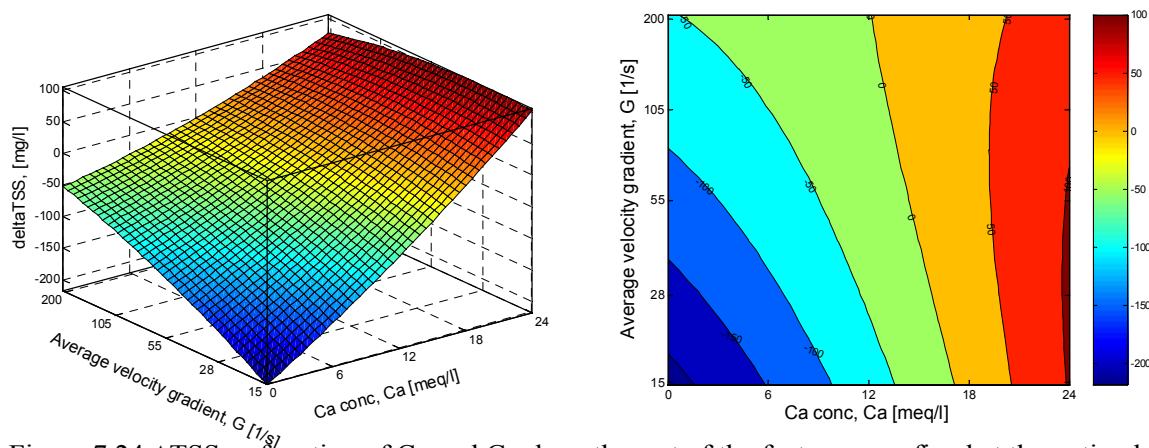


Figure 7.24 Δ TSS as function of Ca and G where the rest of the factors were fixed at the optimal values ($T = 5^{\circ}\text{C}$; $\text{DO} = 4 \text{ mg/l}$ and $X = 4 \text{ g/l}$).

Model simplification

The simplified model gives the following expression:

$$R(\Delta\text{TSS}) = -11.18 - 9.63 \cdot T + 1.66 \cdot G - 2.81 \cdot \text{Ca} + 5.20 \cdot \text{DO} + 6.06 \cdot X - 6.98 \cdot T \cdot G - 11.64 \cdot T \cdot \text{Ca} + 8.51 \cdot T \cdot \text{DO} - 11.61 \cdot G \cdot \text{Ca} + 9.66 \cdot \text{Ca} \cdot \text{DO} + 8.59 \cdot \text{Ca} \cdot X \quad (7.26)$$

It may be observed that all quadratic terms in the model vanished and the simplified model only shows first order dependencies and combined terms. Since the model obtained for the case of turbidity variation was less accurate, a comparison between the factors influence in the turbidity and TSS models cannot be reliably performed.

To investigate a possible link between TSS and floc size an analysis of the first-order effects was performed. The factors were kept at the nominal point (central point design). The model indicated the following:

- An increase of the temperature results in a decrease of Δ TSS. This is however, not in agreement with the observed temperature effect on the floc size dynamics, which showed a slight deflocculation at increasing T . Literature studies also discuss that as temperature increases it produces a rise of the effluent suspended solids concentration (Morgan and Allen, 2003).
- By increasing the average velocity gradient, an increase of Δ TSS occurred. Taking into account the large deflocculation effect at high mixing intensities (see section 6.3.1.) the predicted effect agrees with the previous findings of this work and with the available literature data (Das et al., 1993; Galil et al., 1991; Wilén, 1999).
- Adding Ca to the reactor results in a lower effluent TSS. This is expected as flocculation improves when calcium is added to the system.
- An increase of the DO results in an increase of the effluent TSS. Since short-term changes of DO did not significantly affect the floc size dynamics, a link between those two parameters cannot be directly established. According to Wilén (1999), anaerobic conditions deteriorated supernatant quality, but this is not confirmed by the model.

From the above observations, it can be concluded that a direct link between the floc size dynamics, evaluated under similar conditions, and the supernatant TSS cannot be always found. It seems that only the factors that had a large effect on the floc size (e.g. G and Ca) showed a similar effect on the TSS. The effect of the other factors on the floc sizes did not

show the same expected trend on TSS. However, it may also be possible that the model prediction is not accurate enough for all the considered factors since some of the results do not agree with other literature data.

7.6.2. Final TSS

For the case in which the final TSS, measured after the flocculation experiment, was considered as a response, the generalised as well as the simplified second-order polynomial model resulted are given by equation (7.27) and equation (7.28) respectively.

$$\begin{aligned}
 R(TSS) = & 38.49 - 1.93 \cdot T + 2.82 \cdot G + 2.86 \cdot Ca - 3.69 \cdot DO + 0.68 \cdot X - 0.51 \cdot T \cdot G \\
 & + 5.57 \cdot T \cdot Ca - 3.48 \cdot T \cdot DO + 1.35 \cdot T \cdot X - 2.30 \cdot G \cdot Ca - 4.97 \cdot G \cdot DO \\
 & - 1.38 \cdot G \cdot X - 1.41 \cdot Ca \cdot DO - 2.51 \cdot Ca \cdot X + 9.78 \cdot DO \cdot X \\
 & - 0.42 \cdot T^2 - 1.52 \cdot G^2 - 0.62 \cdot Ca^2 + 3.12 \cdot DO^2 - 0.53 \cdot X^2
 \end{aligned} \tag{7.27}$$

$$R(TSS) = 38.10 - 3.48 \cdot DO + 0.80 \cdot X - 9.83 \cdot DO \cdot X \tag{7.28}$$

The full model is characterised by a very low regression coefficient ($R^2 = 0.4454$), explained by the relatively high pure error (MeanSq=524.13), which occurs due to the large variations of the measurements performed in the central point (Figure 7.25). The detailed statistical analysis, the stationary point and the model optimisation are presented in Appendix 7.6. The simplified model of the final TSS shows that only the first order effect of DO and X, and their interaction have an influence on the response variation. However, this simplified form is hardly supported by previously reported results.

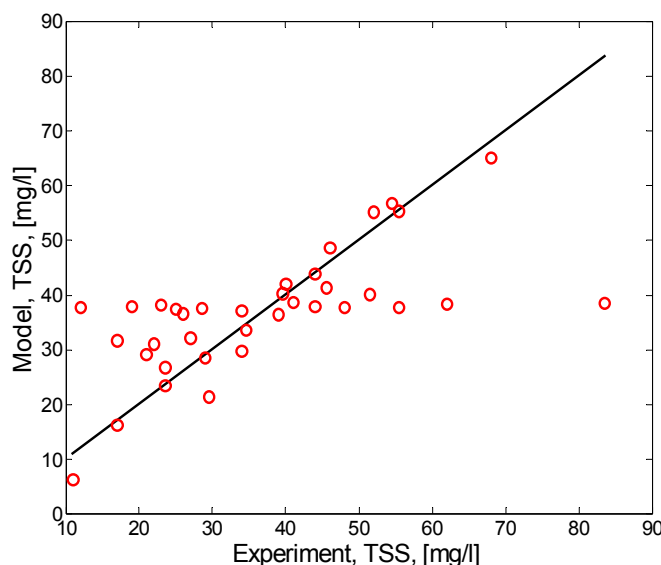


Figure 7.25 Model vs experiment for the final TSS.

The observed differences between the model predictions of ΔTSS and final TSS are considered to be due to variations of the supernatant TSS measured before performing the flocculation experiments.

Due to the relatively low statistical significance of this model, it is concluded that considering TSS as the response of a second-order polynomial model will not give a precise evaluation of the response variations as function of the considered factors.

7.6.3. Conclusions

The analysis of the supernatant total suspended solids concentration by means of DOE and RSM, revealed that the model does not describe the response variations accurately enough and not all the observed effects are in agreement with previous observations and literature data. It seemed that a link between the observed floc size dynamics and supernatant TSS could only be found for the factors which had a sufficiently strong effect on the floc size. For the other factors, the predicted effect was opposite to the trend observed for the floc size.

When the response minimisation was performed, the resulting operating conditions showed that the Ca effect was much more effective than the average velocity gradient. As expected, a minimal TSS at high mixing intensities is only possible when at the same time high calcium concentrations prevail.

The model simplification by using AIC revealed the relevance of all the linear model terms. No quadratic effect survived the simplification procedure.

When considering the final TSS as response, the model shows less statistical relevance as compared to Δ TSS. Model simplification yielded only the relevance of the first-order terms in DO and X, which does not agree with the previous results related to the other factor influences on final TSS.

7.7. Conductivity

An increase of the conductivity is usually associated with a proportional increase of the ions concentration in the solution. In this study, the conductivity was monitored on-line during the (de)floculation process. Since the conductivity mainly represents a measure of the total amount of ions in the solution it may be expected that the calcium addition will have a relevant influence on the conductivity measurements. In this context, Zita and Hermansson (1994) found that the changes in conductivity can rapidly influence the floc formation. However, other factors may have an influence on the conductivity variation as well. This will be investigated further on by considering the conductivity as response.

7.7.1. Δ Conductivity

Firstly, the Δ Conductivity is considered. Similar to the floc size evaluation by $\Delta D[4,3]$, the Δ Conductivity is defined as the difference between the average conductivity values measured when the steady state floc size distribution was obtained and the one measured initially in the flocculation reactor.

Statistical analysis

The highest contribution to Δ Conductivity, as shown in Figure 7.26, comes from Ca. An increase of Ca results in an increase of the response, due to its positive coefficient. However, the linear effect of Ca is not the only way in which this factor influences the response. For instance, the quadratic term in Ca, acts in the same direction and intensifies the Ca effect on the response. Temperature gives the second largest main effect. By analysing the generalised model, it can however be observed that the other factors have a smaller effect on the response as compared with Ca and T. It should be noted that the DO showed the lowest influence on the response, suggesting that this factor should be regarded as a less important factor for the considered response.

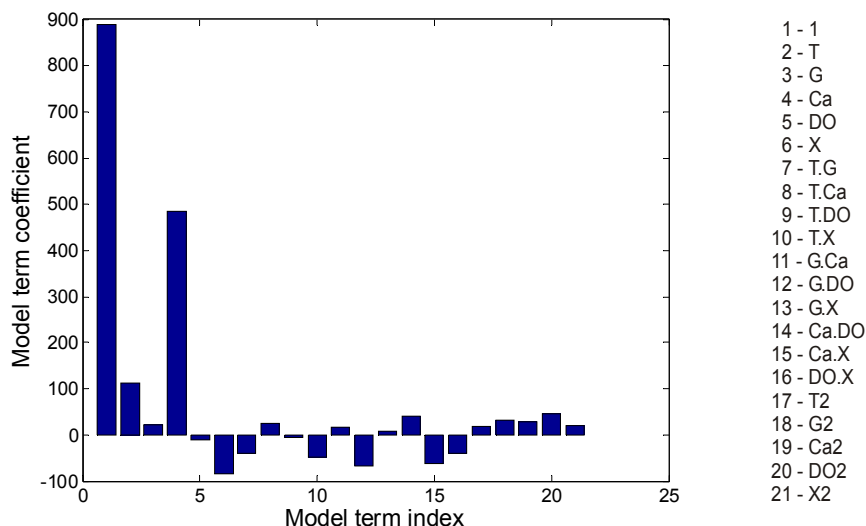


Figure 7.26 Contribution of the model terms to the deltaConductivity response.

The statistical evaluation of the model (Appendix 7.7.) yielded a P-value of only 0.00022. Moreover, the lack-of-fit error had a P-value of 0.6037, indicating that there is no significant lack of model fit error to the experimental data.

The ability of the proposed second-order polynomial model to correctly describe the response is graphically illustrated in the scatter plot of Figure 7.27. The corresponding regression coefficient R^2 measures 0.901, which can be considered a very good result.

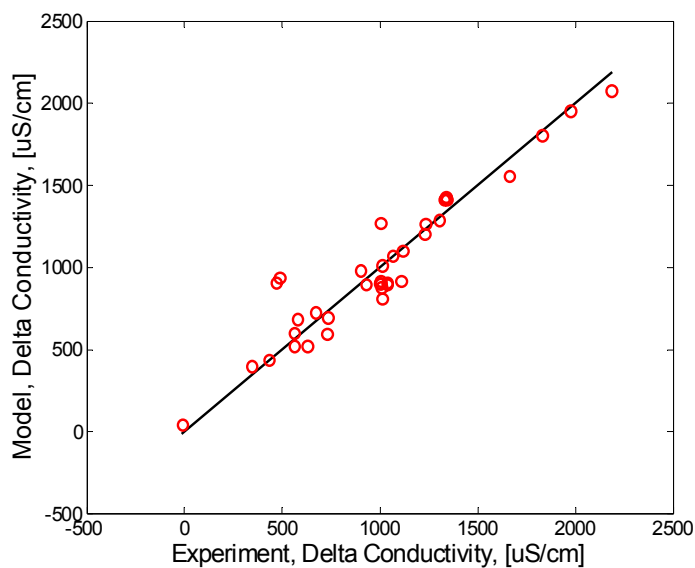


Figure 7.27. Model vs. experiment scatter plot.

Identification and analysis of the stationary point

The model value of the response at the stationary point is 2246.6 $\mu\text{S}/\text{cm}$ and the values of the factors corresponding to the stationary point are listed in Table 7.13.

Table 7.13 The factor values at the stationary point.

Factor	Stationary point (scaled)	Stationary point (unscaled)
T	0.45431	17.272
G	-6.2417	0.99514
Ca	7.9194	59.516
DO	-2.5569	-0.55692
X	12.588	71865.0

The canonical form is found to be:

$$\hat{R}(\Delta\text{Conductivity}) = 2246.6 - 18.938w_1^2 - 8.138w_2^2 + 31.695w_3^2 + 51.223w_4^2 + 94.704w_5^2 \quad (7.29)$$

The canonical form shows that the stationary point is a saddle point. However, most of the values of the factors in the stationary point do not have physical meaning since, as an example negative values for DO or a very high X are impossible to be found in practice. In this context, any model interpretation starting from the stationary point is not feasible.

According to Zita and Hermansson (1994), an increase of the electrolyte concentration determined a corresponding increase of the floc stability and a decrease of the supernatant turbidity. It was suggested that this behaviour depends on the ionic strength values since for very high values, a release of free cells into water occurred. Moreover, van Loosdrecht et al. (1989) showed that the reversible adhesion of bacteria to a surface increased with increasing electrolyte concentrations and finally reached saturation. Based on the above observations, it seems that there is an optimal conductivity, which positively affect the flocculation process. However, this value is difficult to be found in the present case, since the response is almost proportional with the amount of calcium added to the system and therefore it is assumed that an optimal conductivity value will correspond to an optimal calcium concentration value.

Model simplification

Equation (7.30) shows the simplified model for normalised factors.

$$R(\Delta\text{Conductivity}) = 990.47 + 118.02 \cdot T + 485.75 \cdot Ca - 92.72 \cdot X \quad (7.30)$$

The simplified model shows that the response is only dependent on linear variations of temperature, calcium and sludge concentration. Since the model was built with normalised factors, the highest contribution arises from the calcium concentration; this was also found for the complete model. The model confirms the direct proportionality, which exists between the Ca concentration and the conductivity. It was further observed that an increase in temperature leads to an increase of the response as well. The linear effect of the sludge concentration (log-normalized scale) is proportional with the response variation as well. An increase of the sludge concentration will create a decrease of the $\Delta\text{Conductivity}$ value. This may be due to the fact that at high sludge concentration the flocs create cation bridges and the adsorption capacity increases, leading to a decrease of the dissolved salt concentration.

An example of a fitted response surface is given in Figure 7.28 and shows the response as function of G and Ca. It is clearly seen that the variation of the response mainly depends on the Ca concentration, while G has only a small effect.

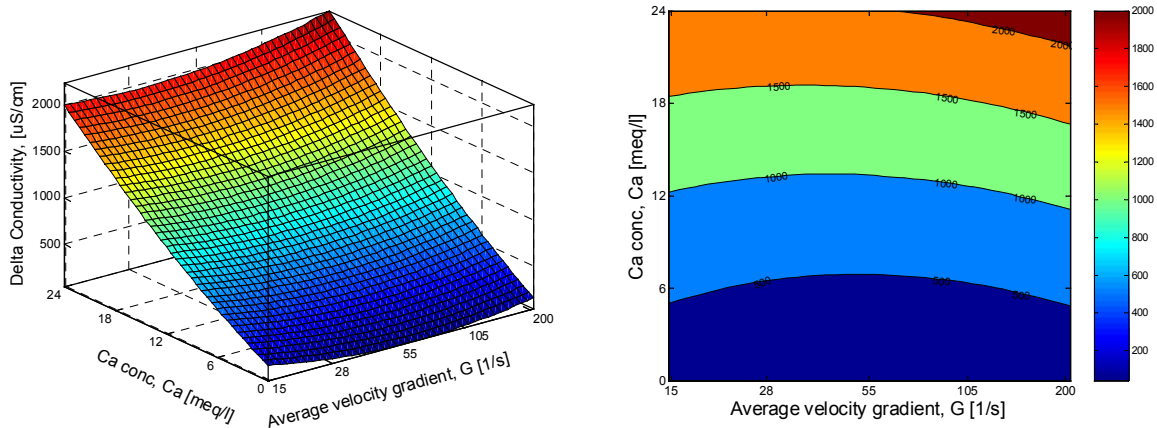


Figure 7.28 The Δ Conductivity as function of G and Ca . The rest of the factors were set to their nominal values ($T = 15^\circ\text{C}$, $\text{DO} = 2 \text{ mg/l}$ and $X = 0.63 \text{ g/l}$).

7.7.2. Final conductivity

As in the previous cases, the final conductivity measured at the steady-state floc size distribution was investigated as well. It resulted in a quadratic polynomial response model.

The complete evaluation of this response is presented in Appendix 7.7. Similar to the case of Δ Conductivity, the quality of the obtained model was very good with $R^2 = 0.8735$ showing no lack-of-fit (P -value = 0.935). However, looking at the scatter plot (Figure 7.29) it seems that one outlier is mainly responsible for the small decrease of the regression coefficient as compared to the one obtained for Δ Conductivity.

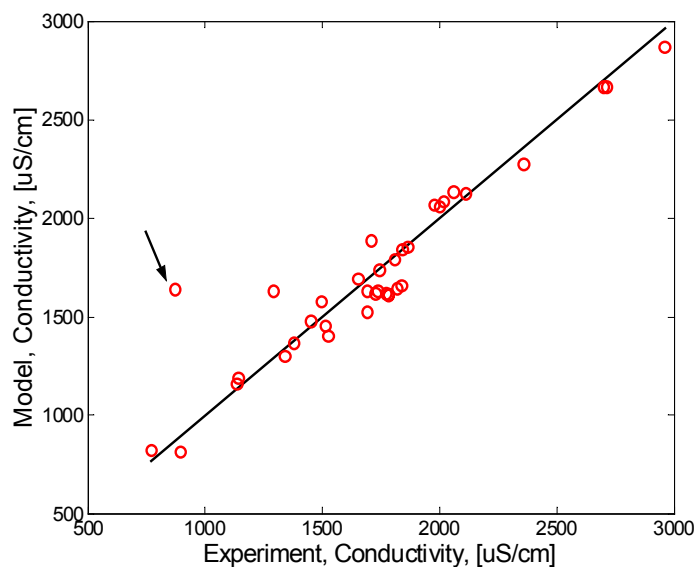


Figure 7.29 Model vs experiment for the final conductivity response.

The model obtained is presented in equation (7.31) and the simplified one in equation (7.32).

$$\begin{aligned}
 R(\text{Conductivity}) = & 1613.84 + 173.71 \cdot T + 67.38 \cdot G + 466.80 \cdot Ca - 16.41 \cdot \text{DO} - 57.55 \cdot X \\
 & - 62.34 \cdot T \cdot G - 0.73 \cdot T \cdot Ca - 2.43 \cdot T \cdot \text{DO} - 92.37 \cdot T \cdot X - 12.25 \cdot G \cdot Ca \\
 & - 79.03 \cdot G \cdot \text{DO} - 39.67 \cdot G \cdot X + 83.19 \cdot Ca \cdot \text{DO} - 111.06 \cdot Ca \cdot X \\
 & - 1.07 \cdot \text{DO} \cdot X + 37.22 \cdot T^2 + 45.29 \cdot G^2 + 35.67 \cdot Ca^2 + 34.11 \cdot \text{DO}^2 + 6.48 \cdot X^2
 \end{aligned} \tag{7.31}$$

$$R(\text{Conductivity}) = 1716.58 + 183.17 \cdot T + 479.20 \cdot Ca - 54.63 \cdot X - 123.61 \cdot Ca \cdot X \quad (7.32)$$

The generalised model shows the same significant relevance of calcium ions addition followed by the temperature as for the case of Δ Conductivity. As their values increase, the response increases as well. Simplifying the model by AIC results in a model similar to the one obtained for Δ Conductivity. Only the mixed effect of Ca and X appears to have an important effect on the final conductivity. Importantly, similar orders of magnitude of the model coefficients have been obtained, indicating a consistency in the model predictions and high reproducibility of the data.

7.7.3. Conclusions

The analysis of the conductivity by means of DOE and RSM revealed that both Δ Conductivity and final conductivity can be accurately reproduced by a second-order polynomial model. Moreover, the high similarity between those two investigated models suggested that the initial conductivity values did not have an important contribution to the final conductivity values. This gives an indication of a constant amount of ions present initially in the investigated sludge samples.

The simplified models predicted a directly proportional relationship between measured conductivity and the calcium ions concentration, which also appeared to have the strongest effect on the response. Temperature and sludge concentration showed to be relevant as well. According to the model prediction, an increase of the temperature would result in a conductivity increase, corresponding to the fact that the water conductivity is dependent on temperature. Instead, the conductivity decreased when the sludge concentration increased possible due to the fact that at high sludge concentration the flocs create cation bridges and the adsorption capacity increases, leading to a decrease of the dissolved salt concentration. It was also shown that average velocity gradient and dissolved oxygen concentration are insignificant factors.

7.8. pH

The optimal pH for biological wastewater treatment is known to be between 6.5 and 8. Although this optimum may be slightly different for particular industrial effluents, chemical neutralisation is usually required only for strongly acidic or alkaline wastewater prior to its activated sludge treatment. For moderately acidic wastewaters, an activated sludge treatment is possible but the sludge may become rich in fungi (Mikkelsen, 2001), while Jenkins et al. (1993) suggested in this context that low pH values favour the growth of nocardioforms. Treatment of slightly alkaline wastewater may be sometimes easier than on neutral industrial wastewater, as a higher pH usually improves the flocculation of activated sludge (Ganczarzyk, 1983).

Changing the pH values to a range that corresponds to acid or alkaline conditions would create significant effects on the activated sludge affecting its structure and properties. In this respect, Liao et al. (2002) showed that the activated sludge flocs in the pH range of 4.5 to 9.5 were more stable in terms of surface charge than those in a pH below 2. Baldwin and Campbell (2001) found that the pH is temperature dependent and even a short-term decrease of it would affect the microbial population of activated sludge. Mikkelsen (2001) demonstrated that an increase in pH leads to a higher shear sensitivity of the particles.

7.8.1. ΔpH

The pH evolution was monitored on-line during the flocculation experiments. Evaluation of ΔpH and the final pH was performed as well. The ΔpH denotes the difference between the average pH measured at the steady-state floc size distribution at the end of the flocculation experiment and the average pH recorded under the initial conditions.

Statistical analysis

The obtained model shows that the response mainly depends on the linear contribution of temperature, shear and calcium (Figure 7.30,a). It is observed that an increase of temperature or calcium concentration would create a decrease of the response whereas an increase of the average velocity gradient would create an increase of ΔpH .

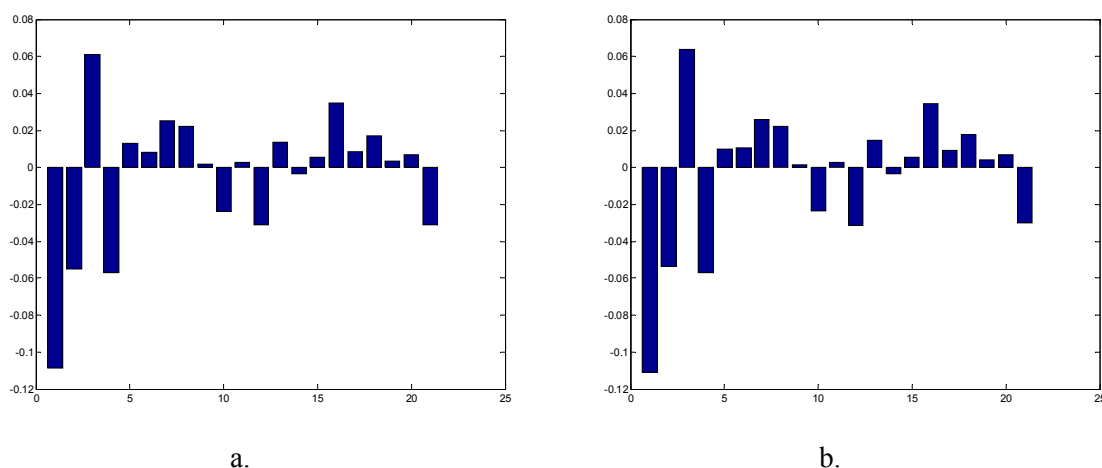


Figure 7.30 Contribution of the model terms to the ΔpH response. a. 36 experiments; b. all experiments except the outliers

The statistical model evaluation indicates a relatively small regression coefficient ($R^2=0.42583$) and a high P-value of 0.8903. In the scatter plot of model vs. experiment it may be observed that two of the experiments performed in the central point gave values that are far from the predicted trend of the other points (Figure 7.31-black arrow). These two points can be considered as outliers. Performing the statistical analysis without taking into consideration those two points, a significant improvement of the model fit was obtained with a regression coefficient of $R^2=0.67997$. However, due to their opposite position relative to the diagonal in the scatter plot, the effect of the outliers is compensated. Indeed, an analysis of the model terms contribution shows highly similar model coefficients (Figure 7.30, b). Due to this observation, the model containing all the experiments will be considered further on. Details regarding the performed statistical analysis are presented in Appendix 7.8.

Identification and analysis of the stationary point

The response value at the stationary point is $\Delta\text{pH}=-0.47$ and the factor values corresponding to the stationary point are listed in Table 7.14. The negative value for DO as well as the very low sludge concentration indicate that the stationary point corresponds to unphysical situations.

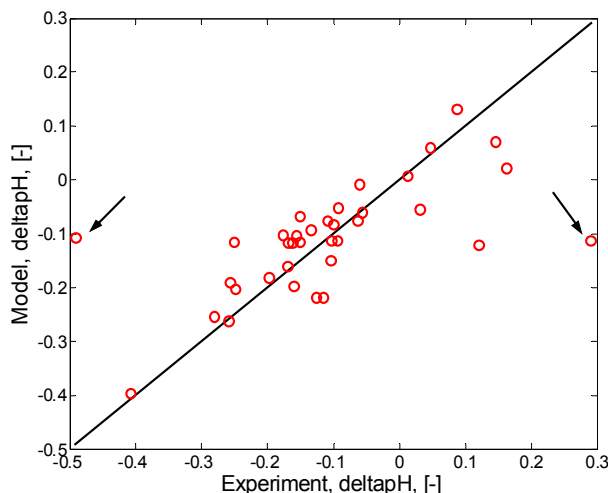


Figure 7.31. ΔpH model vs. experiment scatter plot. The black arrows indicate outliers.

Table 7.14 The factor values at the stationary point

Factor	Stationary point (scaled)	Stationary point (unscaled)
T	2.7801	28.901
G	-5.6983	1.4116
Ca	2.8743	29.246
DO	-3.4782	-1.4782
X	-3.9138	0.01688

The canonical form is found to be:

$$\hat{R}(\Delta pH) = -0.4788 - 0.044w_1^2 - 0.003w_2^2 + 0.004w_3^2 + 0.013w_4^2 + 0.034w_5^2 \tag{7.33}$$

The canonical form indicates that the stationary point is a saddle point.

From a process optimisation point of view the optimal operating conditions are defined by a zero change of pH as, otherwise, it may create a shock effect on the microbial community. By setting the target at ΔpH = 0 and performing the model optimisation, the corresponding objective function gave a value very close to zero. This indicates that it is not possible to find a unique solution and by setting the initial point to a different value, a different set of factors values would be obtained.

However, it may represent interest to evaluate the ΔpH values (minimum and maximum values), occurring when different conditions are imposed. In this way it becomes possible to quantify whether the pH changes are high enough to significantly influence the process. Two different solutions were found for each of the two cases (Table 7.15).

Table 7.15 Optimisation values for minimum and respectively maximum ΔpH

deltapH		0.44/0.55				
Factor	Active constraints	Scaled value	Unscaled value	Active constraints	Scaled value	Unscaled value
T	yes	2/-2	25/5	yes	-2/-2	5/5
G	yes	-2/2	15/200	yes	2/-2	200/15
Ca	-/yes	0.1/2	12.62/24	yes	-2/-2	0/0
DO	yes	-2/2	0/4	yes	-2/2	0/4
X	yes	2/-2	4/0.01	-	-0.04/1.42	0.66/2.33

The predicted relatively low minimal and maximal responses for ΔpH indicate that only a slight variation, at most 1.41, of the pH is expected to occur. It is assumed that these variations are small enough not to affect the flocculation process considerably. The initial average pH (7.48 ± 0.35) was within the recommended operational pH range for the activated sludge process and therefore, the effect of minimal and maximal pH variations may be considered to be too weak to create a harmful effect on the microbial activity.

To decrease the pH value, the Ca concentration is the only one factor which should always be kept at relatively high values. The other factors show variations inside the experimental constrained box from one extreme to another. Instead, a pH increase is obtained by keeping the calcium concentration and temperature as low as possible, while the sludge concentration should take values within the experimental region. The average velocity gradient and dissolved oxygen concentration switch between the maximal and minimal imposed experimental conditions.

Figure 7.32 illustrates an example of the response as function of the calcium and sludge concentration while the other factors were set to the values indicated by the maximal $\Delta\text{pH} = 0.44$. It may be observed that the response decreases by increasing the calcium concentration, while the effect of the sludge concentration is maximal at its middle range values. The surface plot shows that the calcium concentration affects the response more significantly as compared to the sludge concentration.

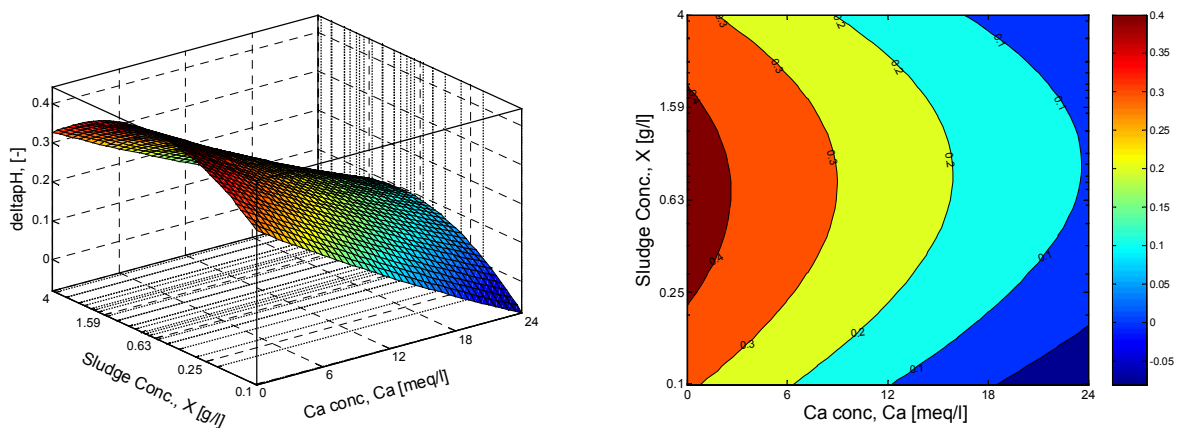


Figure 7.32 The ΔpH variation as function of Ca and X. The other factors were set at the conditions given by $\Delta\text{pH} = 0.44$ ($T = 5^\circ\text{C}$; $G = 200 \text{ s}^{-1}$ and $\text{DO} = 0 \text{ mg/l}$).

Model simplification

Equation (7.34) shows the simplified model for the normalised factors.

$$R(\Delta\text{pH}) = -0.1016 - 0.0548 \cdot T + 0.0592 \cdot G - 0.0576 \cdot Ca + 0.0087 \cdot \text{DO} + 0.0003 \cdot X + 0.0446 \cdot \text{DO} \cdot X \quad (7.34)$$

The response changes linearly with all factors and with a mixed effect of DO and X. By increasing the temperature or calcium concentration a decrease of the response occurs. Any increase in average velocity gradient increases the response due to its positive model coefficient. The DO and X interaction is also relevant.

7.8.2. Final pH

The final pH calculated as the average pH measured at the end of the flocculation experiments will be shortly evaluated as well. Details regarding this response are presented in Appendix 7.8. The obtained model shows an improved regression coefficient ($R^2 = 0.74346$) as compared to the model obtained for ΔpH . The quality of the fitted model improved as well as shown in Figure 7.33. However, one outlier is still observed in the central point (Figure 7.33 – black arrow). This agreed with one of the outlier points also seen for ΔpH . When the outlier is excluded, the regression coefficient increased to $R^2 = 0.8717$. Apparently, neglecting the point significantly changed the model coefficients. Consequently, this is the model considered further on.

As shown in Figure 7.33 the final pH mostly varies between 7 and 8, with only a few values outside this interval. The observed pH is in agreement with the above findings when ΔpH minimal and maximal values were investigated. It therefore may be concluded that the investigated factors did not create significant variations in pH. Hence, no harmful effect on the activated sludge microbial activity or flocculation occurred.

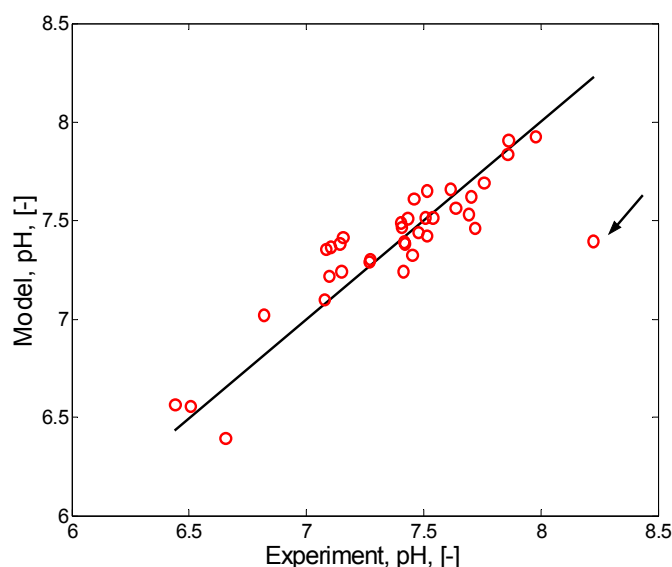


Figure 7.33 Model vs experiment for the final pH response

The pH model obtained by excluding the outlier point is presented in equation (7.35).

$$\begin{aligned}
 R(\text{pH}) = & 7.310 - 0.062 \cdot T + 0.105 \cdot G - 0.047 \cdot Ca - 0.042 \cdot DO - 0.290 \cdot X \\
 & - 0.088 \cdot T \cdot G + 0.096 \cdot T \cdot Ca + 0.116 \cdot T \cdot DO - 0.102 \cdot T \cdot X + 0.055 \cdot G \cdot Ca \\
 & + 0.133 \cdot G \cdot DO - 0.027 \cdot G \cdot X - 0.060 \cdot Ca \cdot DO - 0.013 \cdot Ca \cdot X + 0.028 \cdot DO \cdot X \\
 & - 0.008 \cdot T^2 - 0.090 \cdot G^2 + 0.019 \cdot Ca^2 + 0.055 \cdot DO^2 - 0.090 \cdot X^2
 \end{aligned} \tag{7.35}$$

Using AIC, the model is simplified to:

$$\begin{aligned}
 R(\text{pH}) = & 7.320 - 0.064 \cdot T + 0.102 \cdot G - 0.060 \cdot Ca - 0.042 \cdot DO - 0.279 \cdot X \\
 & - 0.086 \cdot T \cdot G + 0.093 \cdot T \cdot Ca + 0.115 \cdot T \cdot DO - 0.099 \cdot T \cdot X \\
 & + 0.134 \cdot G \cdot DO - 0.092 \cdot G^2 + 0.052 \cdot DO^2 - 0.097 \cdot X^2
 \end{aligned} \tag{7.36}$$

Comparing the simplified models for ΔpH and the final pH, it is clear that the model obtained for the final pH is more complex. Note that the linear effects of the factors remained almost unchanged. Further, the quadratic effects of G and X both indicate that there is a maximum response. By contrast, the quadratic terms of DO indicates a minimum response on the normalised scale. Temperature influences the pH in a linear way, i.e. by its main effect and two-factors interactions. By taking into account the very small model coefficients, it is concluded that the factors lead to rather small pH variations around the average value of $\text{pH}=7.3$.

7.8.3. Conclusions

The analysis of the pH by means of DOE and RSM revealed that the model may describe the response with enough accuracy when a few outliers are neglected.

The small coefficients of the model terms led to changes in the response values that do not differ much with respect to the average pH value of about 7.3. From a physical-meaning viewpoint, it is therefore expected that the observed pH variation does not strongly affect the flocculation process.

7.9. Process optimisation by using RSM

From the above investigation of individual responses it seemed difficult to optimise the flocculation process with respect to the operating conditions. Due to the large number of considered factors, the obtained models generally showed to be very complex. For all cases, the stationary point was found to be a saddle point, which did not allow finding an unconstrained maximum or minimum response value.

In this section, a process optimisation study will be carried out in order to find operating conditions that correspond to optimal responses. In this respect, target values were set for the responses and the associated factors were sought. The optimal targets of the responses were set so that these would ensure an improvement of the flocculation and clarification step in the activated sludge process. It should also be mentioned that the optimisation was performed with the RSM models describing the final response values and not its variations (Δ values).

As shown in section 7.4. from a process tolerance point of view, it is also of interest that the responses corresponding to the optimal design factors have low sensitivity, which would improve the tolerance of the design with respect to the factors' fluctuations. To account for this, an objective function should be constructed in such a way so as to include weighted sensitivities as well. The general form of the objective function, OF, defined by equation (5.36) in Chapter 5 has this ability and it will be consequently considered throughout this section.

In performing the optimisation, two cases will be considered. In the first case, all 7 responses considered will be analysed. The targets will be fixed and their value will be based on the analysis of the individual responses and the prior knowledge on the conditions determining a process improvement. As shown in sections 7.7 and 7.8 respectively, for the conductivity and pH, it is quite difficult to impose a set of optimal targets for the investigated experimental window. For the case of conductivity, this difficulty originates from its direct dependence on the calcium ions addition, whereas for pH it was observed that there was a relatively low impact of all considered factors on the response value. Therefore, these two responses will not be considered in the second optimisation scenario.

7.9.1. Seven response optimisation

Two optimisation approaches were considered. Firstly, only the target part of the objective function FO (see section 7.4.) was accounted for by setting all sensitivity weights to zero. Secondly, the optimisation algorithm accounts for both the target and sensitivity components. Equal weights were considered for target and sensitivity for each of the seven considered responses, except for conductivity. When the conductivity was analysed as an individual response, a maximal value predicted by the model was found to be around 4000 $\mu\text{S}/\text{cm}$ (section 7.7). The conductivity value obviously increases with Ca concentration as long as sludge concentration is not too high. However, it is difficult to relate an optimal process condition to the maximal value of the conductivity, since too much calcium addition would lead to sludge saturation and would slow down the flocculation process. The optimal conductivity value is therefore hard to define. As a first option, the conductivity may be excluded from the set of responses used by the optimisation algorithm. Alternatively, the conductivity may be considered but with a small target weight. As pH does not significantly influence the flocculation process (section 7.8.), the pH may be removed from the set of responses, as considered in a second optimisation stage.

1. Sensitivity weights = 0

Table 7.16 presents the response values obtained after the optimisation. As a consequence of the low target weight for the conductivity, its deviation from the target value is significantly larger as compared to the other responses.

Table 7.16 The optimal response values when adopting zero sensitivity weights

Response No.	Response	Optimum value	Target value	Target weight	Sensitivity weight
1.	D[4,3] [μm]	1711.32	1800	100	0
2.	SVI [ml/g]	121.66	40	100	0
3.	Zeta potential [mV]	-5.11	0	100	0
4.	Turbidity [NTU]	0.03	0	100	0
5.	Conductivity [$\mu\text{S}/\text{cm}$]	1775.49	4000	1	0
6.	pH	6.95	7.5	100	0
7.	TSS [mg/l]	0.03	0	100	0

The optimal operating conditions leading to the response values in Table 7.16 are given in Table 7.17. It should be noticed that the found optima did not depend on the initial estimate.

Table 7.17 Optimal operating conditions

Factor	Scaled	Unscaled
Temperature, T [$^{\circ}\text{C}$]	-1.2453	8.77
Average velocity gradient, G [s^{-1}]	-2.0000	15
Calcium conc., Ca [meq/l]	1.1162	18.69
Diss. Oxygen, DO [mg/l]	-1.0322	0.96
Sludge Conc., X [g/l]	1.7444	3.16

It is observed that the optimum has only one active constraint, i.e. the average velocity gradient reaches its minimal value. It is therefore suggested that the G value should be maintained as low as possible for process optimisation. Note also that a relatively high concentration of calcium is recommended. This can obviously be related to the high conductivity. In agreement with the previous findings (chapter 6) it seems that a relatively low temperature and high sludge concentration are required for process optimisation. Moreover, it is shown that a dissolved oxygen concentration of around 1 mg/l would be enough to maintain a good aggregation of the colloidal material and other wastewater pollutants onto the flocs.

Regarding the optimum values found, it seems that it would be possible to obtain large floc sizes, which will eventually settle well and produce a good effluent quality in terms of suspended solids concentration and turbidity if the above discussed conditions are satisfied.

It may however be observed also that the optimal SVI value is significantly higher than the one imposed as target but this may still be considered acceptable, as it shows good sludge settleability. The zeta potential value indicates the desired presence of some negatively charged particles which, if compared with the very low values of turbidity and TSS, shows that the isoelectric point does not represent a strict condition for the optimal operating conditions.

2. Sensitivity weights = 1

The more complete approach is to include both target and sensitivity in the optimisation study. For this case, the optimal response values and the corresponding operating conditions are given in Table 7.18 and Table 7.19 respectively.

Table 7.18 The response values obtained for the process optimisation

Response No.	Response	Optimum value	Target value	Target weight	Sensitivity weight
1.	D[4,3] [μm]	1712.075	1800	100	1
2.	SVI [ml/g]	118.973	40	100	1
3.	Zeta potential [mV]	-5.043	0	100	1
4.	Turbidity [NTU]	0.027	0	100	1
5.	Conductivity [$\mu\text{S/cm}$]	1762.214	4000	1	1
6.	pH	6.962	7.5	100	1
7.	TSS [mg/l]	0.038	0	100	1

Table 7.19 Optimal operation conditions

Factor	Scaled	Unscaled
Temperature, T [C]	-1.2313	8.84
Average velocity gradient, G [s^{-1}]	-2.0000	15
Calcium conc., Ca [meq/l]	1.0745	18.44
Diss. Oxygen, DO [mg/l]	-1.0449	0.95
Sludge Conc., X [g/l]	1.7504	3.18

Notice that only slight differences were obtained between the responses and factor values when comparing the optimisation results for the cases with and without the sensitivity weights. By increasing the sensitivity weights by one order of magnitude, the attained optimal values changed by up to 10 % (mostly SVI, which decreases), yet the "localization" of the factor values remained in a rather narrow interval, which confirms the confidence in the optimum found.

7.9.2. Five response optimisation

In the next optimisation study, the conductivity and pH were no longer considered as responses. As for the previous case, two types of optimisation were considered.

Again, irrespective of the initialisation point, only one solution was found. As for the previous case, quite similar optimal values were obtained for the considered responses (Table 7.20) as well as for the operating conditions (Table 7.21). The most significant difference was obtained for the calcium concentration indicating that a lower calcium concentration will be enough to obtain optimal operating conditions. Note however that this calcium concentration is very close to the range of calcium concentrations found as optimal when the individual

responses were evaluated and therefore an increase of calcium concentration can be regarded as excess. Another factor, which as compared with the seven response optimisation case slightly decreases (with approx. 1°C) is the temperature, which is in agreement with the conductivity model prediction of the most relevant factors. These small factor value changes seem to particularly affect the SVI, which decreases more towards its target value.

Table 7.20 The response values obtained after the process optimisation

Response No.	Response	Optimum value	Target value	Target weight	Sensitivity weight
1.	D[4,3] [μm]	1718.880	1800	100	0
2.	SVI [ml/g]	98.571	40	100	0
3.	Zeta potential [mV]	-5.282	0	100	0
4.	Turbidity [NTU]	0.011	0	100	0
5.	TSS [mg/l]	0.030	0	100	0

Table 7.21 Optimal operating conditions for five response optimisation without sensitivity weighting

Factor	Scaled	Unscaled
Temperature, T [C]	-1.5716	7.1418
Average velocity gradient, G [s^{-1}]	-2.0000	15
Calcium conc., Ca [meq/l]	0.3573	14.1438
Diss. Oxygen, DO [mg/l]	-1.0026	0.9974
Sludge Conc., X [g/l]	1.7875	3.2943

If the sensitivity is again introduced in the objective function, no significant changes of the responses value and of the optimal factor settings were found as shown in Table 7.22 and Table 7.23 respectively.

If the sensitivity and target weights are all set equal, the optimal point significantly changes, particularly for SVI (strong increase) and for TSS (strong increase). This may be explained as follows: the sensitivity optimisation is related to the stationary point, where the first derivatives of the response vanish. The target optimisation result is a point in the design space, which may change depending on the target specifications. When target and sensitivity parts of the combined objective function have comparable contributions, the result of the optimisation procedure reflects this situation and is in fact the best compromise between the results of the individual (i.e. target and sensitivity) optimisation problems.

Table 7.22 The response values obtained after the process optimisation

Response No.	Response	Optimum value	Target value	Target weight	Sensitivity weight
1.	D[4,3] [μm]	1718.540	1800	100	1
2.	SVI [ml/g]	98.110	40	100	1
3.	Zeta potential [mV]	-5.282	0	100	1
4.	Turbidity [NTU]	0.011	0	100	1
5.	TSS [mg/l]	0.031	0	100	1

Table 7.23 Optimal operating conditions for five response optimisation with sensitivity weighting

Factor	Scaled	Unscaled
Temperature, T [C]	-1.5670	7.1652
Average velocity gradient, G [s^{-1}]	-2.0000	15
Calcium conc., Ca [meq/l]	0.3484	14.0905
Diss. Oxygen, DO [mg/l]	-1.0026	0.9942
Sludge Conc., X [g/l]	1.7875	3.2966

7.9.3. Conclusions

To conclude, by performing the process optimisation using RSM it was possible to find optimal operating conditions, which will lead to an efficient flocculation in terms of large flocs and results in an improvement of the clarification step of the activated sludge process in terms of settling properties and effluent quality.

For the analysed SBR activated sludge samples it seems that optimal operating conditions correspond to the following factors:

- Relatively low temperature values (approx. 7-8°C) are necessary to be maintained. In this way, the model confirmed the observed floc size dynamics, which showed that short term temperature changes would create larger flocs.
- Average velocity gradient should be kept as low as possible. Since this factor was the only constrained factor it is possible that even better flocculation conditions can be found outside the experimental window, i.e. at even lower G values.
- A calcium concentration of 14 - 18 meq/l is enough for a performant process and any higher addition should be regarded as excess. This observation is in agreement with previous finding, which showed that an increase in the calcium concentration did not create a proportional increase in the floc size as recorded by on-line monitoring of the floc size dynamics.
- A dissolved oxygen concentration of approx. 1 mg/l resulted in a high adsorption capacity of colloidal material onto the flocs as evaluated in terms of turbidity and TSS.
- For the analysed sludge sample the optimal sludge concentration was found to be around 3.2 g/l. It sustains the previous observations according to which larger floc sizes are at found at high sludge concentrations.

7.10. Conclusions

In this chapter, the flocculation process performance was evaluated by using DOE and RSM. The effect of five factors, i.e. temperature, average velocity gradient, calcium addition, dissolved oxygen concentration and activated sludge concentration on different process responses (floc size, SVI, zeta potential, turbidity, TSS, conductivity and pH) was investigated by fitting a second order polynomial model to the obtained experimental data.

Good models were obtained for the responses monitored by using on-line sensors (floc size, conductivity and pH). For off-line measurements, moderate and poor statistical model predictions were found. It is therefore concluded that the analysis of off-line data was influenced by additional errors, occurring during the sampling or measurement procedures. As pointed out by Vanrolleghem and Lee (2003), it appears necessary to develop on-line sensors, which should replace the off-line measurements for automatic monitoring of wastewater treatment processes.

The model predictions for the floc size were found to agree with the observations performed on the influence of each factor on the floc size dynamics and with the reported literature data. The average velocity gradient showed the strongest effect on the floc size while the dissolved oxygen concentration was the least important factor.

Further, similar operating conditions were found to be responsible for larger flocs and lower SVIs. It was therefore concluded that large flocs settle better. The most significant factors affecting the SVI were found to be the average velocity gradient and sludge concentration, while the DO showed to be the least important one.

It was however, not possible to find a direct link between the zeta potential and the flocculation process. It was predicted by the model that charge neutralisation is not uniquely determined by the calcium concentration and that other factors too are important, e.g temperature.

A less accurate model was build for the turbidity. This might be due to the observed measurement and sampling errors, which resulted in a high variability, especially for the measurements performed in the central points. Due to this, any evaluation of the factor effects on the supernatant turbidity must be interpreted with caution. However, in agreement with literature data, the model predicted that anaerobic conditions and very low sludge concentrations are mainly responsible for an increase in supernatant turbidity. By contrast, calcium addition was found to have an insignificant effect, which does not agree with previous observations related to the role of calcium in flocculation.

A link between the effects predicted by the RSM models obtained for the supernatant turbidity and total suspended solids concentration was difficult to be found mostly due to the poor statistical accuracy presented by these models. It was indicated that a response minimum (i.e. low turbidity and TSS) is obtained for high mixing intensities and high calcium concentrations.

A very good accuracy was found for the RSM which described the conductivity. In excellent agreement with reported data, the model predicted not surprisingly a direct relationship between conductivity increase and calcium addition. Other factors that have an important effect on the conductivity were the temperature and the sludge concentration.

The small coefficients of the model terms led to changes in pH values that do not changed sufficiently in order to affect significantly the flocculation process.

Finally, it was possible to find the operating conditions which optimise the flocculation process and sludge settling properties. Most of the predicted optimal factor values are in agreement with other reported works. However, they still need to be validated experimentally for other activated sludge samples before the observed trend can be generalised.

To conclude, this study represented a first attempt to evaluate the flocculation process by using the DOE/RSM approach. It is believed that this may be a valuable tool, which may help to better understand the process and its mechanisms and also to improve the performance of the clarification step in the activated sludge process.

Conclusions and perspectives

As emphasized in the literature survey chapter (Chapter 2), the secondary clarifier is one of the most important and critical step of the activated sludge process. Its main objectives are to provide a good quality effluent and a well settled and thickened activated sludge. Most of the research studies focus on the quantitative characteristics of the mixed liquor and restrict to an evaluation, often empirical, of the solids concentrations and settling characteristics. However, the sludge settleability revealed variable characteristics, strongly related to the structure and the properties of the activated sludge flocs. Hence, for an efficient separation process the microorganisms must form flocs, which settle and compact well without leaving a high suspended solids concentration in the effluent. To achieve this goal better than can currently be generated, improving knowledge on the flocculation step represents an essential requirement for an optimal biological wastewater treatment.

Activated sludge flocculation is a very complex process influenced by many interacting factors. Since many of these influences are still poorly understood, predicting and controlling the characteristics of the floc formation is not easy. Moreover, the insufficient knowledge concerning the flocculation mechanism causes the models to eventually fail in their predictions or be unable to capture the effect of changing conditions on essential phenomena such as particles aggregation and breakage or settling characteristics.

This thesis aimed at setting up a systematic approach for the on-line monitoring of the activated sludge flocculation with a special focus on the investigation and analysis of the effects of some physico-chemical factors.

The first step of the developed methodology consisted in the implementation of an experimental technique and of a protocol that allows to monitor the effects of the imposed factors on (de)flocculation dynamics in a consistent way. Secondly, the obtained information was used for evaluating the individual time-dependent as well as the joint total effects of the studied factors on the (de)flocculation dynamics. To this goal, Design of Experiment (DOE) and Response Surface Methodology (RSM) approaches were used and subsequently, second order polynomial models in a normalised factor space were constructed and analysed for a selected set of responses, which were expected to have a role in the flocculation and clarification process. Finally, based on the model predictions, conditions for optimal process operation were searched for. The experiments were performed on sludge samples collected from a pilot-scale SBR operated under stable conditions. Furthermore, standardised sludge samples were used for analysis. To evaluate the sludge stability, its characteristics were intensively monitored and evaluated. To this end, a monitoring procedure was developed as well.

The main conclusions of the conducted research and the perspectives for further investigations are summarised in the next sections.

8.1. Evaluating and obtaining stable sludge samples

A systematic study of the influence of changing the environmental conditions on the flocculation dynamics requires a long experimentation time. Therefore, achieving stable properties of the sludge samples was the first and most important condition to be fulfilled before performing the experiments. Indeed, variations of the initial samples' characteristics would lead to secondary effects, creating difficulties for a correct identification and evaluation of the influences of the analysed factors.

Consequently, a procedure for monitoring the sludge properties in the SBR operated under stable environmental conditions was set up and used for sludge stability evaluations. It consisted in monitoring the activated sludge settling properties (SVI), the floc size and size distribution (FSD) and the microbial community evolution (DGGE) for long and short periods of time. The observation of the sludge samples under the microscope completed the monitoring procedure, allowing its validation by direct visualisation of the floc structural properties.

Long term monitoring of the SBR revealed a dynamic microbial community, which was found to be linked with the evolution of the SVI and FSD, while the microscopic observations confirmed the results. The results showed that stable operating conditions of the SBR in terms of nutrient removal did not imply stable sludge properties.

However, short-term stability of the sludge properties and of the microbial community can be obtained. Obviously any reactor failure or change of the operating conditions should be avoided since they may induce different degrees of perturbation in the sludge properties.

By using the developed monitoring procedures, the stability of the sludge samples was evaluated for the period in which the effects of different factors were assessed experimentally. The results indicated that the sludge properties could be considered rather stable during the experimentation period. These observations satisfy the essential condition required by the proposed experimental design and allowed for a proper identification and evaluation of the imposed factor effects.

The method proposed in this study for monitoring the properties of the activated sludge is believed to be a good procedure, which may be useful to find a link between changes in the activated sludge settling properties, floc structure and the microbial community dynamics.

8.1.1. Further developments and recommendations

Even if many research studies consider DGGE as a perfect and fast tool for monitoring the microbial dynamics as compared with other molecular techniques, the method is merely a qualitative technique, which does not give insights into the structural properties of the flocs.

Although expensive, methods such as Fluorescent In Situ Hybridisation (FISH) in combination with automated image analysis in Confocal Laser Scanning Microscopy (CLSM) and flow cytometry may be used together with DGGE for a quantitative and qualitative analysis of the flocs composition and structure.

8.2. A systematic approach for the on-line quantification of the flocculation dynamics

Given the fragile and complex structure of the activated sludge flocs, the development of the experimental procedure is far from being straightforward. The main steps followed to develop the experimental methodology were:

- Screening out the most important floc properties to be investigated and evaluating the most suitable techniques and procedures to be used for their measurement.
- Elaborating the experimental protocol based on the design of experiment (DOE) theory, which allows the quantification of the joint effect of different considered factors on the flocculation dynamics.
- Developing an experimental set-up in which the flocculation experiments can be performed under controlled operating conditions.

8.2.1. Methodology for on-line measurement of the floc size distribution (FSD)

Among the floc properties, the evaluation of floc size and size distribution proved to be one of the most useful tools to understand the influence of changing the environmental conditions on the flocculation process (Parker et al., 1971; Barbusinski and Koscielniak, 1995; Pochana and Keller, 1999; Biggs and Lant, 2000). In spite of its importance, the knowledge concerning the evolution of floc size and size distribution evolution during a dynamic process is still poor. This is mainly due to a lack of effective techniques able to capture the changes in floc size in a dynamic way.

Therefore, Chapter 3 of this thesis focused on establishing a methodology for the measurement and analysis of the floc size and floc size distributions. Special attention was paid to the selection of the sizing devices. However, since different devices may give different results, depending on their measurement principle, it was assumed that selecting more than one device would allow for a more comprehensive evaluation of the results.

Accordingly, a MastersizerS (Malvern, UK), a CIS-100 (Ankersmid, Belgium) and an automatic image analysis (IMAN) system developed in-house (based on IMAQBuilder and LabView, NI), were found to be the most suitable tools for the measurement purposes. The devices were selected based on their on-line measurement capabilities, complementarity of the measurement principles and similar sample dilution requirements. To allow simultaneous measurements, the devices were coupled in series and their performance for on-line measurement of the activated sludge floc were assessed.

The main conclusions were:

- All devices allow for on-line analysis of the activated sludge sample in a similar concentration range.
- The measurement principle of the devices is of large importance for a correct interpretation of the results, since the transformation of the raw data often leads to misinterpretations.
- The automatic procedure used allows to obtain a floc size distribution measurement every 30 seconds with enough accuracy.
- Each device presented particular limitations in the measurement of small particle sizes (up to 10 μm or even higher for IMAN). Therefore, the interpretation of the results obtained in the range corresponding to small size classes have been performed only for the purpose of comparing the evolution of consecutive

measurements, since any other interpretation of the small size particles could be misleading.

- The particles' shape influenced the MastersizerS results mostly, as it produced a broader distribution. The least influence was observed on the techniques based on image analysis when the equivalent spherical diameter was used to evaluate the particle size.
- It was found that by proper design, the impact of set-up parts and experimental conditions on measurements could be minimised. In this respect, the tubes length should be as short as possible, the pumping procedure should minimise the pulsations, the dilution medium should be filtered effluent (0.45 μm) and the dilution procedure should be in-tube to allow for investigating higher sludge concentrations.

8.2.2. Factors selection and development of the DOE methodology

Many factors may influence the flocculation process simultaneously. Performing the experiments in a conventional way, the effect of just one factor at a time may be investigated. By contrast, in this work a design of experiment (DOE) approach was used to perform the experiments, as it allows for evaluating the effect of the physico-chemical factors in a consistent way and accounts for the joint effect of the factors.

The main steps followed in the present DOE approach were:

- *Selection of the factors with the most relevant effect on the flocculation process.*
A constraint, which limited the number of factors that could be considered, emerged from the necessity of having sludge samples that are as stable as possible for the entire experimentation period. Accordingly, only a number of five factors was selected on the basis of literature reports and easily controllability in a laboratory environment, as follows:
 - average velocity gradient (G),
 - dissolved oxygen concentration (DO),
 - calcium addition (Ca),
 - temperature (T),
 - sludge concentration (X).

For each of these factors, a proper experimental range was defined depending on practical considerations.

- *Selection of the responses, which consisted in a set of on-line or off-line measured variables to evaluate the activated sludge process.* The following variables were considered as responses:
 - floc size evaluated as mass mean size diameter;
 - SVI;
 - supernatant turbidity, suspended solids concentrations and zeta potential;
 - conductivity;
 - pH.
- *Detailed description of the experimental protocol.*

The experimental protocol was constructed having in mind the trade-off between an accurate observation of the flocculation dynamics and the time needed to reach the factor design values in the vessel.

- *Decision on the DOE type/table*

A second-order orthogonal and near rotatable polynomial model was selected as being the most suitable for the final purpose of this study.

8.2.3. The experimental technique

The influence of physical and chemical factors on the (de)flocculation process was investigated in a specifically designed flocculation set-up (FlocUNIT). The set-up was built with a high functionality, allowing the simultaneous investigation of many possible factors over a relatively long experimental time (up to 6 hours).

Therefore, to study the flocculation a five-liters reactor was used, in which samples with different sludge concentrations were analysed. To build the set-up, the methodology developed for on-line measurements of the FSD was considered and the set-up components were connected accordingly.

The FlocUNIT set-up allowed to directly evaluate the flocculation process as it occurred in the reactor under the influence of several well-controlled process parameters.

Different degrees of shear were imposed by using a viscometer, calibrated to measure the average velocity gradient, G . On-line sensors for measurement of pH, conductivity, temperature and dissolved oxygen concentration were used. All set-up devices and sensors were PC-connected by using a program developed in LabView (NI, USA).

To evaluate the influence of the imposed factors on the process effectiveness, off-line measurements of the SVI, supernatant turbidity, suspended solids concentrations and zeta potential were performed before and after the flocculation process.

8.2.4. Further developments and recommendations

The possibility to measure the fractal dimension, which represents an important parameter for evaluating the structural properties of the flocs, was verified for the selected devices. The results turned out to be rather contradictory and characterised by a series of limitations.

Fractal dimension was not considered further in this study. A thorough analysis of this parameter is suggested as a topic for further research.

At the time of performing these experiments, a technique to allow in-situ measurements at high sludge concentration was not accessible.

With a good methodology and careful investigation to overcome some limitations as pointed out by De Clercq (2002b), devices with in-situ measurement capabilities such as those based on the Focused Beam Reflectance Method (FBRM) may be a good alternative for investigating the flocculation dynamics.

Due to the very broad size range, the measurements and size analysis were restricted in general to microflocs larger than $10\mu\text{m}$. The smaller size identification suffered from several drawbacks identified in the measurement principles of the used devices.

It is recommended that more efforts are put to find a method which allows a direct measurement of the entire size range of the particulate material existing in the activated sludge including single bacterial cells and colloids. This would allow for a deeper understanding of the phenomena occurring in activated sludge flocculation when different environmental conditions are imposed.

The developed methodology only allowed for a global evaluation of the floc size and size distribution. The floc structural and biological properties with an emphasis on the role of the microorganisms (floc forming vs filamentous bacteria) and that of the EPS were not considered.

Development of a fully automated technique able to quantify the biological and structural properties of the activated sludge flocs still represents a challenging but required task. It is believed that this would be possible by using in-situ microscopy with high resolutions cameras. Although essential, a standardised procedure is still missing, which complicates the evaluation of the role of the EPS on activated sludge flocculation dynamics.

8.3. Response surface modelling and analysis of the influence of different physico-chemical factors on the (de)flocculation process

The influence of the considered physico-chemical factors on the flocculation process was evaluated in two complementary ways. First, the effect of each factor on the floc size dynamics was studied, whereas in the second, the joint effect of all factors was assessed by using a DOE/RSM approach.

8.3.1. The effect of individual factors on (de)flocculation dynamics

The effect of each factor on the floc size dynamics was first analysed and discussed separately based on the experiments performed in the central, minimum and maximum axial points of the DOE.

The main conclusions drawn from this investigation are:

- A similar evolution between the volume-based floc size diameters and the total number of the particles counted was observed as a general trend. This confirmed the capabilities of the considered devices to measure the floc size dynamics on-line. Moreover, the images recorded by using the IMAN technique visually validated the results.
- Among the five investigated factors, the most significant effect on the floc size originated from average velocity gradient (G) and calcium concentration (Ca) while the least significant was the dissolved oxygen concentration (DO).
- The average velocity gradient imposed showed to be highly important for floc formation and stability. At high mixing intensity a rapid floc break-up phenomenon was observed (with a characteristic time in the order of only a few minutes), followed by a steady size that remained constant for long time periods (up to 55 min.). It was considered that the floc strength plays a role in establishing the observed equilibrium between the aggregation and breakage phenomena. On the contrary, at low mixing intensity values, floc aggregation dominated the

process and resulted in a slightly and continuously increasing floc size trend. The largest flocs formation was recorded for the lowest applied mixing intensity.

- The SBR activated sludge samples showed a high affinity for calcium. Hence, calcium addition resulted in a fast increasing floc size effect. The potential of the floc for re-aggregation was observed even when high mixing intensities were imposed. However, the regrowth effect of the floc was not completely reversible. A floc restructuring factor calculated as the ratio between the difference in size created by calcium addition at high mixing intensities, indicated a 53.41% ability of the flocs to reflocculate at a G value of 200s^{-1} after adding 12 meq/l calcium ions. At low mixing intensities, faster dynamics were observed when increasing the calcium concentration. However, a correlation was not observed between the maximum floc size and the added calcium concentration. These observations suggested that a saturation level of calcium ions occurred and addition of calcium over this level will just accelerate the aggregation process, but will not stimulate larger floc formation.
- Since in the analysed SBR sample, a lack of calcium ions was measured (up to 0.15 meq/l), an additional experiment was performed in order to evaluate the calcium effect on another sludge sample already containing a larger amount of calcium. To this end, a sample collected from a WWTP (Ossemeersen, Ghent, Belgium) with a calcium content of approximately 2.61 meq/l was analysed under the same experimental conditions. The results indicated almost no effect of calcium addition on the floc size. It was found that the short-term response of the flocs to the addition of calcium is highly dependent on the initial amount of calcium ions present in the activated sludge sample. These observations suggest that, by a simple evaluation of the initial calcium concentration, it is possible to quickly evaluate the response of the system to any further calcium additions. In this context it is believed that, as shown in this particular case, a calcium addition will improve the flocculation process performance of the activated sludge with a high content of sodium ions present in their structure. This may be relevant during the winter time, when large amounts of de-icing products are washed out from pavements and increase the sodium concentration of the wastewater influent.
- The tests performed for evaluating the flocculation behaviour at different sludge concentrations showed that larger floc formation occurred at higher sludge concentrations, indicating that the increased collision rate between the microbial aggregates at increasing sludge concentration is effective.
- Larger flocs were formed when temperature decreased in the reactor. Several hypotheses were considered in order to explain the observed behaviour. A possible cause may be related to the microbial activity, which depends on temperature. An important role in deciding the optimal temperature range for the microbial activity is however played by the temperature at which the sludge samples were initially acclimatized. This possibly explains the faster aggregation effect created by calcium addition for the sludge sample operated at 15°C . When temperature was increased to 25°C , a deflocculation effect occurred. A comparison with the available literature studies led to the conclusion that the microbial activity and EPS production are highly influenced by the changes in temperature, even when only short-term investigations are performed.

- Short-term changes in the dissolved oxygen concentration did not have a significant effect on floc size and the observed dynamics was similar for the experiments performed under different dissolved oxygen concentrations.

8.3.2. Modelling the interactive effect of the studied factors on (de)flocculation by using DOE and RSM

The joint effect of all five factors on the considered set of responses was investigated by building response surface models based on the data collected from the DOE. The interaction effects (up to the second order) between all five factors were quantified as well. Furthermore, identification of a set of factor values that optimise the responses was carried out, according to specified optimisation criteria.

In order to account for possible sampling and measurement errors and for validating the models predictions, two models were constructed and evaluated for each response. The first one took into consideration the response as the difference between the final and initial experimental values for the response variables, whereas the second only considered the final response values.

The main conclusions of the RSM analysis are summarised below:

- In general, more accurate statistical models were obtained for the responses monitored by using on-line sensors. For off-line measurements, moderate to poor statistical model predictions were found. It is concluded that the analysis of off-line data was influenced by additional errors occurring during sampling and measurement procedures.
- Accurate statistical models with high similarity between both considered models were obtained when the floc size was considered as a response. By evaluating the interaction effects as obtained after simplification it turned out that the sludge concentration showed mixed second order effects with temperature, average velocity gradient and dissolved oxygen concentration. However, both models predicted that the average velocity gradient had the strongest effect, followed in order by those of calcium and sludge concentration, while the dissolved oxygen concentration and temperature had the weakest influences. The RSM model predictions were consistent with the single-factor time dependence analysis. Furthermore, the RSM model obtained was found to agree well with a power-law relationship between the average velocity gradient and the maximum stable floc size proposed by Parker et al. (1972). Moreover, both models reproduced the experimental data with good accuracy.
- The analysis of the SVI revealed less accurate models characterised by a good to moderate quality of the fit to the experimental data. However, an agreement between models was found in predicting the most important factors, namely the average velocity gradient and the sludge concentration. The DO effect was again the least significant. A similarity between the factor values corresponding to larger flocs formation and those decreasing the SVI allowed to conclude that larger floc formation led to an improvement of the settling properties of the sludge.
- The zeta potential data resulted in models of moderate statistical quality. Evaluation of the calcium effect by keeping the other factors at their nominal values (corresponding to the central point in the design) revealed that an almost complete charge neutralisation corresponded to a calcium concentration of 15.48 meq/l. This indicates that a saturation level with calcium ions may be found, for

given conditions (of the other factors). From the obtained RSM models it was observed that the destabilization phenomena that occur during the (de)floculation process are not entirely due to the charge effects and can not be fully described by using the zeta potential.

- Evaluation of the supernatant turbidity revealed poor statistical models that were not able to reproduce the turbidity variations with satisfactory accuracy. One possible explanation is that the experimental errors drastically influenced the obtained results, since large differences were observed between the two considered models (the response variation versus the final response only). Anaerobic conditions and very low sludge concentration were the main conditions predicted by the models as being responsible for high supernatant turbidities. By contrast, calcium addition was found to have an insignificant effect, which does not agree with previous experimental observations discussing the role of calcium ions in flocculation, especially for the considered sludge samples.
- A very good accuracy was found for the RSM models of the conductivity. The model predicted, not surprisingly, an increase of conductivity with calcium addition. The temperature and the sludge concentration were found to affect the conductivity as well. However, the conductivity is more regarded as a measure of the concentration of the dissolved salts in solution and believed not to play a direct role in flocculation. This is sustained by its continuous tendency to increase with the calcium addition, while it was shown that the relationship between the floc size and calcium concentration is different.
- Accurate statistical models predicted the pH variation with respect to the considered factors well, especially when a few outliers in the central point were neglected. As revealed by the model, the pH was mostly affected by calcium, temperature and average velocity gradient, which nevertheless showed mostly a linear effect on the pH variation. However, under the imposed factor values, the pH did not change sufficiently to affect the flocculation process.
- By using the RSM approach it was possible to find operating conditions that would improve flocculation and settling properties for the particular case of the considered SBR sludge. Accordingly, targets for the analysed variables were imposed in such a way so as to obtain good settling properties (large floc size and low SVI values) and low suspended solids concentration of the supernatant ("zero" values of suspended solids concentration, turbidity and zeta potential). It was found that an optimal process would be achieved at relatively low temperature values of approximately 7-8 °C, as low as possible average velocity gradient values (even lower than the minimum value used in this study, i.e. 15 s⁻¹), a calcium concentration of 14-18 meq/l, a dissolved oxygen concentration of around 1 mg/l and a sludge concentration of around 3.2 g/l. For these factor settings, the model predicted flocs with a mass mean diameter of approximately 1.7 mm size, SVI values between 98 ml/g and 121 ml/g, a suspended solids concentration of around 0.03 - 0.04 mg/l, turbidity values of 0.01 and 0.03 NTU and a zeta potential of around -5mV.

8.3.3. Further developments and recommendations

Evaluating the joint effects of different factors on a considered set of process variables by means of the DOE/RSM methodology is a good way to increase the knowledge on the complex flocculation process. Although empirical, this methodology can provide valuable information relating to the effectiveness of the activated sludge process, with a minimal experimental effort, as it allows to directly correlate the flocculation process with parameters characterising the settling process. However, the results presented in this study were interpreted only for the particular case of the SBR sludge and should not be generalised for other systems, irrespective of their particularities.

For more extensive validation of the results, further research with samples taken from different WWTPs needs to be performed.

A generally valid explanation for the temperature effect on the flocculation dynamics can not be derived from this study alone.

A longer-term investigation of the temperature effect on flocculation, combined with monitoring of the microbial activity and EPS is suggested as a topic for further research.

Because of the complex and especially biological nature of the activated sludge flocs, it may be expected that various sludge samples will react differently to the same experimental conditions.

It is, however, interesting to find out to what extent different activated sludge samples with different structural properties will affect the results and whether it is possible to standardise the effect of some environmental conditions, eventually “parametrised” by the different structural characteristics or properties of the flocs. For a particular activated sludge, it should be possible, with a methodology similar to the one described in this study, to detect, understand and control the role of the most effective factors on the process. This, on the other hand, first requires a screening procedure which will allow for the identification of these factors.

Several other factors which were not considered in this study may play an important role, too. Considering the effect of environmental conditions on the biological properties of the flocs is required to explain the hypothesised theories and phenomena.

In this context, together with biological and structural properties, the effect of other physico-chemical parameters such as influent composition, sludge age, different cations (Na, K, Mg, Fe, Al) and cations ratio, other flocculant additions or ballasting agents, etc. should be considered as well. These however should be determined depending on the particular applications and requirements.

Accurate statistical models were obtained for the responses monitored by using on-line sensors while the analysis of off-line data was influenced by additional measurements errors.

It seems necessary that more effort should be directed to the development of on-line sensors that may eventually replace the off-line measurements that represent a source of larger errors.

The optimal conditions for flocculation found from the RSM approach were not post-checked experimentally.

A further experimental evaluation to verify the optimal conditions is required. An account for long-time process operation under these conditions should be considered as well. Moreover, it would be interesting to investigate how the optimum operating conditions for flocculation correlate to COD and nutrient removal abilities of the activated sludge.

8.4. General conclusions

The work described in this thesis was conducted in the framework of the SediFloc project, which has as an ultimate goal to quantify and model the flocculation process in secondary clarifiers by accounting for the influence of different physico-chemical parameters, in view of a better prediction of the process efficiency.

In the project context, this thesis focused on various aspects related to the measurement, quantification and optimisation of the flocculation process. As a result, a methodology and empirical modelling by using DOE/RSM approaches was developed and used for on-line characterisation of the flocculation dynamics and of its response to the effect of five physico-chemical factors. The thesis was structured in three main parts, which were discussed and investigated accordingly:

- *Stability of the analysed sludge sample*

A pilot-plant SBR operating under stable environmental conditions was intensively monitored for this purpose. A procedure that linked the sludge settling performances with floc size and size distributions and microbial community (using DGGE and microscopical observations) was developed. It was proven that this procedure allows to detect the conditions under which sludge stability occurred and also showed to be a suitable technique for linking the settling properties with floc properties and microbial community dynamics.

Together with DGGE technique, using quantitative molecular techniques (e.g. FISH) coupled with high resolution automated image analysis (e.g. CLSM) systems will allow a closer evaluation of the floc composition and structure and will represent a significant improvement of the developed monitoring procedure.

- *Experimental protocol and analysis methodology*

In order to investigate the (de)flocculation dynamics, an experimental set-up (FlocUNIT) was built, which allowed for the on-line monitoring of the floc size dynamics. The experimental protocol and analysis was developed based on the DOE approach.

A significant improvement of this technique would represent the replacement of the on-line sizing techniques with in-situ techniques. Moreover, more consideration should be given to the measurement of the fractal dimension, which represents an important morphological property of the flocs. Last but not the least, the techniques based on image analysis deserve special attention and should always be used since they allow to directly visualise important information.

- *Response surface modelling and analysis of the influence of different physico-chemical factors on the (de)floculation process*

The effect of each of the considered five factors on the floc size dynamics was first investigated separately. Among the considered factors the most significant effects originated from the average velocity gradient and calcium concentration, while the least significant effect was found for the dissolved oxygen concentration. Large floc formation was observed by decreasing the temperature in the reactor. It was demonstrated that the flocculation is in general a very dynamic process characterised by two phases. During the first phase which is relatively short (in the order of minutes) a fast response of the floc size to changes of the environmental conditions was observed. By contrast, the second phase was a slow process the trend of which was reproducible for longer times (up to a few hours) and strongly depended on the imposed values of the factors. Among the analysed factors the shear rate (average velocity gradient, G) and the calcium concentration were the most responsible for the observed trend in the flocculation dynamics. Therefore, it is suggested that the shear history and the floc strength are useful parameters for evaluating and detecting to what extent and where the flocculation occurs in a WWTP.

An account for microbial activity and EPS characteristics may be helpful for validating and fully explained the observed results.

A DOE/RSM methodology was used for building and analysing empirical models that account for the simultaneous variation of all considered factors. Moreover, this methodology enables optimisation of the flocculation process conditions and of the settling characteristics with respect to some specifically defined optimisation criteria. Acceptable statistical models were generally obtained, which predicted the response variations well. However, the obtained results were not validated for other sludge samples and therefore should rather be regarded as results obtained on a “test vehicle”, where the main achievement is the development of a suitable investigation methodology. On the other hand, the methodology described in this study is rather general and can be applied for different activated sludge systems. Therefore, with only a few experiments, by using the DOE/RSM approach, it is possible to evaluate the response of the activated sludge process to changing parameters as well as to detect the parameter values required to optimise the operating conditions.

The present work may be extended towards the inclusion of changes in biological properties of the flocs. Moreover, the influence of other physico-chemical factors may be very useful as well.

The conducted research demonstrated that for an improved prediction and control of the flocculation process, an integral approach, in which the joint effect of different factors is accounted for simultaneously, should be considered. It was shown that with a relatively low number of experiments, it was possible to investigate the short-term effects of changing environmental conditions and to find the factor values that would optimise the process.

It is further believed that the information accumulated in this research may be useful for a more elaborated modelling of the flocculation process dynamics by using a population balance (PBM) approach. Ultimately, the developed PBM model needs to be incorporated in a 2D Computational Fluid Dynamics (CFD) model able to predict the flow and the solids concentrations fields of a secondary clarifier both in space and time.

However, due to its complexity, a 2D CFD model is difficult to be applied in practice. For this purpose 1D-models are preferred. A frequently occurring problem of the 1D-model represents a lack of experimental data required for model calibration. At this step, in the framework of the Sedifloc project it is aimed that the knowledge of the flocculation and settling process incorporated in the 2D-model will be used to calibrate and validate a 1D-model of the secondary clarifier. Hence, it is assumed that a fully calibrated and validated 1D-model of the secondary clarifier would be able to accurately reproduce the reality.

Moreover, it is believed that that this work provided some stepping stones towards the full understanding of the complex flocculation mechanisms, research of which must be continued.

Appendix to Chapter 3**Appendix 3.1.**

In this appendix the parameters calculated by IMAN are described:

No.	Parameter	Unit	Description
1.	Area (pixels)	pixels	Surface area of a particle
2.	Area (calibrated)	μm^2	Surface area of a particle
3.	Number of Holes	-	Number of holes inside a particle
4.	Hole's Area	μm^2	Surface area of the holes
5.	Total Area	μm^2	Total surface area of a particle (including holes)
6.	Scanned Area	μm^2	Surface area of the entire image
7.	Ratio Area/Scanned Area	%	Percentage of the surface area of a particle in relation to the scanned area
8.	Width	μm	Width of the bounding rectangle
9.	Height	μm	Height of bounding rectangle
10.	Longest segment length	μm	Length of longest horizontal line segment
11.	Perimeter	μm	Length of the outer contour of a particle
12.	Mean chord X	μm	Mean length of horizontal segments
13.	Mean chord Y	μm	Mean length of vertical segments
14.	Max intercept	μm	Length of longest segment in the convex hull of the particle
15.	Particles orientation	-	Direction of the longest segment
16.	Ellipse major axis	μm	Total length of major axis having the same area and perimeter as the particle
17.	Ellipse minor axis	μm	Total length of minor axis having the same area and perimeter as the particle
18.	Elongation factor	-	Max intercept/mean perpendicular intercept
19.	Compactness factor	-	Particle area/ (breadth*width)
20.	Heywood circularity factor	-	Particle perimeter/ perimeter of circle having same area as particle
21.	Waddel disk diameter	μm	Diameter of the disk having the same area as the particle

Appendix to Chapter 4

Appendix 4.1.

In this appendix an overview of the analyses and the measurement frequency performed for off-line SBR monitoring is given:

Table A4-1 Off-line analysis performed for monitoring the activated sludge in the SBR

Analysis	Unit	Frequency
Influent analysis		
COD	mg/l	Day 1 and day 7
COD _{soluble}	mg/l	Day 1 and day 7
N _{tot}	mg N/l	Day 1 and day 7
PO ₄ -P	mg PO ₄ -P/l	Day 1 and day 7
TSS	g/l	Day 1 and day 7
pH	-	Daily
Activated sludge analysis		
SVI	ml/g	Daily
TSS	g/l	Daily
MLVSS	g/l	Twice a week
Microscopical observations	-	Twice a week
Floc size and size distribution	µm	Ones a week
DGGE	-	Ones a week
Effluent analysis		
COD	mg/l	Daily
COD _{soluble}	mg/l	Twice a week
Total - N	mg N/l	Daily
NH ₄ -N	mgNH ₄ -N/l	Once a week
NO ₃ -N	mg NO ₃ -N/l	Daily
PO ₄ -P	mg PO ₄ -P/l	Daily
BOD	mg/l	Twice a week
TSS	mg/l	Twice a week

Appendix 4.2.

This appendix aims to present the effluent and influent analysis performed by using Dr. Lange (Dr. Lange, Germany) technique. The measurement range of each parameter is as well given.

Table A4-2 Overview of the analysis performed by using Dr.Lange technique

Kit code	Parameter	Sample	Range
LCK 314	COD	Effluent	15-150 mg/l
LCK 414	COD _{soluble}	Effluent	5-60 mg/l
LCK 514	COD	Influent	100-2000 mg/l
LCK 614	COD _{soluble}	Influent	50 – 300 mg/l
LCK 238	Total -N	Effluent	5-40 mg/l
LCK 338	Total -N	Influent	20-100 mg/l
LCK 305	NH ₄ -N	Effluent	1-12 mg/l
LCK 340	NO ₃ -N	Effluent	5-35 mg/l
LCK 350	PO ₄ -P	Effluent/Influent	2-20 mg/l

Appendix to Chapter 5

Appendix 5.1.

The aim of this appendix is to present the method by which the design points of each of the considered factors have been calculated. The values of dissolved oxygen, temperature and calcium concentration have been calculated on a linear scale, whereas shear stress and the sludge concentration have been calculated on a logarithmic scale.

The nominal value of each factor corresponds to the centre of the experimental region. Depending on the normalisation type the normalised values of each factor have been calculated, as follows:

- The minimal and the maximal values of the factorial part of the design were assigned to the normalized values of -1 and $+1$, respectively.
- The minimal and maximal values of the axial part of the design were assigned to $-\alpha$ and $+\alpha$, respectively. Since $\alpha > 1$, the extrema of the axial part of the design coincide with the extrema of the experimentation range.

Linear scale:

The unnormalised values for the factors considered on a linear scale are given by:

$$F_{(+\alpha,lin)} = \alpha \frac{F_{max} - F_{min}}{2} + F_{0,lin} = \frac{(\alpha + 1)F_{max} - (\alpha - 1)F_{min}}{2} \quad A5-1$$

$$F_{(-\alpha,lin)} = \alpha \frac{F_{max} - F_{min}}{2} - F_{0,lin} = \frac{(\alpha - 1)F_{max} - (\alpha + 1)F_{min}}{2} \quad A5-2$$

Where: $F_{(-\alpha,lin)}$ and $F_{(+\alpha,lin)}$ are the values in the minimum and maximum axial points respectively, $F_{(min,lin)}$ and $F_{(max,lin)}$ are the minimum and maximum design points which correspond to the normalised values $[-1,1]$.

When considering an orthogonal and rotatable experimental design the axial distance α becomes 2 and the above equations develop into:

$$F_{(max,lin)} = \frac{3 * F_{(+\alpha,lin)} - F_{(-\alpha,lin)}}{4} \quad A5-3$$

$$F_{(min,lin)} = \frac{F_{(+\alpha,lin)} - 3 * F_{(-\alpha,lin)}}{4} \quad A5-4$$

The central point design value is given by the following formula:

$$F_{(0,lin)} = \frac{F_{(min,lin)} + F_{(max,lin)}}{2} \quad A5-5$$

By taking into account that the values on the axial points were imposed from the beginning, the nominal values of the factors can be easily calculated (Table A5-1).

Table A5-1 The nominal values of the factors calculated on a linear scale

Factors	$F_{(-2,lin)}$	$F_{(+2,lin)}$	$F_{(min,lin)}$	$F_{(max,lin)}$	$F_{(0,lin)}$
Dissolved oxygen, DO [mg/l]	0	4	1	3	2
Temperature, T [°C]	5	25	10	20	15
Calcium concentration, Ca [meq/l]	0	24	6	18	12

Logarithmic scale:

The unnormalized values for the factors considered on a logarithmic scale are calculated from equations A5-1 and A5-2

$$F_{(min,log)} = \frac{F_{(+\alpha,log)}}{\left(\frac{F_{(+\alpha,log)}}{F_{(+\alpha,log)}}\right)^{1/4}} \quad \text{A5- 9}$$

$$F_{(min,log)} = F_{(+\alpha,log)} * \left(\frac{F_{(+\alpha,log)}}{F_{(+\alpha,log)}}\right)^{1/4} \quad \text{A5- 10}$$

$$F_{(0,log)} = \sqrt{F_{(min,log)} * F_{(max,log)}} \quad \text{A5- 11}$$

The nominal values of the factors calculated on logarithmic scale are summarised in Table A5-2.

TableA5-2 The nominal values of the factors calculated on logarithmic scale

Factors	$F_{(-2,log)}$	$F_{(+2,log)}$	$F_{(min,log)}$	$F_{(max,log)}$	$F_{(0,log)}$
Shear stress, G [1/s]	15	200	29	105	55
Sludge concentration, X [g/l]	0.1	4	0.25	1.59	0.63

Appendix 5.2.

This appendix shows the experimental design matrix, in terms of coded (normalized) variables, together with the chronological order of the experiments, which minimises the time confounding effect.

Table 5.1 Design Matrix

Exp. code	T	G	Ca	DO	X	Order
1	-1	-1	-1	-1	1	20
2	-1	-1	-1	1	-1	5
3	-1	-1	1	-1	-1	3
4	-1	-1	1	1	1	33
5	-1	1	-1	-1	-1	36
6	-1	1	-1	1	1	4
7	-1	1	1	-1	1	7
8	-1	1	1	1	-1	25
9	1	-1	-1	-1	-1	15
10	1	-1	-1	1	1	30
11	1	-1	1	-1	1	16
12	1	-1	1	1	-1	17
13	1	1	-1	-1	1	29
14	1	1	-1	1	-1	23
15	1	1	1	-1	-1	35
16	1	1	1	1	1	19
17	-2	0	0	0	0	32
18	2	0	0	0	0	8
19	0	-2	0	0	0	24
20	0	2	0	0	0	2
21	0	0	-2	0	0	22
22	0	0	2	0	0	27
23	0	0	0	-2	0	9
24	0	0	0	2	0	14
25	0	0	0	0	-2	12
26	0	0	0	0	2	13
27 (C)	0	0	0	0	0	1
28 (C)	0	0	0	0	0	21
29 (C)	0	0	0	0	0	26
30 (C)	0	0	0	0	0	10
31 (C)	0	0	0	0	0	34
32 (C)	0	0	0	0	0	31
33 (C)	0	0	0	0	0	6
34 (C)	0	0	0	0	0	11
35 (C)	0	0	0	0	0	18
36 (C)	0	0	0	0	0	28

(C) – central point of the design

Appendix to Chapter 6

Appendix 6.1.

The calcium dynamics was investigated by fitting the data to equation 5.17. The time needed for the floc size to reach 95% of the maximum size observed during the fast process was calculated by using the following program written in Matlab 6.5.

```

-----
% set path to the input/output routines
% index of monitored quantities
IdxInp = 2;
IdxOut = 4;
Excelfile = 'diaall.xls';
XlsSheets = { ...
    'exp1','exp2','exp3','exp4','exp5', 'exp6', 'exp7', 'exp8', ...
    'exp9','exp10','exp11','exp12','exp13','exp14','exp15','exp16', ...
    'exp17','exp18','exp19','exp20','exp21','exp22','exp23','exp24', ...
    'exp25','exp26','exp27','exp28','exp29','exp30','exp31','exp32', ...
    'exp33','exp34','exp35','exp36'};
mode = input('Mode (single - 0 / multiple - 1) >>>');
if mode == 0,
    exper = input('Experiment >>>');
    imin = exper;
    imax = exper;
else
    imin = 1;
    imax = length(XlsSheets);
end;
for i=imin:imax,
    [dat,hdr] = xlsread(Excelfile,XlsSheets{i});
    % select the x, y data
    vX = dat(IdxInp,:);
    vY = dat(IdxOut,:);
    % plot data, to see what to select
    f1 = plot(dat(1,:),vY,'o');
    hold on;
    vYfilt = zeros(1,length(vX));
    for j=1:length(vX),
if (j < 3),
    vYfilt(j) = vY(j);
elseif j < length(vX) - 1,
    vYfilt(j) = (vY(j-2) + 2 * vY(j-1) + 4 * vY(j) ...
    + 2 * vY(j+1) + vY(j+2))/10;
else
    vYfilt(j) = vY(j);
end;
end;
end;
    f1 = plot(dat(1,:),vYfilt,'r-');
    hold off;
    pause;
    okFilter = input(' Filter (0-no / 1-yes >>>');
    if (okFilter == 1),
vY = vYfilt;
end;

```

```

% index of initial time window
Record0Init = input('Record Initial start >>>');
Record0Final = input('Record Initial end >>>');

% number of final samples to be considered
RecordfInit = input('Record Final start >>>');
RecordfFinal = input('Record Final end >>>');

% calculate the initial and final values
Yi = mean(vY(Record0Init:Record0Final));
Yf = mean(vY(RecordfInit:RecordfFinal));

% calculate the least square (exp) slope
logYsel = log(abs(vY(Record0Final+1:RecordfInit-1) - Yf));
Xsel = vX(Record0Final+1:RecordfInit-1) - vX(Record0Final+1);
f2 = plot(Xsel,logYsel,'r*');
hold on;
pause;
vC = polyfit(Xsel,logYsel,1);
Xchar= 1/vC(1);
fitlogYsel = vC(1).*Xsel + vC(2);
f2 = plot(Xsel,fitlogYsel,'b-');
error = sqrt(sum((1 - fitlogYsel./logYsel).^2)/(length(logYsel)-1));
fprintf(1,' ==> Fitting interval error: %10.3g\n', error);
pause;
hold off;
vYcalc = zeros(length(vY),1);
for j = 1: length(vY),
if j < Record0Final,
    vYcalc(j) = Yi;
else
    vYcalc(j) = Yf + (Yi-Yf)*exp((vX(j)-vX(Record0Final))/Xchar);
end;
end;
plot(vX,vY,'o');
hold on;
plot(vX,vYcalc,'r-');
hold off;
t95total = vX(Record0Final) + Xchar * log(0.05);
t950 = Xchar * log(0.05);
fprintf(1,' ==> t 95 results:\n\tt95total = %10.3f\n\tt95_0 =
%10.3f\n', ...
t95total,t950);
pause;
close all;
end;

```

Appendix to Chapter 7

Appendix 7.1

In this appendix the factors design values (F_d) and the experimental average values (F_e) are presented as well as the standard deviation (SD) of the latter values. To evaluate the responses by DOE and RSM, the experimental values were taken into account. The calcium concentration was not included in Table A7- 1 since the calcium solution was added into the system with analytical grade and it was considered to be sufficiently accurate.

Table A7- 1 The nominal and experimental values of the imposed factors

Exp	X_d (g/l)	X_e (g/l)	SD	T_d (°C)	T_e (°C)	SD	G_d (s ⁻¹)	G_e (s ⁻¹)	SD	DO _d (mg/l)	DO _e (mg/l)	SD	Ca (meq/l)
1	0.63	0.43	0.14	15	15.16	0.11	55	53.94	0.75	2	2.19	0.13	12
2	0.63	0.74	0.08	15	14.92	0.06	200	199.74	0.18	2	2.38	0.27	12
3	0.25	0.26	0.01	10	10.75	0.53	28	25.51	1.75	1	1.10	0.07	18
4	1.59	1.50	0.06	10	9.76	0.16	105	107.94	2.07	3	3.14	0.10	6
5	0.25	0.24	0.007	10	10.51	0.36	28	26.17	1.29	3	3.12	0.08	6
6	0.63	0.49	0.100	15	15.03	0.02	55	55.28	0.20	2	2.09	0.064	12
7	1.59	1.41	0.12	10	9.81	0.14	105	100.33	3.30	1	1.10	0.074	18
8	0.63	0.57	0.03	25	24.85	0.10	55	54.20	0.56	2	2.08	0.062	12
9	0.63	0.76	0.09	15	15.07	0.05	55	57.92	2.06	0	0.01	0.01	12
10	0.63	0.632	0.004	15	15.57	0.40	55	53.58	1.00	2	2.08	0.059	12
11	0.63	0.59	0.03	15	15.97	0.68	55	56.54	1.08	2	2.09	0.062	12
12	0.1	0.12	0.014	15	16.88	1.32	55	57.52	1.78	2	2.89	0.63	12
13	4	3.89	0.074	15	15.07	0.05	55	54.83	0.11	2	1.96	0.03	12
14	0.63	0.66	0.022	15	15.61	0.43	55	57.96	2.09	4	4.09	0.06	12
15	0.25	0.29	0.033	20	19.95	0.03	28	25.61	1.68	1	1.27	0.19	6
16	1.59	1.50	0.06	20	19.96	0.025	28	24.86	2.22	1	1.03	0.02	18
17	0.25	0.24	0.005	20	20.12	0.09	28	24.21	2.68	3	3.10	0.07	18
18	0.63	0.52	0.079	15	14.96	0.02	55	50.98	2.84	2	2.09	0.06	12
19	1.59	1.46	0.09	20	20.20	0.15	105	97.69	5.16	3	3.17	0.12	18
20	1.59	1.50	0.06	10	10.29	0.21	28	24.99	2.12	1	1.11	0.08	6
21	0.63	0.62	0.007	15	15.54	0.38	55	54.64	0.25	2	2.24	0.17	12
22	0.63	0.68	0.038	15	15.38	0.27	55	51.47	2.49	2	2.11	0.08	0
23	0.25	0.26	0.009	20	20.50	0.35	105	103.83	0.82	3	3.16	0.11	6
24	0.63	0.76	0.097	15	15.15	0.10	15	16.85	1.31	2	2.28	0.19	12
25	0.25	0.27	0.016	10	9.88	0.08	105	102.18	1.99	3	3.12	0.08	18
26	0.63	0.59	0.025	15	14.87	0.093	55	57.54	1.80	2	2.14	0.10	12
27	0.63	0.71	0.05	15	15.15	0.10	55	48.84	4.35	2	2.08	0.05	24
28	0.63	0.70	0.05	15	15.05	0.03	55	56.9	1.34	2	2.05	0.04	12
29	1.59	1.50	0.06	20	20.03	0.02	105	99.60	3.81	1	1.06	0.05	6
30	1.59	1.53	0.03	20	20.05	0.04	28	26.06	1.36	3	3.02	0.02	6
31	0.63	0.634	0.003	15	15.28	0.19	55	51.70	2.33	2	2.11	0.08	12
32	0.63	0.62	0.008	5	5.74	0.52	55	51.7	6.85	2	2.16	0.12	12
33	1.59	1.61	0.017	10	10.03	0.024	28	31.82	2.70	3	3.05	0.03	18
34	0.63	0.72	0.063	15	15.89	0.63	55	60.72	4.04	2	2.06	0.04	12
35	0.25	0.28	0.025	20	20.09	0.07	105	103.55	1.02	1	1.13	0.09	18
36	0.25	0.28	0.024	10	10.57	0.40	105	103.35	1.17	1	1.26	0.18	6

Appendix 7.2

Floc Size

$\Delta D[4,3]$

The model term coefficients values and their statistical analysis are presented in Table A7- 2, while the statistical model evaluation for $\Delta D[4,3]$ is shown in Table A7-3.

Table A7- 2. Response model coefficient values and their statistical analysis

Index	Model term	Coefficient value	P-value
1.	I	268.6985	-
2.	T	1.2436	0.92404
3.	G	-232.6887	0.00000
4.	Ca	43.7874	0.00350
5.	DO	1.4915	0.90494
6.	X	49.6957	0.00206
7.	T*G	3.4977	0.81285
8.	T*Ca	2.5689	0.87130
9.	T*DO	-23.496	0.14697
10.	T*X	-44.0634	0.01708
11.	G*Ca	-32.1000	0.04147
12.	G*DO	1.5762	0.9133
13.	G*X	-30.1708	0.06735
14.	Ca*DO	13.5917	0.39452
15.	Ca*X	11.5056	0.49761
16.	DO*X	-31.0063	0.05737
17.	T ²	-8.6429	0.37676
18.	G ²	37.5650	0.00065
19.	Ca ²	-45.3012	0.00014
20.	DO ²	0.8980	0.9178
21.	X ²	-21.9386	0.04633

Table A7-3 Statistical evaluation for the floc size model

ANOVA ANALYSIS

Source	DegFr	SumOfSq	MeanSq	F-Ratio	P-Value
Total	35	1.7261e+006			
Regression	20	1.6684e+006	8.3421e+004	21.69	1.093e-007
Residual	15	5.7679e+004	3.8453e+003		
- Lack of Fit	6	2.2670e+004	3.7784e+003	0.97	0.47706
- Pure Error	9	3.5009e+004	3.8899e+003		

REGRESSION QUALITY

R ² :	0.96658	(Ideal Value: 1)
R ² adj:	0.92203	(Ideal Value: 1)
RMS Err:	62.01013	(Std. Dev.)

$D[4,3]_f$

The empirical model obtained for $D[4,3]_f$ is presented in this section. The model coefficients were already given in section 7.2.2. The statistical analysis by ANOVA is presented in Table A7-4.

Table A7-4. Statistical evaluation of the model

ANOVA ANALYSIS

Source	DegFr	SumOfSq	MeanSq	F-Ratio	P-value
Total	35	1.9976e+006			
Regression	20	1.8722e+006	9.3608e+004	11.20	0.00001
Residual	15	1.2541e+005	8.3606e+003		
- Lack of Fit	6	4.6257e+004	7.7095e+003	0.88	0.53472
- Pure Error	9	7.9152e+004	8.7947e+003		

REGRESSION QUALITY

R ² :	0.93722	(Ideal Value: 1)
R ² _{adj} :	0.85351	(Ideal Value: 1)
RMS Err:	91.43641	(Std. Dev.)

The stationary point for $D[4,3]_f$ is 358.79 μm and the factor values corresponding to the stationary point are given in Table A7-5.

Table A7-5. The factor values corresponding to the stationary point

Factor	Stationary point (scaled)	Stationary point (unscaled)
T	2.8903	29.452
G	1.1760	117.58
Ca	-1.8652	0.8088
DO	-3.2893	-1.2893
X	-1.4325	0.1675

The canonical form is given by equation A7-1 and indicates that the stationary point is a saddle point.

$$\hat{R}(D[4,3]_f) = 358.79 - 69.003w_1^2 - 36.685w_2^2 - 1.8202w_3^2 + 11.645w_4^2 + 67.050w_5^2 \tag{A7-1}$$

The optimal operating conditions for a maximal response are presented in Table A7-6.

Table A7-6 Optimal factor values for a maximal response

Response $D[4,3]$ (μm)	1880.4		
	Active constrains	Scaled value	Unscaled value
Factor			
T	yes	2	25
G	yes	-2	15
Ca	yes	2	24
DO	yes	-2	0
X	yes	2	4

Appendix 7.3

Sludge Volume Index (SVI)

Δ SVI

The model term coefficients values and their statistical analysis are presented in Table A7- 7, while the statistical model evaluation for Δ SVI is shown in Table A7-8.

Table A7- 7 Δ SVI model coefficient values and their statistical analysis.

Index	Model term	Coefficient value	P-value
1.	1	-41.687	-
2.	T	-1.165	0.78336
3.	G	6.1367	0.14092
4.	Ca	-6.1864	0.15277
5.	DO	-11.2629	0.01275
6.	X	-12.0004	0.01440
7.	T*G	-0.1933	0.96780
8.	T*Ca	3.9821	0.44336
9.	T*DO	-3.5278	0.48998
10.	T*X	3.4752	0.52440
11.	G*Ca	2.1942	0.64531
12.	G*DO	0.6447	0.89085
13.	G*X	5.5208	0.28363
14.	Ca*DO	1.6007	0.75474
15.	Ca*X	-4.4533	0.42001
16.	DO*X	4.2097	0.40267
17.	T ²	-1.4797	0.63772
18.	G ²	2.7981	0.34089
19.	Ca ²	6.3803	0.04415
20.	DO ²	7.7649	0.01357
21.	X ²	-3.8352	0.26025

Table A7-8 Statistical analysis of the model obtained by considering Δ SVI as response

ANOVA ANALYSIS

Source	DegFr	SumOfSq	MeanSq	F-Ratio	P-value
Total	35	1.8520e+004			
Regression	20	1.2447e+004	6.2234e+002	1.54	0.19982
Residual	15	6.0728e+003	4.0485e+002		
- Lack of Fit	6	5.5517e+003	9.2528e+002	15.98	0.00001
- Pure Error	9	5.2111e+002	5.7901e+001		

REGRESSION QUALITY

R2:	0.67209	(Ideal Value: 1)
R2adj:	0.23488	(Ideal Value: 1)
RMS Err:	20.12094	(Std. Dev.)

Final SVI

The quadratic model obtained for the final SVI is presented in this section. The statistical analysis by ANOVA is given in Table A7-9.

Table A7-9 Statistical evaluation of the model

ANOVA ANALYSIS

Source	DegFr	SumOfSq	MeanSq	F-Ratio	P-value
Total	35	5.3044e+004			
Regression	20	3.1700e+004	1.5850e+003	1.11	0.42217
Residual	15	2.1344e+004	1.4229e+003		
- Lack of Fit	6	1.7981e+004	2.9968e+003	8.02	0.00053
- Pure Error	9	3.3629e+003	3.7365e+002		

REGRESSION QUALITY

R ² :	0.59762	(Ideal Value: 1)
R ² _{adj} :	0.06112	(Ideal Value: 1)
RMS Err:	37.72142	(Std. Dev.)

The stationary point is SVI = 132.27 ml/g and the factor values corresponding to the stationary point are given in Table A7-10.

Table A7-10 The factor values corresponding to the stationary

Factor	Stationary point (scaled)	Stationary point (unscaled)
T	1.0196	0.4213
G	-0.3560	43.886
Ca	1.2276	19.366
DO	0.2329	2.2330
X	0.4213	0.9310

The canonical form obtained is given by equation A7-2 and indicates that the stationary point is a saddle point.

$$\hat{R}(SVI) = 132.27 - 16.51w_1^2 - 5.48w_2^2 + 1.54w_3^2 + 8.42w_4^2 + 24.66w_5^2 \tag{A7-2}$$

Appendix 7.4

Zeta potential

$\Delta Zeta$

The model term coefficients values and their statistical analysis are presented in Table A7-11, while the statistical model evaluation for $\Delta Zeta$ is shown in Table A7-12.

Table A7-11 $\Delta Zeta$ model coefficient values and their statistical analysis

Index	Model term	Coefficient value	P-value
1.	1	11.1227	-
2.	T	-1.1009	0.37944
3.	G	-1.3555	0.25811
4.	Ca	1.2994	0.29585
5.	DO	-1.8297	0.13676
6.	X	-2.5616	0.06143
7.	T*G	0.0622	0.96452
8.	T*Ca	-2.8039	0.07712
9.	T*DO	-0.0669	0.96398
10.	T*X	0.3108	0.84447
11.	G*Ca	0.9102	0.51486
12.	G*DO	0.5720	0.67762
13.	G*X	5.3677	0.00213
14.	Ca*DO	-5.7364	0.00141
15.	Ca*X	0.2444	0.87828
16.	DO*X	3.1591	0.04284
17.	T ²	0.7065	0.44429
18.	G ²	0.3005	0.72261
19.	Ca ²	-2.8543	0.00426
20.	DO ²	3.2372	0.00118
21.	X ²	2.8786	0.00886

Table A7-12 Statistical analysis of the model obtained for $\Delta Zeta$

ANOVA ANALYSIS

Source	DegFr	SumOfSq	MeanSq	F-Ratio	P-value
Total	35	2.6630e+003			
Regression	20	2.1449e+003	1.0724e+002	3.10	0.01471
Residual	15	5.1812e+002	3.4541e+001		
- Lack of Fit	6	4.8212e+002	8.0353e+001	20.09	0.00000
- Pure Error	9	3.6000e+001	4.0000e+000		

REGRESSION QUALITY

R ² :	0.80544	(Ideal Value: 1)
R ² _{adj} :	0.54602	(Ideal Value: 1)
RMS Err:	5.87717	(Std. Dev.)

Final zeta potential

The statistical analysis of the quadratic model obtained for final zeta potential is presented in Table A7-13.

Table A7-13 Statistical evaluation of the model

ANOVA ANALYSIS

Source	DegFr	SumOfSq	MeanSq	F-Ratio	P-value
Total	35	4.8506e+002			
Regression	20	3.3044e+002	1.6522e+001	1.60	0.17753
Residual	15	1.5462e+002	1.0308e+001		
- Lack of Fit	6	2.4993e+001	4.1655e+000	0.29	0.93293
- Pure Error	9	1.2963e+002	1.4403e+001		

REGRESSION QUALITY

R ² :	0.68124	(Ideal Value: 1)
R ² _{adj} :	0.25622	(Ideal Value: 1)
RMS Err:	3.21058	(Std. Dev.)

The stationary point for final zeta potential is -6.96 mV and the factor values corresponding to the stationary point are given in Table A7-14.

Table A7-14 Model factor values at the stationary point

Factor	Stationary point (scaled)	Stationary point (unscaled)
T	-0.8935	10.532
G	-1.0027	28.949
Ca	0.8594	17.157
DO	0.0401	2.040
X	0.8283	1.356

The canonical form is given by equation A7-3 and indicates that the stationary point is a saddle point.

$$\hat{R}(Zeta) = -6.96 - 1.47w_1^2 - 0.42w_2^2 + 0.43w_3^2 + 1.01w_4^2 + 1.57w_5^2 \tag{A7-3}$$

The model optimisation shows that two minimal and two maximal values can be found as function of the imposed initial values.

Table A7-15 Optimization parameters for Zeta response

Response Zeta (mV)	-12.196/-29.014			6.07/12.66		
	Active constraints	Scaled value	Unscaled value	Active constraints	Scaled value	Unscaled value
T	yes	2/-2	25/5	yes	2/-2	25/5
G	yes	-2/2	15/200	-	0.52/-1.94	76.90/15.84
Ca	yes	2/-2	24/0	-	-0.07/1.78	11.56/22.7
DO	-	0.24/-0.57	2.24/1.42	yes	2/2	4/4
X	-	0.12/0.34	0.70/0.86	yes	-2/-2	0.1/0.1

Appendix 7.5

Supernatant turbidity

$\Delta Turb$

The model term coefficients values and their statistical analysis are presented in Table A7-16, while the statistical model evaluation for $\Delta Turb$ is shown in Table A7-17.

Table A7-16 $\Delta Turb$ model coefficient values and their statistical analysis

Index	Model term	Coefficient value	P-value
1.	1	-6.7953	-
2.	T	-0.0582	0.96816
3.	G	-0.0409	0.97638
4.	Ca	0.2078	0.88521
5.	DO	1.7239	0.22838
6.	X	0.5377	0.72403
7.	T*G	-0.7521	0.64964
8.	T*Ca	-0.4108	0.81680
9.	T*DO	1.1036	0.53018
10.	T*X	1.0302	0.58317
11.	G*Ca	0.1472	0.92836
12.	G*DO	-0.3726	0.81801
13.	G*X	0.6702	0.70068
14.	Ca*DO	0.9744	0.58227
15.	Ca*X	-0.3507	0.85222
16.	DO*X	1.1121	0.51899
17.	T ²	-0.3299	0.76009
18.	G ²	0.8305	0.41008
19.	Ca ²	1.7590	0.09911
20.	DO ²	-1.0145	0.30577
21.	X ²	0.9334	0.42146

Table A7-17 Statistical analysis for the $\Delta Turb$ model

ANOVA ANALYSIS

Source	DegFr	SumOfSq	MeanSq	F-Ratio	P-value
Total	35	1.0845e+003			
Regression	20	3.6378e+002	1.8189e+001	0.38	0.97795
Residual	15	7.2077e+002	4.8051e+001		
- Lack of Fit	6	3.9547e+002	6.5911e+001	1.82	0.16161
- Pure Error	9	3.2530e+002	3.6145e+001		

REGRESSION QUALITY

R ² :	0.33542	(Ideal Value: 1)
R ² _{adj} :	-0.55069	(Ideal Value: 1)
RMS Err:	6.93190	(Std. Dev.)

Final turbidity

The results of the statistical analysis of the final turbidity model are given in Table A7-18.

Table A7-18 Statistical analysis of the model obtained for the final turbidity (Turbidity)

ANOVA ANALYSIS

Source	DegFr	SumOfSq	MeanSq	F-Ratio	P-value
Total	35	5.9515e+002			
Regression	20	3.5965e+002	1.7982e+001	1.15	0.40024
Residual	15	2.3551e+002	1.5700e+001		
- Lack of Fit	6	8.3821e+001	1.3970e+001	0.83	0.56557
- Pure Error	9	1.5169e+002	1.6854e+001		

REGRESSION QUALITY

R ² :	0.60429	(Ideal Value: 1)
R ² _{adj} :	0.07668	(Ideal Value: 1)
RMS Err:	3.96237	(Std. Dev.)

Appendix 7.6

Supernatant total suspended solids concentration (TSS)

ΔTSS

The model term coefficients values and their statistical analysis are presented in Table A7-19, while the statistical model evaluation for ΔTSS is shown in Table A7- 20.

Table A7-19. ΔTSS model coefficient values and their statistical analysis.

Index	Model term	Coefficient value	P-value
1.	1	-10.1760	-
2.	T	-9.3316	0.03851
3.	G	1.7192	0.66585
4.	Ca	-2.9774	0.47466
5.	DO	4.7627	0.25627
6.	X	5.0613	0.00206
7.	T*G	-6.9920	0.15393
8.	T*Ca	-11.6271	0.03448
9.	T*DO	8.8552	0.09249
10.	T*X	6.5901	0.23033
11.	G*Ca	-11.6742	0.02318
12.	G*DO	-2.8845	0.53709
13.	G*X	3.5923	0.47547
14.	Ca*DO	9.4517	0.07676
15.	Ca*X	8.5283	0.12905
16.	DO*X	3.5952	0.46835
17.	T ²	-3.8540	0.22472
18.	G ²	-3.0734	0.29168
19.	Ca ²	3.3162	0.26613
20.	DO ²	3.1432	0.27020
21.	X ²	-0.2255	0.94544

Table A7- 20 Statistical analysis for the Δ TSS model

ANOVA ANALYSIS

Source	DegFr	SumOfSq	MeanSq	F-Ratio	P-value
Total	35	2.0336e+004			
Regression	20	1.4401e+004	7.2006e+002	1.82	0.12029
Residual	15	5.9345e+003	3.9563e+002		
- Lack of Fit	6	1.5700e+003	2.6166e+002	0.54	0.77030
- Pure Error	9	4.3645e+003	4.8495e+002		

REGRESSION QUALITY

R ² :	0.70817	(Ideal Value: 1)
R ² _{adj} :	0.31907	(Ideal Value: 1)
RMS Err:	19.89054	(Std. Dev.)

TSS

The statistical analysis of the model obtained for the final TSS is presented in Table A7- 21.

Table A7- 21 Statistical evaluation of the model

ANOVA ANALYSIS

Source	DegFr	SumOfSq	MeanSq	F-Ratio	P-value
Total	35	9.6290e+003			
Regression	20	4.2892e+003	2.1446e+002	0.60	0.85641
Residual	15	5.3398e+003	3.5598e+002		
- Lack of Fit	6	6.2265e+002	1.0377e+002	0.20	0.97228
- Pure Error	9	4.7171e+003	5.2413e+002		

REGRESSION QUALITY

R ² :	0.44545	(Ideal Value: 1)
R ² _{adj} :	-0.29395	(Ideal Value: 1)
RMS Err:	18.86756	(Std. Dev.)

The stationary point is TSS = 11.23 mg/l and the values of the factors corresponding to the stationary point are given in Table A7-22.

Table A7-22 Factors value corresponding to the TSS stationary point

Factor	Stationary point (scaled)	Stationary point (unscaled)
T	-3.2642	-1.3210
G	2.5448	283.66
Ca	-2.1291	-0.7748
DO	-3.6884	-1.6884
X	-0.8560	0.2856

The canonical form is given equation A7-4 and indicates that the stationary point is a saddle point.

$$\hat{R}(TSS) = 11.23 - 1.45w_1^2 - 1.09w_2^2 - 7.01w_3^2 - 1.48w_4^2 + 1.71w_5^2$$

Appendix 7.7

Conductivity

Δ Conductivity

The model term coefficients values and their statistical analysis are presented in Table A7-23, while the statistical model evaluation for Δ Conductivity is shown in Table A7- 24.

Table A7-23. Δ Conductivity model coefficient values and their statistical analysis.

Index	Model term	Coefficient value	P-value
1.	1	888.2365	-
2.	T	111.7434	0.02685
3.	G	23.2754	0.59796
4.	Ca	484.0480	0.00000
5.	DO	-8.6600	0.84523
6.	X	-82.9574	0.10098
7.	T*G	-39.7524	0.45253
8.	T*Ca	26.0433	0.64474
9.	T*DO	-5.2247	0.92497
10.	T*X	-47.4126	0.42915
11.	G*Ca	17.2626	0.74027
12.	G*DO	-64.7891	0.21939
13.	G*X	8.7641	0.87400
14.	Ca*DO	41.9065	0.45835
15.	Ca*X	-60.6441	0.31851
16.	DO*X	-38.8971	0.47831
17.	T ²	19.0898	0.57937
18.	G ²	33.4767	0.29920
19.	Ca ²	30.4565	0.35310
20.	DO ²	46.0728	0.15033
21.	X ²	21.4497	0.55879

Table A7- 24 Statistical analysis for Δ Conductivity model

ANOVA ANALYSIS

Source	DegFr	SumOfSq	MeanSq	F-Ratio	P-value
Total	35	7.3462e+006			
Regression	20	6.6190e+006	3.3095e+005	6.83	0.00022
Residual	15	7.2725e+005	4.8483e+004		
- Lack of Fit	6	2.4714e+005	4.1189e+004	0.77	0.60371
- Pure Error	9	4.8011e+005	5.3346e+004		

REGRESSION QUALITY

R ² :	0.90100	(Ideal Value: 1)
R ² _{adj} :	0.76901	(Ideal Value: 1)
RMS Err:	220.18896	(Std. Dev.)

Final Conductivity

Table A7-25 Statistical evaluation of the model

ANOVA ANALYSIS

Source	DegFr	SumOfSq	MeanSq	F-Ratio	P-value
Total	35	8.1163e+006			
Regression	20	7.0899e+006	3.5449e+005	5.18	0.00108
Residual	15	1.0264e+006	6.8425e+004		
- Lack of Fit	6	1.6395e+005	2.7324e+004	0.29	0.93501
- Pure Error	9	8.6243e+005	9.5826e+004		

REGRESSION QUALITY

R ² :	0.87354	(Ideal Value: 1)
R ² _{adj} :	0.70493	(Ideal Value: 1)
RMS Err:	261.58209	(Std. Dev.)

The stationary point is found at a point Conductivity= 1624.9 μS/cm and the corresponding factor values are given in Table A7- 26.

Table A7- 26 The factor values corresponding to the stationary point for Conductivity.

Factor	Stationary point (scaled)	Stationary point (unscaled)
T	-0.22582	13.871
G	-1.7287	18.147
Ca	0.65321	15.919
DO	-2.5211	-0.5211
X	2.9263	9.4456

The canonical form indicates that the stationary point is a saddle point.

$$\hat{R}(\text{Conductivity}) = 1624.9 - 62.32w_1^2 - 21.55w_2^2 + 55.87w_3^2 + 73.06w_4^2 + 113.73w_5^2 \tag{A7- 5}$$

The maximal value for Conductivity as predicted by model and the corresponding factor values are listed in Table A7- 27.

Table A7- 27 Optimal factor values required for obtaining the maximum response in Conductivity.

Response Conductivity (μS/cm)	4472.63		
Factor	Active constraints	Scaled value	Unscaled value
T	yes	2	25
G	yes	2	200
Ca	yes	2	24
DO	yes	-2	0
X	yes	-2	0.01

Appendix 7.8

pH

ΔpH

The model term coefficients values and their statistical analysis are presented in Table A7-28, while the statistical model evaluation for ΔpH is shown in Table A7- 29.

Table A7-28 ΔpH model coefficient values and their statistical analysis.

Index	Model term	Coefficient value	P-value
1.	1	-0.1087	-
2.	T	-0.0549	0.15902
3.	G	0.0610	0.10326
4.	Ca	-0.0570	0.13998
5.	DO	0.0129	0.72140
6.	X	0.0081	0.83628
7.	T*G	0.0252	0.55745
8.	T*Ca	0.0219	0.63390
9.	T*DO	0.0014	0.97586
10.	T*X	-0.0238	0.62255
11.	G*Ca	0.0026	0.95079
12.	G*DO	-0.0309	0.46408
13.	G*X	0.0136	0.76191
14.	Ca*DO	-0.0036	0.93760
15.	Ca*X	0.0053	0.91322
16.	DO*X	0.0348	0.43665
17.	T ²	0.0084	0.76328
18.	G ²	0.0169	0.51490
19.	Ca ²	0.0034	0.89821
20.	DO ²	0.0067	0.79110
21.	X ²	-0.0309	0.30686

Table A7- 29 Statistical analysis for the ΔpH model

ANOVA ANALYSIS

Source	DegFr	SumOfSq	MeanSq	F-Ratio	P-value
Total	35	8.3774e-001			
Regression	20	3.5673e-001	1.7837e-002	0.56	0.89035
Residual	15	4.8101e-001	3.2067e-002		
- Lack of Fit	6	8.9616e-002	1.4936e-002	0.34	0.90287
- Pure Error	9	3.9139e-001	4.3488e-002		

REGRESSION QUALITY

R ² :	0.42583	(Ideal Value: 1)
R ² _{adj} :	-0.33973	(Ideal Value: 1)
RMS Err:	0.17907	(Std. Dev.)

pH

Table A7- 30 Statistical evaluation of the pH model

ANOVA ANALYSIS

Source	DegFr	SumOfSq	MeanSq	F-Ratio	P-value
Total	35	5.2255e+000			
Regression	20	3.8850e+000	1.9425e-001	2.17	0.06487
Residual	15	1.3405e+000	8.9369e-002		
- Lack of Fit	6	3.2858e-001	5.4763e-002	0.49	0.80802
- Pure Error	9	1.0120e+000	1.1244e-001		

REGRESSION QUALITY

R ² :	0.74346	(Ideal Value: 1)
R ² _{adj} :	0.40141	(Ideal Value: 1)
RMS Err:	0.29895	(Std. Dev.)

The stationary point is pH = 7.58 and the factor values corresponding to the stationary point are given in Table A7-31.

Table A7-31 The factor values corresponding to the stationary point for pH.

Factor	Stationary point (scaled)	Stationary point (unscaled)
T	0.46280	17.314
G	-0.34463	44.209
Ca	-0.89567	6.626
DO	0.01228	2.0123
X	-1.3738	0.1769

The canonical form indicates that the stationary point is a saddle point.

$$\hat{R}(pH) = 7.58 - 0.164w_1^2 - 0.0847w_2^2 + 0.0361w_3^2 + 0.056w_4^2 + 0.123w_5^2 \tag{A7- 6}$$

Statistical evaluation of the final pH obtained for the case in which one central point experiment (no.21) was not considered in the evaluations is presented in Table A7- 32:

Table A7- 32 Statistical evaluation of the model

ANOVA ANALYSIS

Source	DegFr	SumOfSq	MeanSq	F-Ratio	P-value
Total	34	4.4972e+000			
Regression	20	3.9201e+000	1.9601e-001	4.76	0.00227
Residual	14	5.7708e-001	4.1220e-002		
- Lack of Fit	6	-4.9411e-001	-8.2352e-002	-0.62	1.00000
- Pure Error	8	1.0712e+000	1.3390e-001		

REGRESSION QUALITY

R ² :	0.87168	(Ideal Value: 1)
R ² _{adj} :	0.68837	(Ideal Value: 1)
RMS Err:	0.20303	(Std. Dev.)

Table A7-33 The factor values corresponding to the stationary point (pH = 7.58)

Factor	Stationary point (scaled)	Stationary point (unscaled)
T	0.574	17.870
G	-0.095	51.903
Ca	-1.061	5.632
DO	-0.222	1.777
X	-1.872	0.111

The canonical form indicates that the stationary point is a saddle point.

$$\hat{R}(pH) = 7.58 - 0.144w_1^2 - 0.061w_2^2 + 0.054w_3^2 + 0.075w_4^2 + 0.141w_5^2$$

A7- 7

References

- Abbassi B., Dullstein S. and Rabiger N. (1999) Minimization of excess sludge production by increase of oxygen concentration in activated sludge flocs; Experimental and theoretical approach. *Wat. Res.* **34**(1): 139-146.
- Allen T. (1997) *Particle size measurement. Vol.1 - Powder sampling and particle size measurement*. Fifth edition. Chapman and Hall LTD., London
- Altschul S.F., Madden T.L., Schaffer A.A., Zhang J., Zhang Z., Miller W. and Lipman D.J. (1997) Gapped Blast and PSI-BLAST: a new generation of protein database search programs. *Nucleic Acids Res.* **25**: 3389-3402.
- Andreadakis A.D. (1993) Physical and chemical properties of activated sludge floc. *Wat. Res.* **27**(12): 1707-1714.
- Ankersmid (2004) <http://www.ankersmid.com>
- APHA (1992) *Standard methods for the examination of water and wastewater* 18th ed. American Public Health Association, Washington DC, USA.
- Argaman Y. and Kaufman W.J. (1970) Turbulence and flocculation. *J. Sanit. Eng. Div. ASCE* **96**: 223-231.
- Artan N., Wilderer P., Orhon D., Tasli R. and Morgenroth E. (2002) Model evaluation and optimisation of nutrient removal potential for sequencing bath reactors. *Water S.A.* **28**(4): 423-432.
- Baldwin D.D. and Campbell C.E. (2001) Short-term effect of low pH on the microfauna of an activated sludge wastewater treatment system. *Water Qual. Res. J. Canada* **36**(3): 519-535.
- Barbusinski K. and Koscielniak H. (1995) Influence of substrate loading intensity on floc size in the activated sludge process. *Wat. Res.* **29**(7): 1703-1710.
- Baudu M., Laroye M.Y., Gaudriot P.H. and Mazet M. (1995) Turbidity measurement contribution for biological waste-water treatment process. *Environ. Technol.* **16**(4): 355-366.
- Biggs C.A. (2000) Activated sludge flocculation: investigating the effect of shear rate and cation concentration on flocculation dynamics. *PhD Thesis*, Advanced Wastewater Management Center, Dept. of Chem. Eng., University of Queensland, Australia.
- Biggs C.A., Lant P. and Hounslow M. (2003) Modelling the effect of shear history on activated sludge flocculation. *Wat. Sci. Tech.* **47**(11): 251-257.

Blanco A., De la Fuente E., Negro C, Monte M.C. and Tijero J. (2002) Focused beam reflectant measurement as a tool to measure flocculation. *TAPPI Journal* **1**(10): 14-20.

Boeije G. (1999) Chemical fate prediction for use in geo-referenced environmental exposure assessment. *PhD Thesis*, Faculty of Agricultural and Applied Biological Sciences, Ghent University.

Boon N., Goris J., de Vos P., Verstraete W. and Top E. (2000) Bioaugmentation of activated sludge by an indigenous 3-Chloroaniline-degrading *Comamonas testosteroni* Strain, I2gfp. *Appl. Environ. Microbiol.* **66**(7): 2906-2913.

Boon N., De Windt W., Verstraete W. and Top E. (2002) Evaluation of nested PCR-DGGE (denaturing gradient gel electrophoresis) with group-specific 16S rRNA primers for the analysis of bacterial communities from different wastewater treatment plants. *FEMS Microbiology Ecology* **39**: 101-112.

Bott C.B. and Love N.G. (2002) Investigating a mechanistic cause for activated sludge deflocculation in response to shock loads of toxic electrophilic chemicals. *Water Environ. Res.* **74**(3): 306-315.

Bowen P. (2002) Particle size measurement from millimeters to nanometers and from rods to platelets. In proceeding: World Congress on Particle Technology. Sydney, Australia, July 21-25 2002 (on CD-ROM).

Bratby J. (1980) *Coagulation and Flocculation with an emphasis on water and wastewater treatment*. Uplands Press Ltd, Publishers of "Filtration & Separation" magazine, Croydon CR 1LB, England.

Bruus J.H., Nielsen P.H. and Keiding K. (1992) On the stability of activated sludge flocs with implications to dewatering. *Wat. Res.* **26**: 1597-1604.

Busalmen J.P, Sancez De S.R. and Schiffrin D.J. (1998) Ellipsometric measurement of bacterial film at metal-electrolyte interfaces. *Appl. Environ. Microbiol.* **64**(10): 3690-3697.

Bushell G. and Amal R. (2000) Measurement of fractal aggregates of polydisperse particles using small-angle light scattering. *J. Colloid Interface Sci.* **221**: 186-194.

Bushell G., Jan Y.D., Woodfield D., Raper J. and Amal R. (2002) On techniques for the measurements of the mass fractal dimension of aggregates. *Adv. Colloid Interface Sci.* **95**: 1-50.

Bye M.C. and Dold L.P. (1998) Sludge volume index settleability measures: effect of solids characteristics and test parameters. *Water Environ. Res.* **70**(1): 87-93.

Camp T.R. and Stein P.C. (1943) Velocity gradients and internal work in fluid motion. *J. Boston Soc. Civil Eng.* **30**: 219-237.

Cenens C., Jenné R. and Van Impe J.F. (2002) Evaluation of different shape parameters to distinguish between floc and filaments in activated sludge images. *Wat. Sci. Tech.* **45**(4-5): 85-91.

- Chaignon V., Lartiges B.S., El Samrani A. and Mustin C. (2002) Evolution of size distribution and transfer of mineral particles between flocs in activated sludges: an insight into floc exchange dynamics. *Wat. Res.* **36**: 676-684.
- Chakraborti R.K., Gardner K.H., Atkinson J.F. and Van Benschoten J.E. (2003) Changes in fractal dimension during aggregation. *Wat. Res.* **37**: 837-883.
- Chin C.-J., Yiacoumi S. and Tsouris C. (1998) Shear Induced Flocculation of Colloidal Particles in Stirred Tanks, *J. Coll. Inter. Sci.* **206**: 532-545
- Choi Y.C. and Morgenroth E. (2003) Monitoring biofilm detachment under dynamic changes in shear stress using laser-based particle size analysis and mass fractionation. *Wat. Sci. Tech.* **47**(5): 69-76.
- Chudoba J., Ottava V. and Madera V. (1973a) Control of activated sludge filamentous bulking –I. Effect of the hydraulic regime or degree of mixing in aeration tank. *Wat. Res.* **7**: 1163-1182.
- Chudoba J., Grau P. and Ottava V. (1973b) Control of activated sludge filamentous bulking – II. Selection of microorganisms by means of selector. *Wat. Res.* **7**: 1389-1406.
- Chudoba J., Blaha J. and Madera V. (1973c) Control of activated sludge filamentous bulking –III. Effect of sludge loading. *Wat. Res.* **8**: 231-237.
- Chudoba J. (1989) Discussion of: Effect of culture history on the determination of biodegradation kinetics by batch and fed-batch techniques, by Laura L. Templeton and C. P. Leslie Grady Jr., *Journal WPCF* **61**: 367-369.
- Cooke M., Bolton G., Jones D.H. and Housley D. (2001) Demonstration of a novel retrofit tomography baffle cage, for gas-liquid mixing studies under intense operating conditions. In Proceedings: 2^{ed} World Congress on industrial process tomography. Hanover, Germany, 29-31 August 2001.
- Cousin C. and Ganczarczyk J. (1998) Effects of Salinity on Physical Characteristics of the Activated Sludge Flocs, *Water Qual. Res. J. Canada* **33**(4): 565-587.
- Cousin C. and Ganczarczyk J. (1999) Effect of calcium ion concentration on the structure of activated sludge flocs. *Environ. Technol.* **20**: 1129-1138.
- Curtis T.P. and Craine N.G. (1998) The comparison of the diversity of activated sludge plants. *Wat. Sci. Tech.* **37**(4-5): 71-78.
- Daigger G.T., Buttz J.A. and Stephenson J.P. (1992) Analysis of techniques for evaluating and optimising existing full-scale wastewater treatment plants. *Wat. Sci. Tech.* **25**: 103-118.
- Dagot C., Pons M.N., Casellas M., Guibaud G., Dollet P. and Baudu M. (2001) Use of image analysis and rheological studies for the control of settleability of filamentous bacteria: application in SBR reactor. *Wat. Sci. Tech.* **43**(3): 27-33.
- Dammel E.E. and Schroeder E.D. (1991) Density of activated sludge solids. *Wat. Res.* **25**(7): 841-846.

Das D., Keinath T.M., Parker D.S., Wahlberg E.J. (1993) Floc breakup in activated sludge plants. *Wat. Environ. Res.* **65**(2): 138-145.

Davenport J.R., Curtis P.T., Goodfellow M., Stainsby M.F. and Bingley M. (2000) Quantitative use of Fluorescent In Situ Hybridization to examine relationships between mycolic acid-containing actinomycetes and foaming in activated sludge plants. *Appl. Environ. Microbiol.*, **66**(3): 1158-1166.

De Clercq B., Brannock M., Lant P.A. and Vanrolleghem P.A. (2002a) In situ particle size characterization on a circular clarifier of a wastewater treatment plant. In: Proceedings 2002 World Congress on Particle Technology. Sydney, Australia, July 21-25 2002 (on CD-ROM).

De Clercq B., Lant P.A. and Vanrolleghem P.A. (2002b) On-line particle size measurements in secondary clarifiers. In: Proceedings International IWA Conference on Automation in Water Quality Monitoring (AutMoNet2002). Vienna, Austria, May 21-22 2002 (on CD-ROM).

De Clercq B. (2003) Computational fluid dynamics of settling tanks: development of experiments and rheological, settling and scraper submodels. *PhD Thesis*, Faculty of Agricultural and Applied Biological Science, Ghent University, Belgium.

Derjaguin B.V. and Landau L. (1941) Theory of the stability of strongly charged lyophobic sols and the adhesion of strongly charged particles in solutions of electrolytes. *Acta Physiochim. URSS* **14**: 633-662.

Devisscher M., Bogaert H., Gernaey K. and Verstraete W. (1998) Use of bubbleless aeration to improve the performance of titrimetric sensors for the study of denitrification processes. In: Proceedings BNR' 98 – New Advances in Biological Nitrogen and Phosphorous Removal for Municipal or Industrial Wastewaters. Narbonne, France, October 12-14 1998.

Dick R.I. and Ewing B.B. (1967) Evaluation of activated sludge thickening theories. *J. Sanit. Eng. Div. Am. Soc. Civ. Eng.* **93**: 9-29.

Dick R.I. and Vesilind A.P. (1969) The sludge volume index – What is it? *Journal WPCF.* **41**(7): 1285-1291.

Dignac M.F., Urbain V., Rybacki D., Bruchet A., Snidaro D. and Scribe P. (1998) Chemical description of extracellular polymers: implications on activated sludge structure. *Wat. Sci. Tech.* **38**(8/9): 45-53.

Droppo I.G., Leppard G.G., Flannigan D.T. and Liss S.N. (1997) The freshwater floc: a functional relationship of water and organic and inorganic floc constituents affecting suspended sediment properties. *Water, Air and Soil Pollution*, Kluwer Academic Publishers **99**: 43-54.

Duan J. and Gregory J. (2003) Coagulation by hydrolyzing metal salts. *Adv. Colloid Interface Sci.* **100-102**: 475-502.

Eichner A.C., Erb R.W., Timmis K.N. and Wagner-Dobler I. (1999) Thermal gradient gel electrophoresis analysis of bioprotection from pollutant shocks in the activated sludge microbial community. *Appl. Environ. Microbiol.* **65**(1): 102-109.

- Eikelboom D.H., Andreadakis A and Andreasen K. (1998) Survey of filamentous populations in nutrient removal plants in four European countries. *Wat. Sci. Tech.* **37**(4-5): 281-289.
- Eikelboom D.H. (2000) *Process control of activated sludge plants by microscopic investigation*. IWA Publishing, London, England.
- EPA (1997) *The causes and control of activated sludge bulking and foaming*. Summary Report - U.S. Environmental Protection Agency, Centre for Environmental Research Information, Cincinnati, USA.
- EPA (1999) *Wastewater technology fact sheet: Sequencing Batch Reactors*. U.S. Environmental Protection Agency, Centre for Environmental Research Information, Cincinnati, USA.
- Eriksson L. and Alm B. (1991) Study of flocculation mechanisms by observing effects of a complexing agent on activated sludge properties. *Wat. Sci. Tech.* **24**: 21-28.
- Eriksson L. and Alm B. (1993) Characterization of activated sludge and conditioning with cationic polyelectrolytes. *Wat. Sci. Tech.* **28**(1): 203-212.
- Fernandez A., Huang S., Seston S., Xiang J., Hickey R., Criddle C. and Tiedje J. (1999) How stable is stable? Function versus community composition. *Appl. Environ. Microbiol.* **65**(8): 3697-3704.
- Francis L, Reyes D.L., Ritter W. and Raskin L. (1997) Group-specific small-subunit rRNA hybridization probes to characterize filamentous foaming in activated sludge systems. *Appl. Environ. Microbiol.* **63**(3): 1107-1117.
- Fitzpatrick C.S.B., Fradin E. and Gregory J. (2003) Temperature effects on flocculation, using different coagulants. In Proceedings: IWA Specialist Conference on Nano and Microparticles in Water and Wastewater Treatment. Zurich, Switzerland, September 22-24 2003: 225-230.
- Frølund B. and Keiding K. (1994) Implementation of an HPLC polystyrene divinylbenzene column for separation of activated sludge exopolymers. *Appl. Microbiol. Biotechnol.* **41**(6): 708-716.
- Frølund B., Palmgren R., Keiding K. and Nielsen P.H. (1996) Extraction of extracellular polymers from activated sludge using cation exchange resin. *Wat. Res.* **30**(8): 1749-1758.
- Fuchs A. and Staudinger G. (1999) Characterising the clarification of the supernatant of activated sludges. *Wat. Res.* **33**(11): 2527-2534.
- Galil N., Stahl N., Novak T.J. and Rebhun M. (1991) The influence of mixing on the physical characteristics of biological flocs. *Research Journal WPCF* **63**(5): 768-772.
- Ganczarczyk J. J. (1983) *Activated Sludge Process – Theory and Practice*. Marcel Dekker, INC, NY, USA.
- Gaval G. and Pernelle J.-J. (2003) Impact of repetition of oxygen deficiencies on filamentous bacteria proliferation in activated sludge. *Wat. Res.* **37**: 1991-2000.

- Giokas D.L., Daigger G.T., von Sperling M., Kim Y. and Paraskevas P.A. (2003) Comparison and evaluation of empirical zone settling velocity parameters based on sludge volume index using a unified settling characteristics database. *Wat. Res.* **37**: 3821-3936.
- Govoreanu R., Koegst T., Nopens I., Malisse K., De Clercq B. and Vanrolleghem P.A. (2003) *The FloccUNIT Manual*. BIOMATH Technical Report, Department of Applied Mathematics, Biometrics and Process Control, Ghent University, Belgium.
- Gregory J. (1997) The density of particles aggregates. *Wat. Sci. Tech.* **36**(4): 1-13.
- Gregory J. (1989) Fundamentals of flocculation. *CRC Critical Rev. Environ. Control.* **19**: 185-230.
- Grijpsperdt K. (1996) Development of an on-line sensor for the sedimentation process in activated sludge plant. *PhD Thesis*, Faculty of Agricultural and Applied Biological Science, Ghent University, Belgium.
- Grijpsperdt K. and Verstraete W. (1997) Image analysis to estimate the settleability and concentration of activated sludge. *Wat. Res.* **31**(6): 1126-1134.
- Guan J., Waite D.T. and Amal R. (1998a) Rapid structure characterization of bacterial aggregates. *Environ. Sci. Technol.* **32**: 3735-3742.
- Guan J., Waite D.T. and Amal R. (1998b) Rapid determination of fractal structure of bacterial assemblages in wastewater treatment: implications to process optimization. *Wat.Sci.Tech.* **38**(2): 9-15.
- Han M. and Lawler F.D. (1992) The (relative) insignificance of G in flocculation. *J. Am. Water Works Assoc.* **84**: 79-91
- Han H.Y., Shim J.S., Chung Y.K. and Park Y.H. (2002) Diagnosing and optimizing water treatment processes by using particle counter: a case study in Korea. *Wat. Sci. Tech.* **45**(4-5): 511-518.
- Higgins M.J. and Novak J.T. (1997a) The effect of cations on the settling and dewatering of activated sludges: Laboratory results. *Water Env. Res.* **69**(2): 215-224.
- Higgins M.J. and Novak J.T. (1997b) Dewatering and settling of activated sludges: The case for using cation analysis. *Water Env. Res.* **69**(2): 225-232.
- Higgins M.J. and Novak J.T. (1997c) Characterization of exocellular protein and its role in bioflocculation. *J. Env. Eng.* **123**: 479- 485.
- Hillgardt M. and Hoffmann E. (1997) Particle size analysis and sedimentation properties of the activated sludge flocs. *Wat. Sci. Tech.* **36**: 167-175.
- Houghton J.I., Burgess J.E. and Stephenson T. (2002) Off-line particle size analysis of digested sludge. *Wat. Res.* **36**: 4643-4647.
- Hounslow M.J., Ryall R.L. and Marshall V.R. (1988). A discretized population balance for nucleation, growth and aggregation. *AIChE Journal* **34**(11): 1821-1832.

- Hultman B., Lowen M., Karlsson U, Li P.H. and Molina L. (1991) Prediction of activated sludge sedimentation based on sludge indexes. *Wat. Sci. Tech.* **24**(7): 33-42.
- Insel G., Sin G., Lee D.S. and Vanrolleghem P.A. (2004) A calibration methodology and model-based system analysis for nutrient removing SBR. In Proceedings: 3rd IWA International Conference on SBRs. Noosa, Australia, February 22-26 2004.
- Irvine, R. and Busch, A. (1979) Sequencing batch biological reactors-an overview. *Journal WPCF* **51**(2): 244-254.
- Irvine R.L. and Ketchum L.H. (1989) Sequencing Batch Reactors for biological wastewater treatment. *CRC Critical Reviews in Environmental Control* **18**(4): 255-294.
- Jenkins D. (1992) Towards a comprehensive model of activated sludge bulking and foaming. *Wat. Sci. Tech.* **25**: 215- 230.
- Jenkins D., Richard M.G and Daigger G.T. (1993) *Manual on the causes and control of activated sludge bulking and foaming*. 2nd Ed., Lewis Publisher, Boca Raton, USA.
- Jiang Q. and Logan B. (1991) Fractal dimensions of aggregates determined from steady-state size distribution. *Environ.Sci.Technol.* **25**(12): 2031-2038.
- Jiang Q. and Logan B. (1996) Fractal dimension of aggregates from shear devices. *Journal AWWA* **88**(2): 100-113.
- Jin B., Wilen B.-M. and Lant P. (2003) A comprehensive insight into floc characteristics and their impact on compressibility and settleability of activated sludge. *Chem. Eng. J.* **95**: 221-234.
- Johnson C.P., Li X. and Logan B.E. (1996) Settling velocity of fractal aggregates. *Environ. Sci. Technol.* **30**: 1911-1918.
- Jorand F., Zartarian F., Thomas F., Block J.C., Bottero J.Y., Villemin G., Urbain V. and Manem J. (1995) Chemical and structural (2D) linkage between bacteria within activated sludge flocs. *Wat. Res.* **29**(7): 1639-1647.
- Jorand F., Boué-Bigne F., Block J.C. and Urbain V. (1998) Hydrophobic/hydrophilic properties of activated sludge exopolymeric substances. *Wat. Sci. Tech.* **37**(4/5): 307-316.
- Kaewpipat K. and Grady Jr. C.P.L. (2002) Microbial population dynamics in laboratory scale activated sludge reactors. *Wat. Sci. Tech.* **46** (1-2): 19-27.
- Keiding K. and Nielsen P.H. (1997) Desorption of organic macromolecules from activated sludge: effect of ionic composition. *Wat. Res.* **31**(7): 1665-1672.
- Keller J., Yuan Z. and Blackall L. (2002) Integrating process engineering and microbiology tools to advance activated sludge wastewater treatment research and development. *Re/Views in Environmental Science & Bio/Technology* **1**: 83-97.
- Kjellerup B.V., Keiding K. and Nielsen P.H. (2001) Monitoring and troubleshooting of non-filamentous settling and dewatering in an industrial activated sludge treatment plant. *Wat. Sci. Tech.* **44**(2-3): 155-162.

- Krishna C. and Van Loosdrecht van M.C.M (1999) Effect of temperature on storage polymers and settleability of activated sludge. *Wat. Res.* **33**: 2374-2382.
- Kusters K.A. (1991) The influence of turbulence on aggregation of small particles in agitated vessels. *PhD Thesis*. Technical University Eindhoven, Nederland.
- Lakehal D., Krebs P., Krijgsman J. and Rodi W. (1999) Computing shear flow and sludge blanket in secondary clarifiers. *J. Hydr. Eng.* **31**: 215-224.
- LaPara T.M., Nakatsu C.H., Pantea L.M. and Alleman J.E. (2002) Stability of the bacterial communities supported by a seven-stage biological process treating pharmaceutical wastewater as revealed by PCR-DGGE. *Wat. Res.* **36**: 638-646.
- Lee D.S., Nopens I., Govoreanu R. and Vanrolleghem P.A. (2003) *The operation manual of the SBR*. Biomath Technical Report. Department of Applied Mathematics, Biometrics and Process Control, Ghent University, Belgium.
- Lee S.E., Koopman B., Bode H. and Jenkins D. (1983) Evaluation of alternatives sludge settleability indices. *Wat. Res.* **17**(10): 1421-1426.
- Li D.H. and Ganczarczyk J. J. (1987) Stroboscopic determination of settling velocity, size and porosity of activated sludge flocs. *Wat. Res.* **21**(3): 157-262.
- Li D.H. and Ganczarczyk J.J. (1989) Fractal geometry of particle aggregates generated in water and wastewater treatment processes. *Environ. Sci. Technol.* **23**: 1385-1389.
- Li D.H. and Ganczarczyk J. J. (1991) Size distribution of activated sludge flocs. *Research Journal WPCF* **63**(5): 806-814.
- Li D.H. and Ganczarczyk J.J. (1990) Structure of activated sludge flocs. *Biotech. Bioeng.* **35**: 57-65.
- Li D.-H. and Ganczarczyk J.J. (1993) Factors affecting dispersion of activated sludge flocs. *Wat. Environ. Res.* **65**: 258-263.
- Li X.Y., Passow U. and Logan B.E. (1996) Fractal dimensions of small (15-200 μm) particles in Easter Pacific coastal waters. *Deep – Sea Research* **45**: 115-131.
- Li X.Y. and Logan B.E. (1997) Collision frequencies between fractal aggregates and small particles in a turbulently sheared fluid. *Environ. Sci. Technol.* **31**: 1237-1242.
- Li X.Y. and Logan B.E. (2001) Permeability of fractal aggregates. *Wat. Res.* **35**(14): 3373-3380.
- Li X.Y. and Yuan Y. (2002) Settling velocities and permeabilities of microbial aggregates. *Wat. Res.* **36**: 3110-3120.
- Liao B.Q., Allen D.G., Droppo I.G., Leppard G.G. and Liss S.N. (2001) Surface properties of sludge and their role in bioflocculation and settleability. *Wat. Res.* **35**(2): 339-350.
- Liao B.Q., Allen D.G., Leppard G.G., Droppo I.G. and Liss S.N. (2002) Interparticle interactions affecting the stability of sludge flocs. *J. Colloid Interf. Sci.* **249**(2): 372-380.

- Liu Y., Lam M.C. and Fang H.P.H (2001) Adsorption of heavy metals by EPS of activated sludge. *Wat. Sci. Tech.* **43**(6): 59-66.
- Liu Y. and Fang H.P.H (2002) Extraction of extracellular polymeric substances (EPS) of sludges. *J. Biotechnol.* **95**(3): 249-256.
- Liu Y. and Fang H.P.H (2003) Influences of extracellular polymeric substances (EPS) on flocculation, settling and dewatering of activated sludge. *Critical Reviews in Env. Sci. Tech.* **33**(3): 237-273.
- Mace S. and Mata-Alvarez J. (2002) Utilization of the SBR technology for wastewater treatment: an overview. *Ind. Eng. Chem. Res.* **41**: 5539-5553.
- Madoni P., Davoli D. and Gibin G. (2000) Survey of filamentous microorganisms from bulking and foaming activated-sludge plants in Italy. *Wat. Res.* **34**: 1767-1722.
- Malvern (2004) <http://www.malvern.co.uk>
- Martins A.M.P., Heijnen J.J. and van Loosdrecht M.C.M. (2004) Effect of feeding pattern and storage on the sludge settleability under aerobic conditions. *Wat. Res.* **37**: 2555-2570.
- Martins A.M.P., Pagilla K., Heijnen J.J. and van Loosdrecht M.C.M. (2004) Filamentous bulking sludge – a critical review. *Wat. Res.* **38**(4): 793-817.
- Michaud R. and Morgenroth E. (2003) The influence of particle size on microbial hydrolysis of particulate organic matter. In Proceedings: IWA Conference on Nano- and Microparticles in Water and Wastewater Treatment. Zurich, Switzerland, September 22-24 2003.
- Mikkelsen L.H., Gottfredsen A.K., Agerbæk M.A., Nielsen P.H. and Keiding K. (1996) Effects of colloidal stability on clarification and dewatering of activated sludge. *Wat. Sci. Tech.* **34**: 449-457.
- Mikkelsen L.H. and Keiding K. (1999) Equilibrium aspects of the effects of shear and solids content on aggregate deflocculation. *Adv. Colloid Interface Sci.* **80**: 151-182.
- Mikkelsen L.H. and Keiding K. (2001) Effects of solids concentration on activated sludge deflocculation, conditioning and dewatering. *Wat. Sci. Tech.* **44**(2-3): 417-425.
- Mikkelsen L.H. (2001) The shear sensitivity of activated sludge. Relations to filterability, rheology and surface chemistry. *Colloid Surface A* **182**(1-3): 1-14.
- Mikkelsen L.H. and Keiding K. (2002) Physico-chemical characteristics of full scale sewage sludges with implications to dewatering. *Wat. Res.* **36**: 2451-2462.
- Mori T., Sakai Y., Honda K., Yano I. and Hashimoto S. (1988) Stable abnormal foam in activated-sludge process produced by *Rhodococcus* with strong hydrophobic properties. *Environ. Technol. Lett.* **9**: 1041-1048.
- Motta da M., Pons M.N. and Roche N. (2001) Automated monitoring of activated sludge in a pilot plant using image analysis. *Wat. Sci. Tech.* **43**(7): 91-96.

- Murthy S.N. and Novak J.T. (1999) Factors affecting floc properties during aerobic digestion: implications for dewatering. *Water Environ. Res.* **71**(2): 197-202.
- Muthumbi W., Boon N., Boterdaele R., De Vreese I., Top E.M. and Verstraete W. (2001) Microbial sulfate reduction with acetate: process performance and composition of the bacterial communities in the reactor at different salinity levels. *Appl. Microbiol. Biotechnol.* **55**: 787-793.
- Muyzer G., De Waal C.E. and Uitterlinden G.A. (1993) Profiling of complex microbial populations by denaturing gradient gel electrophoresis analysis of polymerase chain reaction-amplified genes coding for 16S rRNA. *Appl. Environ. Microbiol.* **59**(3), 695-700.
- Myers R.H. (1976) *Response surface methodology*. 2nd Ed., Edwards Brother Inc., Distributors Ann Arbor, Michigan, USA.
- Myers R.H., Khuri A.I. and Carter Jr. W.H. (1989) Response surface methodology: 1966-1988. *Technometrics* **31**(2): 137-157.
- Naito M., Hayakawa O., Nakahira K., Mori H. and Tsubaki J. (1998) Effect of particle shape on the particle size distribution measured with commercial equipment. *Powder Technology* **100**(1): 52-60.
- Neis U. and Tiehm A. (1997) Particle size analysis in primary and secondary waste water effluents. *Wat. Sci. Tech.* **36**(4): 151-158.
- Nielsen P.H., Frølund B. and Keiding K. (1996) Changes in the composition of extracellular polymeric substances in activated sludge during anaerobic storage. *Appl. Microb. Biotech.* **44**: 823-830.
- Nielsen P.H. and Keiding K. (1998) Disintegration of activated sludge flocs in the presence of sulfide. *Wat. Res.* **32**: 313-320.
- Nopens I., Capalozza C. and Vanrolleghem P.A. (2001) *Stability analysis of a synthetic municipal wastewater*. Biomath Technical Report. Department of Applied Mathematics, Biometrics and Process Control, Ghent University, Belgium.
- Nopens I., Biggs C.A., De Clercq B., Govoreanu R., Wilén B.-M., Lant P. and Vanrolleghem P.A. (2002) Modelling the activated sludge flocculation process combining laser diffraction particle sizing and population balance modelling (PBM). *Wat. Sci. Tech.* **45**(6), 41-49.
- Novak J.T., Nancy G.L., Smith M.L. and Elliott R.W. (1998) The effect of cationic salt addition on the settling and dewatering properties of an industrial activated sludge. *Wat. Environ. Res.* **70**(5): 984-996.
- Novák L., Larrea L., Wanner J., Garciaheras J.L. (1993) Non-filamentous activated sludge bulking in a laboratory-scale system. *Wat. Res.* **27**(8): 1339-1346.
- Novák L., Larrea L., Wanner J., Garciaheras J.L. (1994) Non-filamentous activated sludge bulking caused by *Zoogloea*. *Wat. Sci. Tech.* **29**(7): 301-304.
- Örmeci B. and Vesilind P.A. (2001) Effect of dissolved organic material and cations of freeze-thaw conditioning of activated and alum sludge. *Wat. Res.* **35**(18): 4299-4306.

- Ozinski A.E. and Ekama G.A. (1995) Secondary settling-tank modelling and design. 2. Linking sludge settleability measures. *Water SA*. **21**(4): 333-349.
- Panswad T., Doungchai A. and Anotai J. (2003) Temperature effect on microbial community of enhanced biological phosphorus removal system. *Wat. Res.* **37**: 409-415.
- Parker D.S., Kaufman W.J. and Jenkins D. (1970) *Characteristics of biological flocs in turbulent flows*. SERL Report No. 70-5, University of California, Berkely, USA.
- Parker D.S., Kaufman W.J. and Jenkins D. (1971) Physical conditioning of activated sludge flocs. *Jornal WPCF*. **43**: 1817-1833.
- Parker D.S., Kaufman W.J. and Jenkins D. (1972) Floc breakup in turbulent flocculation processes. *J. Sanitary Eng. Div.* **98**(SA1): 79-99.
- Parker D.S., Wahlberg E.J and Gerges H.Z. (2000) Improving secondary clarifier performances and capacity using a structured diagnostic approach. *Wat. Sci. Tech.* **41**(9):201-208.
- Patry G.G. and Takács (1992) Settling of flocculent suspensions in secondary clarifiers. *Wat. Res.* **26**(4): 473-479.
- Peng Y., Gao C., Wang S., Ozaki M. and Takigawa A. (2003) Non-filamentous sludge bulking caused by a deficiency of nitrogen in industrial wastewater treatment. *Wat. Sci. Tech.* **47**(11): 289-295.
- Piirtola L., Uusitalo R. and Vesilind P.A. (1999) Effect of mineral and cations on activated and alum sludge settling. *Wat. Res.* **34**(1): 191-195.
- Pochana K. and Keller J. (1999) Study of factors affecting simultaneous nitrification and denitrification (SND). *Wat. Sci. Tech.* **39**(6):61-68.
- Pons M.N., Vivier H., Belaroui K., Bernard-Michel B., Cordier F., Oulhana D. and Dodds J.A. (1999) Particle morphology: from visualisation to measurement. *Powder Technology* **103**: 44-57.
- Pujol R. and Canler J.P. (1992) Biosorption and dynamics of bacterial populations in activated sludge. *Wat. Res.* **26**: 209-212.
- Ranjard L., Poly F. and Nazaret S. (2000) Mini-review. Monitoring complex bacterial communities using culture-independent molecular techniques: applications to soil environment. *Res. Microbiol.* **151**: 167-177.
- Rasmussen H., Bruus J.H., Keiding K. and Nelsen P.H. (1994) Observations on dewaterability and physical, chemical and microbiological changes in anaerobically stored activated sludge from a nutrient removal plant. *Wat. Res.* **28**(2): 417-425.
- Rasmussen M.R. and Larsen T. (1997) On-line measurements of settling characteristics in activated sludge. *Wat.Sci.Tech.* **36**(4): 307-312.

- Robertson B.R., Button D.K. and Koch A.L. (1998) Determination of the biomass of small bacteria at low concentrations in a mixture of species with forward light scatter measurements by flow cytometry. *Appl. Environ. Microbiol.* **64**(10): 3900-3909.
- Rudd T., Sterrit R.M. and Lester J.W. (1983) Extraction of extracellular polymers from activated sludge. *Biotechnol. Lett.* **5**: 327-332.
- Russ J.C. (1990) *Computer- Assisted Microscopy. The measurement and analysis of images.* Plenum Press, NY, USA.
- Schmid M., Thill A., Purkhold U., Walcher M., Bottero J.Y., Ginestet P., Nielsen P.H., Wuertz S. and Wagner M. (2003) Characterization of activated sludge flocs by confocal laser scanning microscopy and image analysis. *Wat. Res.* **37**: 2043-2052.
- Sanin D. and Vesilind P.A. (1999) A comparison of physical properties of synthetic sludge with activated sludge. *Wat. Env. Res* **71**(2): 191-196.
- Sanin D. and Vesilind P.A. (2000) Bioflocculation of activated sludge: The role of calcium ions and extracellular polymers. *Environ. Technol.* **21**(12): 1405-1412.
- Segers D. (2004) Impact of agrochemicals on the microbial diversity within soil and plant. *Ph.D. thesis*, Faculty of Agricultural and Applied Biological Science, Ghent University, Belgium
- Séka M.A., Cabooter S. and Verstraete W. (2001) A test for predicting propensity of activated sludge to acute filamentous bulking. *Wat. Env. Res.* **73**(2): 237-242.
- Séka M.A. (2002) Monitoring tests and upgrading additives for activated sludge sedimentation. *Ph.D. thesis*, Faculty of Agricultural and Applied Biological Science, Ghent University, Belgium.
- Serra T., Colomer J. and Casamitjana X. (1997) Aggregation and breakup of particles in shear flow. *J. Colloid Interface Sci.* **187**: 466-473.
- Serra T. and Casamitjana X (1998) Structure of the aggregates during the process of aggregation and breakup under a shear flow. *J. Colloid Interface Sci.* **206**: 505-511.
- Serra T. and Logan B.E. (1999) Collision frequencies of fractal bacterial aggregates with small particles in a shared fluid. *Environ. Sci. Technol.* **33**: 2247-2251.
- Sezgin M., Jenkins D. and Parker D.S. (1978) A unified theory of filamentous activated sludge bulking. *J. Water Polln. Control Fedn.* **50**: 362-381.
- Sezgin M. (1982) Variation of sludge volume index with activated sludge characteristics. *Wat. Res.* **16**: 83-88.
- Sibelco (2004) <http://www.sibelco.be>
- Sievers M., Schroeder C., Bormann H., Onyeche T.I., Schlaefer O. and Schaefer S. (2003) Automation in sludge dewatering by novel on-line characterization of flocculation. *Wat. Sci. Tech.* **47**(2): 157-164.

- Sin G., Insel G., Lee D.S. and Vanrolleghem P.A. (2004) Optimal but robust N and P removal in SBRs: A systematic study of operating scenarios. In: Proceedings 3rd IWA International Conference on SBRs. Noosa, Australia, February 22-26 2004.
- Smith N.R., Yu Z. and Mohn W.W. (2003) Stability of the bacterial community in a pulp mill effluent treatment system during normal operation and a system shutdown. *Wat. Res.* **37**: 4873-4884.
- Smoczynski L. and Wardzynska R. (1996) Study on macroscopic aggregation of silica suspension and sewage. *J. Colloid Interface Sci.* **183**: 309-314.
- Smoluchowski M. (1917) Versuch einer Mathematischen Theorie der Koagulationskinetik Kolloider Lösungen. *Z. Phys. Chem.* **92**: 129-168.
- Snidaro D, Zartarian F., Jorand F., Bottero J.Y., Block J.C. and Manem J. (1997) Characterization of activated sludge structure. *Wat. Sci. Tech.* **36**: 313-320.
- Sobeck D.C. and Higgins M. (2002) Examination of three theories for mechanisms of cation-induced bioflocculation. *Wat. Res.* **36**: 527-538.
- Spicer P.T. and Pratsinis S.E. (1996) Shear-induced flocculation: the evolution of floc structure and the shape of the size distribution at steady state. *Wat. Res.* **30**(5): 1049-1059.
- Spicer P.T., Pratsinis S.E., Raper J., Amal R., Bushell G. and Meesters G. (1998) Effect of shear schedule on particle size, density, and structure during flocculation in stirred tanks. *Powder Technol.* **97**: 26-34.
- Stasinakis A.S., Nikolaos S.T., Mamais D., Papanikolaou E.C., Tsakon A. and Themistokles L.D. (2003) Effects of chromium (IV) addition on the activated sludge process. *Wat. Res.* **37**: 2140-2148.
- Sudhir N.M. and Novak J.T. (2001) Influence of cations on activated sludge effluent quality. *Wat. Environ. Res.* **73**(1): 30-36.
- Sürücü G. and Çetin F.D. (1989) Effect of temperature, pH and DO concentration on filterability and compressibility of activated sludge. *Wat. Res.* **23**: 1389-1395.
- Sutherland I.W. (1988) Bacterial surface polysaccharides: structure and function. *Inv. Rev. Cyt.* **113**:187-231.
- Takács I., Party G.G. and Nolasco D. (1991) A dynamic model for the clarification-thickening process. *Wat. Res.* **25**: 1263 – 1271.
- Tang S., Ma Y. and Sebastine I.M. (2001) The fractal nature of *Escherichia coli* biological flocs. *Colloids Surf. B: Biointerfaces* **20**: 211-218.
- Tchobanoglous G. and Burton F.L. (1991) *Wastewater Engineering: Treatment, Disposal and Reuse*. 3rd ed. Metcalf and Eddy Inc., McGraw Hill Inc., New York.
- Tchobanoglous G., Burton F.L. and Stensel H.D. (2003) *Wastewater Engineering: Treatment, and Reuse*. 4th ed. Metcalf and Eddy Inc., McGraw Hill Inc., New York.

- Tiehm A., Herwig V. and Neis U. (1999) Particle size analysis for improved sedimentation and filtration in wastewater treatment. *Wat. Sci. Tech.* **39**(8): 99-106.
- Thomas D.N., Judd S.J. and Fawcett N. (1999) Flocculation modelling: a review. *Wat. Res.* **33**(7): 1579-1592.
- Thompson G. and Forster C. (2003) Bulking in activated sludge plant treating paper mill wastewaters. *Wat. Res.* **37**(11): 2636-2644.
- Thomsen T.R., Nielsen J.L., Ramsing N.B. and Nielsen P.H. (2004) Micromanipulation and further identification of FISH-labelled microcolonies of a dominant denitrifying bacterium in activated sludge. *Env. Microbiol.* **6**(5): 470-479.
- Tsai C.H. and Rau S.R. (1992) Evaluation of Galai CIS-1 for measuring size distribution of suspended primary particles in the ocean. *TAO* **3**(2): 147-163.
- Tsai C.H. (1996) An assessment of a time-of-transition laser sizer in measuring suspended particles in ocean. *Marine Geology* **134**: 95-112.
- Twardowski M.S., Boss E., Macdonald J.B., Pegau W.S., Bernard A. H. and Zaneveld J.R.V. (2001) A model for estimating bulk refractive index from the optical backscattering ratio and the implications for understanding particle composition in case I and case II waters. *J. Geophys. Res.* **107**(C7): 14129-14142.
- UNEP (2000) Environmentally sound technologies in wastewater treatment for the implementation of the UNEP global program of action "Guidance on municipal wastewater", United Nations Environment Programme (UNEP), www.unep.or.jp
- Urbain V., Block C.J. and Manem J. (1993) Bioflocculation in activated sludge: an analytical approach. *Wat. Res.* **27**(5): 829-838.
- Vanderhasselt A., De Clercq B., Vanderhaegen B., Verstraete W. and Vanrolleghem P.A. (1999) On-line control of polymer addition to prevent massive sludge wash-out. *J. Environ. Eng.* **125**: 1014-1021.
- Vanderhasselt A. and Vanrolleghem P.A. (2000) Estimation of sludge sedimentation parameters from single batch settling curves. *Wat. Res.* **34**(2): 395-406.
- van de Hulst H.C. (1981) *Light scattering by small particles*. Dover Publications Inc. USA
- Van der Meeren P., Saveyn H., and Leysen R. (2004) Colloid-membrane interaction effects on flux decline during cross-flow ultrafiltration of colloidal silica on semi-ceramic membranes. *Phys. Chem. Chem. Phys.* **6** (in press).
- Vanrolleghem P.A., Van der Schueren D., Krikilion G., Grijspeerdt K., Willems P. and Verstraete W. (1996) On-line quantification of settling properties with in-sensor-experiments in an automated settlometer. *Wat. Sci. Tech.* **33**(1): 37-51.
- Vanrolleghem P.A. and Lee D.S. (2003) On-line monitoring equipment for wastewater treatment processes: state of the art. *Wat. Sci. Tech.* **47**(2): 1-34.

- Veerapaneni S. and Wiesner M. (1996) Hydrodynamics of fractal aggregates with radially varying permeability. *J. Colloid Interface Sci.* **177**: 45-57.
- Verstraete W. and Van Vaerenbergh E. (1986) Aerobic activated sludge. *Biotechnology* **2**(8): 43-112.
- Verwey E.J.W. and Overbeek J.G. (1948) Theory of the stability of lyophobic colloids. Elsevier, Amsterdam, Netherlands.
- Vigneau E., Loisel C., Devaux M.F. and Cantoni P. (2000) Number of particles for the determination of size distribution from microscopic images. *Powder Technology* **107**:243-250.
- Vogelaar J.C.T., Bouwhuis E., Klapwijk A., Spanjers H. and van Lier J.B. (2002) Mesophilic and thermophilic activated sludge post-treatment of paper mill process water. *Wat. Res.* **36**(7): 1869-1879.
- Wahlberg E.G. and Keinath T.M. (1988) Development of settling flux curves using SVI. *Journal WPCF* **60**(12): 2095-2100.
- Wahlberg E.G., Keinath T.M. and Parker D.S. (1994) Influence of activated sludge flocculation time on secondary clarification. *Wat. Environ. Res.* **66**(6): 779-786.
- Waite T.D., Guan J. and Amal R. (1998) Rapid determination of bacterial assemblage structure: Implications to process optimisation in wastewater treatment. In: *Chemical Water and Wastewater Treatment V*. Hahn H.H., Hoffmann E. and Ødegaard H. (Eds.), Springer-Verlag, Berlin, Germany. pp.:269-283.
- Waite T.D. (1999) Measurement and implications of floc structure in water and wastewater treatment. *Colloids Surf. A: Physicochemical and Engineering Aspects* **151**: 27-41.
- Wanner J., Chudoba J., Kucman K. and Proske L. (1987) Control of activated sludge filamentous bulking – VII. Effect of anoxic conditions. *Wat. Res.* **21**(12): 1447-1451.
- Wanner J. (1994) Activated sludge bulking and foaming control. *Technomic publishing*, Basel, Switzerland.
- Ward J.H. (1963) Hierarchical grouping to optimize an objective function. *Journal of the American Statistical Association* **58**: 236-244.
- Weiner B.B., Tscharnuter W.W. and Karasikov N. (1998) Improvements in accuracy and speed using the time-of-transition method and dynamic image analysis for particle sizing. In: Symposium Series 693, Particle Size Distribution III. Ed. Provder T., American Chemical Society.
- Wilén B.-M. (1999) Properties of activated sludge flocs. *PhD dissertation*, Dept. Sanitary Eng., Chalmers University of Technology, Goteborg, Sweden.
- Wilén B.-M. and Balmer P. (1999) The effect of dissolved oxygen concentration on the structure, size and size distribution of activated sludge flocs. *Wat. Res.* **33**(2): 391-400.

- Wilén B.-M., Nielsen J.L., Keiding K and Nielsen P.H. (2000) Influence of microbial activity on the stability of activated sludge flocs. *Colloids Surf.: Biointerfaces* **18**(2): 145-156.
- Wilén B.-M., Jin B. and Lant P. (2003) Impacts of structural characteristics of activated sludge floc stability. *Wat. Res.* **37**: 3632-3645.
- Wilderer P., Irvine R.L. and Goronszy M.C. (2001) *Sequencing Batch Reactor Technology*. IWA Scientific and Technical Report No:10, London, UK.
- Wilderer P.A., Bungartz H.-J., Lemmer H., Wagner M., Keller J. and Wuertz S. (2002) Modern scientific methods and their potential in wastewater science and technology. *Wat. Res.* **36**: 370-393.
- Wu R.M., Feng W.H., Tsai I.H. and Lee D.J. (1998) An estimate of activated sludge floc permeability: a novel hydrodynamic approach. *Wat. Environ. Res.* **70**(7): 1258-1264.
- Wu R.M. and Lee D.J. (1998) Hydrodynamic drag force exerted on a moving floc and its implication to free-settling tests. *Wat. Res.* **32**(3): 760-768.
- Wu R.M., Lee D.J., Waite T.D. and Guan J. (2002) Multilevel structure of sludge flocs. *J. Colloid Interface Sci.* **252**: 383-392.
- Wuertz S., Spaeth R., Hinderberger A., Griebe T., Flemming H.C. and Wilderer P.A. (2001) A new method for extraction of extracellular polymeric substances from biofilm and activated sludge suitable for direct quantification of sorbed metals. *Wat. Sci. Tech.* **43**(6): 25-31.
- Xu R. and Guida O.A.D. (2002) Particle size and shape analysis using light scattering, coulter principle and image analysis. In proceeding: World Congress on Particle Technology. Sydney Australia. July 21-25 2002 (on CD-ROM).
- Yun Z., Jo W., Yi Y., Choi S., Choi E. and Min K. (2000) Effects of sludge settling characteristics in BNR system. *Wat. Sci. Tech.* **42**(3/4): 283-288.
- Zanoni A.E. and Blomquist M.W. (1975) Column settling tests for flocculant suspensions. *J. Env. Eng. Division* **101**(3): 309-318.
- Zartarian F., Musin C. Bottero J.Y., Vilemin G., Thomas F., Aillères L., Champenois M., Grulois P. and Manem J. (1994) Spatial arrangement of the components of activated sludge flocs. *Wat. Sci. Tech.* **30**(11): 243-250.
- Zita A. and Hermansson M. (1994) Effect of ionic strength on bacterial adhesion and stability of flocs in a wastewater activated sludge system. *Appl. Environ. Microbiol.* **60**(9): 3041-3048.

List of abbreviations and symbols

Abbreviations

1D, 2D, 3D	one-, two- and three- dimensiona
AIC	Akaike Information Criterion
AR	Aspect Ration
BOD	Biological Oxygen Demand
CF	Compactness Factor
CFD	Computational Fluid Dynamics
COD	Chemical Oxygen Demand
DAQ	Data Acquisition
DLA	Diffusion Limited Aggregation
DLVO	Derjaguin, Landau, Verwey and Overbeek (theory)
DO	Dissolved Oxygen
DGGE	Denaturing Gradient Gel Electrophoresis
DSVI	Diluted Sludge Volume Index
EPS	Extracellular Polymeric Substances
EF	Elongation Factor
FBRM	Focus Beam Reflectance Measurement
FF	Form Factor
FI	Filament Index
FISH	Fluorescent In Situ Hybridisation
FSD	Floc Size Distribution
HCF	Heywood Circularity Factor
IMAN	Automatic Image Analysis system
LALLS	Long Angle Laser Light Scattering
MLSS	Mixed Liqueur Suspended Solids
MLVSS	Mixed Liqueur Volatile Suspended Solids
MS_{reg}	Regression Mean of Squares
MS_{res}	Residual Mean of Squares
OF	Objective Function

PBM	Population Balance Modelling
PCR	Polymerase Chain Reaction
RD	Roundness
RGD	Rayleigh-Gans-Debye approximation
RLA	Reaction Limited Aggregation
RMSE	Root Mean Square Errors
SBR	Sequencing Batch Reactor
SHAPE	Image analysis channel of CIS-100 device
SNF	Signal Normalisation Factor
SDU	Solution Density Uncalibrated
SS	Sum of Squares
SVI	Sludge Volume Index
TGGE	Thermal Gradient Gel Electrophoresis
TOT	Time Of Transition/laser channel of CIS-100 device
TSS	Total Suspended Solids (concentration)
VI	Virtual Instrument
WWTP	Waste Water Treatment Plant

Symbols

$2n$	axial number of experiments
2^n	factorial number of experiments
A	surface area
c_1, \dots, c_p	models parameters
df	degree of freedom
d_s	maximum stable floc size
$D_1; D_2; D_3$	one-, two- and three dimensional fractal
$D[4,3]$	mass mean diameter
D_{50}	median diameter
D_f	fractal dimension
D_p	perimeter-based fractal dimension
$D(n, 10 \dots 90)$	number-based average diameters representing 10%, ..., 90% of the particles size
$D(v, 10 \dots 90)$	volume-based average diameters representing 10%, ..., 90% of the particles size
$f(x)$	probability density function

F	normalised values of the DOE factors
F_0	nominal (central points) value of the DOE factors
G	root-mean square velocity gradient/shear stress
i	size interval
k	number of central points experiments
l	maximum size length
m	real refractive index of the particles
m'	imaginary refractive index of the particles
n	number of factors
n_{par}	number of parameters in the fitted model.
N	number of particles/flocs
N_a	agitation speed
p	number of terms
P	power dissipation/sonication power (Chapter 3)
Pr	Perimeter
R	model response
\hat{R}	fitted response surface
R^2	regression
R^2_{adj}	adjusted regression
Re	Reynolds number
sw	sensitivity weight
tw	target weight
t	time
T	temperature
T_a	torque
V	volume
w_i	canonical variables
X	sludge concentration
X_{16}, X_{50}, X_{84}	particle size at 16%, 50%, 84%
X_g	geometric mean of the size distribution
X_1, X_2, \dots, X_5	factors considered in design

Greek symbols

α	axial points of the DOE
ε	energy dissipation

$\varepsilon(x)$	solid fraction of the flocs
ε_m	model errors
ν	kinematic viscosity
ρ	density
σ_g	geometric standard deviation

Summary

The activated sludge process is one of the most widespread biological wastewater treatment method. For an effective process, the solid-liquid separation represents a crucial step. In order to obtain a successful solid-liquid separation and to meet the latest regulations regarding effluent quality, the microorganisms must form flocs, which settle and compact well without leaving a high suspended-solids concentration in the effluent. The activated sludge flocculation, however, is a very complex process in which many factors interact and may have an influence. Since a large number of these influences are poorly understood, the characteristics related to the floc-formation are still difficult to be predicted and controlled. Hence, improving knowledge on the flocculation step is an essential requirement for an optimal biological wastewater treatment.

The work described in this thesis was conducted in the framework of the "Sedimentation and Flocculation" (*SediFloc*) project conducted through several PhD studies. The objectives of this project were to quantify and model the flocculation process in secondary clarifiers by accounting for the influence of different physico-chemical parameters. Therefore, putting together the information concerning the flocculation dynamics and its modelling may represent one step forward in process understanding and a more accurate prediction of effluent quality.

This thesis aimed at developing a methodology for the on-line evaluation of the flocculation dynamics and at investigating the process response to variations of different physico-chemical factors. Finally, the joint effect of these parameters was investigated. To this end, Design of Experiment (DOE) and Response Surface Methodology (RSM) approaches were used. The knowledge resulting from this systematic study was used to explain the behaviour of a set of process characteristics.

The possibility of on-line monitoring of the activated sludge flocculation dynamics was demonstrated for the first time by Biggs (2000). Starting from this method, an important part of this work was devoted to the development of techniques that allow for the direct evaluation of the relationship between different operational parameters, the flocculation process and the effectiveness of the clarification step.

Initially, attention was paid to the possibility of measuring the floc morphological properties (e.g. the floc size and size distributions and fractal dimension). Due to the fragile biological nature, irregular structure and heterogeneous composition of the flocs, the measurement procedure may affect the results and lead to a misinterpretation of the data. Following a comprehensive literature study of the available sizing devices, a MastersizerS (Malvern, UK), a CIS-100 (Ankersmid, Belgium) and an automatic image analysis system (IMAN) developed in house in LabView (NI, USA) were selected for measurements. These devices were selected because of their different measurement principles, which allows obtaining much (sometimes complementary) information regarding the process dynamics, as well as because of their on-line analysis capabilities and similar sample preparation and manipulation requirements. The devices performance for activated sludge floc size and size distributions measurements was systematically evaluated and compared. To this end, the influences of some set-up

components, the concentration range and the possibility to in-line dilute the samples were investigated in order to find the operating conditions creating minimal floc disturbances during measurements. Moreover, the influence of floc shape and measurement principle on the size measurements was evaluated and the results were compared with those obtained for inorganic particles (round glass beads and irregular sand particles). It was found that all techniques used turned out to be fast and reliable methods for direct quantification of the floc size distributions.

For a correct evaluation of the influence of different physico-chemical factors on the flocculation process, the sludge samples should first be standardised. For this purpose, a Sequencing Batch Reactor (SBR) was built and operated under stable environmental conditions. An intensive monitoring procedure allowed for the evaluation of the sludge stability. In order to carry out this task, a procedure that linked the sludge settling performance with the evolution of the floc size and size distributions and microbial community dynamics (using DGGE and microscopical observations) was developed. It was found that sludge stability can be achieved only for relatively short time periods (e.g. of approximately one month) and, therefore, the experimental duration for performing the flocculation experiments should be restricted as well.

For evaluating the flocculation dynamics, an experimental set-up (FlocUNIT) was built. It consisted in a five-liter reactor in which the flocculation process took place. Different environmental conditions were applied in the reactor and their effect was monitored on-line by using specific sensors and off-line at the end of each experiment. A number of 36 experiments was performed by following an orthogonal and rotatable DOE. The influence of five relevant factors (temperature, shear stress, dissolved oxygen concentration, sludge concentration and calcium concentration) on a set of selected process responses (floc size, SVI, supernatant turbidity and suspended solids concentration, zeta potential, pH, conductivity) was evaluated.

Initially, the effect of each of the considered factors on the floc size dynamics was investigated separately. Among these factors, the most significant contribution on the size originated from the shear stress and the calcium concentration. High shear stress values produced deflocculation. However, calcium addition allowed the flocs to partially reaggregate even at high shear stress values. At low shear stress values, aggregation dominated and resulted in a slight and continuous increase of the floc size. The high affinity of the SBR sludge for calcium was not observed when different sludge samples collected from a WWTP were analysed. It was therefore concluded that the response of the activated sludge sample to the calcium addition is highly dependent of the initial calcium content of the sludge. At a higher solids concentration a tendency to form larger flocs was observed. Larger floc sizes were also observed when the temperature decreased in the reactor, while the dissolved oxygen concentration did not have a significant short-term effect on the floc size dynamics.

Finally, the joint effect of all five factors on the considered responses was investigated. The responses were evaluated by using a quadratic polynomial model, constructed from the experimental data after each factor underwent a linear or logarithmic scale normalisation. Accurate statistical models were obtained when the measurements were performed by using on-line sensors. The off-line analyses were influenced by the additional errors due to the sampling and measurements procedure, leading to model predictions with a moderate to poor statistical quality. Among the considered factors, the highest influence on the floc size dynamics came from shear stress. Similar operating conditions were found to be responsible for both larger floc formation and lower SVIs, demonstrating the link between the settling properties and floc size. The destabilisation process occurring during the (de)flocculation processes is not entirely due to charge effects and can not be fully described by using zeta

potential. Anaerobic conditions and low sludge concentrations led to an increase of the supernatant turbidity. However, a poor statistical model accuracy was found for models aimed at predicting the supernatant suspended solids concentrations and turbidity. It was suggested that the selected quadratic models can not predict the behaviour of these responses accurately. Conductivity showed, as expected, a direct relationship with the calcium concentration present in the system, while temperature and sludge concentration only had a small influence. Under the imposed factors, the pH did not change sufficiently to affect the flocculation process.

A process optimisation by using RSM was performed for the particular case of SBR sludge. Its goal was to find the conditions necessary for obtaining good settling properties (large floc size and low SVI) and low suspended solids concentrations of the supernatant ("zero" values for turbidity, suspended solids concentrations and zeta potential). It was found that, in order to obtain the imposed targets, the optimal operating conditions corresponded to the following factor values: temperature of approx. 7-8 °C; as low as possible shear stress values (even lower than the minimum value (15 s^{-1}) considered in these experiments); a calcium concentration of 14-18 meq/l; a dissolved oxygen concentration of approx. 1 mg/l and a sludge concentration of around 3.2 g/l.

In conclusion, this dissertation focused on various aspects related to the measurement, quantification and optimisation of the flocculation process. As a result, a methodology and empirical modelling by using DOE/RSM was developed and used for on-line characterisation of the flocculation dynamics and of its response to the effect of five physico-chemical factors. The conducted research also demonstrated that for a better prediction and control of the flocculation process, an integral approach, in which the cumulative effect of different factors is accounted for simultaneously, should be considered. It was shown that with a relatively low number of experiments, it is possible to investigate the short-term effect of changing environmental conditions and to find the factor values that would optimise the process. Moreover, the obtained results may be further used for a more elaborated modelling of the flocculation process dynamics by using a population balance formulation.

Samenvatting

Het actief slib proces is één van de meest verspreide methodes voor biologische afvalwaterzuivering. De scheiding van de vaste en vloeibare fase vormt hierbij een cruciale stap. Om de vaste en vloeibare fase succesvol te scheiden en aldus de meest recente effluent kwaliteitsnormen te halen, is het belangrijk dat de micro-organismen compacte vlokken vormen die goed bezinken zonder een hoge concentratie aan gesuspendeerde vaste deeltjes in het effluent achter te laten. Het actief slib flocculatieproces is echter een complex proces waarin verschillende factoren kunnen interageren en het proces beïnvloeden. Aangezien een groot aantal van deze invloedsfactoren slecht begrepen zijn, is het nog steeds moeilijk om de karakteristieken van de vlokvorming te voorspellen en te controleren. Dit impliceert dat een verbeterde kennis van de flocculatiestap essentieel is voor het optimaliseren van het biologische waterzuiveringsproces.

Het werk dat beschreven wordt in deze thesis werd uitgevoerd in het kader van het “Sedimentatie en Flocculatie” (Sedifloc) project, dat verscheidene doctoraten overkoepelde. De doelstelling van het project waren het kwantificeren en modelleren van het flocculatieproces in secundaire bezinkers, rekening houdend met verschillende fysico-chemische parameters. Het samenbrengen van informatie betreffende de flocculatiedynamica en de modellering ervan zou een stap voorwaarts kunnen betekenen in het doorgronden van het proces en aanleiding kunnen geven tot een betere voorspelling van de effluentkwaliteit.

Deze thesis had tot doel het ontwikkelen van een methodologie voor on-line evaluatie van de flocculatiedynamica en het onderzoeken van de procesrespons op variaties van verschillende fysico-chemische factoren. Tenslotte werd ook het gecombineerde effect van deze parameters bestudeerd. Hiervoor werd gebruik gemaakt van “Design of Experiment (DOE)” en “Response Surface Methodology (RSM)”. De kennis die hieruit voortvloeide werd gebruikt om het gedrag van een aantal proceskarakteristieken te verklaren.

De mogelijkheid om de actief slib flocculatiedynamica on-line op te volgen werd voor het eerst aangetoond door Biggs (2000). Uitgaande van deze methode werd een belangrijk deel van dit werk gewijd aan het ontwikkelen van technieken die een rechtstreekse beoordeling van de relatie tussen verschillende operationele parameters, het flocculatieproces en de klarings efficiëntie toelaten

Initieel werd aandacht besteed aan de mogelijkheid om de morfologische eigenschappen van de vlokken (vb. de vloggrootte, vloggroottedistributie en fractale dimensie) te meten. Door de fragiele biologische aard, de onregelmatige structuur en de heterogene samenstelling van de vlokken kan het resultaat beïnvloed worden door de meettechniek en zo aanleiding geven tot een foutieve interpretatie van de data. Na een grondige literatuurstudie van de beschikbare apparaten voor het meten van deeltjesgrootte werden de MastersizerS (Malvern, VK), de CIS-100 (Ankersmid, België) en een geautomatiseerd beeldanalysesysteem (IMAN) dat zelf werd ontwikkeld in LabView (NI, VS) gekozen voor het uitvoeren van de metingen. Zij werden enerzijds gekozen voor hun verscheidenheid van meetprincipe, wat aanleiding geeft tot een grote hoeveelheid (soms complementaire) informatie betreffende de procesdynamica. Anderzijds werd de keuze ook gedreven door het feit dat on-line analyse mogelijk was en de

staalvoorbereiding en –manipulatie analoog was. De performantie van de verschillende apparaten voor het meten van de actief slib vloggrootte en –distributie werd systematisch geëvalueerd en vergeleken. Hiertoe werden de invloed van sommige apparaatcomponenten, het concentratiebereik en de mogelijkheid voor in-line staalverdunding onderzocht met het oog op de bepaling van die bedrijfscondities die de minste vlokverstoring veroorzaken tijdens de metingen. Meerbepaald werd de invloed van de vlokvorm en meetprincipe op de vloggroottemetingen geëvalueerd. De resultaten werden vergeleken met deze verkregen met anorganische partikels (ronde glaspartikels en onregelmatige zandpartikels). Het bleek dat alle technieken snelle en betrouwbare methoden waren voor directe kwantificatie van vloggroottedistributies.

Om een correcte evaluatie van de invloed van verschillende fysico-chemische factoren op het flocculatieproces toe te laten, dienden de slibstalen eerst gestandaardiseerd te worden. Hiervoor werd een “Sequencing Batch Reactor (SBR)” gebouwd die bedreven werd onder stabiele omgevingscondities. Een rigoureuze en intensieve meetprocedure liet toe de slibstabiliteit te evalueren. Hiertoe werd een procedure ontwikkeld die slibbezinkingseigenschappen linkte aan de evolutie van vloggrootte, vloggroottedistributies en microbiële gemeenschapsdynamica (d.m.v. DGGE en microscopische observaties). Er werd gevonden dat slibstabiliteit enkel voor relatief korte periodes (grootte orde van een maand) kon worden bekomen. Dit limiterde de periode tijdens dewelke flocculatie-experimenten konden worden uitgevoerd.

Voor het evalueren van de flocculatiodynamica zelf werd een tweede experimentele opstelling (Flocunit) gebouwd, die onder meer bestond uit een 5L vat waarin het flocculatieproces plaatsgreep. Verschillende omgevingscondities werden aangelegd in de reactor en hun effect werd on-line opgevolgd door specifieke sensoren en off-line aan het einde van elk experiment. In totaal werden 36 experimenten uitgevoerd die deel uitmaakten van een orthogonaal en roteerbaar DOE. De invloed van 5 relevante factoren (temperatuur, wrijvingskrachten, opgeloste zuurstofconcentratie, slibconcentratie en calciumconcentratie) werd geëvalueerd op een set van geselecteerde responsvariabelen (vloggrootte, SVI, supernatant turbiditeit en supernatant gesuspendeerde deeltjes, zeta potentiaal, pH en conductiviteit).

Eerst werd het effect op de vloggroottedynamica van alle beschouwde factoren afzonderlijk onderzocht. Hieruit bleek dat de wrijvingskrachten en de calciumadditie het meest uitgesproken effect hadden op de vloggrootte. Grotere wrijvingskrachten resulteerden in deflocculatie, hoewel de calciumadditie gedeeltelijke re-aggregatie toeliet, zelfs bij grote wrijvingskrachten. Bij kleinere wrijvingskrachten was aggregatie dominant wat resulteerde in een lichte, maar continue stijging van de vloggrootte. De hoge affiniteit voor calcium van het SBR-slib werd niet teruggevonden bij verschillende andere slibstalen genomen in een RWZI. Er kon dan ook besloten worden dat de respons van een actief slib staal op een calciumadditie sterk afhankelijk is van het initiële calciumgehalte van het slib. Bij een hogere concentratie aan vaste stof werd een tendens tot grotere vlokken vastgesteld. Hetzelfde werd geconstateerd bij lagere temperaturen in de reactor, terwijl het opgeloste zuurstofgehalt geen uitgesproken korte termijn effect had op de vloggroottedynamica.

Tenslotte werd het gezamenlijk effect van alle 5 factoren op de verschillende responsvariabelen onderzocht. De responsvariabelen werden geëvalueerd met behulp van een kwadratische polynoom geconstrueerd uit de experimentele data nadat elke factor een lineaire of logaritmische normalisatie had ondergaan. Accurate statistische modellen werden bekomen wanneer de metingen met on-line sensoren werden uitgevoerd. De off-line analyses werden beïnvloed door additionele fouten veroorzaakt door staalname en meetprocedure, wat aanleiding gaf tot modelvoorspellingen met een matig tot slechte statistische kwaliteit. Van alle beschouwde factoren hadden de wrijvingskrachten de grootste impact. Gelijkaardige

bedrijfscondities veroorzaakten zowel grotere vlokken als lagere SVI-waarden, wat duidelijk het verband aantoont tussen de bezinkingseigenschappen en de vloggrootte. Het destabilisatieproces dat plaatsgrijpt tijdens (de)floculatie is niet volledig te wijten aan ladingseffecten en kan niet volledig beschreven worden door de zeta potentiaal. Anaerobe condities en lage slibconcentraties resulteerden in een toename van de supernatant turbiditeit. Een slechte statistische modelaccuraatheid werd echter gevonden voor modellen die trachtten de supernatant gesuspendeerde stoffen en turbiditeit te voorspellen. Er werd dan ook gesteld dat de geselecteerde kwadratische modellen het gedrag van de responsvariabelen niet accuraat konden voorspellen.

Conductiviteit vertoonde, zoals verwacht, een direct verband met de calciumconcentratie in het systeem, terwijl de temperatuur en slibconcentratie slechts een kleine invloed hadden. Onder de aangelegde bedrijfsfactoren waren de pH-fluctuaties te klein om het flocculatieproces dusdanig te beïnvloeden.

Een procesoptimalisatie door middel van RSM werd uitgevoerd voor het SBR-slib met als doel het bepalen van die procescondities noodzakelijk voor het bekomen van goede bezinkingseigenschappen (grote vloggrootte en lage SVI) en lage supernatant gesuspendeerde stof concentraties ("nul" waarden voor turbiditeit, gesuspendeerde stof concentratie en zeta potentiaal). Er werd gevonden dat, voor deze vooropgestelde criteria, de optimale bedrijfscondities overeenkwamen met de volgende waarden voor de respectievelijke factoren: een temperatuur van ca. 7-8°C; zo laag mogelijke wrijvingskrachten (zelfs lager dan de minimum waarde (15 s^{-1}) die werd beschouwd in deze experimenten); een calciumconcentratie van 14-18 meq/l; een opgelost zuurstofgehalte van ca. 1 mg/l en een slibconcentratie om en bij 3.2 g/l.

Dit werk spitste zich toe op de verscheidene aspecten gerelateerd met het meten, kwantificeren en optimaliseren van het flocculatieproces. Een methodologie en empirisch model door gebruik van DOE/RSM werd ontwikkeld en aangewend voor on-line karakterisatie van de flocculatiedynamica en haar respons op 5 fysico-chemische factoren. Het uitgevoerde onderzoek toonde aan dat voor een betere predictie en controle van het flocculatieproces een geïntegreerde aanpak moet worden genomen, waarin het cumulatieve effect van de verschillende factoren gelijktijdig in rekening wordt gebracht. Er werd aangetoond dat het, met relatief weinig experimenten, mogelijk is het korte termijn effect van wijzigende omgevingscondities te onderzoeken en de factorwaarden te bepalen die het proces optimaliseren. De resultaten kunnen aldus gebruikt worden voor een diepgaandere modelstudie van de flocculatiedynamica door middel van populatiebalansen.

Curriculum Vitae

Ruxandra Govoreanu

PERSONAL DATA

Nationality: Romanian
Place of Birth: Horezu, Romania
Home address: Kesseldallaan 10/302; B-3010 Leuven; Belgium
E-mail: ruxandra.govoreanu@biomath.ugent.be or rgovoreanu@hotmail.com

EDUCATION

2002 – present **Ph.D. research** in *Applied Biological Science and Environmental Technology*, Faculty of Agricultural and Applied Biological Sciences, Ghent University, Ghent, Belgium.
2000 – 2004 **Ph.D. training** in *Applied Biological Science and Environmental Technology*, Faculty of Agricultural and Applied Biological Sciences, Ghent University, Ghent, Belgium.
1995 – 1996 **M.Sc.** in *Chemical Engineering*, Faculty of Chemical Engineering, Technical University of Bucharest, Bucharest, Romania
1990 – 1995 **Licentiate** in *Chemical Engineering*, Faculty of Chemical Engineering, Technical University of Bucharest, Bucharest, Romania

RESEARCH AND EMPLOYMENT HISTORY

2000 – present **Research Assistant**, Department of Applied Mathematics, Biometrics and Process Control (BIOMATH), Ghent University, Ghent, Belgium
1998 – 2000 **Teaching Assistant**, Department of Inorganic Chemistry Engineering and Environmental Protection; Faculty of Chemical Engineering, Technical University of Bucharest, Bucharest, Romania
1996 – 1998 **Quality Control Engineer, R&D Engineer** - in charge with new pharmaceutical products development, S.C. OmegaProinvest S.A., Bucharest, Romania
1995 – 1996 **Research Engineer**, Research Institute for Environmental Engineering, Bucharest, Romania

PROFESSIONAL MEMBERSHIPS

2001 – present International Water Association (IWA)
1998 – 2001 Romanian Chemical Society

PUBLICATIONS

Refereed International Journals

Govoreanu R., Saveyn H., Van der Meeren P. and Vanrolleghem P.A. (2003) Simultaneous determination of activated sludge floc size distribution by different techniques. *Wat. Sci. Tech.* (submitted)

Govoreanu R., Seghers D., Nopens I., De Clercq B., Saveyn H., Capalozza C., Van der Meeren P., Verstraete W., Top E. and Vanrolleghem P.A. (2003) Linking floc structure and settling properties to activated sludge population dynamics in an SBR. *Wat. Sci. Tech.* 47(12), 9-18.

Nopens I., Biggs C.A., De Clercq B., Govoreanu R., Wilén B.-M., Lant P. and Vanrolleghem P.A. (2002) Modelling the activated sludge flocculation process combining laser diffraction particle sizing and population balance modelling (PBM). *Wat. Sci. Tech.*, 45(6), 41-49.

Conference Proceedings

Govoreanu R., Nopens I., Seghers D. and Vanrolleghem P.A. (2003) Investigation of low suspended solids concentration and calcium addition effects by on-line measurements of the activated sludge floc size and size distribution. In: *Proceedings Natural Waters and Water Technology, EuroConference on the Roles of Colloids and Particles in Water Technology*, Acquafreda di Maratea, Italy, 4-9 October 2003

Govoreanu R., Saveyn H., Van der Meeren P. and Vanrolleghem P.A. (2003) Simultaneous determination of activated sludge floc size distribution by different techniques. In: *Proceedings IWA International Conferences on Nano and Microparticles in Water and Wastewater Treatment*, Zurich, Switzerland, September 22-24 2003. pp.51-59

Govoreanu R., Seghers D., Nopens I., De Clercq B., Saveyn H., Capalozza C., Van der Meeren P., Verstraete W., Top E. and Vanrolleghem P.A. (2002) Linking floc structure and settling properties to activated sludge population dynamics in an SBR. In: *Proceedings 3rd IWA World Water Congress*. Melbourne, Australia, April 7-12 2002.

Govoreanu R., Vandegheuchte K., Saveyn H., Nopens I., De Clercq B., Van Der Meeren P and Vanrolleghem P.A. (2002) An automated image analysis system for on-line structural characterization of the activated sludge flocs. *Med. Fac. Landbouww. Univ. Gent*, 67/4, 175-178.

Govoreanu R., Nopens I., De Clercq B., Saveyn H., Van der Meeren P. and Vanrolleghem P.A. (2001) Influence of experimental parameters for on-line determination of floc size distribution. In: *Proceedings 12th Romanian International Conference on Chemistry and Chemical Engineering*. Bucharest, Romania, September 13-15 2001 (on CD-ROM).

Nopens I., Biggs C.A., De Clercq B., Govoreanu R., Wiln B.-M., Lant P. and Vanrolleghem P.A. (2001) Modelling the activated sludge flocculation process combining laser diffraction particle sizing and population balance modelling (PBM). In: *Proceedings 5th IWA Seminar on Modelling of Activated Sludge Processes in Theory and Practise*. Kollokole, Denmark, September 10-12 2001

Govoreanu R., Apostol G., Costache C., Stanescu R. and Constantinescu I. (2001) Determination of optimal coagulant dosing rate using empirical models. In: *Proceedings 12th Romanian International Conference on Chemistry and Chemical Engineering*. Bucharest, Romania, September 13-15 2001 (on CD-ROM).

De Clercq B., Nopens I., Govoreanu R., Vanrolleghem P.A. and Van Der Meeren P. (2000) Sludge (de)floculation dynamics in secondary clarifiers. *Med. Fac. Landbouww. Univ. Gent*, 65/4, 235-240.

Costache C., Constantinescu I., Lanyi S., Stanescu R., Govoreanu R. and Codescu A. (2000) Thermodynamic Study of the Phosphoric Acid Extraction with Solvents. In: *Proceedings of the 2nd International Conference of the South-Eastern European Countries on Chemical Sciences for Sustainable Development*, Chalkidiki, Greece, June 2000;

Govoreanu R., Apostol G., Stefan S., Costache C., Stanescu R., Lanyi S. and Constantinescu I. (1999) Optimization study on coagulation process based upon empirical models. In: *Proceedings of the 11th International Conference on Chemistry and Chemical Engineering*, Bucharest, Romania, September 1999. (on CD-ROM);

Drost A., Apostol G., Govoreanu R., Stefan S., Costache C., Stanescu R., Lanyi S. and Constantinescu I. (1999) Potassium Ion Dynamics in Sandy Soils. In: *Proceedings of the 11th International Conference on Chemistry and Chemical Engineering*, Bucharest, Romania, September 1999. (on CD-ROM)

Apostol G., Govoreanu R., Stefan S., Costache C., Stanescu R., Lanyi S. and Constantinescu I. (1999) Thermodynamics of phenol adsorption and electroadsorption on granular activated carbon. In: *Proceedings of the 8th Symposium "Technologies, Plants and Equipment for Improvement of Environmental Quality"*, Bucharest, Romania, November 1999;

